THE DRYING OF RYEGRASS SEEDS IN DEEP LAYERS

by

M. E. NELLIST, B.Sc(Agric), M.Sc(Agric.Eng),(Dunelm)

VOLUME 1

A thesis submitted for the degree of

Doctor of Philosophy

in the

University of Newcastle upon Tyne

January, 1974

BEST COPY

AVAILABLE

Poor text in the original thesis.
Some text bound close to the spine.
Some images distorted

ACKNOWLEDGEMENTS.

This work was carried out under the supervision of Professor J. R. O'Callaghan. Thrcugh the original initiative and continued support of Professor C.J. Moss, it was financed by the National Institute of Agricultural Engineering with the approval of the Agricultural Research Council. This support extended to 3 terms in residence at the University.

The author would like to thank all those many colleagues at Silsoe and Newcastle who helped in some way. The following are but a few.

Mrs. S. J. Matthews for technical and clerical assistance.

W. P. Billington, O. Harries, T. W. Layton and D. V. H. Rees for major contributions to the design and construction of the apparatus.

M. Hughes and colleagues of the Central Laboratory, N.I.A.E., for laboratory tests on the seed.

J. Bowler and R. Gowen, former vacation students, for help with experimental work and data analysis.

Control and Instrumentation Division, N.I.A.E., for maintenance of electronic equipment.

P. A. Clark of Rothamsted Experimental Station for help with data processing and the use of the London University computer.

Dr. D. J. Menzies for advice and help with computing at Newcastle.

A. Evers of the Cereals Research Station, St. Albans, for cutting sections through ryegrass seeds.

H. M. Roberts of the Welsh Plant Breeding Station for supplying tetraploid hybrid ryegrass seed.

F. S. Mitchell, G. Shepperson, Dr. D.S. Boyce, M. A. Moore and P. H. Bailey for discussion and advice.

Mrs. J. E. Caspall and Miss R. Brown for typing.

B. A. Watt and colleagues for photographic services.

ABSTRACT

Preservation of quality is the primary consideration in the drying of grass seed. Quality may be lost through destruction of seed viability and contamination by mould. Both result from the establishment, within the drying bed, of undesirable temperature and moisture conditions generated by the interaction of the seed and drying air. The work was based on the assumption that such moisture and temperature changes could be calculated from a knowledge of the heat and mass transfer properties of the seed and air, and that it would be possible to proceed from this physical framework to the calculation and imposition of biological restraints upon the selection of drying conditions.

Experimental work was carried out with a large and a small seeded strain of ryegrass of similar shape and structure. For each strain, potential germination was expressed as a function of moisture content at threshing.

Apparatus was developed for determining exposed layer drying curves at a wide range of air conditions and numerical procedures were developed for fitting the data to alternative diffusion equations. The fitted constants were expressed as functions of drying air temperature, humidity and seed initial moisture content. Effects on germination were expressed as functions of drying air temperature, exposure time and potential germination.

A mathematical model of the drying process was programmed in FORTRAN and used the exposed layer constants to predict moisture and temperature changes in deep beds subjected to fluctuating inlet air conditions. The model was stable, economical in computing time and gave reasonable overall agreement with experimental deep bed results. Consistent over-optimism of the drying time predictions was identified with cumulative error in temperature changes. Possible revisions of the basic equations pose problems of integration beyond the scope of the present work.

CONTENTS

VOLUME 1 - TEXT

ACKNOWLEDGEMENTS. i

ABSTRACT. ii

CONTENTS. iii

LIST OF TEXT TABLES. x

LIST OF TEXT FIGURES. xiii

KEY TO SYMBOLS. xxi

1. INTRODUCTION. 1

2. RYEGRASS SEED - RELEVANT PROPERTIES. 5

2.1. SEED ANALYSIS. 5

2.2. EXPERIMENTAL MATERIAL. 7

2.2.1. Ripening studies. 8

2.2.1.a. Sabrina and Sabel 8

2.2.1.b. S.23 12

2.2.2. Anatomy. 15

2.2.3. Size and weight. 21

2.2.3.a. Theory 21

2.2.3.b. Experimental 23

2.2.3.c. Results and discussion 25

3. DETERMINATION OF DRYING PROPERTIES - THIN-LAYER EXPERIMENTS. 31

3.1. INTRODUCTION. 31

3.2. THEORY. 31

3.2.1. Mass Transfer. 31

3.2.2. Equilibrium moisture content. 37

3.2.3. Biological damage. 41

3.3. EXPERIMENTAL. 45

3.3.1. Apparatus. 45

3.3.1.1. Thin-layer weighing units 47

3.3.1.2. Temperature control 51

3.3.1.3. Humidity measurement 51

3.3.1.4. Humidity control 53

3.3.1.5. Data logger 55

3.3.2. Data Processing. 56

3.3.2.1. Weight loss 58

3.3.2.2. Temperature 68

3.3.3. Experimental Details. 69

3.3.3.1. Mass transfer experiments, 1970-71 69

3.3.3.2. Germination experiment, 1972 71

3.4. RESULTS. 73

3.4.1. Mass Transfer. 73

3.4.1.1. 1970 Experiments 73

3.4.1.2. 1971 Experiments 80

3.4.2. Germination. 96

3.4.2.1. Effect of long-term exposure to drying air temperature 96

3.4.2.2. Results of 1972 experiments 104

3.4.2.2.a. Controls 104

3.4.2.2.b. Air temperature and humidity 105

3.4.2.2.c. Final moisture contents 105

3.4.2.2.d. Germination 109

3.5. DISCUSSION. 118

3.5.1. Drying rate. 118

3.5.1.a. 1970 results 118

3.5.1.b. 1971 results 120

3.5.2. Equilibrium moisture content. 129

3.5.3. Germination. 132

3.6. SUMMARY AND CONCLUSIONS. 140

3.6.1. Experimental. 140

3.6.2. Data Processing. 140

3.6.3. Drying Rate Constant. 141

3.6.4. Asymptotic moisture content. 152

3.6.5. Germination. 142

4. DEEP BED EXPERIMENTS. 144

4.1. INTRODUCTION. 144

4.2. APPARATUS. 144

4.2.1. General description. 144

4.2.2. Drying bins. 145

4.2.3. Fan and heater bank. 149

4.2.4. Flow measurement. 150

4.2.5. Temperature measurement. 151

4.3. EXPERIMENTAL. 152

4.3.1. Procedure for parallel flow runs. 153

4.3.1.a. 1970 (Runs 1,2,3) 153

4.3.1.b. 1971/2 (Runs 4-12) 154

4.3.2. Procedure for radial-flow runs. 156

4.3.3. Pressure resistance to airflow. 157

4.4. RESULTS AND DISCUSSION. 159

4.4.1. Drying runs. 159

4.4.2. Pressure resistance to airflow. 201

4.5. SUMMARY AND CONCLUSIONS. 206

5. SIMULATION OF DRYING IN DEEP BEDS. 209

5.1. INTRODUCTION. 209

5.1.1. Review of previous work. 209

5.2. DEVELOPMENT OF A MODEL FOR GRASS SEEDS. 213

5.2.1. Heat and mass transfer equations. 214

5.2.1.1. Moisture balance 215

5.2.1.2. Heat transfer equation 215

5.2.1.3. Heat balance equation 216

5.2.1.4. Drying rate 217

5.2.1.5. Method of solution 220

5.2.1.6. Condensation and re-evaporation 221

5.2.1.7. Heat transfer coefficient 225

5.2.2. Solution of the equation of the wet-bulb line. 229

5.2.3. Other properties. 232

5.2.3.1. Specific heat capacity 232

5.2.3.2. Latent heat 233

5.2.4. The computer programme. 233

5.3. SIMULATION OF EXPERIMENTAL RESULTS. 236

5.3.1. Preliminary tests. 236

5.3.1.1. Sensitivity to increment size 236

5.3.1.2. Sensitivity to heat transfer coefficient 239

5.3.2. Comparison of observed and predicted results. 243

5.3.2.1. Input data 243

5.3.2.2. Comparison of drying times and final moisture contents 244

5.3.2.3. Examination of individual runs 247

5.4. DISCUSSION. 269

5.4.1. Validation: 269

5.4.2. Application. 274

5.5. SUMMARY AND CONCLUSIONS. 275

6. CONCLUSIONS. 277

6.1. RYEGRASS SEED - RELEVANT PROPERTIES. 277

6.2. DETERMINATION OF DRYING PROPERTIES - THIN-LAYER EXPERIMENTS. 278

6.3. DEEP BED EXPERIMENTS. 280

6.4. SIMULATION OF DRYING IN DEEP LAYERS. 281

7. REFERENCES. 283

CONTENTS

VOLUME 2 - APPENDIX

CONTENTS i

LIST OF APPENDIX TABLES iv

LIST OF APPENDIX FIGURES ix

1. INTRODUCTION 291

2. RYEGRASS SEED - RELEVANT PROPERTIES 292

3. DETERMINATION OF DRYING PROPERTIES - THIN-LAYER EXPERIMENTS 305

3.1. DATA PROCESSING

3.1.1. Computer program DECODE for code-to-cycle conversion 305

FORTRAN listing of DECODE 308

3.1.2. Development of curve fitting procedures 309

3.1.2.1. 2 term-exponential. Equation 3.10 309

3.1.2.2. Exponential series. Equations 3.38 and 3.39 310

3.1.3. Implementation of curve-fitting procedures 313

3.1.3.1. Main program + MCTCON + DOUBEX 313

FORTRAN listing of main programme, MCTCON and DOUBEX 317

Example output from main programme, MOTCON and DOUBEX 326

3.1.3.2. Main program + subroutines SEREX and SINGEX 328

FORTRAN listing of main programme, SINGEX and SEREX 332

Example output from main programme, SINGEX and SEREX 343

3.1.3.3. Ancillary facilities 345

3.1.3.3.(a) Plotting program PPLOT 345

FORTRAN listing of PPLOT 346

3.1.3.3.(b) Plotting program PLOT 348

FORTRAN listing of PLOT 350

3.1.4. Program to analyse thermocouple readings 353

FORTRAN listing of MENTEM 356

Example output from MENTEM - a low humidity run 360

Example output from MENTEM - a high humidity run 361

3.2. RESULTS OF THIN-LAYER TESTS. 362

3.2.1. Analysis of results from 1972 germination experiment 416

3.2.1.1. Analysis of variance of germination results for Sabel 416

3.2.1.2. Analysis of variance of germination results for S.23 424

3.2.1.3. Analysis of variance for 14 day vigour results for Sabel 429

3.2.1.4. Analysis of variance for 14 day vigour results for S.23. 435

4. DEEP BED EXPERIMENTS. 442

4.1. APPARATUS 442

4.1.1. Fan performance and control 442

4.1.2. Air velocity and pressure resistance in the radial-flow batch drier. 443

4.1.2.1. The general case 443

4.1.2.2. The experimental rig 445

4.1.3. Data processing 447

4.1.3.1. Programs DEEP and RDEEP for processing data read from Honeywell-Brown recorder charts 447

FORTRAN program DEEP 450

FORTRAN program RDEEP 452

4.1.3.2. Plotting programs SIMPLT and RADPLT 454

FORTRAN programme SIMPLT 457

FORTRAN programme RADPLT 459

4.2. RESULTS 461

5. SIMULATION OF DRYING IN DEEP LAYERS. 577

5.1. Deep bed simulation programs 577

5.1.1. Parallel flow 577

FORTRAN programme for parallel-flow 587

Example output from parallel-flow simulation -Run 1 598

Example output from parallel-flow simulation -Run 4 605

5.1.2. Radial flow 609

FORTRAN program for radial-flow 610

TABLES

Table No.	Title	Page
2.1.	Comparison of direct and indirect threshed samples of Sabel, 1972.	12
2.2.	Sieve sizes.	24
2.3.	Mean dimensions, 1000 seed weight and some derived parameters of size and shape.	25
2.4.	Mean 1000 seed weights, g, in major size fractions. Bracketed values=% by weight in each class.	27
2.5.	Diameters derived from sieving results.	27
3.1.	Details of drying curves in Figs. 3.9 and 3.10	73
3.2.	Values of constants in fitted curves of Figs. 3.11 and 3.12.	76
3.3.	Values of the constants A and B in equation 3.41	76
3.4.	Drying conditions in 1971 thin-layer experiments.	80
3.5.	Standard deviations of predicted from observed values derived from fits of 4 alternative diffusion equations	81
3.6.	Drying conditions and standard deviations of the fitted curves for Runs 66, 106 and 207 drawn in Fig. 3.16.	82
3.7.	Values of coefficients in equation 3.44 expressing drying constant, k, as a function of temperature, initial moisture content and absolute humidity.	85
3.8.	Values of the constants a,b,c in equation 3.42 for asymptotic moisture content. Classified by variety and source of values.	91
3.9.	Constants in equation 3.42 for all 1971 data and for 1971 plus 1972 data.	94
3.10.	Dates of harvest, initial moisture contents and properties of control samples.	104
3.11.	Means and standard deviations of drying air temperatures with grand mean at each level and standard deviation of that mean.	105
3.12.	Final moisture contents, % d.b.	106
3.13.	Mean 14 day germination counts.	110
3.14.	Analysis of variance of 14 day germination counts (transformed to angles) and percent vigour of Sabel and S.23. seeds.	111

Table No.	Title	Page
3.15.	Germination as a straight line function of temperature at each exposure time and moisture content.	115
3.16.	Drying temperature, °C, giving 90% germination predicted by the linear equations of the parallel curve analysis, Table 3.15.	115
3.17.	Mean vigour percentages (7/14 day)	117
3.18.	Coefficients in the expression y=A.exp(bT) where y= p or q of equations 3.50 or 3.51	123
3.19.	Values of the quantity, $(\sqrt{k_{S23}/k_{Sabel}})$ at 5 temperatures for the 4 alternative diffusion equations.	125
4.1.	Summary of the deep-bin runs.	152
4.2.	Summary data for parallel-flow deep bed Runs 1 - 6. Imperial units.	160
4.3.	Summary data for parallel-flow deep bed Runs 7 - 12. Imperial units.	161
4.4.	Summary data for radial-flow deep bed Runs 13 - 15. Imperial units.	162
4.5.	Some approximate measures of air utilisation	163
4.6.	Coefficients a and n in equation 4.6, $p=aV^n$, derived from various groups of data.	201
5.1	Effect on M of modifying equation 5.6 to form 5.7.	217
5.2.	Values of E_2, E_1 and E_2/E_1 as affected by kθ	218
5.3.	Triangular matrix of x_{ii} derived from values of x and y arranged in ascending order of y.	224
5.4.	Specific heats of S.24 ryegrass - unpublished data of R.B.Sharp[107]	232
5.5.	Effect of depth and time increments on predicted drying time, minutes, for Run 7 (T_a = 55.4°C) and Run 9 (T_a = 26.0°C)	237
5.6.	Effect of value of heat transfer coefficient on predicted drying time and final moisture profile in Run 7 (hS = 460 kJ/min K m^3)	242
5.7.	Simulation of experimental runs. Constants used in equation 3.44 for evaluating the drying constant, k.	243
5.8.	Simulation of experimental runs. Constants used in equation 3.42 for evaluating the asymptotic moisture content, Me.	244

Table No.	Title	Page
5.9.	Simulation of experimental runs. Comparison of drying times and final mean bed moisture contents.	246
5.10.	Differences between experimental and predicted drying times and mean bed moisture contents in relation to total drying time and percentage moisture removed.	271

FIGURES

Fig. No.	Title	Page
1.1.	Seasonal variation in grower's prices for S.23 ryegrass seed.	1
2.1.	Moisture content (top), 1000 seed weight (centre) and germination (bottom) plotted against harvest data for Sabrina and Sabel.	9
2.2.	Germination of Sabrina and Sabel as a function of moisture content (top) and 1000 seed weight (bottom).	11
2.3.	Moisture content (top), 1000 seed weight (centre) and germination (bottom) plotted against harvest date for S.23.	13
2.4.	Germination of S.23 as a function of moisture content (top) and 1000 seed weight (bottom).	14
2.5.	Typical seeds of S.23 (top) and Sabrina (bottom) x 7.	16
2.6.	Longitudinal section through a Sabrina seed showing pales enclosing the endosperm. Embryo not visible (x40).	17
2.7.	Transverse section through typical portions of the seed of Sabrina. Embryo and endosperm at blunt end of seed (top); endosperm and folds of pales near the apex of the kernel; pericarp and pales beyond kernel (bottom).	18
2.8.	Internal structure of the ryegrass seed kernel (x120).	19
2.9.	Plan and cross-sectional views of S.23 (left) and Sabrina (right) to illustrate comparative size, shape and derived parameters.	28
3.1.	The N.I.A.E. multi-unit drier in 1969.	46
3.2.	The N.I.A.E. multi-unit drier in 1972 following modification for thin-layer drying.	46
3.3.	Thin-layer weighing unit.	48
3.4.	Circuit for incorporating photo-switch (PS) and read-switch (RS) into automatic weighing system.	49
3.5.	Aspirated dry-and wet-bulb thermocouple units.	52
3.6.	Schematic layout of single-packed tower.	54

Fig. No.	Title	Page
3.7.	Flow chart of main programme and subroutine MOTCON used for the generation of moisture contents at each cycle time.	60
3.8.	Flow chart for subroutine SEREX	66
3.9.	Replicate drying curves for 28.8°C. Solid line = curve predicted by equation 3.38 (1970 data).	74
3.10.	Replicate drying curves for 61.7°C. Solid line = curve predicted by equation 3.38 (1970 data.)	74
3.11.	Comparative fits of Equations 3.1 and 3.10 to experimental points (for key see Fig.3.12)	75
3.12.	Comparative fits of equations 3.1. and 3.10 to experimental points. ——— ——— . ——— . ———log least squares equ 3.1. - - - - - - - - - - - - - - - direct least squares equ 3.1. ——————————direct least squares equ 3.10.	75
3.13.	Plots of drying constant,k, against drying air temperature for logarithmic least squares fit of equation 3.1. (top) and direct least squares fit of equation 3.10. (bottom).	77
3.14.	Plot of drying constant,k, against drying air temperature for direct least squares fit of equation 3.1.	78
3.15.	Plot of equilibrium moisture constants against relative humidity with fitted lines of equation 3.42. at 30°C and 60°C (1970 data).	79
3.16.	Comparative fits given by equations 3.1. (- - -) 3.10(———), 3.38 (- . . - . . -) and 3.39 (— . — . —) for Runs 66 (top), 106 (middle) and 207 (bottom), 1971 data.	83
3.17.	Plots of drying constant k given by the fit of equation 3.39 to 1971 data for Sabel (top) and S.23 (bottom). Fitted line plotted at mean humidity and initial moisture content of each data set.	86
3.18.	Drying constants, k_2, of equation 3.10 as a function of temperature for Sabel and S.23. Solid lines = 1971 data. Dotted line = 1970 data.	87
3.19.	Drying constant k_2 of equation 3.10 as a function of air humidity for Sabel (o) and S.23 (Δ). 1971 data.	89

Fig. No.	Title	Page
3.20.	Drying constant k as a function of temperature for 4 alternative drying curve equations fitted to 1971 data for S.23.	90
3.21.	Asymptotic constants, Me, derived from fits of equation 3.10. plotted against relative humidity for Sabel (o) and S.23 (Δ) 1971 data.	92
3.22.	Correlation of asymptotic moisture contents, Me, with temperature and humidity given by equation 3.42. for values of Me obtained for the 2 term exponential equation for Sabel (left) and S.23 (right).	93
3.23.	Final moisture contents, M_f, plotted against relative humidity for 1971 results for Sabel (o) and S.23 (Δ) and for results from both varieties in the 1972 germination experiment (□). Continuous curve = plot of equation 3.42 for constant absolute humidity.	95
3.24.	Germination results from 1970 tests in S.23 seed with fitted curve of equation 3.45.	97
3.25.	Effect of drying air temperature in depressing germination of Sabel (1) and S.23 (2).	98
3.26.	Effect of long-term exposure to temperature on the germination of Sabel. Fitted curves at 23.2 (top), 68.2 (centre) and 99.9 (bottom) moisture content, % d.b.	100
3.27.	Effect of long-term exposure to temperature on the germination of S.23. Fitted curves at 31.1 (top), 62.3 (centre) and 93.9 (bottom) moisture content, % d.b.	101
3.28.	Effect of long term exposure to temperature on the vigour of Sabel with fitted curve of equation 3.48.	102
3.29.	Effect of long-term exposure to temperature on the vigour of S.23 with fitted curve of equation 3.49.	103
3.30.	Final moisture contents after 10 hours exposure to temperatures in the range 57.3 - 78.7°C plotted against corresponding relative humidities for Sabel, Runs 1 (□), 2 (o) and 3 (Δ) and S.23, Runs 4 (□), 5 (o) and 6 (Δ).	108

Fig. No.	Title	Page
3.31.	Effect of temperature on germination of Sabel seeds after 15 min. (left) and 10h (right) exposure from initial moisture contents of 80.0 (Δ), 64.2 (o) and 46.6 (□)% dry basis.	113
3.32.	Effect of temperature on germination of S.23 seeds after 15 min. (left) and 10h (right) exposure from initial moisture contents of 71.5 (Δ), 53.4 (o) and 36.1 (□)% dry basis.	113
3.33.	Comparison of experimental and predicted drying rates given by data in Fig. 3.9.	119
3.34.	Sum (top) and product (bottom) of the constants, k, and k_2 in equation 3.10 for Sabel (•) and S.23 (Δ) with fitted lines represented by continuous and dotted lines for Sabel and S.23 respectively.	122
3.35.	Comparative drying rate constants, k, for S.23 (1) and Sabel (2) ryegrasses (equation 3.10), barley (3) (Boyce, ref.17) and wheat (4) (M'Ewen and O'Callaghan ref. 68).	127
3.36.	Comparative diffusivities of S.23 (1) and Sabel (2) ryegrass, with other grains. 3 = Wheat-M'Ewen and O'Callaghan (68) 4 = Barley-Boyce (17) 5 = Maize) 6 = Wheat)-Pabis (93) 7 = Beans)	128
3.37.	Comparison of experimental and predicted germinations of Sabel as a function of exposure time, equation 3.53, at 57.7 (◊), 63,2 (o), 68.8 (Δ), 74.2 (□) and 78.5 (▽)°C at moisture levels of 80.0 (top), 64.1 (middle) and 46.5 (bottom) % d.b.	137
3.38.	Comparison of experimental and predicted germinations of S.23 as a function of exposure time, equation 3.53, at 57.7 (◊), 63.2 (o), 68.8 (Δ), 74.2 (□) and 78.5 (▽) °C at moisture levels of 75.1 (top), 53.4 (middle) and 31.1 (bottom) % d.b.	138
4.1.	Apparatus for parallel and radial-flow deep bed tests.	145
4.2.	Deep bin drier, Air duct, plenum chamber and small drying bin (top) and fan, heater, electrical controls and inclined tube gauges (bottom).	146
4.3.	False floor insert for small drying bin with thermocouple leads fastened to central stalk at 3 in. intervals.	147

Fig. No.	Title	Page
4.4.	Section of radial bin drier. Thermocouple locations indicated by numbered dots.	148
4.5.	Flat sampling pan for the deep bin drier.	155
4.6.	Initial (x) and final (o) moisture gradients for parallel-flow runs 1 (top) and 2 (bottom)	165
4.7.	Temperature profile, Run 1, 10:7:70	166
4.8.	Temperature profile, Run 2, 28:7:70	167
4.9.	Initial (x) and final (o) moisture gradients for parallel-flow Runs 3 (top) and 4(bottom).	170
4.10.	Temperature profile, Run 3, 4:8:70.	171
4.11.	Temperature profile, Run 4, 12:7:71.	172
4.12.	Initial (x) and final (o) moisture gradient for parallel-flow Runs 5 (top) and 6 (bottom).	173
4.13.	Temperature profile, Run 5, 14:7:71.	174
4.14.	Temperature profile, Run 6, 19:7:71.	175
4.15.	Initial (x) and final(o) moisture gradients for parallel-flow Runs 7 (top) and 8 (bottom)	177
4.16.	Temperature profile, Run 7, 22:7:71.	178
4.17.	Temperature profile, Run 8, 26:7:71.	179
4.18.	Initial (x) and final (o) moisture gradients for parallel-flow Runs 9 (top) and 10 (bottom).	181
4.19.	Temperature profile, Run 9, 30:7:71.	182
4.20.	Temperature profile, Run 10, 4:8:71.	183
4.21.	Initial (x) and final (o) moisture gradients for parallel-flow Runs 11 (top) and 12 (bottom).	186
4.22.	Temperature profile, Run 11, 16:8:71.	187
4.23.	Temperature profile, Run 12, 17:7:72.	188
4.24.	Intermediate and final moisture gradients for radial-flow Runs 13 (top) and 14 (bottom)	190
4.25.	Temperature (o) and moisture (x) gradients sampled at 19h in Run 13 (top) and 45h in Run 14 (bottom).	191
4.26.	Temperature profile, Run 13, 25:7:72.	192
4.27.	Temperature profile, Run 14, 3:8:72.	193
4.28.	Intermediate and final moisture gradients for radial flow Run 15.	195

Fig. No.	Title	Page
4.29.	Temperature (o) and moisture (x) gradients sampled at 46h in Run 15.	196
4.30.	Temperature profile, Run 15, 10:8:72.	197
4.30a.	Effect of moisture reduction upon shrinkage.	199
4.31.	Pressure resistance for Sabel. Parallel-flow Runs 5,6,8 and 12.	202
4.32.	Pressure resistance for S.23 parallel-flow Runs 9 and 10 and curves derived from radial-flow runs 16 and 15.	203
4.33.	Pressure resistance for S.23, Radial flow Runs 14 and 15.	204
5.1.	Interacting variables in the thin-layer.	214
5.2.	Principle of adjusting ΔM to contain exhaust r.h. within the feasible range (where the symbol ΔM represents $\Delta M.\left(\frac{\rho.\Delta z}{G.\Delta\theta}\right)$.	223
5.3.	Simplified flow chart of parallel-flow deep bed drying programme.	234
5.4.	Effect of depth increment on predicted final moisture profile in Run 9.	238
5.5.	Effect of heat transfer coefficient on final temperature profile predicted for Run 7. Experimental observations at real final time denoted by ●.	240
5.6.	Effect of heat transfer coefficient h3 on temperatures in layer 1 at iteration 1 (continuous lines) and in the 39th layer of the last iteration (dotted lines)	241
5.7.	Comparison of experimental and predicted final moisture contents (top) and drying times (bottom) for Sabel and Sabrina (o) and S.23 (x).	245
5.8.	Run 1. Observed (•) and calculated (1) final moisture profiles. The effect on the calculated profile of using an alternative relation for M_e is shown at the experimental time and at the time required to reach the final mean bed moisture content.	247
5.9.	Run 2. Predicted drying curve (1) and input air temperature (2).	249
5.10.	Run 2. Calculated (1) and observed (•) final moisture contents within the bed.	250

Fig. No.	Title	Page
5.11.	Run 3. Observed (•) and calculated (1) final moisture profiles.	251
5.12.	Run 3. Variation in predicted mean bed moisture content with time (1) and comparison of calculated (2) and observed (3) exhaust air temperatures.	252
5.13.	Run 4. Final moisture profiles predicted at (1) experimental time (=23.0h) and (2) calculated final time (26.4h) compared with experimental data (•).	253
5.14.	Run 5. Final moisture profile predicted at 79.4h (1) and at 114 h (2) compared with experimental data (•).	254
5.15.	Run 5. Predicted drying curve. X = experimental final moisture content.	255
5.16.	Run 6. Predicted temperature-time profiles (----) compared with observed profiles (——) from Fig. 4.14. A = predicted average drying curve.	256
5.17.	Run 6. Final moisture profile at predicted drying time (1) compared with experimental data (•).	257
5.18.	Run 7. Predicted temperature-time profiles (----) compared with observed profiles (——) from Fig. 4.16. A = predicted average drying curve.	258
5.19.	Run 7. Final moisture profile at predicted drying time (1) compared with experimental data (•).	259
5.20.	Run 8. Predicted temperature-time profiles (----) compared with observed profiles (——) from Fig. 4.17. A = predicted average drying curve.	260
5.21.	Run 8. Final moisture profiles predicted at experimental time (1) and at 99.8 h (2) compared with experimental data (•).	261
5.22.	Run 10. Final moisture profile predicted at 88.5 h (1) compared with experimental profile at 136 h. (•).	262
5.23.	Run 10. Predicted temperature-time profiles (---) compared with observed profiles.(——) from Fig. 4.20. A = predicted average drying curve.	264
5.24.	Run 12. Predicted temperature-time profiles (---) compared with observed profiles (——) from Fig. 4.23. A = predicted average drying curve.	265
5.25.	Run 12. Final moisture profile at predicted drying time (1) compared with experimental data (•).	266

Fig. No.	Title	Page
5.26.	Run 13. Final moisture profile at predicted drying time (1) compared with experimental data (o).	267
5.27.	Run 14. Predicted temperature-time profiles (- - -) compared with observed profiles (——) from Fig. 4.27. A = predicted average drying curve.	268
5.28.	Example of predicted (——) and experimental (- - -) deep bed profiles given by O'Callaghan et al [88] Depths from surface 1 = 0.28m, 2 = 0.23 m, 3 = 0.15 m, 4 = 0.075 m, 5 = surface.	272

KEY TO SYMBOLS.

Operators

ln	logarithm to base e
log	logarithm to base 10
exp( )	exponent of
f( )	function of
f'( )	first differential function of
h( )	function of
δ	increment of difference
d	differential
$\int$	integral
Δ	incremental
Σ	summation

Lower case.

a, b, c, d	constants
d_c	diameter of cylinder, m
d_e	effective diameter based on density, m
d_g	geometric mean diameter, m
d_m	equivalent spherical diameter, m
d_s	effective diameter of cylinder, m
d_{vs}	volume-surface mean diameter, m
e	basis of natural logarithms
f	frequency
h	number of classes(Section 2)
h	coefficient of heat transfer, kJ/min m^2 K
hS	volumetric heat transfer coefficient, kJ/min m^3 K
i, j	integer constants

j_h dimensionless group for heat transfer

k drying constant, time^{-1}

k_1, k_2 drying rate constants in equation 3.10

k thermal conductivity of air, kW/m K

k_g rate of germination depression, time^{-1}

l length of finite cylinder, m

n integer constant

p sum of k_1 and k_2

p numerical constant in wet-bulb equation

q product of k_1 and k_2

q quantity of heat

r radius of drying particle

r correlation coefficient

r numerical constant in wet-bulb equation

rh relative humidity, ratio or %

s constant in wet-bulb equation

t temperature, °F

t cycle time

v air velocity, m/sec

x space coordinate

x independent variable

x_k values of independent variable

y space coordinate

y dependent variable

y_k values of dependent variable

z space coordinate

z half-thickness of plane sheet(Section 3)

z depth of deep bed(Section 5)

Upper case

A empirical constant (Section 3)

A abbreviated term in model equations (Section 5)

A_s surface area of layer edge, m^2

A empirical constant (Section 3)

A abbreviated term in model equations (Section 5)

B empirical constant (Section 3)

B abbreviated term in model equations (Section 5)

B_m, B_n } Bessel function expressions

C concentration of diffusing substance (Section 3)

C specific heat capacity of wet seed, kJ/kg K

Cpa specific heat capacity of air, kJ/kg K

Cpg specific heat capacity of seed dry matter, kJ/kg K

Cpl specific heat capacity of water liquid, kJ/kg K

Cpw specific heat capacity of water vapour, kJ/kg K

D bed depth, m (Section 2)

D diffusion coefficient, m^2/min (Section 3)

D_P bed depth in parallel flow

D_R depth normal to radius in radial bin section

D_p average particle diameter, m

D_O diffusivity at absolute zero

DM dry matter, g

E activation energy

E abbreviated term in model equations (Section 5)

F rate of transfer of diffusing substance through unit area

F abbreviated term in model equations (Section 5)

G mass rate of flow, lb/h or kg/h (Section 4) or mass rate of flow per unit area, kg/min m^2 (Section 5)

G seed germination, %

G_O value of germination predicted for seed of initial moisture content, M_O

G_e asymptotic germination, %

G_D germination depression, %

H	absolute humidity of air, ratio
J_o	Bessel function of μ_n
L	latent heat of vapourisation of water at T_{wb}, kJ/kg
La	latent heat of vapourisation of water at 0°C, kJ/kg
Lg	latent heat of vapourisation of water in seed, kJ/kg
M	seed moisture content, % d.b.(Ratio in equations in Section 5)
M	mean bed moisture content, % d.b.
M_b	bound moisture content, ratio d.b.
M_e	equilibrium or asymptotic moisture content, % or ratio d.b.
M_f	final moisture content, % or ratio d.b.
M_i	intermediate value of moisture content at time, θ_i
M_d	moisture content, dry basis (% or ratio)
M_w	moisture content, % wet basis
M_o	initial moisture content, % or ratio d.b.
N	number of estimated values.
P	pressure, N/m^2
P_{at}	atmospheric pressure, N/m^2
P_s	saturated vapour pressure, N/m^2
P_{swb}	saturated vapour pressure af water at T_{wb}, N/m^2
P_v	partial vapour pressure, N/m^2
P_P	pressure drop in parallel flow
P_R	pressure drop in radial flow
Q	volume flow of air, ft^3/min or m^3/min
R	universal gas constant
R	radius of finite cylinder
R_1	radius of inner wall of radial bin
R_2	radius of outer wall of radial bin
R_L	radius of annular layer in radial bin
S	surface area per unit volume of seed bulk, m^{-1}
S_v	surface area per unit volume of seed, m^{-1}

S_p	surface area of individual particle or seed, m^2
T	temperature, °C
T_a	air temperature, °C
T_{abs}	absolute temperature, °K
T_{amb}	ambient temperature , °C
T_{db}	temperature of the dry bulb, °C
T_g	seed temperature, °C
T_{max}	maximum permissible temperature for seed viability, °C
T_s	temperature of surface of seed and air at layer edge, °C
T_{wb}	temperature of the wet bulb, °C
U	conductance, kJ/m^2 C min
V_p	volume of individual seed or particle, m^3
W_i	weight of moisture at θ_i, g
W_{1000}	weight of 1000 seeds, kg
Y_k	estimated values of dependent variable

Greek

Δ	adjustment in solution of equation of wet-bulb line
ΔD	shrinkage, % original depth
ϵ	porosity, ratio
θ	time
μ	dynamic viscosity, kg/m min
μ_n	roots of Bessel function
ρ	density
σ	standard deviation
σ_g	geometric standard deviation
σ^2	variance
ϕ	R_1/R_2

1. INTRODUCTION.

1. INTRODUCTION

The ryegrasses are the most important grass species in British farming. Perennial ryegrasses alone account for 45% of U.K. grass seed consumption and the ryegrass group accounts for over 72%.(101) In physical terms this represents an annual consumption of the perennial varieties of between 230 and 273 thousand cwt. Grass seed has no use other than for sowing. As a result demand is inelastic and yet yields and hence national production are notoriously variable. Growers are thus in a weak marketing position and have had to face large seasonal price fluctuations. These are illustrated by the plot of growers' prices for the variety S.23 for the years 1957-1971 in Figure 1.1.(33) This diagram also demonstrates that the general price level has not reflected the inflation of the last few years. This situation has been met by the increasing concentration of grass seed production into the hands of fewer and more specialist seed growers who have remained

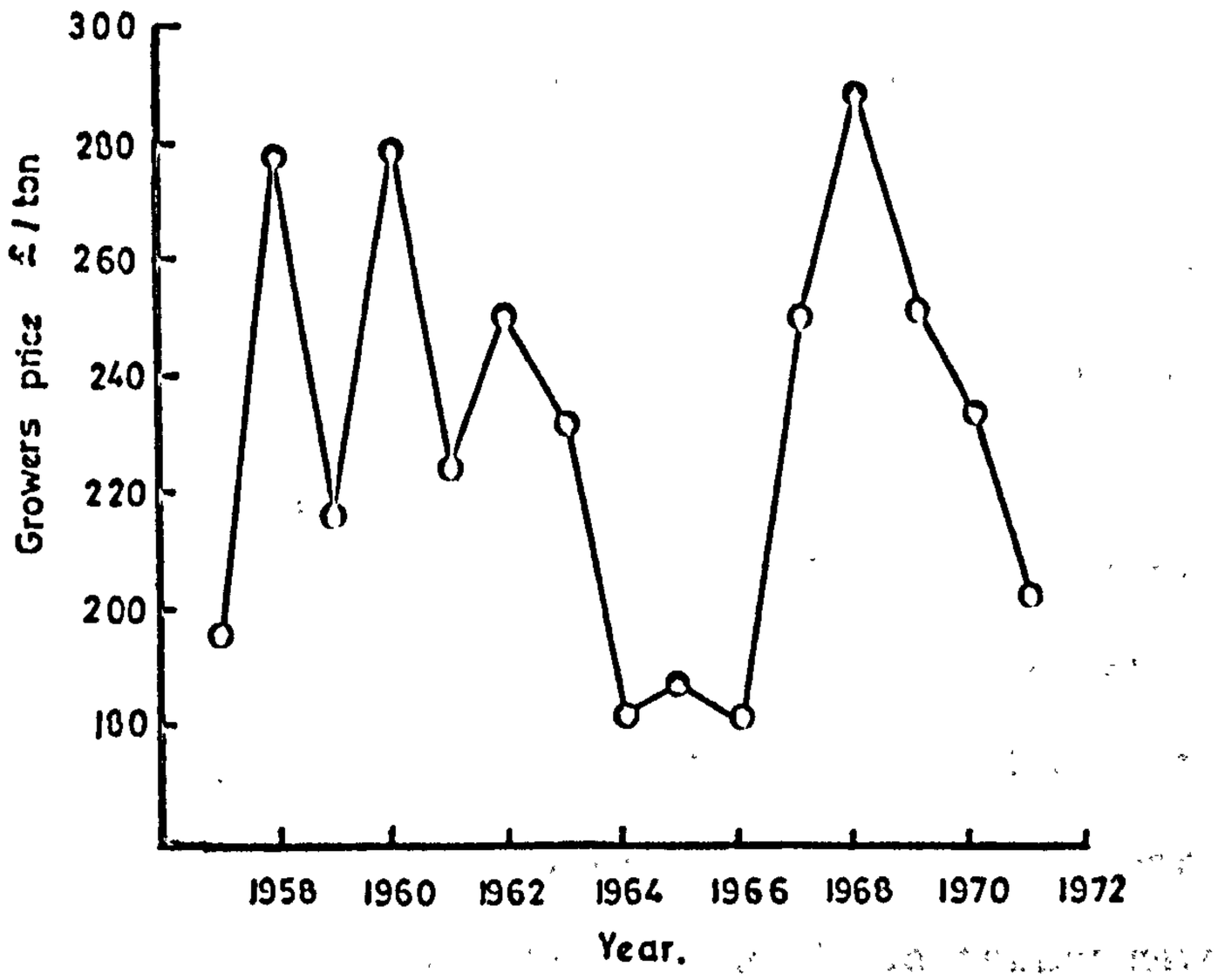

Fig. 1.1 Seasonal variation in grower's prices for S23 ryegrass seed.

in business by obtaining better or more consistent seed yields at reduced cost. The greatest cost reductions have resulted from the change in harvesting techniques, away from the traditional binder method, first to windrow harvesting and then to cutting and threshing direct by combine harvester.

This change in method has been more gradual than the equivalent change in the cereal harvest because it created greater problems. Grasses begin to shed seed at an early stage of ripening and it is necessary to thresh the crop before the seed is fully ripe if a reasonable yield is to be obtained. Thus the seed is normally harvested over a moisture range greater than that commonly encountered with cereal grains. It is possible, although not good practice, to thresh S.24 perennial ryegrass at moisture contents as high as 50% w.b. and still obtain seed of acceptable quality. A small proportion of the national ryegrass harvest may be harvested in this condition but the bulk is probably threshed in the range 35–25% w.b. Drying is, therefore, an essential component of the modern ryegrass harvesting system.

Most types of agricultural drier can be used to dry the seed although the on-floor method is the most popular. Continuous flow or batch-type driers have tended to decline in popularity for three main reasons.

(a) The seed does not flow easily particularly at high moisture content.

(b) It is difficult to match drier capacity with combine-harvester output and high-moisture seed will begin to heat even whilst still in the combine-harvester tank.

(c) There is some prejudice against the use of heated air because of the possibility of depression of viability. Previous work by the present author suggests that this prejudice may be unfounded for diploid ryegrass seeds[79]. Low temperature drying, particularly the on-floor type of installation, is popular because it does away with the handling problem, the seed need not be precleaned before drying and the intake capacity of the drier can vary with the output of the harvesters. In addition there is no danger of seed damage from heated air: there is, however, a hazard from moulding of wet seed if it is dried too slowly. The problem is that the conditions under which moulding may occur are those which would be the most economical. That is, where a complete drying zone remains within the drying bed for the greatest possible proportion of the total drying time. Most of the difficulty in striking the correct balance between seed depth and air velocity arises from the high initial moisture content of the seed which will be at, or close to, equilibrium with saturated air. In addition the situation is aggravated by the high and often uneven pressure resistance to airflow.

Previous work[79] had indicated that to determine optimum drying conditions by empirical experimentation alone was not feasible in time or cost. This applies to both high and low temperature drying, but more so to the low temperature drying because of the longer time scale and greater variability in inputs.

The objective of this present study was to attempt to specify such optimum conditions by developing a mathematical simulation of the drying process in deep layers of ryegrass seeds to enable the extrapolation of a limited number of experimental observations to a wide range of conditions. Particular attention was to be paid to low temperature drying and the use of biological changes as restraints within the model.

2. RYEGRASS SEED - RELEVANT PROPERTIES.

2. RYEGRASS SEED - RELEVANT PROPERTIES

2.1. SEED ANALYSIS

Almost all of the experimental work described in this thesis has involved the taking and analysis of seed samples for the determination of one or more of the following properties:-

Moisture content

Purity

1000 seed weight

Germination

Standard methods for their determination are prescribed by the International Seed Testing Association (I.S.T.A.)[55] and these methods have been followed with only minor modifications. The main features of the methods are:-

Moisture content

2 replicate, unground 5 g samples dried for 1 hour in a ventilated oven regulated at 130°C.

Purity

2 replicate 2.5g sub-samples were sorted by hand into pure seed, multiple florets and rubbish. Purity was defined as the percentage of pure seed. The purity analysis provides a useful check on the cleanliness of the samples but its main use was in providing pure seed for the 1000 seed weight and germination tests.

1000 seed weight

The pure seed fractions from the purity analysis were used to count out either 3 or 4 lots of 100 seeds each, which were weighed. The weights were multiplied by 10 and the mean taken. No prescription was made in the I.S.T.A. rules concerning correction for moisture content but B.S. 3986:1966[20] specifies a moisture content of 15% for wheat used in grain drier tests. Attempts to correct the

ryegrass 1000 seed weights to a common moisture content based on the values determined at the start of the purity analysis proved unrealistic because the seeds tended to equilibrate to between 10-12% whilst exposed to the laboratory atmosphere. Thus the 1000 seed weights quoted in this report refer to a moisture value of 10-12%.

Germination

The replicate 100s counted for the 1000 seed weight test were carried forward into this test. The 100 seeds were germinated on 90 mm diameter filter paper pads supplied with water through paper wicks dipping into continuously circulating water. The pads were soaked initially in a 0.2% solution of KNO_3 to assist the breaking of dormancy. Alternating temperatures of 17° and 22°C for both air and water were employed in a diurnal cycle of 16 hours dark and 8 hours light respectively. As an additional aid to breaking dormancy, the change in the water temperature from 22°C to 17°C was made rapidly. The number of seedlings germinating normally in 14 days was the germination percentage. An intermediate count was carried out at 7 days (5 days in the official test) and seedlings germinating by that time removed. In the experiment described in Section 3.3 the tests were extended up to 21 days.

2.2. EXPERIMENTAL MATERIAL

Two types of ryegrass were used in the experimental work. Aberystwyth S.23 is a diploid variety of Lolium perenne. A pasture variety with a prostrate growth habit it runs to seed late in the season and has very small seeds. Sabrina [103] and Sabel are both tetraploid hybrid crosses between Lolium perenne and Lolium multiflorum. The seeds are very large and ripen earlier in the season than S.23. They are new varieties which are only now being made available commercially and seed for this work was obtained by special arrangement with the Welsh Plant Breeding Station (WPBS).

2 acres each of S.23 and Sabrina were established at Silsoe in time for 1970 harvest. Sabrina was replaced by Sabel for the 1971 and 1972 harvests because it was found, both at Silsoe and at the WPBS[103], that Sabrina exhibited secondary and tertiary heading which confused the ripening picture.

The best guide to the harvesting of ryegrass seeds is moisture content. In the case of S.23 it was known from previous studies [77] that satisfactory germination could be obtained from seed harvested at moisture contents as high as 50% but that better quality and seed weight could be obtained without excessive loss through shedding if harvesting was delayed until moisture content was reduced below 35% w.b. The ripening characteristics of the tetraploid hybrids were unknown and hence the routine sampling of these crops during the maturation period took on a special significance.

2.2.1. Ripening studies

At appropriate intervals during the ripening phase crop samples were either cut by hand shears and threshed on a ststionary threshing rig or cut and threshed direct by combine-harvester. For both machines a threshing drum peripheral speed of 25.4 m/s (5000 ft/min) and 9.5 mm ($\frac{3}{8}$ in) was used, not only to thresh these control samples but for the threshing of all the seed used in the experimental work. Immediately after threshing the control samples were sub-sampled for moisture content determination and the remainder dried with ambient air on a multi-hole sample drier. When dry ($\simeq$13% w.b.) they were stored in sealed tins at 50°F (10°C) for from 2 to 4 months until they could be analysed for purity, 1000 seed weight and germination. In 1972, on each of 4 harvest dates of the tetraploid Sabel, some additional crop was cut but not threshed until it had been allowed to dry naturally for several days in an unheated store; this was to simulate an indirect harvesting method e.g. swath harvesting.

The results of these tests are plotted in Figs. 21-24 and the data given in Appendix 2.

2.2.1.(a) Sabrina (1970) and Sabel (1971/2)

Fig.2.1 is of interest because it indicates the period over which the crop may be harvested and shows how much the properties measured fluctuate from one date to the next, mainly as a result of sampling error. In the single year that Sabrina was grown it ripened earlier than did the Sabel in the following two years, but the ripening of the Sabrina was also confused by the development of unripe-seed in late formed tillers. These gave an upward twist to the moisture content curve and as the phenomenon appeared to be characteristic of the variety (103), led to its replacement with Sabel in the following two years. The differences between Sabrina and Sabel disappear if the

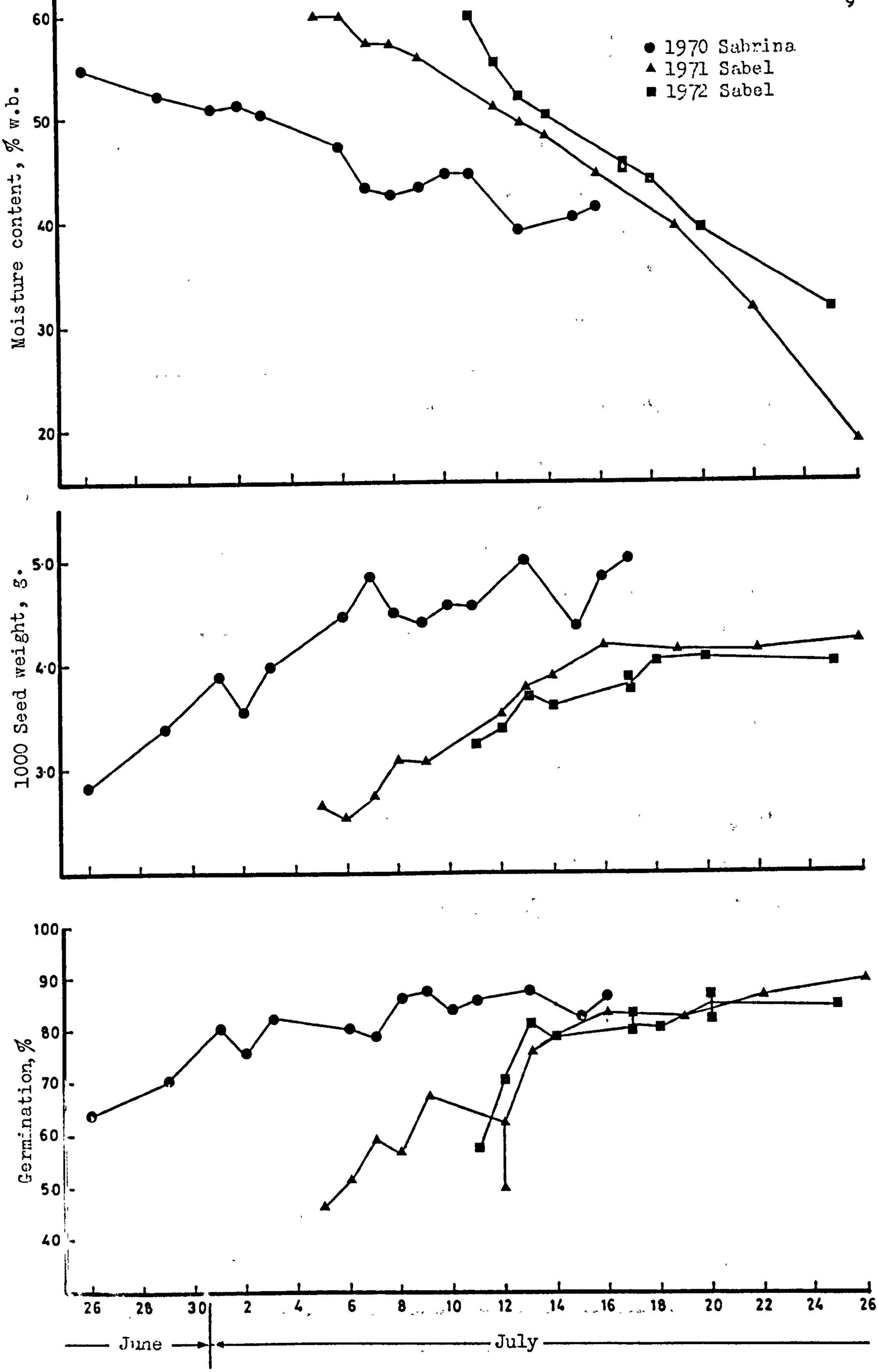

Fig.2.1. Moisture content (top), 1000 seed weight (centre) and germination (bottom) plotted against harvest date for Sabrina and Sabel

germinations of the control samples are plotted against the moisture content. In Fig.2.2 (top) the moisture content scale is in wet basis since this is the one commonly used in correlating biological properties. However it was found that the data were more highly correlated with the dry basis moisture content and the equation of the curve plotted in Fig.2.2 (top) is

$$G = 94.9 - 3.336 \exp (C.0173.Md) \quad \ldots\ldots\ldots\ldots \quad 2.1$$

$$\text{or} \quad G = 94.9 - 3.336 \exp (1.73.Mw/(10C-Mw) \quad \ldots\ldots\ldots\ldots \quad 2.2$$

As would be expected, the increase in germination as moisture content falls is reflected by an increase in 1000 seed weight and this relationship is plotted in Fig.2.2.(bottom). The direct correlation between these two factors is quite small if the moisture content effect is eliminated and inclusion of 1000 seed weight as a separate factor in equation 2.1 would not have been justified.

Equation 2.1 predicts that 90% germination, the normal commercial minimum requirement, is not reached until 18% w.b. (22% d.b.). Roberts [103] has shown that Sabrina is capable of yielding 90% germination at 52% w.b. if threshed gently by hand rubbing but is severely damaged if threshed in a laboratory mill. He concluded that the tetraploid is extremely sensitive to damage and since seed shedding begins at about 45%, recommends that the variety should be swath-harvested. The seeds in the present work were by no means as severely damaged as the mill threshed samples of Roberts but nevertheless the data of Fig.2.2. (top) support the conclusion that direct threshing may not be suitable. Table 2.1 compares the results of direct and indirect threshing of material from four dates for Sabel in 1972. It confirms that seed cut at a moisture content as high as 55.4% will continue to ripen on the cut stalks. The germinations of these indirect

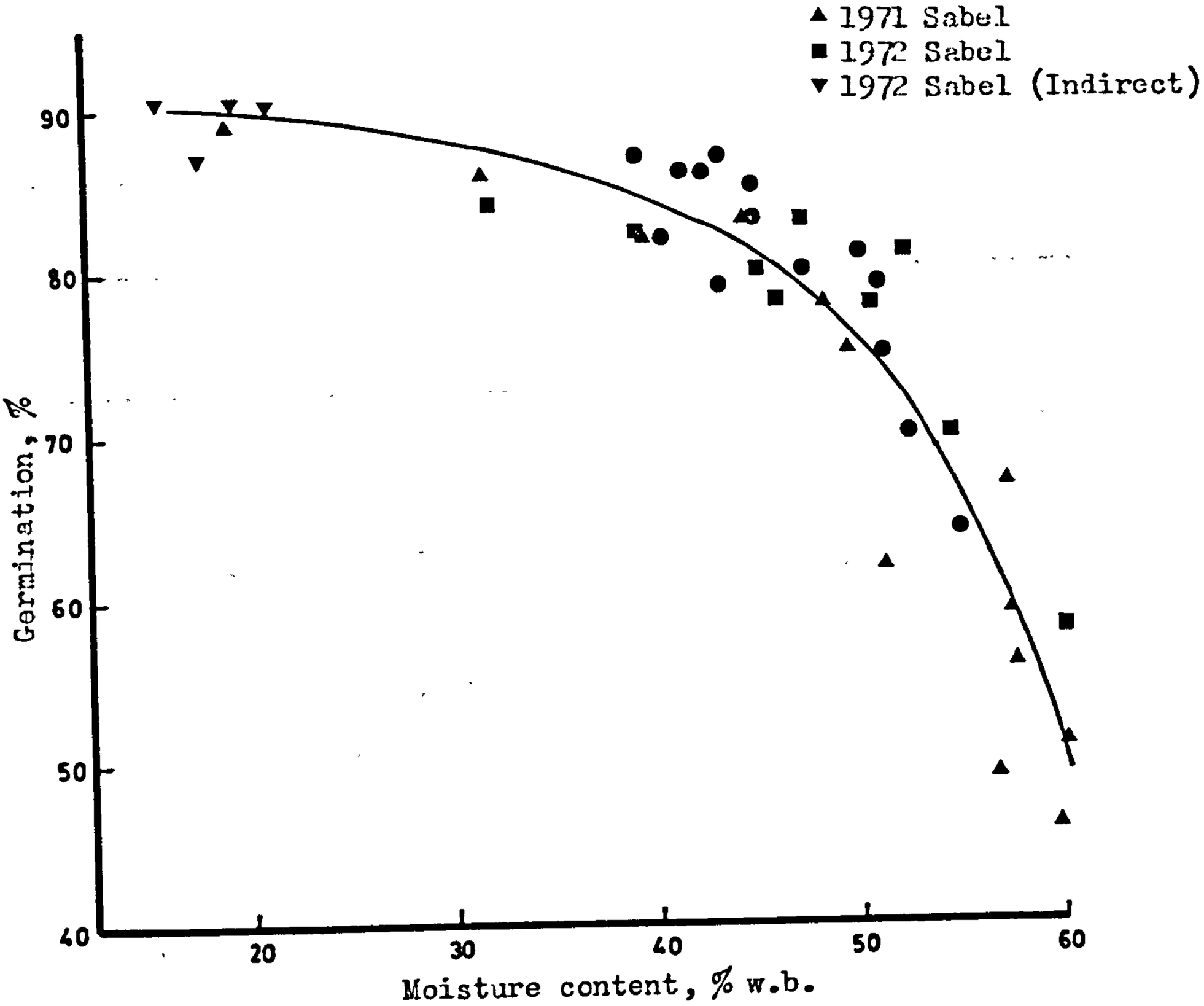

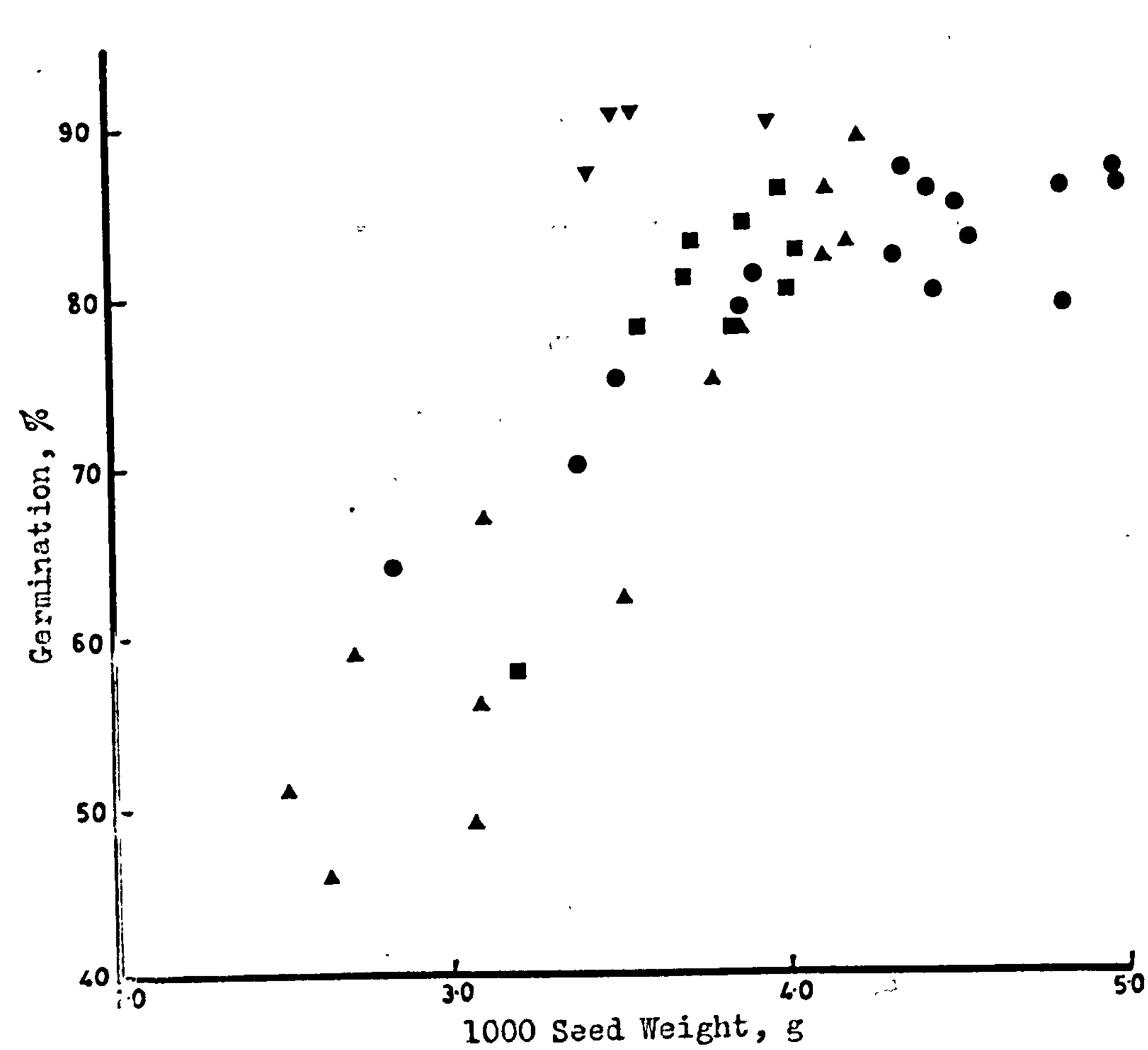

Fig.2.2. Germination of Sabrina and Sabel as a function of moisture content (top) and 1000 seed weight (bottom)

Table 2.1

Comparison of direct and indirect threshed samples of Sabel, 1972

Date of cutting, July	Moisture content threshing, % w.b.		1000 seed weight g.		Germination %	
	Direct	Indirect	Direct	Indirect	Direct	Indirect
12	55.4	18.0	3.39	3.43	70	87
13	52.1	19.7	3.72	3.53	81	90
14	50.5	15.8	3.59	3.58	78	90
17	45.6	21.7	3.81	3.99	81	9(

harvest samples are also plotted in Fig.2.2 (top) and fit neatly onto the line predicted by equation 2.1 although not used in its derivation.

2.2.1 (b) S.23

The 3 years harvests of S.23 are plotted in Fig.2.3. In all 3 years the trends of moisture content and germination were similar but the 1000 seed weights of the seed obtained in the first year were higher than those obtained in the two subsequent years. This may be a reflection of the husbandry of the crop e.g. diminished soil fertility or increased plant population in the 2nd and 3rd years. Since it did not affect the germination/moisture content pattern the difference is not serious. This relationship is plotted in Fig.2.4 (top) together with a fitted curve defined by equation 2.3.

$$G = 96.0 - 0.1588 \exp (C.0445.Mc) \quad \ldots\ldots\ldots\ldots\ldots 2.3.$$

or $$G = 96.0 - 0.1588 \exp (4.45Mw/(100-Mw) \quad \ldots\ldots\ldots\ldots 2.4.$$

This equation predicts the attainment of 90% germination at 45% w.b. (82% d.b.) and clearly confirms the feasibility of direct harvesting already established in current practice [76,77].

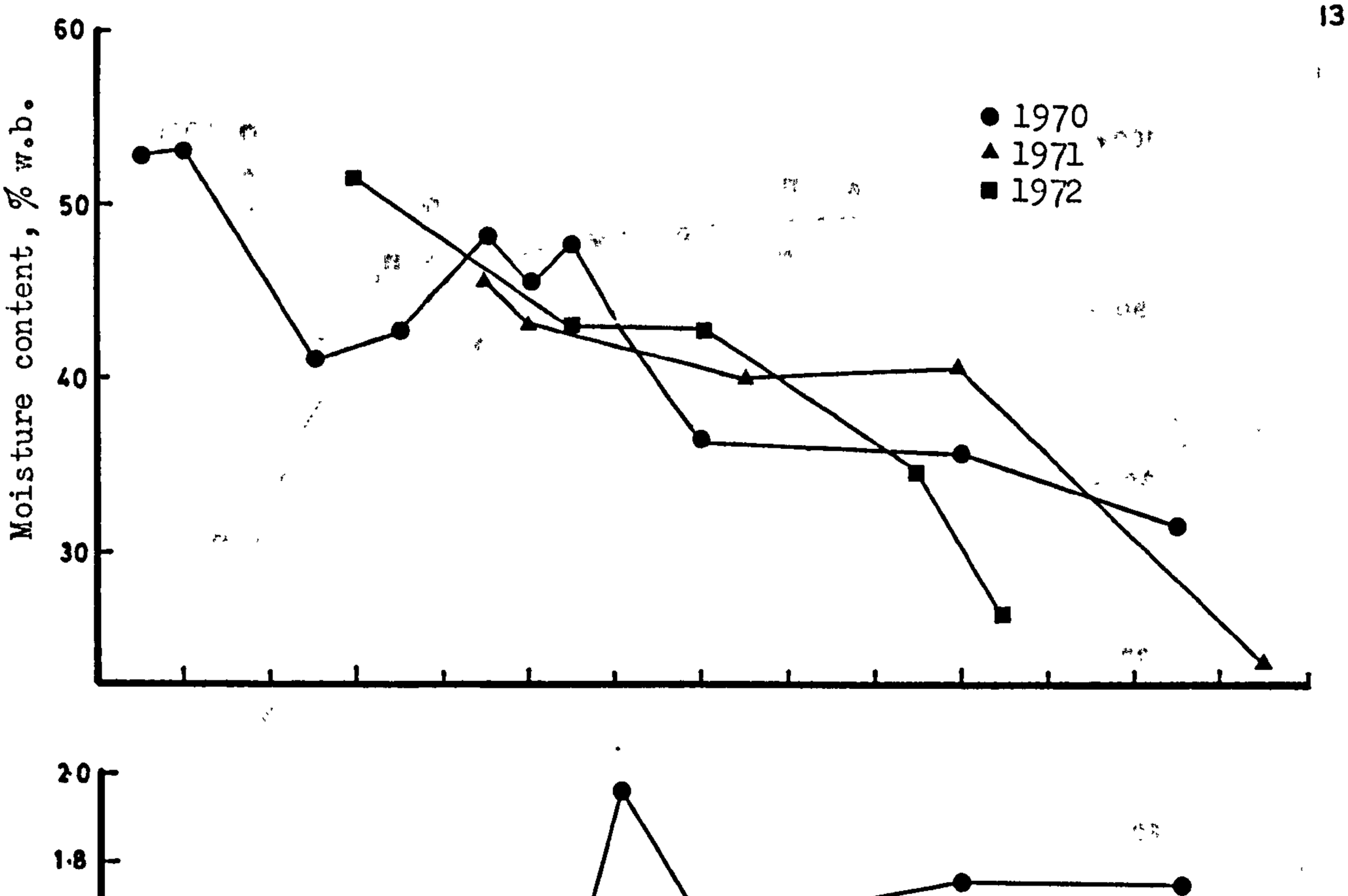

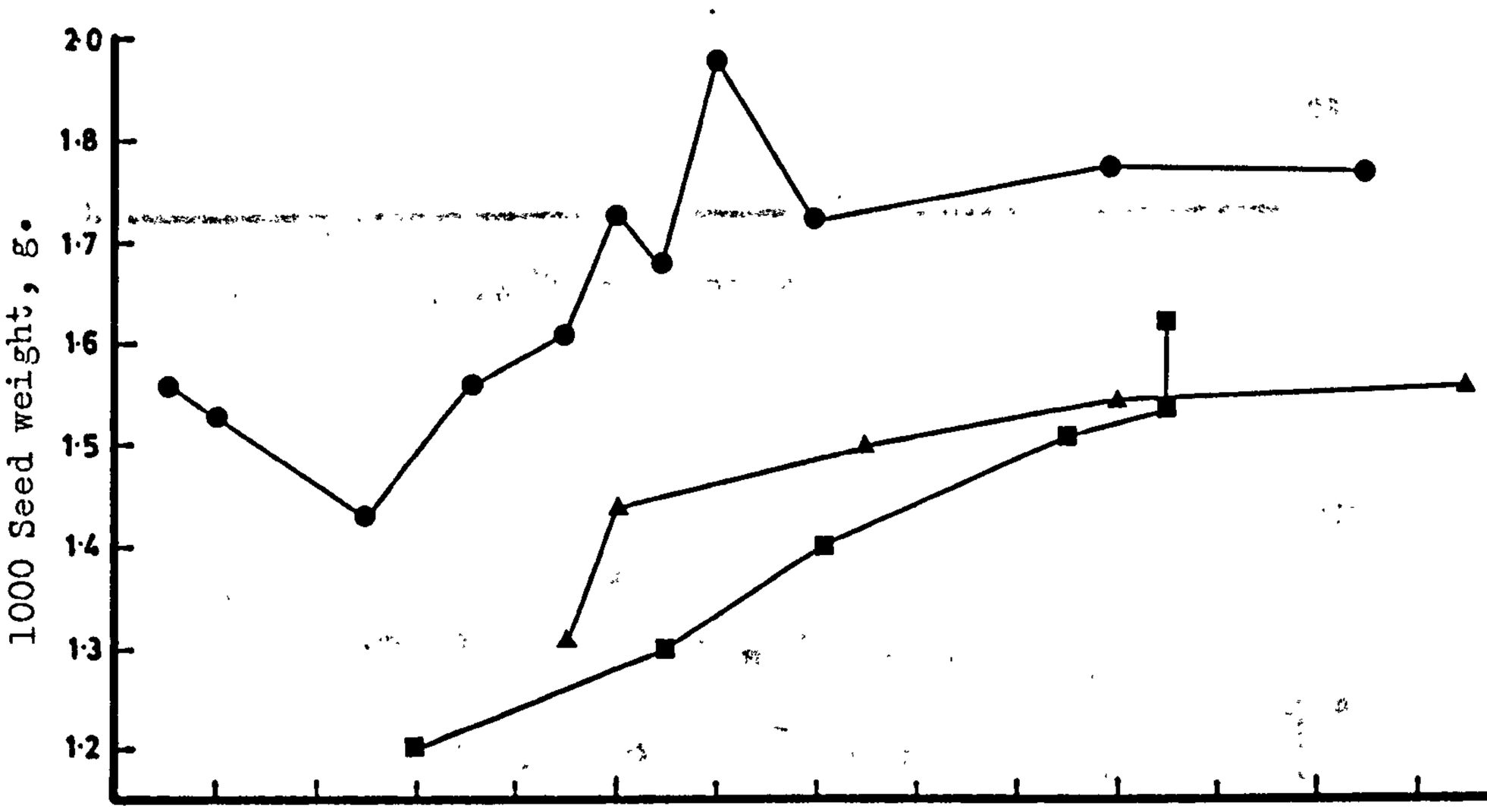

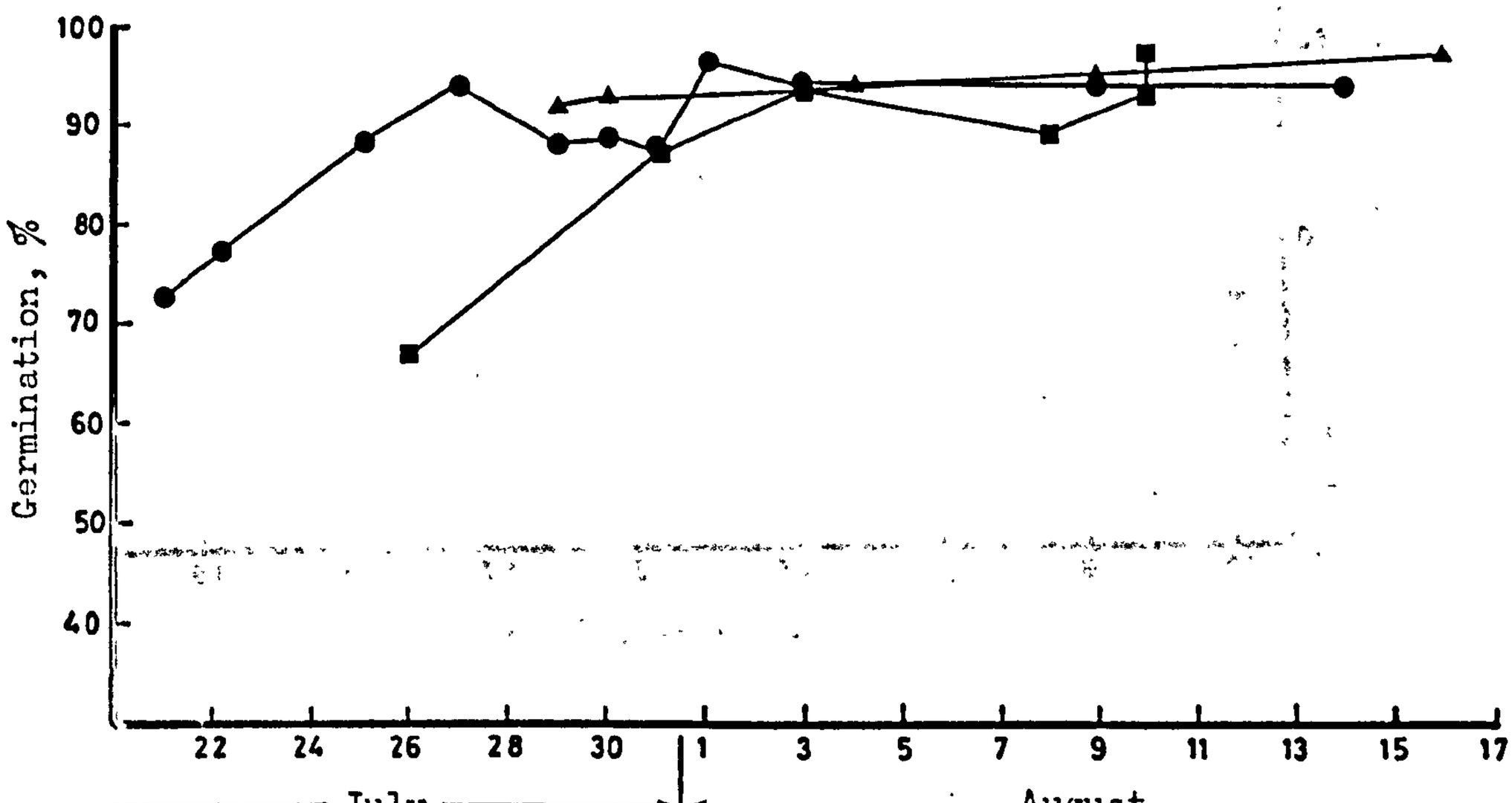

Fig.2.3. Moisture content (top), 1000 seed weight (centre) and germination (bottom) plotted against harvest date for S23

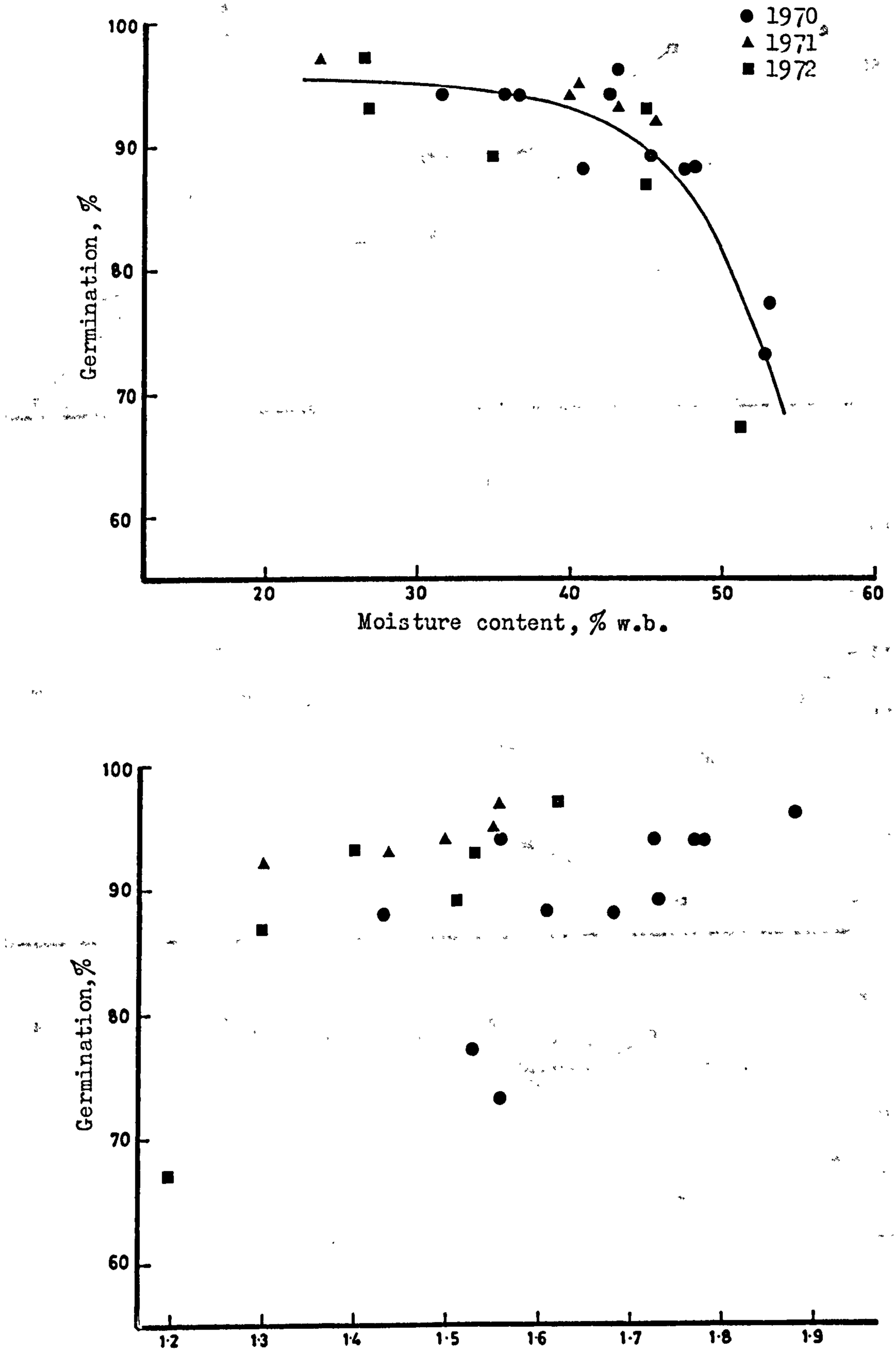

Fig.2.4. Germination of S23 as a function of moisture content (top) and 1000 seed weight (bottom)

2.2.2. Anatomy

The simplest theory describing the drying of seeds assumes that they can be regarded as capsules of water enclosed by a pervious membrane; other more complex, but more realistic, models take into account the internal resistance to moisture diffusion [96] but whilst still regarding the seeds as homogeneous particles. Recently attempts have been made to write equations of drying in which the seed can be regarded as concentric layers of varying materials.[138] Clearly in this context the anatomy of the seeds becomes important.

The anatomy of a ryegrass seed is similar to that of a cereal grain. The grain or kernel develops within a pair of bracts or leaves called the lemma and palea and although these do not become fused to the grain as they do in barley, they are firmly attached and are not readily removed at threshing as they are in wheat or rye. Naked seeds are normally regarded as an indication of over-severe threshing. The complete seed is shaped like a long boat (Fig.25) but when viewed against a powerful light can be seen to be much longer than the kernel which only occupies the bottom half of it. This feature is visible in the longitudinal section through a Sabrina seed shown in Fig.2.6. In cross-section, Fig.2.7, the pales are folded around the seed and upwards to form two longitudinal ribs.

The internal structure of the kernel is summarised by Fig.2.8. The endosperm and the embryo are surrounded by a dark thin layer which is difficult to differentiate into pericarp, testa and hyaline layers but beneath this layer the large cells of the aleurone layer surrounding and forming part of the endosperm are clearly visible.

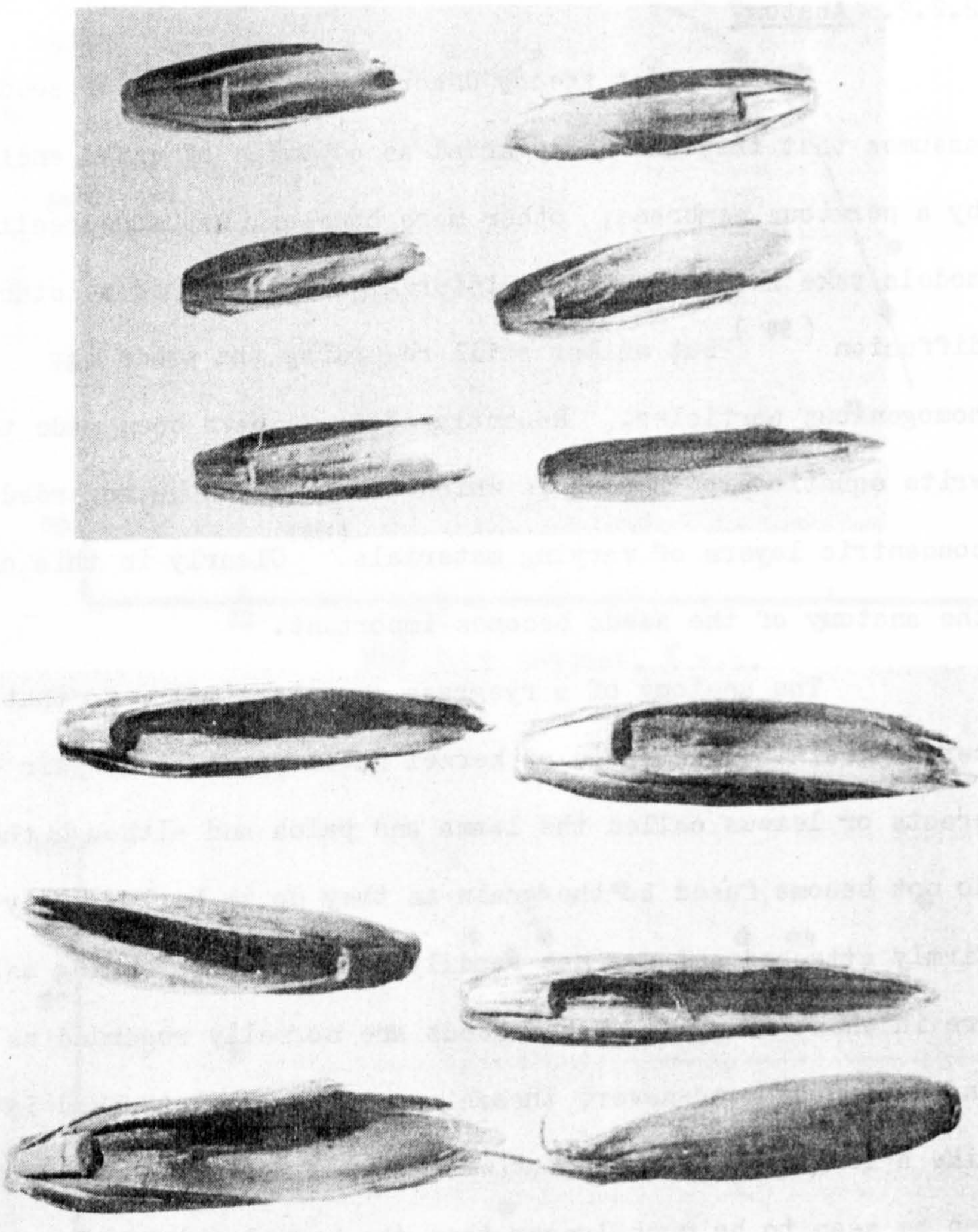

Fig. 2.5. Typical seeds of S.23 (top) and Sabrina (bottom) X 7

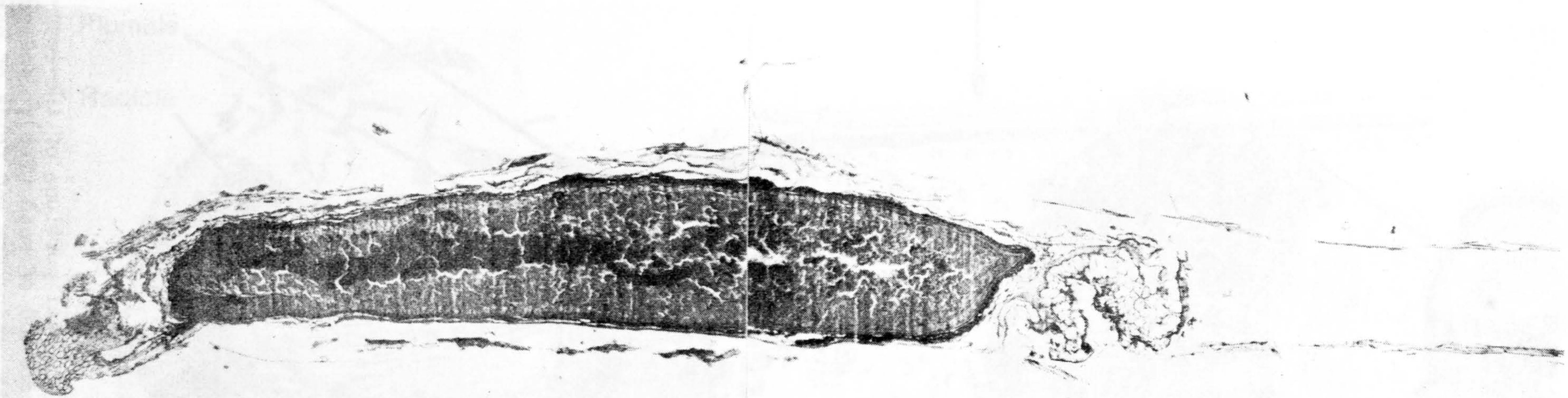

Fig.2.6 Longitudinal section through a Sabrina seed showing pales enclosing the endosperm. Embryo not visible. (x 40)

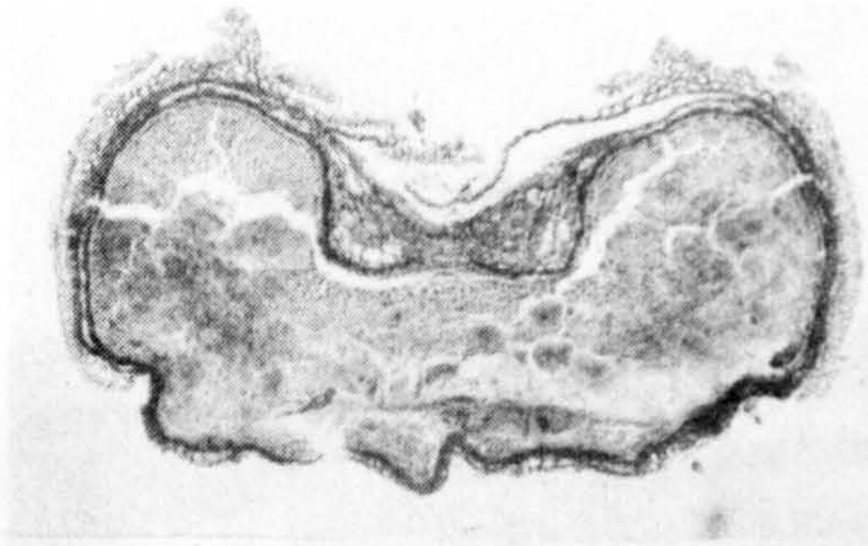

(x47)

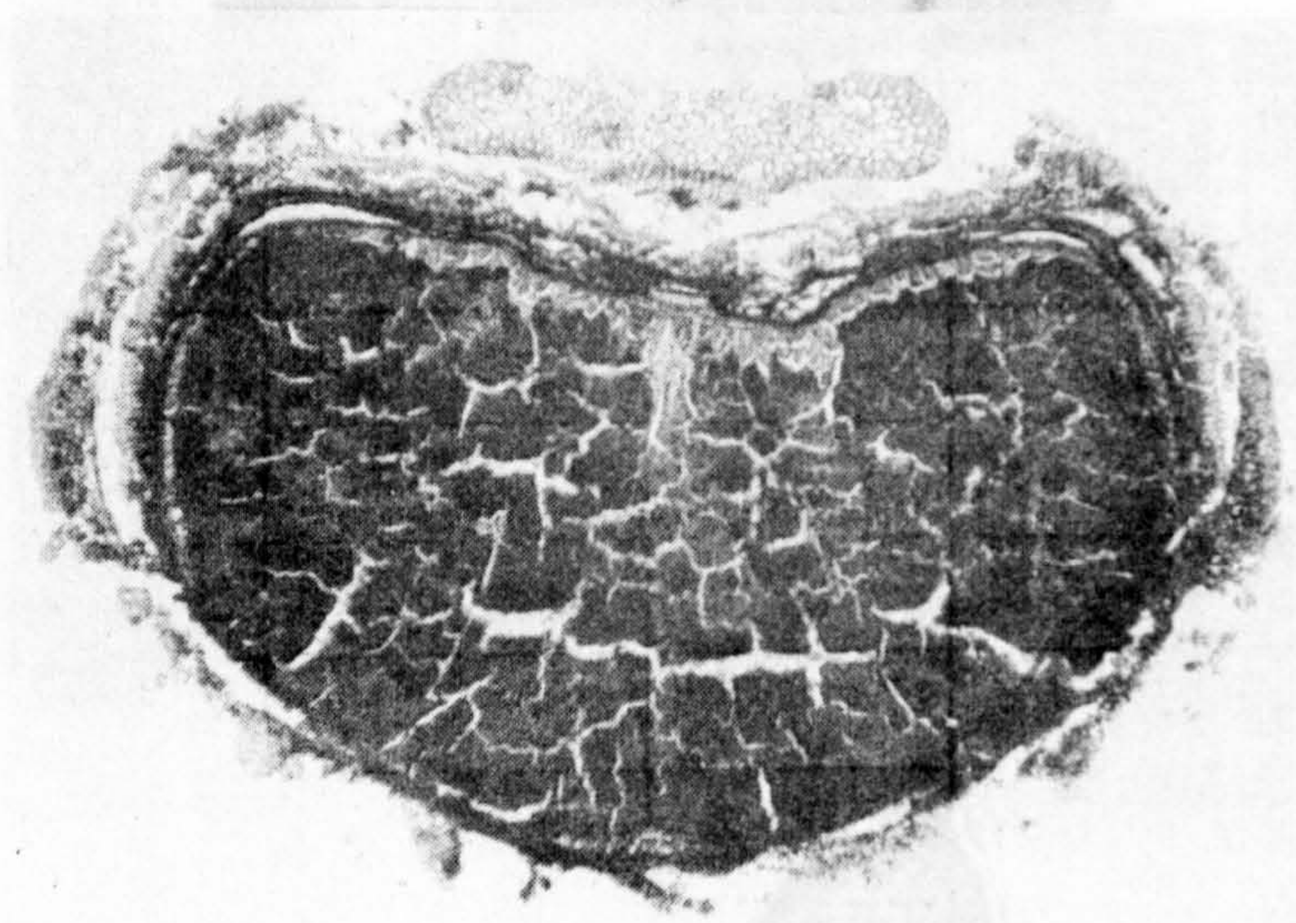

(x47)

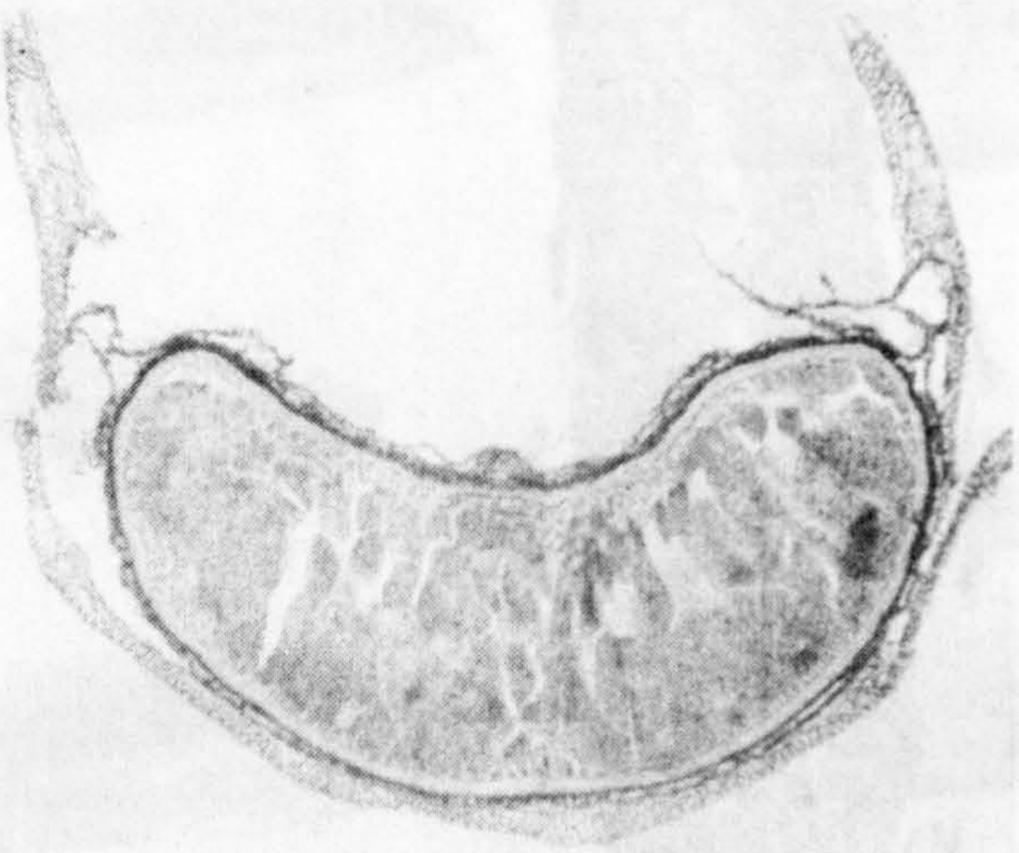

(x47)

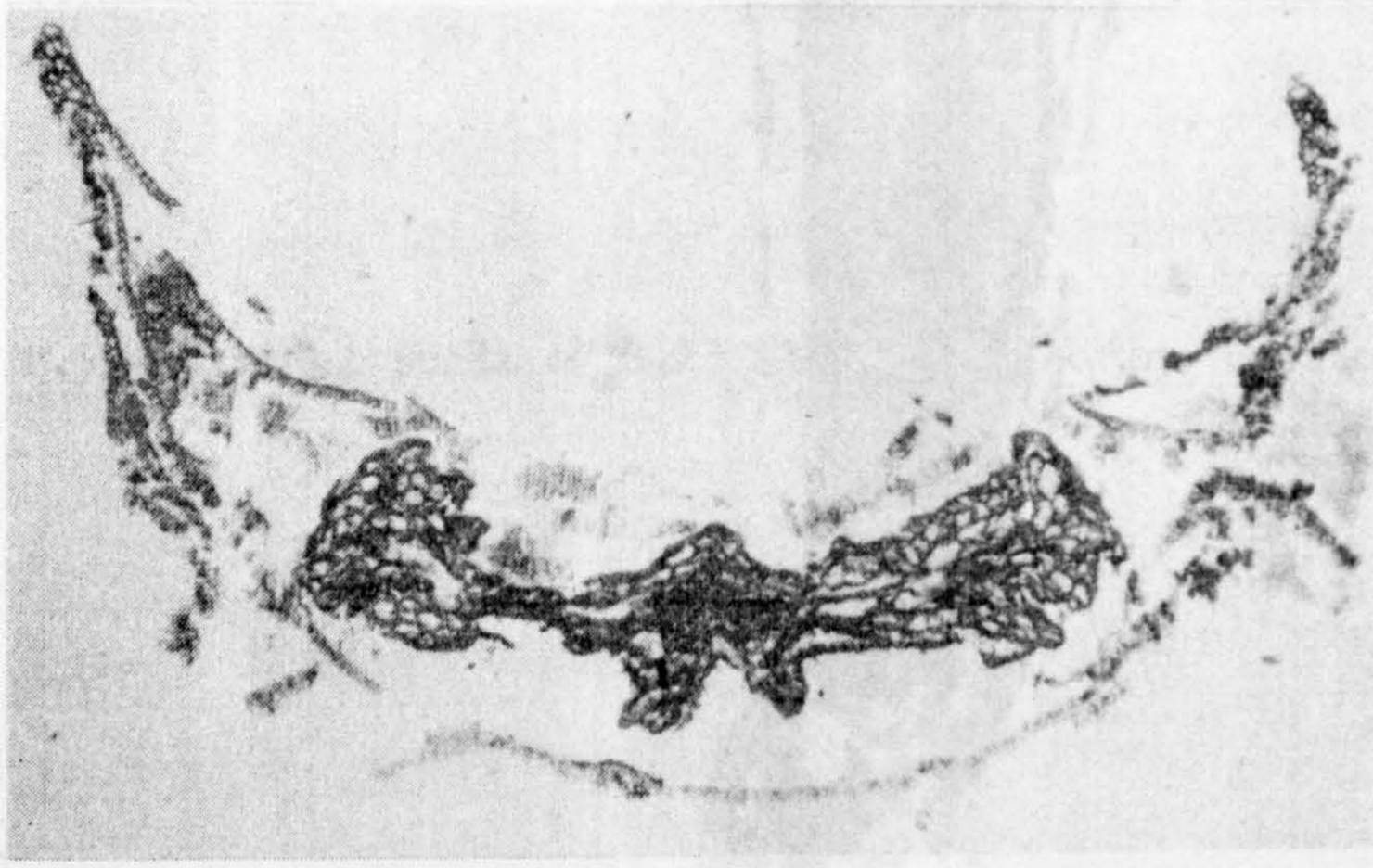

(x49)

Fig. 2.7 Transverse sections through typical portions of the seed of Sabrina. Embryo and endosperm, at blunt end of seed (Top); endosperm and rachis at the broadest point; endosperm and folds of pales near the apex of the kernel; pericarp and pales beyond kernel (Bottom).

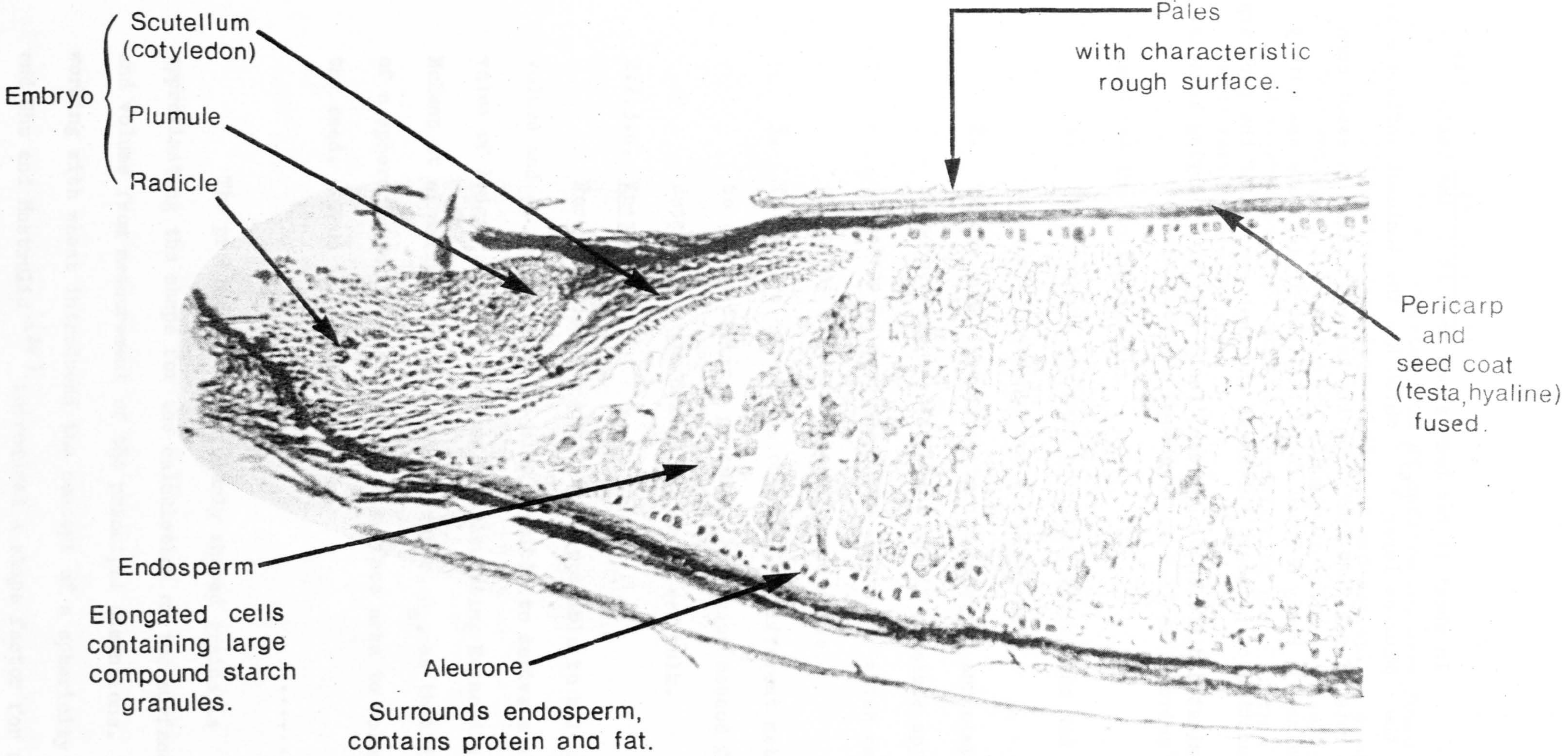

Fig. 2·8 Internal structure of the ryegrass seed kernel (x120)

In wheat it has been shown that it is the testa [48] not the aleurone layer [67] which has the dominant influence on the rate of moisture loss from the kernel. Also in sweet corn (Zea mays), Purdy & Crane [98] found that the drying rate was mainly a function of pericarp thickness and that removal of the pericarp eliminated differences between 'fast' and 'slow' drying kernels.

2.2.3. Size and weight

It was expected that if differences were found between the drying characteristics of diploid and tetraploid seeds then they would be, in large part, a function of differences in size and weight and might also be a function of shape if this property also varied between them.

A comparison was made between S.23 and Sabrina seeds and had the following aims.

1. To determine the mean principal dimensions and weights and their distributions about the mean.
2. To use such dimensions to characterise and compare shape between the varieties and if possible approximate the shape to some geometric figure for which calculation of volume and surface area is possible.
3. To compare dimensions obtained by different methods and to choose the most practical effective method for determining the dimensions in a seed bulk.

2.2.3.a. Theory

For particles for which it is possible to calculate volume and surface area it is also possible to derive a single value of length suitable for use in calculating Reynold's number. McEwen et al (68) define the spherical diamater, d_m, as that diameter of a sphere having the same ratio of surface area to volume as the seed. Thus in its simplest form

$$d_m = \frac{6 \cdot V_p}{S_p} \qquad \ldots\ldots\ldots 2.5$$

The problem with irregularly shaped grains is approximating the shape for the calculation of the surface area and volume from measurement of the principal dimensions. Becker (13) working with wheat introduced the concept of a sphericity factor and Chu and Hustrulid (26) introduced a shape factor for maize.

For correlating heat transfer data for spheres and cylinders, Gamson, Thodos and Hougen [36] used an effective diameter for the cylinders corresponding to a sphere having the same surface area as the cylinder.

$$d_s = \sqrt{d_c . l_c + \frac{d_c^2}{2}} \qquad \ldots\ldots\ldots 2.6$$

where d_c = diameter of the cylinder,

and l_c = length.

A similar approach was taken with wheat by Pabis and Henderson [94] who used the geometric average of the 3 principal dimensions as being the diameter of an equivalent sphere. Pabis [96] later defined the effective diameter, d_e, as

$$d_e = \sqrt[3]{\frac{6 . W_{1000}}{1000\ \rho\ \pi}} \qquad \ldots\ldots\ldots 2.7$$

where ρ = density of seed and W_{1000} = 1000 seed weight. Since 1000 seed weight is an easily measured property this is clearly an attractive method.

For more irregularly shaped particles than the large cereal grains, various 'diameters' can be obtained from the frequency distributions of dimensions obtained by various methods. [22]

That of sieving is the one most applicable to particles of the size of grass seeds. Particulate materials are generally found to follow the log-normal distribution and the geometric mean, d_g and standard deviations are normally reported. The geometric mean is given by the equation

$$\ln d_g = \frac{1}{n} \sum_{i=1}^{h} (f_i . \ln d_i) \qquad \ldots\ldots\ldots 2.8$$

where f_i = frequency within each class d_i

h = number of classes

and $n = \sum (f_i \ldots\ldots f_n)$ = 100 when f_i is in percentage form.

The standard deviation of the geometric mean is then given by

$$\ln \sigma_g = \sqrt{\frac{1}{n} \sum_{i=1}^{h} \left[f_i (\ln d_i - \ln d_g)^2 \right]} \qquad \ldots\ldots\ldots 2.9$$

Other diameters are defined and are more suitable for some purposes. For surface-area determinations, the volume-surface mean particle size is appropriate and is defined as follows

$$d_{vs} = \frac{\Sigma f_i d_i^3}{\Sigma f_i d_i^2} \qquad \ldots\ldots\ldots 2.10$$

It is the diameter of a sphere of equivalent volume to surface ratio and is analogous to the spherical diameter, d_m, defined by M'Ewen et al.[68] If the specific surface area, S_v, is defined as the surface area per unit volume then

$$S_v = \frac{6}{d_{vs}} \qquad \ldots\ldots\ldots 2.11$$

For particles other than spheres or cubes, the proportionality factor is not 6 but this factor is usually considered to be sufficiently close to the correct value to give a reasonable estimate of the area.

2.2.3.b. Experimental. (i) Measurements on individual grains

Surplus seed from the original bulk used to sow the S.23 and Sabrina crops and seed from the subsequent harvest in 1970 was used to provide 2 samples of each variety. Each bulk was divided down to a quantity just sufficient to provide 10 replicate samples of 100 seeds each. These were weighed to 0.001 g to provide an estimate of 1000 seed weight.

Then from each separate 100, 10 seeds were taken at random and measured for length and width by means of a projection microscope of 10x magnification, and for thickness by means of micrometer. The measurements were reported to 0.01 mm.

The experiment was thus a 2 x 2 design in which each treatment combination was split into 10 sub-samples and for the

measurement of dimensions, the sub-samples were further split into 10. It was set up in this form to examine the variation in dimensions within the samples rather than to examine differences between them. Such a comparison could not have been carried out without a larger number of samples of independent origin of both varieties.

(ii) Sieve analysis

For each variety x year combination, four 50g samples were sieved by means of a Pascall Sieve Shaker using a shaking time of 5 minutes. The sieves used in mesh numbers and equivalent metric hole sizes are listed in Table 2.2 .

Table 2.2

Sieve sizes

B.S. Mesh size	Aperture size - microns	Class boundaries	Class mark (di)
7	2.400	3.000-2.400	2.700
10	1.680	2.400-1.680	2.040
12	1.405	1.680-1.405	1.5425
14	1.200	1.405-1.200	1.3025
16	1.003	1.200-1.003	1.1015
18	0.853	1.003-0.853	0.928
22	0.699	0.853-0.699	0.776
25	0.599	0.699-0.599	0.649
30	0.500	0.599-0.500	0.5495

It was found that for each variety, the bulk of the seed was contained in 3 oversize fractions. These were mesh sizes 14, 16, 18 for S.23 and 10, 12, and 14 for Sabrina. From each of these major fractions, 4 replicates of 100 seeds each were counted and weighed, as before, to 0.001 g.

2.2.3.c. Results

Although there were differences between the mean results obtained from the two samples of each variety, these were small compared to those between varieties and only the means for the varieties are differentiated in the text. Full details of all the results are contained in Appendix 2.

The results of the measurements on individual grains are summarised by Table 2.3 in which each value is the mean of 200 observations. The range of each dimension within each variety is indicated by the standard deviations and where appropriate the relative magnitude of Sabrina relative to S.23 is indicated.

Table 2.3

Mean dimensions, 1000 seed weight and some derived parameters of size and shape

Property	S.23 ± S.D.	Sabrina ± S.D.	Relative Magnitude	Mean
1000 seed weight, g	1.744	4.124	2.365	
Length, mm	5.3 ± 0.72	7.0 ± 0.76	1.32	
Width, mm	1.21 ± 0.15	1.59 ± 0.19	1.31	
Thickness, mm	0.78 ± 0.11	1.09 ± 0.17	1.40	
Length/Width	4.41 ± 0.59	4.43 ± 0.46		4.42
Length/thickness	6.8 ± 1.17	6.50 ± 1.05		6.68
Width/thickness	1.57 ± 0.26	1.47 ± 0.12		1.52
$\sqrt[3]{\text{Length x width x thickness}}$	1.71 ± 0.17	2.30 ± 0.24	1.34	
d_e (equation 2.7)	1.36	1.81	1.33	

The mean 1000 seed weight of Sabrina, 4.124 g, is 2.365 times that of S.23, 1.744 g, and this is reflected in the larger dimensions. Since the relative increases in all 3 dimensions are of a similar order, it may be assumed that the shape of both varieties is the same and this conclusion is further borne out by comparison of the

shape factors. In general the seeds are 4.42 times as long as they are wide and 6.68 times longer than they are thick, and the distribution of each variety about its mean values is very similar.

The cube root of the relative magnitude of the 1000 seed weights is 1.33 which is of similar order to the increases in both individual dimensions and their geometric mean which indicates that the two varieties also have similar density. In calculating the effective diameters, d_e, by equation 2.7 a density of 1.32 g/cm has been assumed.(62)

Although there are consistent differences in mean size and weight between varieties, the size distribution within each variety is quite wide so that there is considerable overlap between them. For example, the 95% confidence limits on length are 3.89 - 6.71 mm for S.23 and 5.51 - 8.49 mm for Sabrina and a similar overlap occurs between the other dimensions. This would also suggest a wider range in seed weight than is indicated by the standard deviation of the 1000 seed weight measurements, which, being based on random selections of 100 seeds, do not (and should not) reflect the variation in size between individual seeds. The sieving procedure deliberately separated the seed into size fractions and the 1000 seed weights of these fractions (Table 2.4) exhibit the variations that the variation in seed dimensions would lead one to expect.

Table 2.4

Mean 1000 seed weights, g in major size fractions
Bracketed values = % by weight in each class

B.S. Mesh size	Class boundary microns	S23		Bb1237	
		1969	1970	1969	1970
10	2.400-1.680	-	-	6.19 (17.8)	5.66 (4.96)
12	1.680-1.405	-	-	4.74 (52.1)	4.94 (54.6)
14	1.405-1.200	2.24 (41.1)	2.31 (21.9)	3.3 (28.5)	3.27 (33.4)
16	1.200-1.003	1.66 (39.0)	1.81 (50.3)	-	1.93 (5.0)
18	1.003-0.853	1.16 (15.3)	1.29 (20.9)	-	-

The geometric and volume-surface mean diameters derived from the sieving results by equations 2.8, 2.10 are presented in Table 2.5 . As would be expected from the nature of the sieving process the geometric mean diameter is of the same order as the seed width and the volume-surface diameters are in even closer agreement with the width. Once again the magnitude of increase in size from S.23 to Sabrina is $1\frac{1}{3}$.

Table 2.5

Diameters derived from sieving results

Diameter, mm	S.23	Sabrina	Relative magnitude
Geometric mean	1.118	1.479	1.32
Volume-surface mean	1.181	1.584	1.34

To illustrate these results, in Fig. 2.9 the average dimensions have been used to draw to scale, plan and cross sectional views of the seeds based on the shape given by the photographs and sections. The derived diameters are represented by a series of concentric half circles beneath the shape drawings.

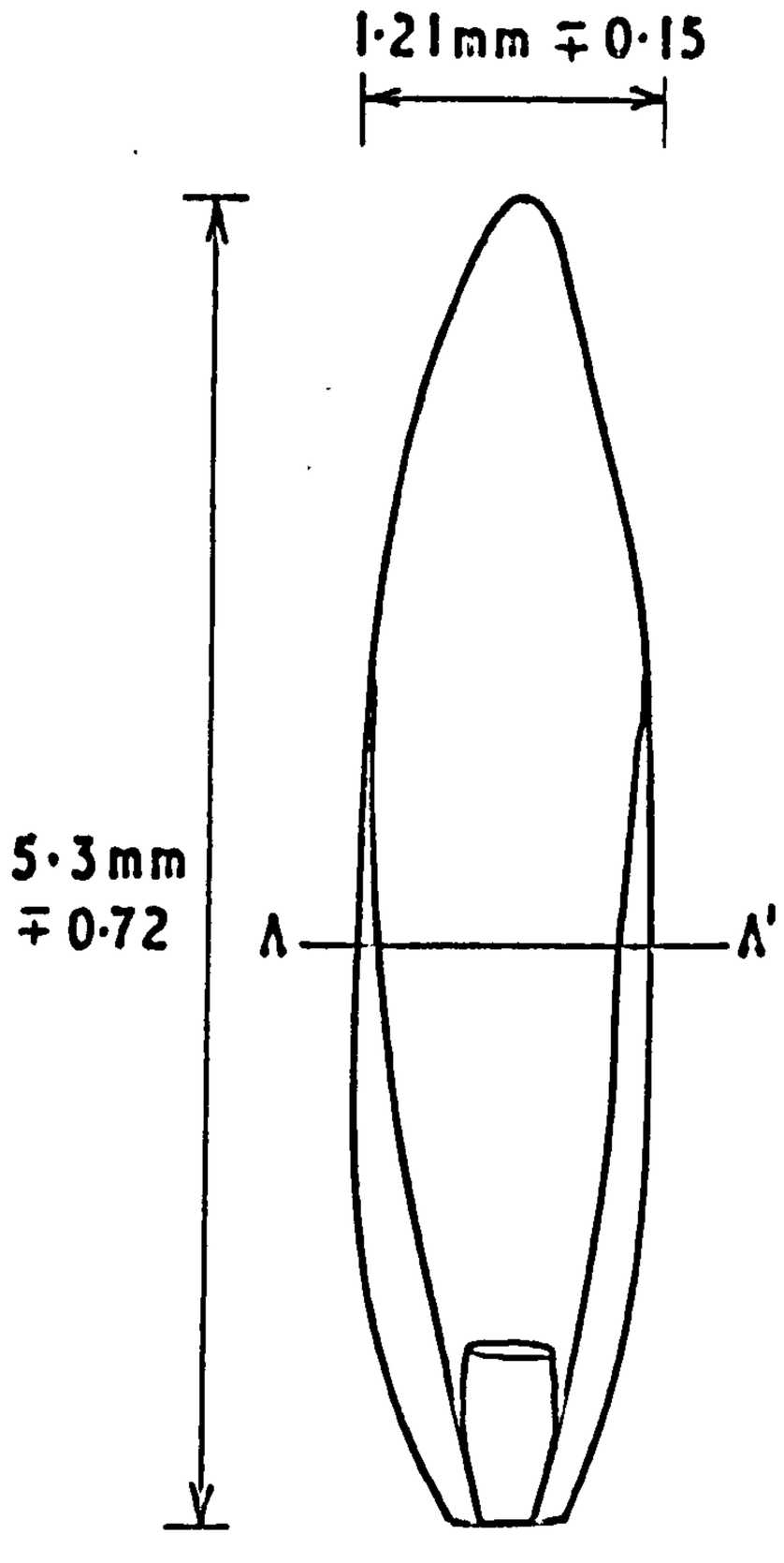

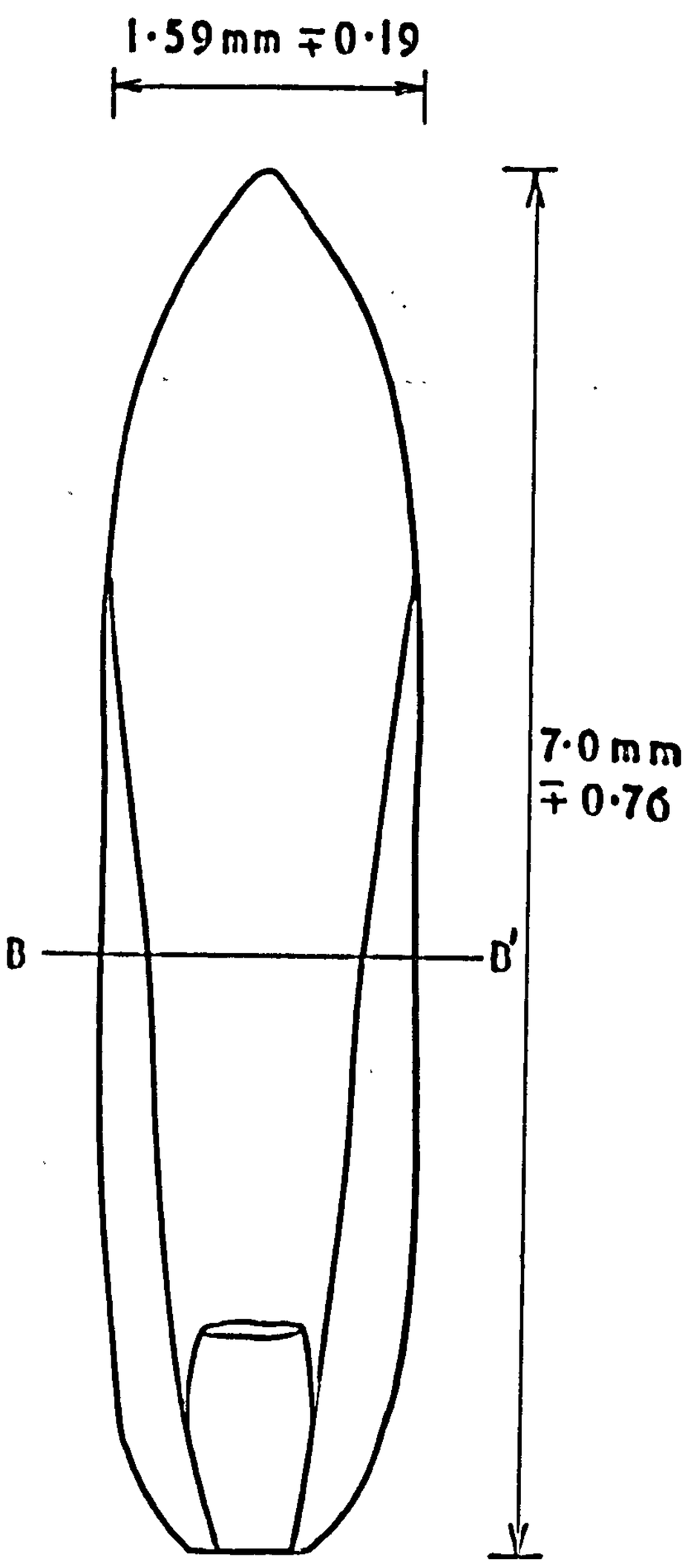

Sections

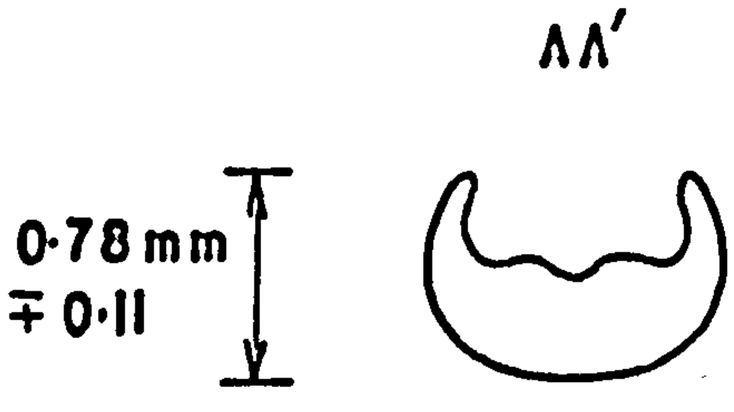

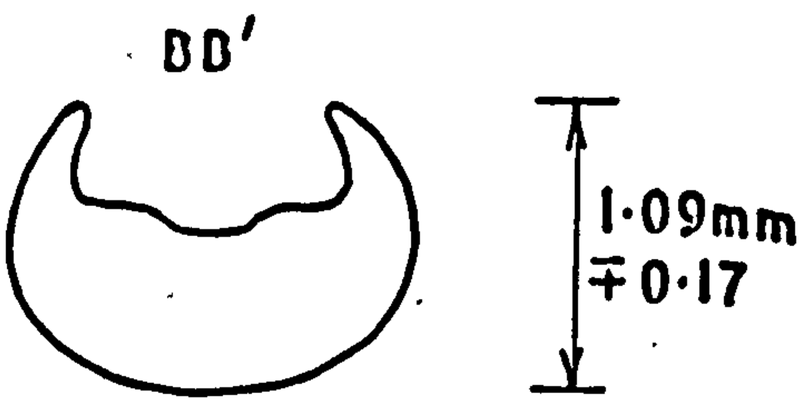

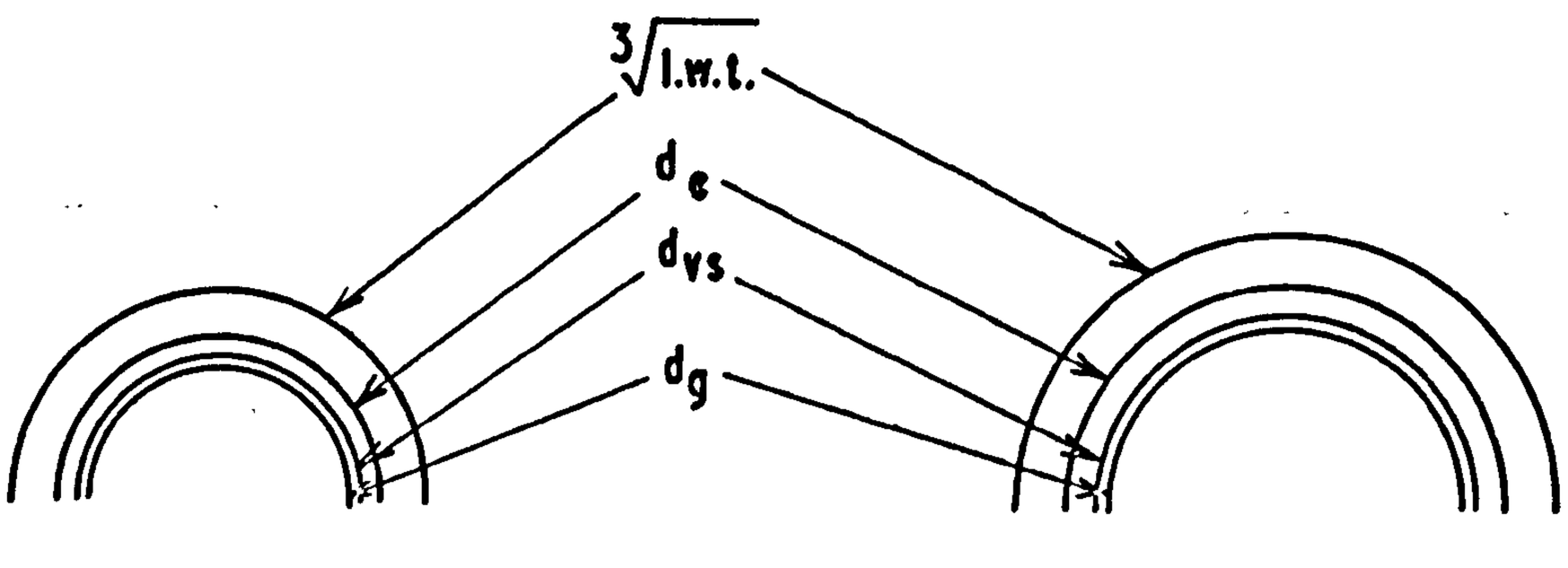

Fig 2.9. Plan and cross-sectional views of S23 (left) and Sabrina (right) to illustrate comparative size, shape and derived parameters.

Since the relative magnitude between varieties of all of the diameters is similar, the choice of characteristic "dimension" by which to compare varieties would seem to be best determined by (a) their relevance for comparison with other seed species and (b) the ease with which they are determined. From both points of view, the effective diameter, d_e, as calculated by equation 2.7 would seem to be the most suitable since it is derived from 1000 seed weight, a property which is readily determined for most species. For ryegrass seed its value also lies between the geometric mean of the principal dimensions and the geometric mean diameter calculated from the sieving results. It therefore represents a compromise between these values.

In addition to providing some indication of "dimension" for use in say, Reynold's number or in calculating diffusion coefficients, it was hoped that this study might provide some guide to the surface area per unit volume, S_v, a property relevant to the process of heat transfer. Substitution of the volume-surface mean diameters in equation 2.11 gives specific areas of 5081 and 3787 m^2/m^3 for S.23 and Sabrina respectively.

Orr and Dallavalle[90] suggest that for long cylindrical particles the 6 in equation 2.11 should be replaced by 4. This reduces the two estimates to 3587 and 2525 m^2/m^3 respectively. An approximate check on these values is to use them together with d_{vs} and the mean 1000 seed weights (Table 2.3) to calculate the solid densities. Using the smaller pair of estimates, solid densities of 1368 and 1321 kg/m^3 are obtained. These agree extremely well with the value of 1320 kg/m^3 measured by Lawton[62] for S.24 and 1290 kg/m^3 measured by Osborne[91] for S.101. A final calculation which confirms that these specific surface areas are in the right range is that of approximating the seed to a rectangular box of dimensions equal to the mean principal dimensions.

Since this ignores the tapered shape, it might be expected to overestimate the surface area. The values obtained, 4325 and 3180 m^2/m^3 for S.23 and Sabrina respectively are higher than those obtained with the modified form of equation 2.11.

Another method of calculating surface area is to use the Kozeny-Carman formula for the air permeability of a granular solid. In simple form this is[57]:

$$S_V = \sqrt{\frac{P}{5\mu D_V} \cdot \frac{\epsilon^3}{[1-\epsilon]^2}} \qquad \ldots\ldots\ldots 2.12$$

where P = pressure drop, N/m^2

D = bed depth, m

v = air velocity, m/sec

μ = dynamic viscosity

ϵ = porosity

and using data for S.23 and Sabrina obtained in the experiments described in Section 4 indicates specific surface areas of the order of 11,000 to 19,000 m^2/m^3 i.e. more than twice the values given by sieving or simple measurement. This result seems doubtful but cannot be dismissed for two reasons. Firstly, they were derived from pressure measurements on uncleaned seed and may reflect a high level of contamination with small particles. Secondly as a through-flow method, this may give answers most relevant to through-flow drying.

3. DETERMINATION OF DRYING PROPERTIES. THIN-LAYER EXPERIMENTS.

3. DETERMINATION OF DRYING PROPERTIES. THIN-LAYER EXPERIMENTS

3.1. INTRODUCTION

This section is concerned with the determination of the mass transfer properties of the seeds. The work involved

1. The development of apparatus in which thin layers of seed could be dried at controlled temperatures and humidities and with continuous monitoring of loss of weight.
2. The development of procedures for analysing the data and for expressing the properties as functions of drying conditions.

The mass transfer experiments provided information on the effect of drying treatments on seed germination, and this property was also studied in a separate experiment using the same apparatus. Finally the apparatus was used for some preliminary attempts to determine heat transfer coefficients.

3.2. THEORY

3.2.1. Mass Transfer

The removal of water from a mass of seed by the through-flow of air can be divided into 2 phases. In the first, water moves from within the seed to its surface; in the second, there is evaporation from the surface into the interstitial air. Irrespective of the mechanism by which the moisture moves within the seed, it does so in response to the external conditions. Its rate of movement will be affected by the rate of movement of air through the interstitial spaces only if stable conditions are not maintained. In a normal deep-bed drying situation, the balance of heat and mass transfer is such that the external conditions surrounding individual seeds are constantly changing, but virtually stable conditions can be maintained experimentally

by drying the seeds in a 'thin' or 'exposed' layer with an excess of airflow. The work in this section assumes that functional relationships describing the moisture movement within the seed under constant external conditions can be used to calculate the moisture movement when the conditions are varying.

It was shown in Section 2 that ryegrass seeds are similar in structure to the common cereal grains but are smaller and are harvested over a greater range of moisture content and ripeness. Nevertheless, it would be reasonable to expect that their behaviour during drying would also be similar and that the following relationship, put forward for wheat [67,69] and barley [16,49] might adequately describe the falling rate period.

$$\frac{M-M_e}{M_o-M_e} = \exp(-k\theta) \qquad \ldots\ldots\ldots 3.1$$

The derivation of this equation [67] is based upon the assumption that the resistance to drying of the cereal grain is in the aleurone layer enclosing the endosperm and not diffusion through the endosperm itself. Hinton [48] in an ingenious series of experiments demonstrated that, although wheat did have a water resistant layer, the testa, and not the aleurone layer, it was the much greater relative thickness of the endosperm which really limited the rate of movement of water into and out of the grain. This supports earlier work by Babbitt who demonstrated that the removal of the wheat pericarp and testa had no effect on the drying rate. In contrast Purdy & Crane [99] found that varietal differences in pericarp thickness could effect the drying rate of maize, but it is evident from their results that the endosperm tissue was still the basic determinant of the rate.

(2)

(10,53,25,40,93,96,127,118)

Thus it has been shown by several investigators that equation 3.1 does not give a satisfactory description of the whole curve and several alternative equations have been proposed. Some of these are empirical (118,34) but where there is a theoretical base it is usually Fick's Law of Diffusion.

Fick's first law states that the rate of transfer of a diffusing substance through unit area of a section is proportional to the concentration gradient measured normal to the section.

$$F = -D.\frac{\delta C}{\delta x} \qquad \ldots\ldots\ldots 3.2$$

From this equation it is possible to derive the second law which defines the rate of change of concentration with time. In three-dimensional form this is

$$\frac{\delta C}{\delta \theta} = D\left(\frac{\delta^2 C}{\delta x^2} + \frac{\delta^2 C}{\delta y^2} + \frac{\delta^2 C}{\delta z^2}\right) \qquad \ldots\ldots\ldots 3.3$$

Solutions to equation 3.3. are given in standard textbooks (see Crank, 1964 (30)) and because of the difficulty of exactly characterising a seed shape it is convenient to accept solutions from standard geometrical shapes (10,96,26,139). The most obvious shape with which to approximate a seed is that of a sphere for which the solution, if moisture content is used to replace concentration is

$$\frac{M-M_e}{M_o-M_e} = \frac{6}{\pi^2}\sum_{n=1}^{\alpha}\frac{1}{n^2}.\exp\left(-n^2.\frac{D\pi^2}{r^2}.\theta\right) \qquad \ldots\ldots\ldots 3.4$$

This series converges rapidly as $\underline{\theta}$ increases so that for large θ it can be written

$$\frac{M-M_e}{M_o-M_e} = \frac{6}{\pi^2}.\exp(-k\theta) \qquad \ldots\ldots\ldots 3.5$$

where $k = D\frac{\pi^2}{r^2}$ The analogy with equation 3.1 is immediately clear and for practical purposes the replacement of $D\frac{\pi^2}{r^2}$ with the single term k allows the mass transfer constant to be determined without specific reference to seed size and shape.

For a plane sheet of half-thickness, z, the solution is

$$\frac{M-M_e}{M_o-M_e} = \frac{8}{\pi^2}\sum_{n=1}^{\alpha}\frac{1}{(2n-1)^2}\cdot\exp\left(-(2n-1)^2\cdot\frac{D\pi^2}{z^2}\cdot\Theta\right) \quad \ldots\ldots\ldots 3.6$$

This is similar to equation 3.4 but converges more rapidly because of the omission of alternate terms. Henderson & Henderson (47) found that the first 2-terms of this series provided an adequate description of the drying of rice for use in a simulation model.

A solution for a finite cylinder was proposed by Pabis (96)

$$\frac{M-M_e}{M_o-M_e} = \sum_{n=1}^{\alpha}\sum_{m=1}^{\alpha} B_n B_m \exp\left[-\left(\mu_n^2 + \frac{R\mu_m^2}{l}\right)\frac{D}{R^2}\Theta\right] \quad \ldots\ldots\ldots 3.7$$

where R = radius l = length

$$B_n = \frac{4}{\mu_n^2} \qquad B_m = \frac{2}{\mu_m^2}$$

$$\mu_m = (2m-1)\frac{\pi}{2} \qquad J_0(\mu_n) = 0$$

The μ_n values are the roots of the Bessel function of the first kind of order zero, ($\mu_1 = 2.405$, $\mu_2 = 5.520$, $\mu_3 = 8.654$, $\mu_4 = 11.792$.) A similar solution was developed by Young & Whitaker (139) in a study of the drying of peanuts in the hull but was found to give a reasonable description of the drying curve only when the ratio of radius to length bore no physical resemblance to the peanuts. Husain, Chen and Clayton (52) concluded that when the ratio of

length to diameter is greater than 5 the end effects are negligible and the drying of a long seed such as rice could be approximated by the solution for the infinite rather than the finite cylinder.

Such a simplification is probably reasonable since all the solutions are based on assumptions which are almost certainly not true. These are

1. That the initial distribution of moisture content is uniform.
2. That the seed is homogeneous.
3. That diffusivity is constant (and therefore independent of moisture content).
4. That the seed surface instantaneously reaches equilibrium with the drying air.

Numerical approximations to the solution of Fick's Law with variable diffusivity have been presented (Chu & Hustrulid [27] Young [137] Whitaker et al [131], Husain, Chen & Clayton [51]) and extended [138] to represent the drying body as a series of composite shells which for non-homogeneous bodies, can be composed of materials of differing hygroscopic properties.

Becker & Sallans [10,11] found that the drying curve for wheat could be described by two periods of constant diffusivity, the transition occurring at approximately 10% m.c.d.b. The diffusion coefficient was approximately 10 times smaller below this level. A similar phenomenon was found in the drying of non-fatty fish muscle [58] and it was suggested that the transition point is that at which the adsorbed water is reduced to a monomolecular layer.

In the present work it was nccessary to strike a balance between the possibility of greater precision given by the more complex equations and utility within a simulation programme. Repeated evaluation of the differential of the drying curve equation is the whole basis of the deep layer calculations described in Chapter 5 and a simple function with the minimum number of constants can save considerably on computing time. Thus equation 3.1 was the first relation investigated. This equation has two constants k and Me and other investigators have derived these either graphically or by a least squares fit of the differential forms of equation 3.1. (37, 16, 110)

$$\frac{dM}{d\theta} = -k(M - M_e) \qquad \ldots\ldots\ldots 3.8$$

$$\ln \frac{dM}{d\theta} = -k\theta - \ln k(M_o - M_e) \qquad \ldots\ldots\ldots 3.9$$

In a preliminary study of data for rapeseed obtained by manual weighing in 1969 (78), the present author concluded that the equation was best fitted in the undifferentiated form either by logarithmic or direct (iterative) least squares. Although the latter gave a better overall fit, the former gave a better fit to the final portion of the curves because of the logarithmic weighting and because the asymptotic constant, Me, was fixed close to the final moisture content. This difference tended to confirm that equation 3.1 did not fit the whole curve particularly well and that the extra terms of the series equations 3.4 and 3.6 might provide a better description. ✓ Clearly one way of evaluating the constants for the series equations would be to fit a modified equation 3.1 to only that

portion of the drying curve for which the series has converged. But the problem here is in deciding at what point the series has converged, when k is, by definition, not known and the experimental curves relate to varying initial moisture contents and drying air temperatures.

Rather than make some arbitrary choice of this point it was decided that, in addition to fitting equation 3.1 by logarithmic and direct least squares, the data would also be fitted to a 2 term exponential equation

$$M = A.\exp(-k_1.\theta)+B.\exp(-k_2.\theta)+M_e \qquad \cdots\cdots\cdots 3.10$$

in which the extra term, A exp $(-k_1\theta)$, would approximate the higher order terms of equation 3.4 or 3.6. Programmes to fit equations 3.1 and 3.10 were developed and a paper describing their application to data from 1970 was published (81). Subsequently the programmes were further refined and an additional programme developed to fit the series equations 3.4 and 3.6 simplified by the substitution of the drying rate constant k, for the respective term $\frac{D\pi^2}{r^2}$ and $\frac{D\pi^2}{z^2}$

This work is described in detail in Section 3.3.2 and Appendix 3.

3.2.2. Equilibrium moisture content

The term Me in equations 3.1 - 3.10 has been termed the dynamic equilibrium moisture content because it is usually found to differ from the static e.m.c. reached under long term exposure to a constant atmosphere. Its existence as a distinct quantity has been doubted (27) although it has been suggested that it may represent some average of the surface moisture over a certain period. This would be reasonably consistent with the hypothesis of a second falling rate period.(58) But it seems

to the present author that an additional reason for the discrepancy is that the dynamic value is usually derived from a curve fitting procedure which is concerned to find a value which minimises the variance of the whole curve rather than to find an absolute value of e.m.c. Clearly in drying calculations in which equilibrium conditions are approached, the value of the Me used must deviate little from the static value if realistic answers are to be obtained. Thus it is to be expected that the dynamic Me will be a function of relative humidity and temperatures in a similar manner to the static value. That is, a plot of Me against r.h. would be expected to be of sigmoid form, rising steeply from zero but levelling off and increasing almost linearly over most of the r.h. range and rising steeply again to become asymptotic to 100% r.h. The only equation which has been proposed specifically for correlating dynamic e.m.c.(69) values does not have this form and although it has been used in models of the drying process (16,17,88) it has been found necessary to introduce an empirical modification.(3) Numerous theories and equations to explain adsorption and desorption equilibria have been put forward, and some of these have been found reviewed in more detail elsewhere by the present author.(82)

If water is visualised as adsorbing onto the internal surfaces of the seed then the layer of molecules adsorbing directly onto the surface will be the one most tightly held. Subsequent layers of molecules will be more and more loosely held until they are removable by the normal heat of evaporation. For convenience Smith (111) simplified this model into 2 categories of adsorbed moisture, that which was 'loosely' held and that which was 'bound' to the seed surface by forces stronger than the normal heat of evaporation. He visualised that the bound water fraction must

reach a maximum value well short of saturation and that it could be represented by a convex curve asymptotic to a relatively low moisture content. In contrast the loosely held fraction would increase progressively as saturation vapour pressure was approached and would produce a concave curve. The summation of these two curves would produce the characteristic sigmoid shape. He proposed the equation

$$Me = Mb - a \ln (1-rh) \quad \ldots\ldots\ldots\ldots\ldots 3.11$$

where Mb represents the maximum bound water. Hence the equation does not describe that part of the curve in which all of the moisture is in the bound state. However, the results of Becker & Sallans [11] for wheat would suggest that Mb is below the safe storage moisture content and that this relatively simple equation can be of practical value. A number of similar equations have been proposed the most widely used being that of Henderson.[45]

$$(1 - rh) = \exp. (-a\ T.M^n) \quad \ldots\ldots\ldots\ldots\ldots 3.12$$

or a modification proposed by Day and Nelson [32] in which all the temperature dependency is transferred to the constants a and n

$$(1 - rh) = \exp (-a\ M^n) \quad \ldots\ldots\ldots\ldots\ldots 3.13$$

From a consideration of the Othmer plot Strohman and Yoerger [116] have proposed the equation

$$\ln (rh) = a \ln P_s \exp (bM) + c \exp (dM) \quad \ldots\ldots\ldots 3.14$$

where a, b, c & d are constants independent of temperature and the saturation vapor pressure term $\ln P_s$ provides the temperature dependency. A simpler, but similar equation has been given by Chung and Pfost [28].

$$\ln (rh) = -\frac{a}{RT_{abs}} \exp (-bM) \quad \ldots\ldots\ldots\ldots 3.15$$

But like the Henderson equation, the use of the RT term does not eliminate the temperature dependency of the constants a and b and the independently proposed equation of Chen and Clayton [23] simply removes the RT term. None of these equations take account of hysteresis except by empirical determination of separate constants for the adsorptive and desorptive phases. Young and Nelson [135,136] have put forward an equation which represents a combination of the equation of Smith with the molecular BET equation. This equation does account for hysteresis but is cumbersome. An even more complex theory has been proposed by Ngoddy & Bakker-Arkema[84,85,86,87].

Very few workers have determined isotherms at more than one or two temperatures so that the temperature dependency of the empirically determined constants in some of the equations cited is difficult to determine. Data for the e.m.c. at different temperatures collated from other published data were presented by Day and Nelson[32]. Pixton & Warburton [97] present their data in an unusual manner. Lines of constant e.m.c. are plotted against rh and temperatures in the range 0 to 30°C such that ln (rh) = a + bT and the constants a and b are both functions of the moisture content.

An interesting finding by Tuite & Foster [125] was that the e.m.c. of maize can be reduced by high drying temperatures and that this effect is independent of hysteresis. The converse of this is that artificially dried seed may support higher interstitial relative humidities than more naturally dried seed and may therefore need to be dried to lower moisture contents for safe storage.

Static equilibria for ryegrass seeds have been reported by Kreyger[60], Sijbring[109] and Kulik & Justice[61].

3.2.3. Biological damage

The first priority of the thin-layer experiments was to establish the important physical properties of the drying seeds. However it is clear from the literature that work on the physical and biological aspects of drying have for too long been carried out in isolation with neither the engineer/physicist nor the agronomist/botanist always appreciating the significance of each other's findings [82]. It was felt, therefore, that as far as possible a study of the effects on seed quality should parallel the determination of the physical properties.

In the context of the thin-layer drying experiments, the type of biological damage to be expected was that due to heat and this is most conveniently measured by germination. The author has reviewed elsewhere [82] work on the effects of heat on the germination of a wide range of agricultural seeds. Suffice it to say here that the experiments may be divided into two main types.

(a) Those in which the seeds are heated without drying.

(b) Those in which they are heated with drying.

Although less representative of the practical situation experiments of type (a) have given the more repeatable results because of the precision with which they can be performed e.g. the use of sealed tubes in water baths, and because moisture content is held constant. In the type (b) experiment, the drying is not only altering the moisture content but also the evaporation may be affecting the temperature of, or the temperature gradient in, the seed. For a given temperature it has been shown that damage is more severe in the type (a) experiment and that the type of damage sustained differs from that of type (b) [129, 134, 64].

Attempts to describe damage as a function of temperature, time of exposure and moisture content have all been based on type (a) experiments. As long ago as 1917, Groves [38] found that the maximum permissible temperature to which wheat at 12% m.c.w.b. could be heated was a logarithmic function of exposure time.

$$T_{max} = 96.9 - 10.4 \log \theta \quad \ldots\ldots\ldots\ldots 3.16$$

A similar equation for wheat, put forward by Hutchinson [54] included moisture content and was valid for the range 35-14% w.b.

$$T_{max} = a - 5.4 \log \theta - 43.87 \log Mw \quad \ldots\ldots\ldots 3.17$$

where Mw is in percent and a = a constant whose value was 122.0 or 130.3 for the start of damage and complete kill respectively. An equation of this type has also been found to describe the loss of viability in storage of wheat, barley, broad beans and peas.[102]

In the formula suggested by Ptitsin [98] moisture dependency is accounted for by the use of the specific heat capacity, C.

$$T_{max} = 23.5/C + 20 - 10 \log \theta \quad \ldots\ldots\ldots\ldots 3.18$$

Bailey [3] has attempted to use the Hutchinson and Ptitsin formulae for the prediction of damage in the mathematical simulation of high temperature grain drying. None of these equations take account of the varying response to the treatments given by seeds dependent upon their initial condition or previous history. That this is important is recognised in the British Standard grain drier test [20] in which a type (a) heating test is used as a means of providing a response tolerance within which grain used for the test must fall [50]. The important factors in the previous history of the seed appear to be the severity of threshing and maturity at that time and the age of the seed when used for drying experiments. There is evidence to show that

freshly harvested mature seeds are more resistant to heat than re-wetted seeds [128] and unpublished work by the author with barley and wheat demonstrated over 2 season's an increasing sensitivity to drying damage with increasing drum speed although the magnitude of effect varied between years. In that work the grains were not harvested until mature. It has been shown in Chapter 2 that the potential germination of ryegrass seed is also a function of maturity at harvest.

In addition to the variability in results introduced by the rather ill defined factors outlined in the previous paragraph, a difficulty common to the determination of most biological properties is the variability introduced by the germination test itself. The standard germination test [55] is an attempt to provide repeatable, uniform and favourable germination conditions under which any viable seed ought to germinate. Light, humidity, water supply and temperature are all strictly defined and controlled within narrow limits. It has been shown, however, that unless the seeds have a viability in excess of 80% the variability in germination results is usually much greater than would be expected from random sampling alone [117]. This variability has been attributed to:

(a) A diminished tolerance of damaged seeds to variation in germination conditions. Small differences in light, temperature or water supply within the germinator may be critical or the condition required by the seed may now be outside the normal range.

(b) The greater difficulty for the analyst in distinguishing between abnormal seedlings and those which are merely late developing.

(c) Heat damaged seeds may be viable but slow to germinate (54,129); in these circumstances they are susceptible to attack from fungi which may suppress germination altogether. Delayed germination is, in a sense, induced dormancy and dormancy arising from other causes may also be a factor introducing variability into the results. The tetraploid hybrid ryegrasses have been shown to be particularly prone to dormancy.(103)

There are a limited number of experimental data for ryegrass seeds. Williams (133) reported damage at 49°C in thin layers of S101 and S23 perennial ryegrass dried with high airspeeds from initial moistures of 17.6 and 18.3% w.b. respectively. In sealed heating experiments with seeds rewetted to 22% w.b. germination was decreased after 2 hours at 50°C but not after 3 hours at 40°C.(60) A critical temperature of 70°C was reported by Woodforde and Lawton(134) for seed rewetted to 20% w.b. and dried in a thin layer for 1 hour. Using unpublished results of experiments on drying 6 inch beds of freshly-harvested S24 ryegrass seed, the present author has published a chart relating combinations of moisture content and temperature above which germination was depressed below 90% (79). Similar charts for the grass seeds, cocksfoot and timothy indicated that, of the three species, ryegrass was the least sensitive to heat damage.

3.3. EXPERIMENTAL

3.3.1. APPARATUS

At the time that the present work was begun, the N.I.A.E. multi-unit drier (Fig. 3.1) was a research apparatus built for the experimental determination of the effects of drying conditions on the quality and drying rate of seeds and other crops, when dried by through-flow of air in layers from 3 to 12 in deep.[75] It consisted of 8 independent drying units grouped together into one complex to allow certain common services to be shared. In particular an automatic weighing system utilised a common electronic package[100] A N.I.A.E. built data logger for recording weight loss and temperature data had been installed in 1968 and had been replaced by a commercial unit in 1969.

For the present work it was necessary to adapt and improve this apparatus to allow the continuous and automatic weighing of a thin-layer of seed of only one grain thick but with a sample weight of between 100 and 200g, so as to provide sufficient dried material for moisture content and seed analysis. This modification was developed during the winter of 1969-70 and the necessary hardware put out for manufacture by a local firm in the spring of 1970. Only two units were available at the start of the 1970 harvest but the remaining 8 were commissioned before it ended. Another modification which was partially completed by the second (1971) harvest was the addition on 3 units of apparatus to control humidity. Only those parts of the apparatus which have not been described previously[75,100] are described in this thesis. The modified drier is illustrated in Fig. 3.2.

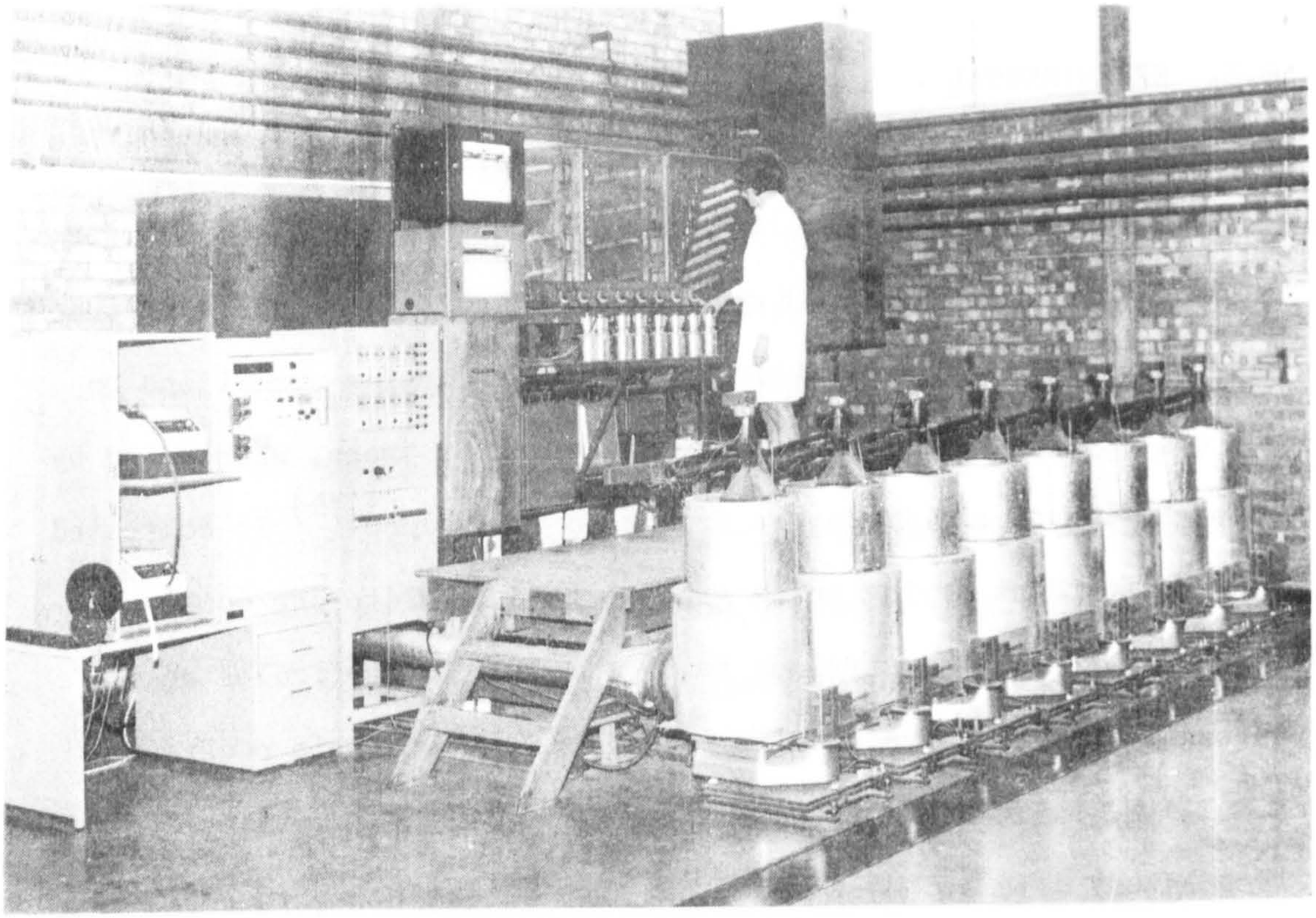

Fig. 3.1. The N.I.A.E. multi-unit drier in 1969.

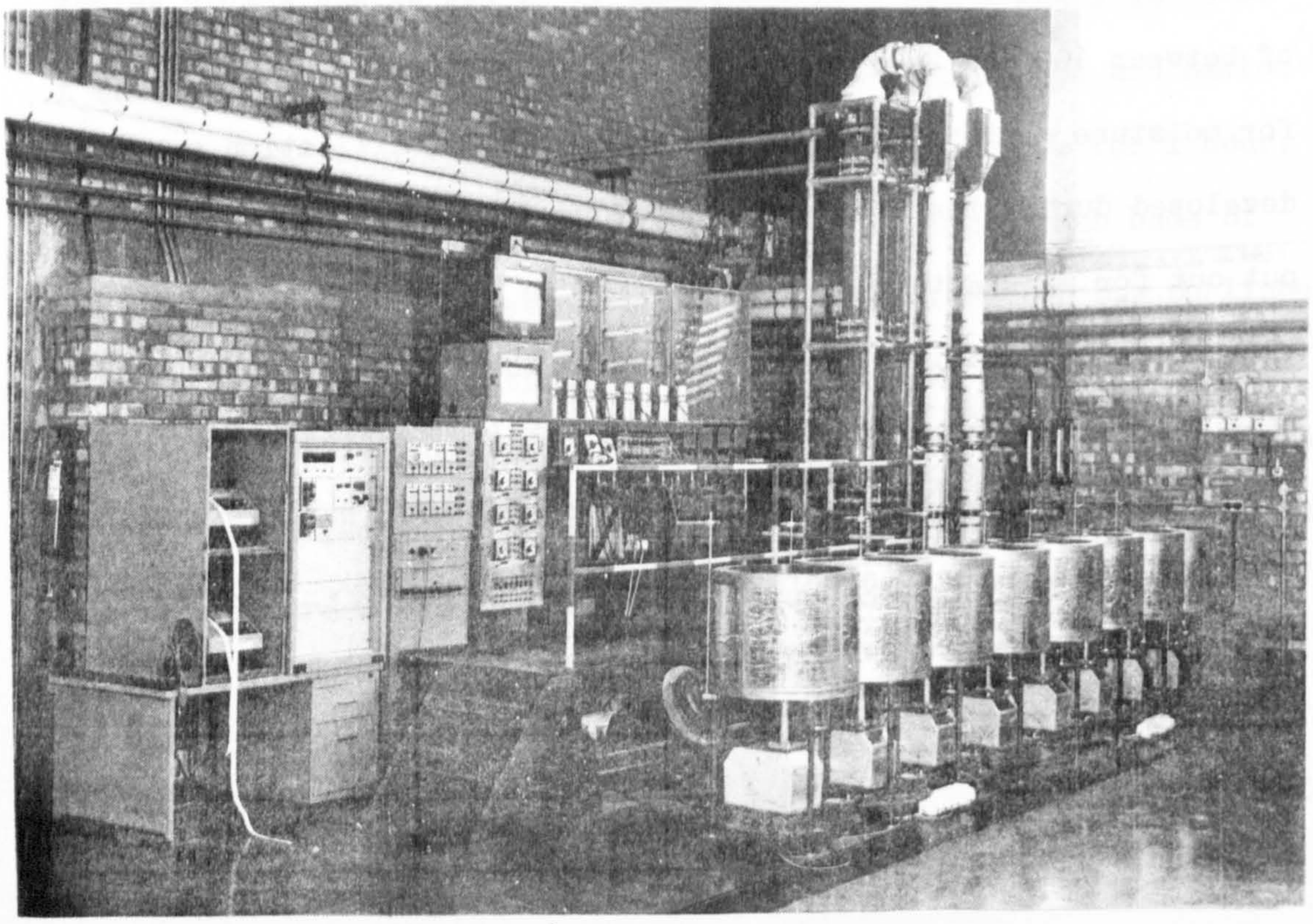

Fig. 3.2. The N.I.A.E. multi-unit drier in 1972 following modification for thin-layer drying.

3.3.1.1. Thin layer weighing units

In principle the apparatus to be described was similar to that used by Greig[37] and was based upon the assumption that if air is blown at a constant velocity upwards through the base of a perforated tray containing the drying sample, then the upthrust of that air can be regarded as constant and the change in weight of the pan will be due to loss of weight of the sample. To implement this system it was necessary to replace the complete drying container, plenum chamber and platform balance assembly previously described[100].

Each replacement unit (Fig. 3.3) consisted of a circular drying pan, A, of 2 sq. ft. in area with an aluminium frame and nylon mesh base resting upon an aluminium stalk, B, 27 in long and rigidly attached at its bottom-end to the main beam of a Sauter-Toppan top-loading balance, G. The stalk projected upwards and through an outer tube, D, which separated it from an insulated plenum chamber, E, into which air was led at the base and escaped, via a gauze, F, and honeycomb flow straightener, G, through the drying pan. The clearance between the pan and the sides of the plenum was of the order of $\frac{1}{8}$ in. At the base of the stalk a small platform, supported a removeable container, H, into which small steel weights could be added from an automatic dispensing mechanism, I. In 1971, an additional baffle of $2\frac{1}{2}$ in of Dunlopreme 97 open pore polyurethane (J) was added to the top of the flow straightener, G, and acted to prevent dust and dirt from falling through into the plenum chamber.

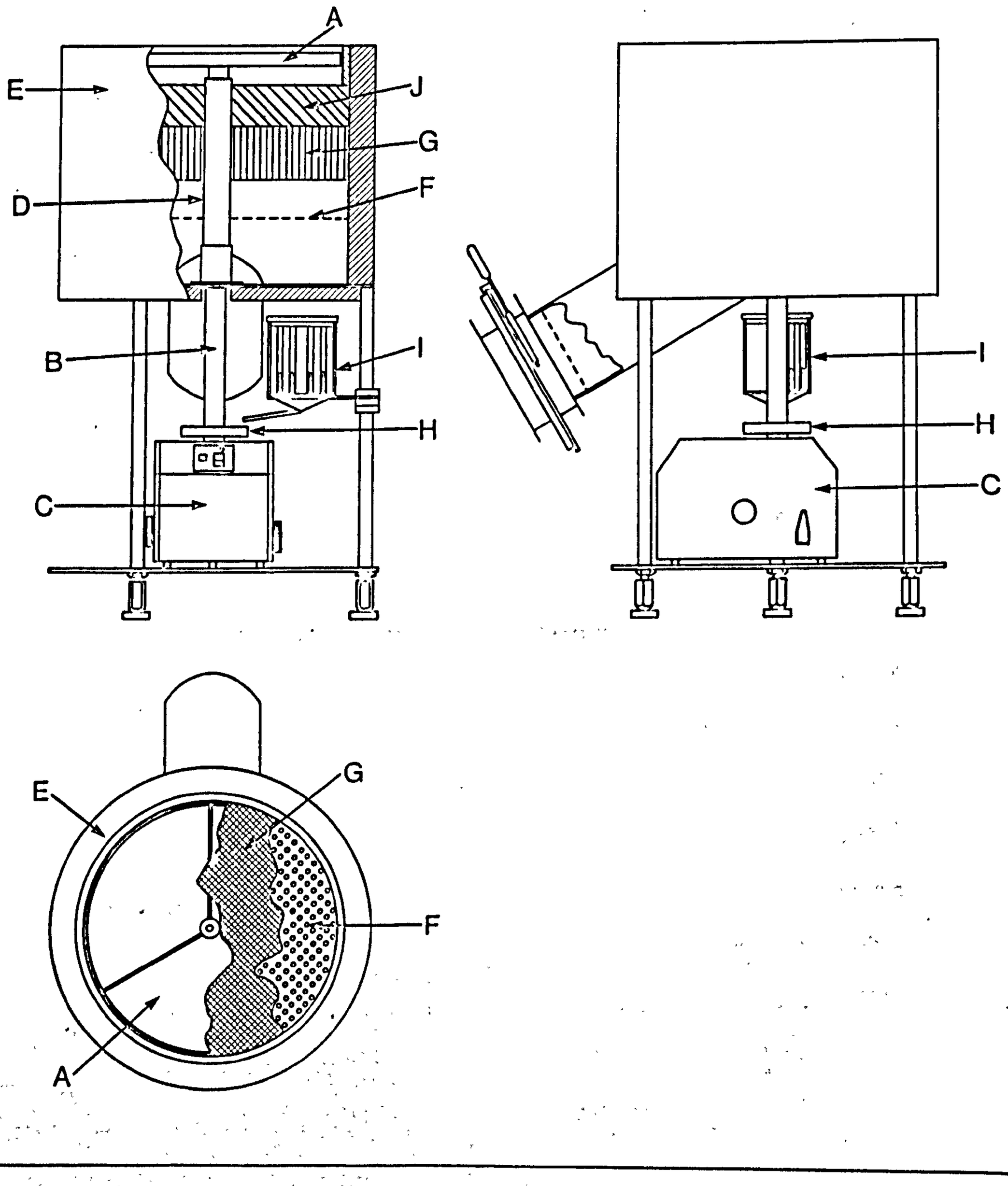

Fig. 3.3 Thin layer weighing unit.

The capacity of each balance was 1000g, and the projected graticule range was 100g, reading to 0.1g. For use with the automatic weighing system the balance was fitted with a Photain light switch which was positioned so as to be activated by the graticule projection when the balance was reading 100g or less. Activation of the switch caused the closure of reed contacts which replaced the steel and mercury contacts of the previous system[100]. The additional electronic circuitry is shown in Fig. 3.4[43].

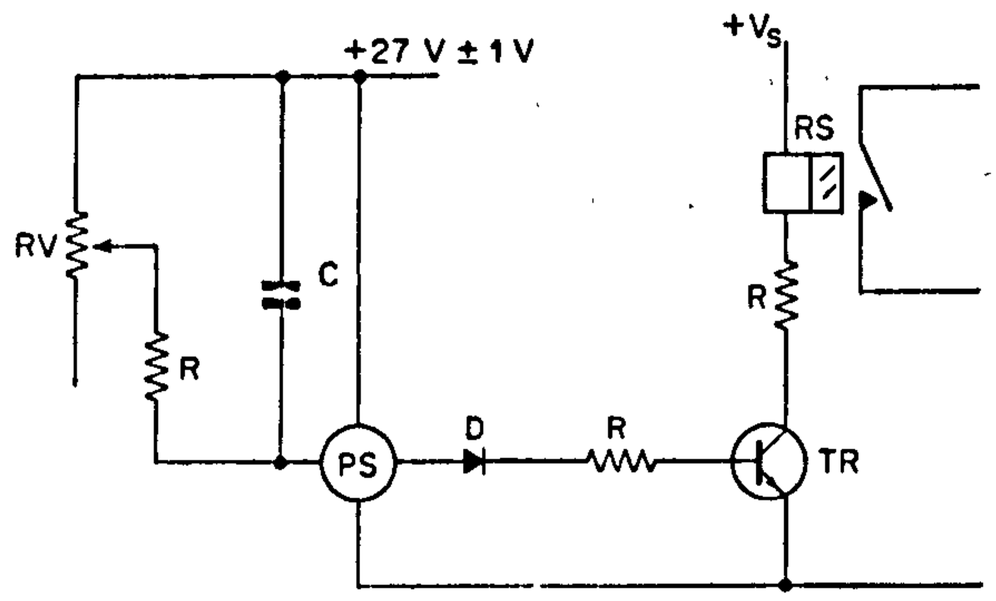

Fig. 3.4 Circuit for incorporating photo-switch (PS) and reed-switch (RS) into automatic weighing system

Contact closure caused the time at which it occurred to be both printed and punched on to tape and the weight dispenser to release one weight. These operations were controlled by a timing pulse, which occurred at 4 second intervals.

The system operated as follows. The drying pan was placed on a separate balance and the sample carefully sprinkled on until the required sample weight was reached. With the air already blowing through the plenum chamber at a known speed and temperature, the pan was then positioned on to the stalk, and as this was done the printing counter for the individual unit was zeroed. The balance was then rapidly adjusted by means of the rapid tare knob until it read 100g and the photo-switch circuit was connected. This caused the addition of a $\frac{1}{2}$g weight from the dispenser and increased the balance reading to 100.5g.

In this position the light switch was inactivated and remained so until loss of weight by drying returned the reading to 100g when another weight would be added and the cycle repeated. By this means the system provided a list of times in units of 4 secs. for equal increments of weight loss. Drying was normally, but not necessarily, terminated at a weight addition and the final weight of the sample was determined on a separate static balance.

Calibration

Initial drying tests, at first using lawn clippings and then tetraploid ryegrass seeds, gave discrepancies between the indicated weight loss from the automatic system and the actual loss obtained from static weighings, carried out immediately before and after drying, which were greater than would have been expected from experimental error alone. Further tests with the small-seeded ryegrass, Aberystwyth S23, showed that thechief cause of the discrepancies was progressive variation in resistance of the seed sample causing a decrease in upthrust on the drying pan. During the harvest period of this particular grass seed the number of drying units was increased, first to four and then to six, and it was possible to carry out comparative runs using different airflows on replicate seed samples and with additional periodic checks of true weight loss.

It was shown that the decrease in upthrust was almost entirely a function of time. When the effective change was expressed as a percentage of the total discrepancy (thus bringing the errors on to a common scale) the pattern of change was similar in all cases.

This was of an exponential type of decay to a steady level normally reached after about 12,000 cycles (13.3 h) but in most cases reaching an insignificant level at around 5000 cycles. The data were fitted with several alternative error correction functions and it was found that the one developed for the high airflow runs could also be used for the low airflow curves since the discrepancies in these cases were of a much smaller order. The application of the error correction function is discussed further in Section 3.3.2.

3.3.1.2. Temperature control

Temperature was controlled originally by an N.I.A.E. designed and built system. The controllers, using thermistor sensing heads, provided on/off control of 2 kw heaters. These were divided into 4 banks of 300, 400, 500 and 800 watts, each of which could be switched on to either manual or automatic control. Although adequate for previous work, it was realised in 1970 that the control was too coarse for the thin-layer experiments. Early in 1971 the thermistor units were replaced with Nuelectrohm TINICON type 1920/100 time based proportional controllers employing resistance thermometer sensors. The excellence of the control these provided is demonstrated by the figures included in Table 3.11 (Section 3.4.2.2.).

3.3.1.3. Humidity measurement

With the installation of the thin-layer weighing units and the packed towers, the original common duct was removed and each drier allowed to obtain its air from the laboratory atmosphere. The previous single aspirated dry- and wet- bulb thermocouple unit was therefore replaced by 8 similar units, one at the inlet to each drier. As the packed towers were completed the units in driers 7 & 8 were repositioned at the top of the towers (see 3.3.1.4.) A typical unit is shown in Fig. 3.5.

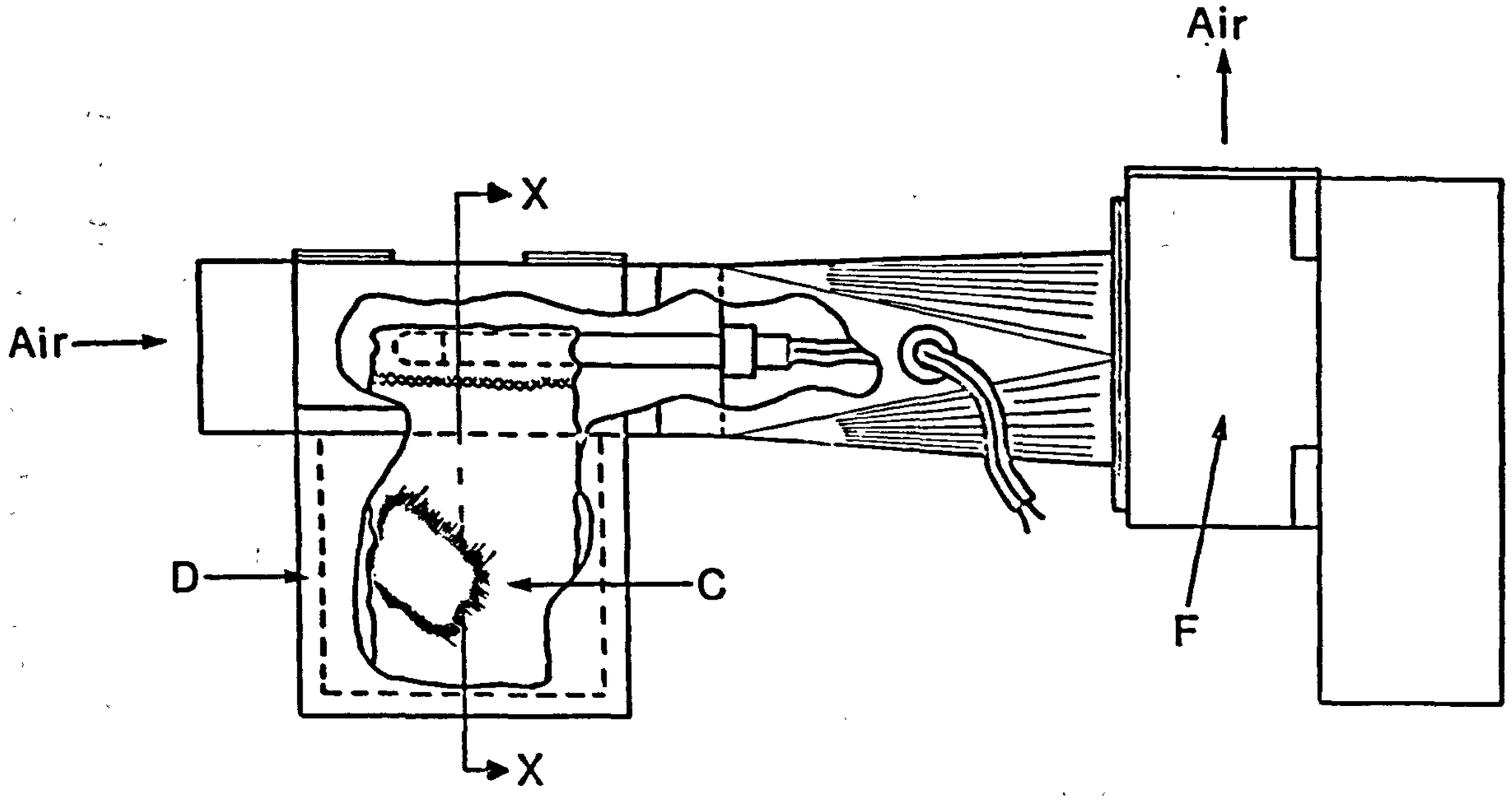

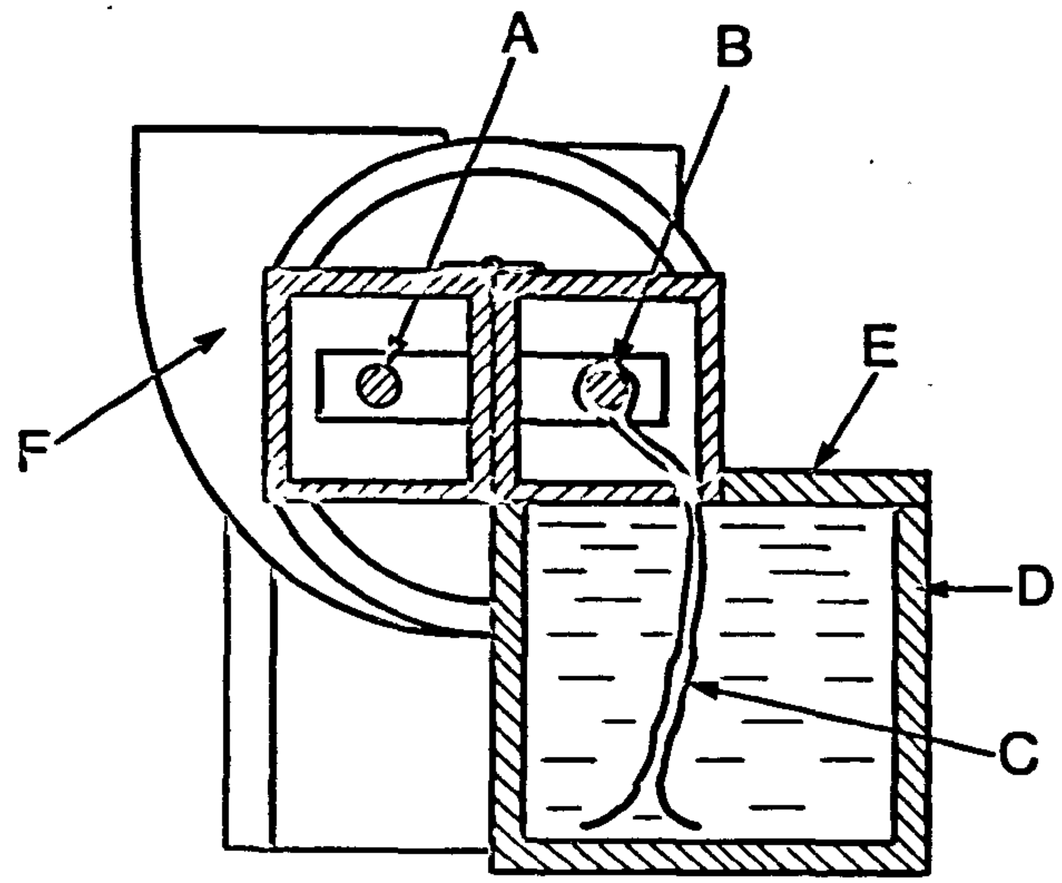

Section on X.X.

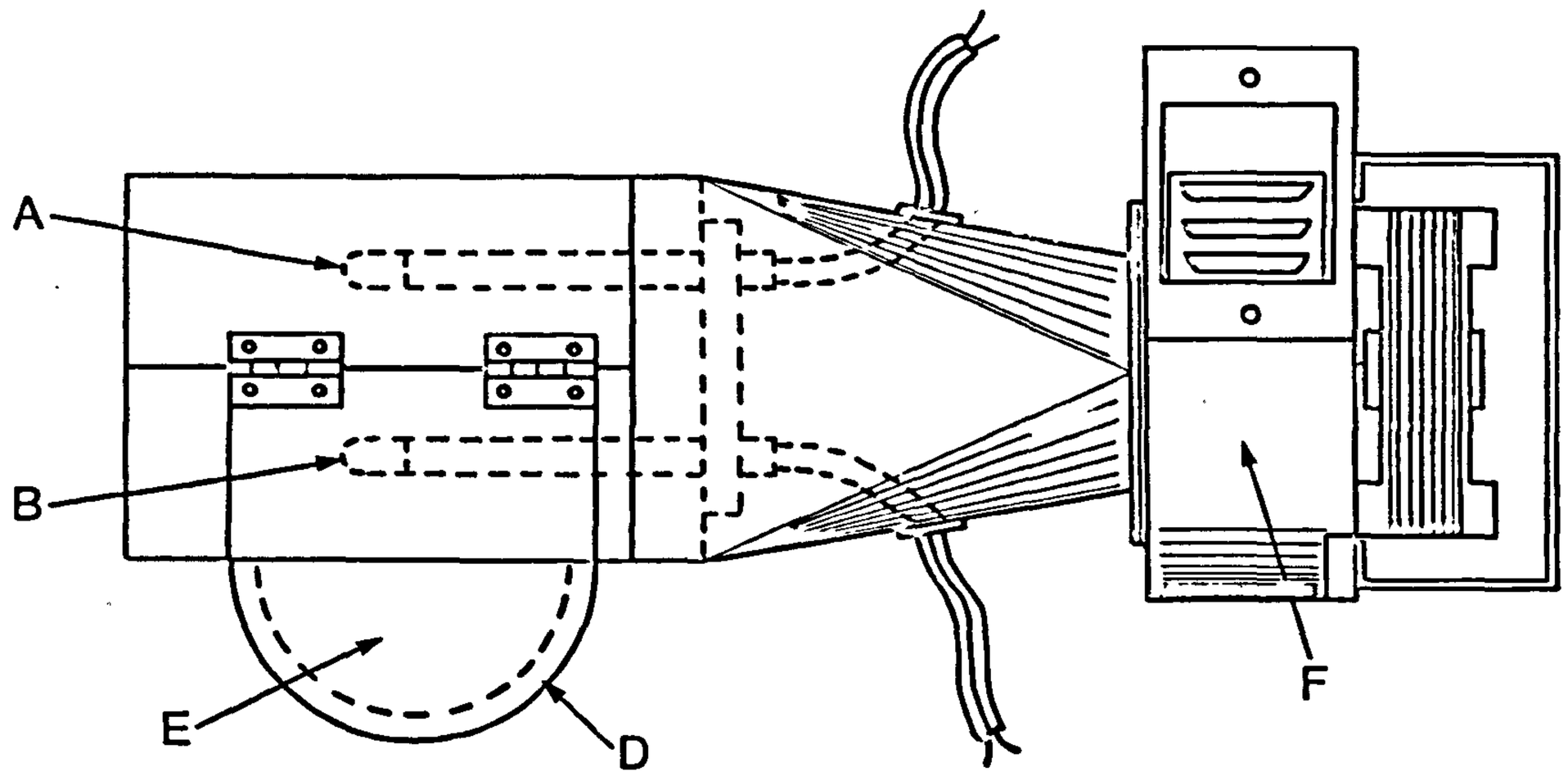

Fig. 3.5 Aspirated dry- and wet-bulb thermocouple units.

The thermocouples are embedded in copper bulbs, A and B projecting along 2 separate airways formed from 1 5/16 in square section Tufnol tube. Thermocouple B is enclosed in a muslin wick, C, fed with deionised water from a reservoir, D. Access to the wick and reservoir is gained via a small hinged lid, E. Air is drawn over the bulbs and then discarded to atmosphere by a small centrifugal fan, F. These units give results comparable with those given by a clockwork Assman aspirated psychrometer.

3.3.1.4. Humidity control

Two forms of control were installed. On 2 of the units, the air was conditioned by means of 2 packed towers and on a third, a refrigeration unit was used to cool the air to approximately 5°C (41°F). Since this was normally less than the dew point, the resulting condensation ensured a reasonably stable and low humidity in the drying air.

The refrigeration unit a Prestcold Condensing Unit Model AS 50-1/H was connected to a finned heat exchanger positioned on the inlet side of the fan before the heater unit. Moisture, condensed from the air, drained away below the unit and was prevented from collecting as ice in the fins by correct adjustment of the refrigerant pressure (and hence temperature).

The 2 packed towers are visible on the right hand side of the drier in Fig. 3.2. They are explained by the simplified diagram of a single unit in Fig. 3.6. The tower, A, was constructed of QVF glass sections and had a total height of just over 3 metres and internal diameter of 225 mm. Over an approximate length of 2 m (the shaded area of A in Fig. 3.6.) it was packed with 20 mm x 20 mm diameter glass Raschig rings.

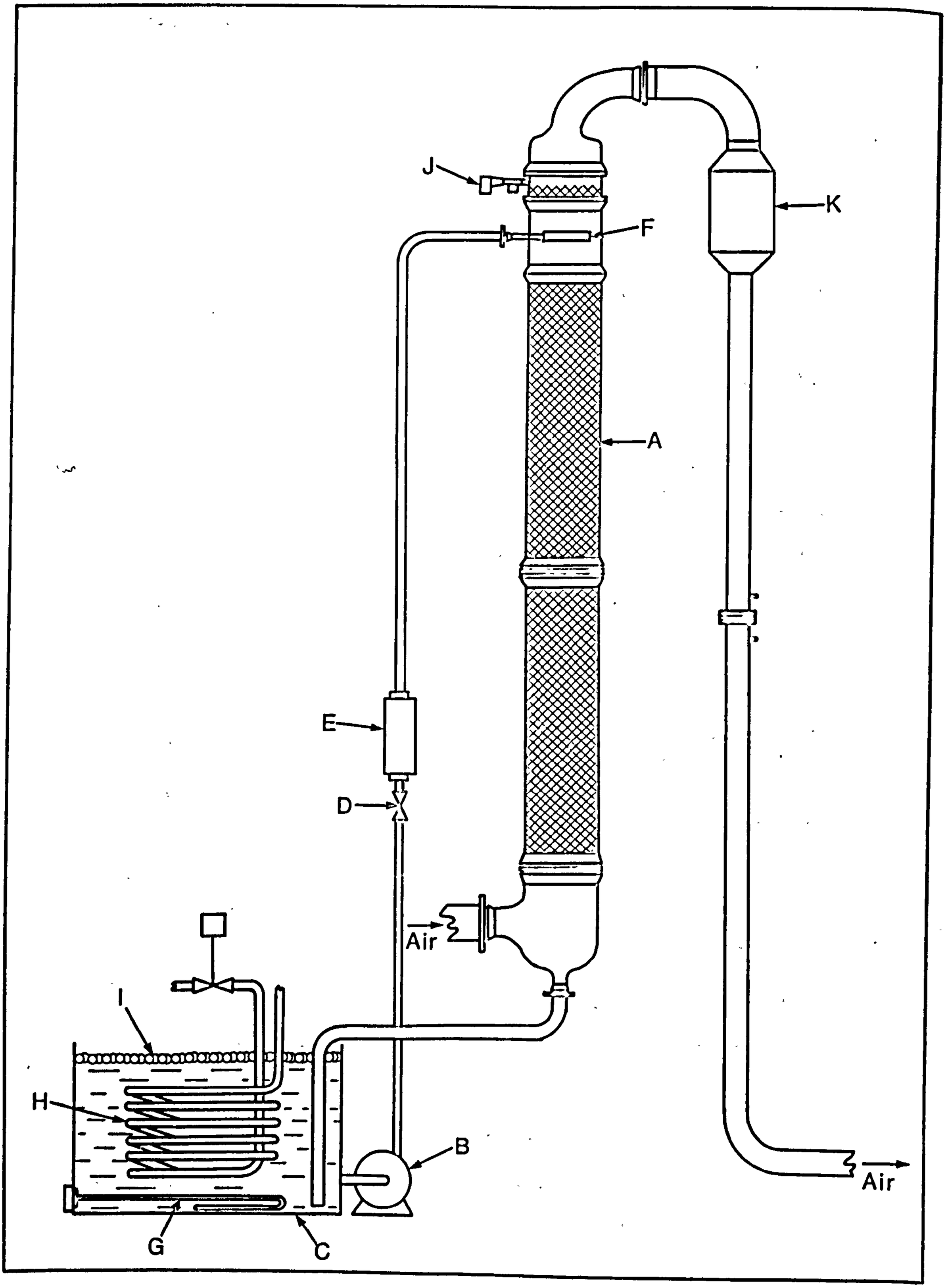

Fig. 3.6 Schematic layout of single packed tower.

An impeller pump, B, of 120 gall/h capacity, lifted deionised water from an 80 gallon tank, C, through a control valve D, and Rotameter, E, to the top of the tower where it was distributed by the spray section, F. A 3 kw immersion heater, G, and a refrigerating coil, H, were used to modulate water temperature under the control of a Nuelectrohm TINICON proportional controller. Evaporation from the top of the tank was reduced by means of floating plastic spheres, I, and normal water loss was made good from a header tank (not shown in Fig. 3.6.). Provided an excess flow of water was maintained through the tower, the air passing up it would exit at the top saturated and at the water temperature. This condition was monitored by the aspirated hygrometer unit, J. From this point onward the airway was heavily lagged with fibre glass insulation and in addition the section between the hygrometer unit and the heater, K, was wrapped with electrical heating tapes controlled by a Simmerstat type of regulator. Their function was merely to maintain the walls of the airway above the air dew-point and prevent condensation. Heating of the air to the required dry-bulb temperature was carried out by the heater unit, K, switched as on the other driers, by a Nuelectrohm controller.

3.3.1.5. Data Logger

A Solartron Compact Series 2 data logger and 2 Addo Type 5 paper tape punches were used to record weight loss and temperature data on separate punched paper tapes. An interface, designed and built by the Control and Instrumentation Department linked the logger with an automatic weighing system. This allowed the weight loss data to be recorded as a series of scans, each consisting of a time, in 4 second cycles, followed by a series of 8 digits, which, depending upon the state of the weighing units, could be any combination of noughts or ones.

Thus in the following example scan

0045 01010C00

the cycle time is 45 and weight addition has occurred in that cycle on drier numbers 2 and 4. A scan was initiated by a change of state in the weighing units and thus a line of zero's only was a fault. Equally a line of ones, although possible, was highly unlikely statistically and when such lines began to occur rather frequently in the 1971 season were found to be caused by 'noise' on the electrical power supply and were finally cured by the installation of interference suppressors and a constant voltage regulator. The advantage of this system of recording weight loss is that the 8 digit code allowed the information from 8 driers to be recorded on one paper tape.

For recording temperature, the logger incorporated a 50 channel scanner receiving millivolt inputs from chromel-constantan thermocouples "bridged" with a temperature compensated offset voltage. The readings were output as millivolts x 100. The scanner was programmed to scan in 6 blocks of 8 thermocouples, each block comprising one of 6 thermocouple locations on each drier. These were ambient dry-bulb, ambient wet-bulb, inlet, exhaust, exhaust dry-bulb and exhaust wet-bulb temperatures. Any serial combination of these six blocks could be selected by setting switches on the logger console, but in the work reported here only the first 3 blocks were used. Scans were controlled by a digital clock and could be set to occur at any of the following intervals:- 1 min., 10 min., $\frac{1}{2}$ h, 1 h, or 2 h.

3.3.2. DATA PROCESSING

In 1970 the procedure for analysing the data tapes was necessarily cumbersome. This was because:-

(a) The A.R.C. computing facilities at Rothamsted Experimental Station (R.E.S.) were in a state of transition. The Orion computer which used the Ferranti EMA language was being replaced by the ICL 470 computer on which FORTRAN was to be the language. This change was well behind schedule and the A.R.C. had been forced to hire time on the IBM 360 at University College, London.

(b) The author was due to spend a term in residence at Newcastle University where a FORTRAN compiler was available.

(c) The data had been punched on 5 track-tape in Ferranti code.

The problem of using 5-track tape with FORTRAN programmes on the U.C.L. computer had been solved in 1969 by P.A. Clarke of the Computer Department, R.E.S. A library package, ROTHAM 52 CARD was used in conjunction with 2 sub-routines written into the FORTRAN programme and called in place of the normal READ statements. Thus the first part of the processing of the weight loss tapes (code to cycle conversion see 3.3.2.1.) was carried out at U.C.L. and the decoded data punched on to cards. These cards were then used to complete the processing at Newcastle University on the IBM.

The temperature tapes from 1970 were not processed through this system. They were printed through a teleprinter and the data entered manually into a Wang desk computer.

By 1971, the ICL 470 computer at R.E.S. had been installed and was beginning to function under the Multijob operating system. The Addo punches were converted to punching 8 track type in ISO code and both weight loss and temperature tapes were processed through the new computer.

3.3.2.1. Weight loss

There were 3 stages in the processing of the weight loss tapes.

1. The conversion of the 8 digit code to lists of cycle times for each drier and drying run on that drier.
2. The conversion of these cycle times into parallel lists of moisture contents and time.
3. The fitting of the appropriate equations to determine the drying constants.

Apart from minor differences necessary to adapt them to the different computer, the same FORTRAN programmes were used in both years for stages 1 and 2. The programmes used for stage 3 were subject to continuous development throughout the period of this work. Full details and flow-charts of these programmes as currently implemented on the ICL 470 are given in Appendix 3.1

Stage 1 Code-to cycle conversion

In addition to the 8 digit code, this programme requires information on the starting and finishing cycle of each run and the drier number which it occupied. Because of the large variation in drying times with temperature it was often possible to carry out 2 or 3 runs on one drier whilst a single run was being completed on another drier. For this reason the programme can cope with a total of 24 runs on one tape, i.e. 3 on each drier, none of which need necessarily have been started at cycle 0. The printed output from this programme could be compared with the printed records of cycle times from the Sodeco printers[100] and any other information noted during each run and any errors corrected. In 1970 these corrections were made to the punched card output and in 1971 they were made via the remote terminal at N.I.A.E. to disc files copied from magnetic tape storage on the ICL 470 at R.E.S.

Stage 2 Generation of moisture content at each cycle time

This stage is summarised by the flow chart of Fig. 3.7.

The main programme performed the following functions.

(a) Reading in, and printing out, of the error correction function constants.

(b) Reading in of the data for each run and the subsequent calculation and printing of such run parameters as dry matter and initial moisture content.

(c) Reading of a directive, ID, which depending upon its value, would cause.

(i) all error correction functions to be used on a particular data set

(ii) a single error correction function to be used on a particular data set

(iii) transfer to (b) to read in another data set

(iv) terminate the entire programme

The programme continued to return to read the directive ID until type (iv) was enccuntered.

(d) If the directive ID had indicated that a certain error correction function should be applied to the data, subroutine MOTCON was called.

MOTCON used the appropriate error function and cycle times to generate an array of moisture contents. It was then used either to print this information or to call one ore more of 3 subroutines, SINGEX, DOUBEX, SEREX which fit diffusion equations or a subroutine SIMDIF which carries out a simple differentiation of the drying curve. In Fig. 3.7. MOTCON is shown calling both SINGEX and DOUBEX; this was the form in which it was used initially in 1970.

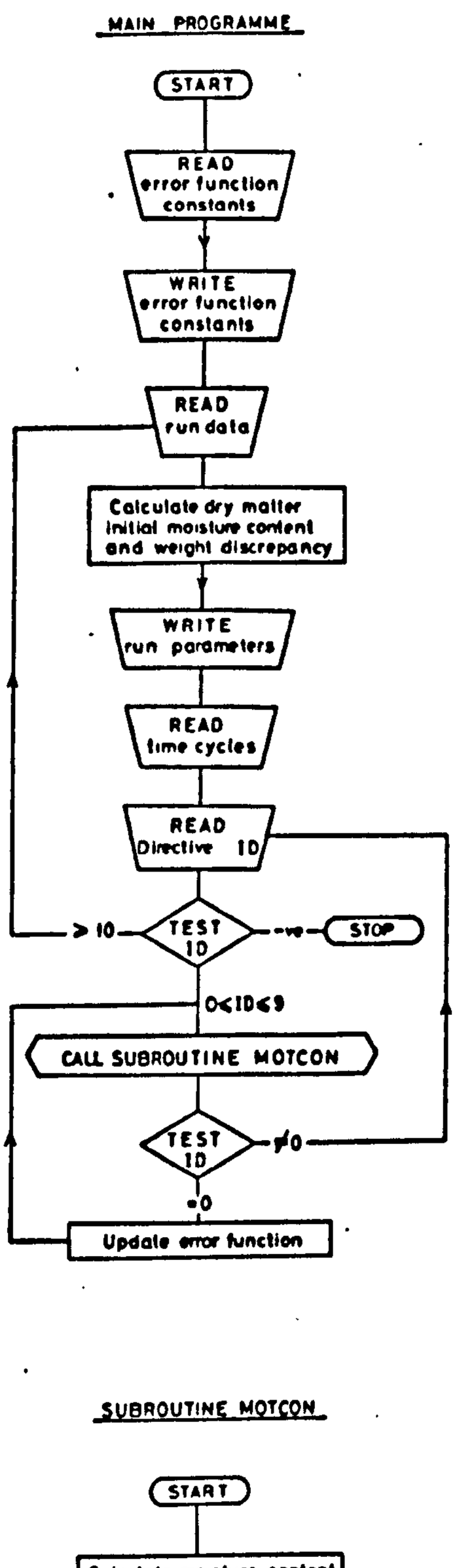

Fig. 3.7 Flow chart of main programme and subroutine MOTCON used for the generation of moisture contents at each cycle time.

These subroutines represent stage 3 of the weight loss processing and in later programmes were used independently of MOTCON but using the moisture content/drying time lists produced by MOTCON as input data.

The main function of MOTCON was the application of the error correction function in generating the moisture content values.

In the ideal situation where no discrepancy exists between the weight loss and that indicated by the static weighings, then the intermediate moisture contents could be calculated simply by using the formula.

$$Mi = \left(\frac{W_{i-1} - 0.51}{DM}\right) \times 100\% \text{ d.b.} \qquad \ldots 3.19$$

where Mi = moisture content at cycle θ_i, % d.b.

W_{i-1} = wt of moisture at cycle θ_{i-1}, % d.b.

DM = dry matter, g

and 0.51 is the value of the weight added at θi, g.

In practice the decreasing resistance of the drying sample means that the actual weight loss between two successive weight addition cycles is greater than 0.51 by an amount depending upon the total change in resistance, i.e. the discrepancy, and the value of the cycle times.

From a consideration of the error readings, the general form of the error correction function was chosen as

$$ER = Ae^{-Bt} + Ce^{-Dt} \qquad \ldots 3.20$$

where t = cycle time

and A,B,C & D = constants chosen such that ER = 1 at t = 0 and approaches 0 at cycle times indicated by experiment.

By appropriate choice of constants, the function can be reduced to a single exponential and can be made to be very nearly linear for the whole run.

Thus at any time, the value ER indicates the proportion of weight discrepancy remaining. Between any two weight additions the amount of weight lost

$$= 0.51 + (ER_{t(i-1)} - ER_{t(i)}) \times \text{Discrepancy}$$

In practice it was possible for short runs to terminate before the error function faded to zero so that in order that the recorded discrepancy was fully allocated it was necessary to calculate an amended discrepancy.

$$\text{Amended discrepancy} = \frac{\text{Discrepancy}}{1 - ER_{t(\text{last})}} \quad \ldots 3.21$$

As the sample became very dry, intervals between weight additions became very large and it was sometimes necessary to terminate the run before the balance equilibrium was restored. In this case the weight lost in the interval since the previous weight addition was taken to consist of the amount allocated by the error function plus any end correction which could be made if the balance reading was less than 0.5g from equilibrium.

Given that the asymptotic moisture value, M_e can be found or estimated, the simple single exponential equation,[3.1] can be written in the logarithmic form

$$\log (M-M_e) = \log (M_o-M_e)-k\theta \qquad \ldots 3.22$$

and a value of k obtained by fitting a straight line by linear least squares. A convenient method of estimating M_e is to use the formula

$$M_e = \frac{M_1 M_2-M_t^2}{M_1+M_2-2M_t} \qquad \ldots 3.23$$

where M_1, M_2, M_t are values of M such that $\theta_t = \frac{\theta_2-\theta_1}{2}$ and the values of θ_t are large.

However the values of k and M_e so determined are not necessarily the best values because (a) M_e is estimated from 3 observations only and (b) the least squares procedure minimizes the sum of the squares of the deviations of $\log (M-M_e)$ rather than the true variable M. But having obtained initial estimates by this method an iterative correction procedure can be applied as suggested by Southworth and Deleeuw,[129] Guest[39] and Oliver.[89]

The basic equation can be written in the form

$$y = ae^{bx}+c \qquad \ldots 3.24$$

where $y = M$
$a = (M_o-M_e)$
$C = M_e$
$b = k$
$x = 0$

and $$y = f(a,\ b, c) \qquad \ldots 3.25$$

If the initial estimates of the constants a_o, b_o and c_o then

$$y = f(a_o+\Delta_a, b_o+\Delta_b, c_o+\Delta_c) \qquad \ldots 3.26$$

and expanding by one term in Taylor's series about the point (a_o, b_o, c_o)

$$y = f(a_o, b_o, c_o) + \Delta_a\left(\frac{\delta f}{\delta a}\right)_o + \Delta_b\left(\frac{\delta f}{\delta b}\right)_o + \Delta_c\left(\frac{\delta f}{\delta c}\right)_o \qquad \ldots 3.27$$

where the partial derivatives are to be evaluated at (a_o, b_o, c_o).

From Eqn (3.24) $$\frac{\delta f}{\delta a} = e^{bx}, \frac{\delta f}{\delta b} = axe^{bx}, \frac{\delta f}{\delta c} = 1.$$

Substituting in Eqn (3.27)

$$y = f(a_o, b_o, c_o)+\Delta_a e^{b_o x}+\Delta_b a_o x e^{b_o x}+\Delta_c. \qquad \ldots 3.28$$

Eqn (14) is linear in Δa, Δb and Δc and the method of least squares is directly applicable to the calculation of these values. Given a series of N estimates of moisture, Y_k against time, x_k, where $k = 1, N$, then the least squares function to be minimized is

$$\sum_{k=1}^{N} d_k^2 = \Sigma[y_k-f(a_o, b_o, c_o)-\Delta_a e^{b_o x_k}-\Delta_b a_o x_k e^{b_o x_k}-\Delta_c]^2 \qquad \ldots 3.29$$

$$= h(a_o, b_o, c_o)^2 \qquad \ldots 3.30$$

and is minimized when the partial derivatives

$$\frac{\delta h}{\delta \Delta_a}, \frac{\delta h}{\delta \Delta_b}, \frac{\delta h}{\delta \Delta_c} \quad \text{are equal to 0.}$$

Thus $$\frac{\delta h}{\delta \Delta_a} = -2\,\Sigma[h(a_o, b_o, c_o)]e^{b_o x_k} = 0 \qquad \ldots 3.31$$

$$\frac{\delta h}{\delta \Delta_b} = -2\,\Sigma[h(a_o, b_o, c_o)]a_o x_k e^{b_o x_k} = 0 \qquad \ldots 3.32$$

$$\frac{\delta h}{\delta \Delta_c} = -2\,\Sigma[h(a_o, b_o, c_o)]\,1 = 0 \qquad \ldots 3.33$$

Let $$D_k = Y_k-f(a_o, b_o, c_c) = [Y_k-a_o e^{b_o x_k}-c_o] \qquad \ldots 3.34$$

and expand Eqns (3.31,32,33) into simultaneous equations linear in Δa, Δb, and Δc.

$$\Sigma e^{b_o x_k} D_k = \Delta_a \Sigma e^{2b_o x_k}+\Delta_b a_o \Sigma x_k e^{2b_o x_k}+\Delta_c \Sigma e^{b_o x_k} \qquad \ldots 3.35$$

$$\Sigma x_k e^{b_o x_k} D_k = \Delta_a \Sigma x_k e^{2b_o x_k}+\Delta_b a_o \Sigma (x_k)^2 e^{2b_o x_k}+\Delta_c \Sigma x_k e^{b_o x_k} \qquad \ldots 3.36$$

$$\Sigma D_k = \Delta_a \Sigma e^{b_o x_k}+\Delta_b a_o \Sigma x_k e^{b_o x_k}+\Delta_c N \qquad \ldots 3.37$$

The solution of equations (3.35, 3.36, 3.37) provides values of the adjustments Δa, Δb and Δc by which the original estimates a_o, b_o and c_o may be modified. The process may then be repeated until convergence is achieved. The subroutine SINGEX was written to carry out these calculations and two other subroutines were developed to perform similar calculations to fit equation 3.10, (DOUBEX) and equations 3.4 and 3.6 (SEREX) in the modified form of 3.38 and 3.39.

$$M = (M_o - M_e)\frac{6}{\pi^2}\sum_{n=1}^{\alpha}\frac{1}{n^2}.\exp(-n^2.k\theta) + M_e \qquad \ldots\ldots\ldots 3.38$$

$$M = (M_o - M_e)\frac{8}{\pi^2}\sum_{n=1}^{\alpha}\frac{1}{(2n-1)^2}\exp(-(2n-1)^2.k\theta + M_e \qquad \ldots\ldots\ldots 3.39$$

The sets of simultaneous equations for DOUBEX and SEREX are developed in the appendix; since there are 5 constants in equation 3.10, DOUBEX derived 5 simultaneous equations. All 3 subroutines used another subroutine, MATINV, for the solution of the simultaneous equations. This was a slightly simplified version of that given under the same name by McCormack and Salvadori [63] and used the Gauss-Jordan method of solution.

In the original versions of SINGEX and DOUBEX, a condition that all the adjustments should be less than 0.2% of their respective constants was used as the criterion for convergence. This was later altered to work directly on the sums of squares of the deviation (SSD) which was considered to be minimised if the change in SSD caused by the new adjustments was less than 0.2%. In this revised form, a method suggested by Hartley [44] was used to increase the rate of convergence. Using this method the original estimates of the constants were

not modified until the SSD they generated had been compared with that which would have resulted if first one-half and then all of the adjustments had been made. These 3 estimates of SSD were then assumed to be on a parabola of which the minimum was estimated by the formula.

$$VMIN = 0.5 + 0.25 (SSD_0 - SSD_1) / (SSD_1 - 2(SSD_{\frac{1}{2}}) + SSD_0) \quad \ldots\ldots\ldots 3.38$$

where VMIN was the factor by which to correct the indicated adjustments. The SSD given by using this factor was evaluated. If it was indeed less than the original SSD then (VMIN x adjustment) was used in the next iteration. Otherwise the adjustment was halved and a new VMIN calculated. If the original starting values were reasonable this assisted convergence; if they were bad it prevented divergence and the failure of the program. Starting values were originally estimated solely by the subroutines, but in later versions they could be supplied from the calling programme. This option proved useful when the internally generated values were clearly leading to an erroneous solution. A maximum of 20 iterations was allowed and if this maximum was reached the acceptance of the fit depended upon the size and relative degree of oscillation in the constants and sums of squares and on visual inspection of the results. Normally however, convergence was achieved within 4 or 5 iterations. With only minor modification the flow chart of Fig.3.8 is applicable to all three subroutines.

Ancillary facilities

As a means of making visual checks of the drying curves and fitted equations,2 FORTRAN programmes were written to produce plots on an incremental graph plotter. Both operated on lists of

Subroutine SEREX

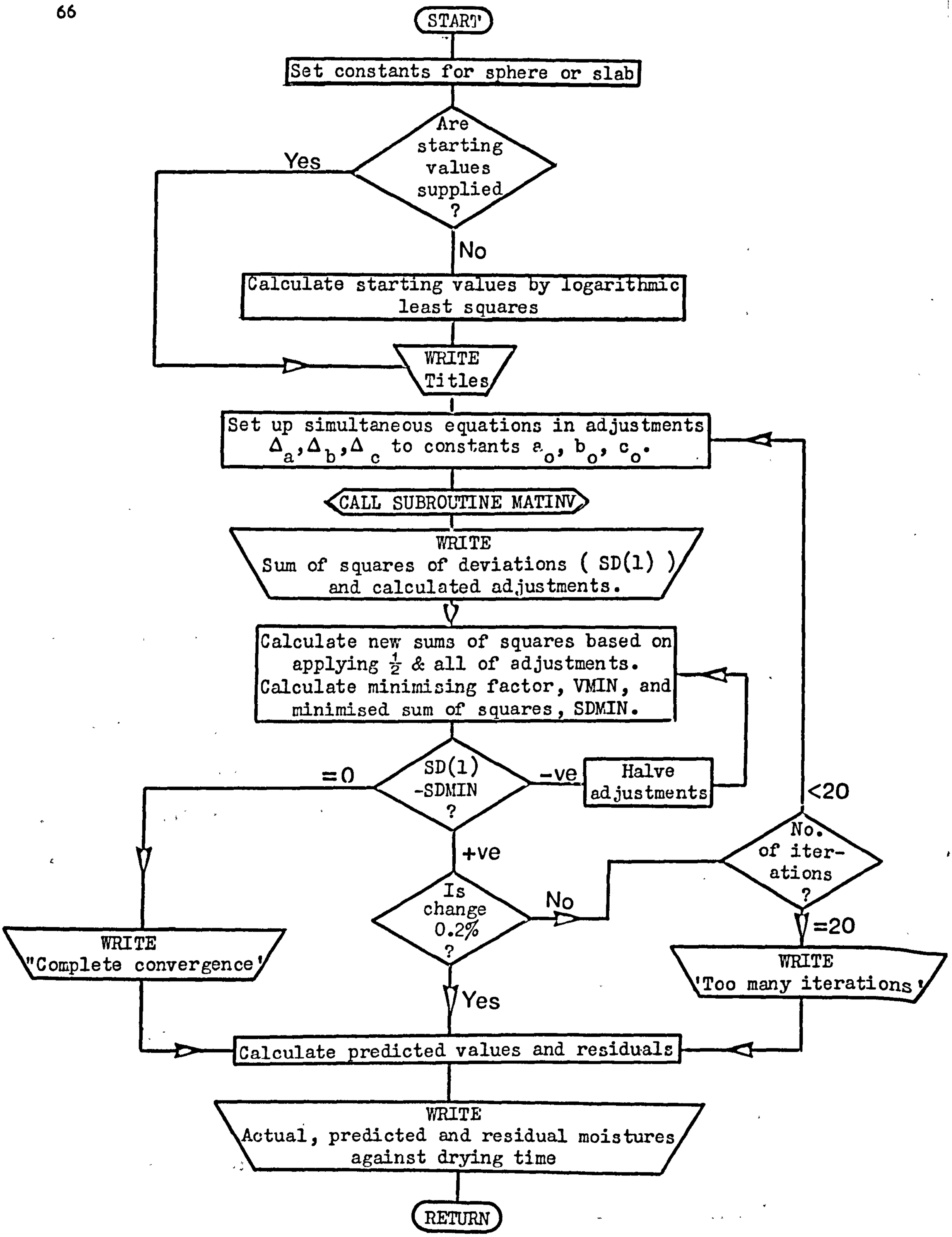

Fig. 3.8 Flow chart for subroutine SEREX

values of time and moisture content output to a separate line file by one of the curve-fitting programmes. PPLOT plotted all the curves from one run on one graph and in the form of continuous lines. Irregularities in the data were indicated by obvious kinks in the lines. PLOT plotted each curve on a separate graph as data points and had the facility to plot the fitted equations 3.1, 3.10, 3.38 and 3.39 given the derived constants. The original plots of the example runs in Fig.3.16 were done in this way.

3.3.2.2. Temperature

In 1970 the temperature data tapes were processed through a Wang desk computer which simply converted the readings (millivolts x 100) into temperatures Celsius and printed the mean values on each channel. In 1971 and 1972 the tapes were processed through the 470 using the FORTRAN programme MENTEM (Appendix 3.1). Three thermocouple positions per drier were scanned by the logger. These were the dry and wet bulb locations in the inlet to each drier fan (or in the case of the packed towers, at the air exit from the top of the towers) and the location in the plenum chamber immediately beneath the drying pan. The programme converted the readings to degrees Celsius and calculated for each time scan, the humidity of the air entering the drier and hence the relative humidity of the air entering the seed. The information from each scan was printed together with the means, standard deviation and maximum and minimum values of the principal quantities. Finally if the differential pressure across the orifice plate was supplied in the input data, the airflow during the run was calculated and printed. The programme could cope with up to 3 drying runs of independent length or any one channel. A specimen output is given in Appendix 3.1

3.3.3. Experimental details

Thin-layer drying experiments were carried out in the 3 seasons, 1970, 1971 and 1972. Those in the first 2 years were primarily concerned with the determination of the mass transfer properties but they also provided some information on the effect of drying treatments on germination. The experiments specifically concerned with determining the effect on germination and the preliminary attempts to determine heat transfer coefficients were carried out in 1972.

3.3.3.1. Mass-transfer experiments, 1970-71

The harvest periods and the method of harvest have been defined in Chapter 2. In farming practice, grass seed is normally dried in the uncleaned condition, but, to reduce variation between samples, the seed used in these tests was all cleaned on a small laboratory cleaner. Whenever possible the drying runs were carried out with freshly-harvested seed but in both years some seed was stored in sealed polythene bags at 1.6°C (35°F) and used on wet days and as a means of prolonging the drying season. Such storage did not appear to harm the seed physically and subsequent germinations were unaffected. In 1971 seed which had been deep frozen to (-15)-(-18)°C was also used to prolong the drying season. When thawed the physical appearance was unchanged but about 80% of the seeds had been killed.

The procedure for setting up the drying runs has already been described in Section 3.3.1.a.

Immediately after drying the samples were transferred to airtight metal tins. The tins were sampled, usually in small batches, for the determination of final moisture content and were stored at 10°C (50°F). To avoid dormancy effects germination testing was delayed until December in both years.

In 1970, 180 runs were carried out, 40 of those were with the variety Sabrina and the remainder with S23. Runs with the Sabrina were necessarily limited because for most of the harvest period only two thin-layer drying units were available. The numbers were gradually increased to 8 during the season. The data obtained in this year contained a number of imperfections chiefly arising from the use of air velocities in the range 9-27 m/min (30-88 ft/min). These gave rise to relatively large weight loss discrepancies and worsened the existing poor response of the temperature controllers. Finally the results which were included in the analysis published in 1971 [81] were taken from the 140 runs with S23. The runs were carried out at temperatures from 27.7°C (82°F) to 61.7°C (143°F) and at initial moisture contents from 40 to 117% d.b. In most cases the runs were allowed to continue until their weight loss had almost ceased, and run times varied between 4 and 50 hours. 95 runs were logged onto punched tape. 36 were not logged but used the automatic weighing system. 9 were manually recorded. The first 21 runs were carried out using a sample size of 150g and the remainder with 100g. 84 were carried out at air velocities in the range 9-11 m/min and gave an average weight loss discrepancy of 3.74 ± 1.56 g.

In 1971, the problems of upthrust were largely solved by the use of lower airflows (4.4 - 6.6 m/min (14-21.5 ft/min)) and the new temperature controllers. But a new problem arose. Early in 1971 the Institute had been connected to a new power supply line and 'noise' in this line began interfering with the automatic weighing system. The interference proved extremely difficult to trace because it occurred irregularly at an average frequency of 3 timesper day and a number of possible 'noise' generating installations within the Institute were suspected and had to be gradually eliminated. Towards the end of the drying season, the problem was almost completely cured by the installation

of a high quality voltage regulator and during the winter of 1971 was completely cured by the addition of further suppression upon individual channels of the automatic weighing system. The effect of the 'spikes' was to cause spurious weight additions on all 8 and occasionally on fewer channels. In the majority of cases the error these caused could be rectified and the data records amended but some runs, particularly those in which the drying rate was low, were lost. The average discrepancy between actual and indicated weight loss was 1.2 ± 1g. The effect of the changing upthrust was now small in comparison with other possible sources of error (e.g. delay in setting up balance, shift in balance zero during run, weight change during pan transfers) and was shown by the number of very small and some negative discrepancies. 210 runs were started in 1971 but only 192 were successfully analysed. The remainder were discarded either because of spurious weight additions or because of excessive fluctuation of temperature or humidity. Such fluctuations were caused either by controller malfunction or inexperience in operation of the packed towers.

3.3.3.2. Germination experiment, 1972

At each of 3 harvest dates for each variety, 100g samples of seed were dried on the thin-layer drier at nominal temperatures of 55°, 60°, 65°, 70° and 75°C and for exposure times at each temperature of $\frac{1}{4}$, $\frac{1}{2}$, 1, 2, 4 and 10 hours. Since drier temperatures can be controlled and recorded with considerable precision, it was felt unnecessary to randomise drier temperatures between each treatment and once each drier had been set to a particular temperature, the setting was left unchanged throughout the experiment. For any particular variety x moisture content combination, the exposure times were carried out serially and, to take account of possible short term storage effects, these treatments were randomised.

Drier temperatures were logged onto punched tape and analysed by MENTEM. A single mean and standard deviation was calculated for each series of exposure times. Differential pressure across the orifice plates was held constant at 0.1 in. which was equivalent to airflows of from 5.9 - 6.1 m/min (19.5 - 20.1 ft/min) depending on air temperature.

At each variety x moisture level, the seed samples were taken from a sieved and aspirated bulk of $\doteq$ 5,000g, direct-harvested immediately before the experiment and stored throughout its duration in a room controlled at 4.5°C (40°F). The bag was removed from this room and allowed to warm up in the laboratory for about 15 minutes before being used. At the end of each exposure, a sub-sample of 11g was taken for moisture content determination and the remainder of the sample transferred to a sample drier for drying to be completed at ambient temperature. A control sample from each bulk was also dried in this way. As the experiment progressed and those treatments which dried the seed below a safe storage moisture content were identified, it became unnecessary to transfer some of the samples to the sample drier. All the dry samples were stored in sealed tins at 10°C (50°F) and were later aspirated once more, as a preliminary to being analysed for purity, 1000 seed weight and germination. The germination tests, which were carried out during October-November, 1972, were performed in the normal way but were allowed to overrun the normal 14 day limit by 7 days to ensure that all delayed germination was recorded. Subjective assessments of mould growth were also made at the end of these extra periods.

3.4. RESULTS

3.4.1. Mass Transfer

3.4.1.1. 1970 Experiments

The analysis of the results from 1970 is based on that published in the Journal of Agricultural Engineering Research (81) in 1971. Subsequent to this analysis, improvements were made to the curve fitting programmes and the subroutine SEREX was developed. With the exception of some once-over fits of the exponential series equations the data was not reanalysed. This was because the data was considered to be markedly inferior to that of 1971 and the necessary extra work involved in transferring the data onto the ICL 470 computer would not be justified.

The results presented are derived from 117 data sets from which the drying curves were calculated using the following experimentally determined error correction function.

$$ER = e^{-0.0045\theta} \qquad \cdots 3.40$$

An impression of the measure of agreement between replicate curves can be gained from *Figs* 3.9 and 3.10 in which are plotted curves for drying air temperatures of 28·8°C (84°F) and 61·7°C (143°F) respectively. The actual conditions are defined in Table 3.1

TABLE 3.1

Details of drying curves in *Figs* 3.9 & 3.10

Fig. no.	*Curve*	*Symbol*	*Temperature (°C)*	*Airspeed (m.min)*	*Initial m.c. (% d.b.)*
3.9	A	X	28·7	9·7	46·3
	B	0	27·9	10·1	46·2
	C	Δ	29·0	9·3	45·7
	D	+	29·2	9·7	45·1
	E	□	29·4	9·2	46·0
3.10	F	X	61·7	10·4	61·9
	G	0	61·7	10·2	60·0
	H	Δ	61·7	10·4	61·0

In all but one case the direct least squares fit of Eqn 3.1 by SINGEX converged, but the similar fits of Eqn 3.10 by DOUBEX failed to do so in 12 cases. In another 8 cases DOUBEX also failed to find starting values for the rapidly decaying exponential term and in another 2 cases gave extremely bad fits. Two examples of the goodness of fit to individual curves are provided by *Figs* 3.11 and 3.12 Plotted in these are the experimental and fitted curves for curve A of *Fig.* 3.9 and curve F of *Fig.* 3.10. The pattern they show is typical of the rest of the data. The logarithmic least-squares fit of Eqn 3.1 tends to fit reasonably well at the end of the curve but badly at the beginning. The direct least-squares fit is much better at the beginning but much worse at the end and with an

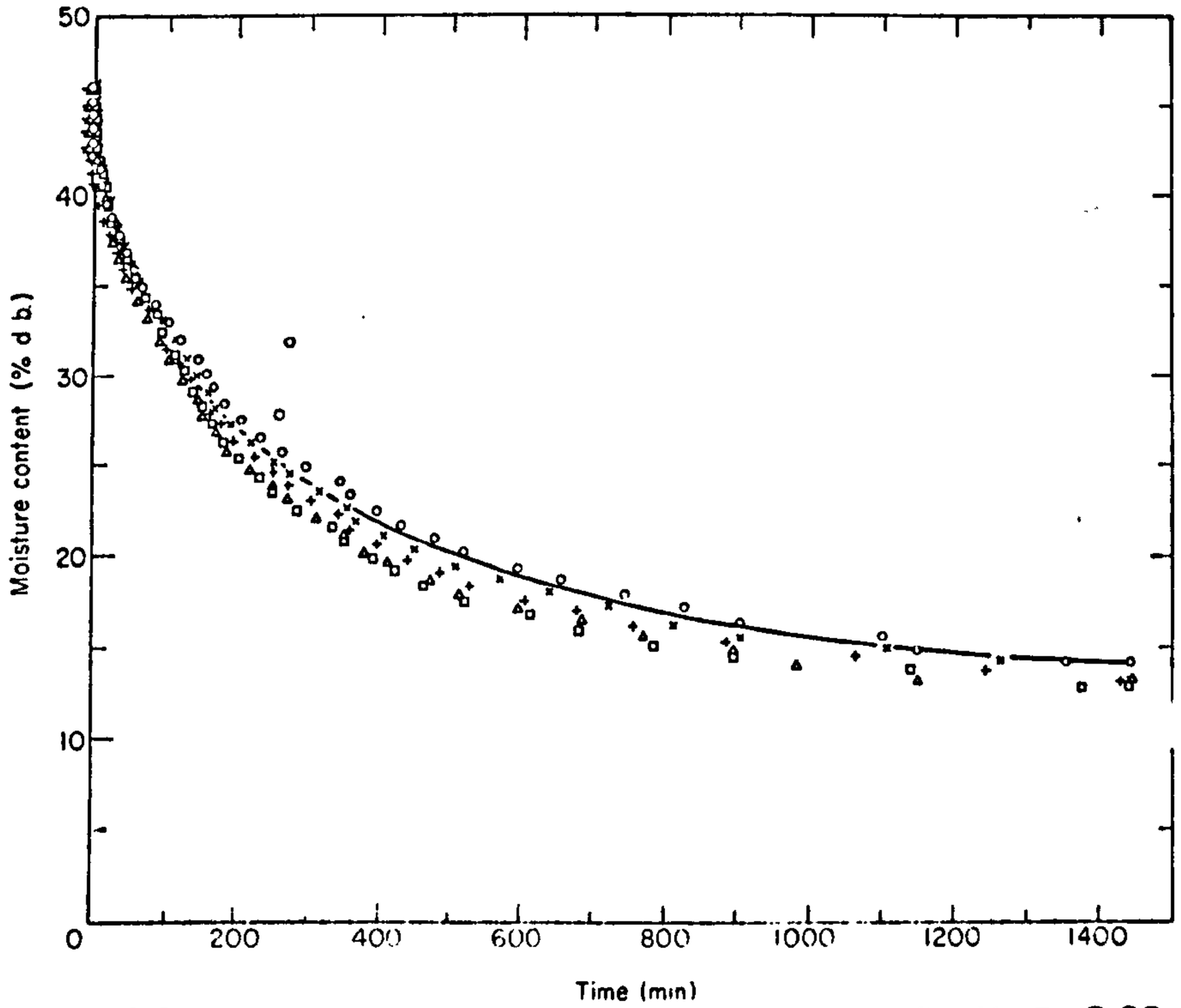

Fig 3.9 *Replicate drying curves for 28·8°C. Solid line = curve predicted by Eqn* 3.38 (1970 data)

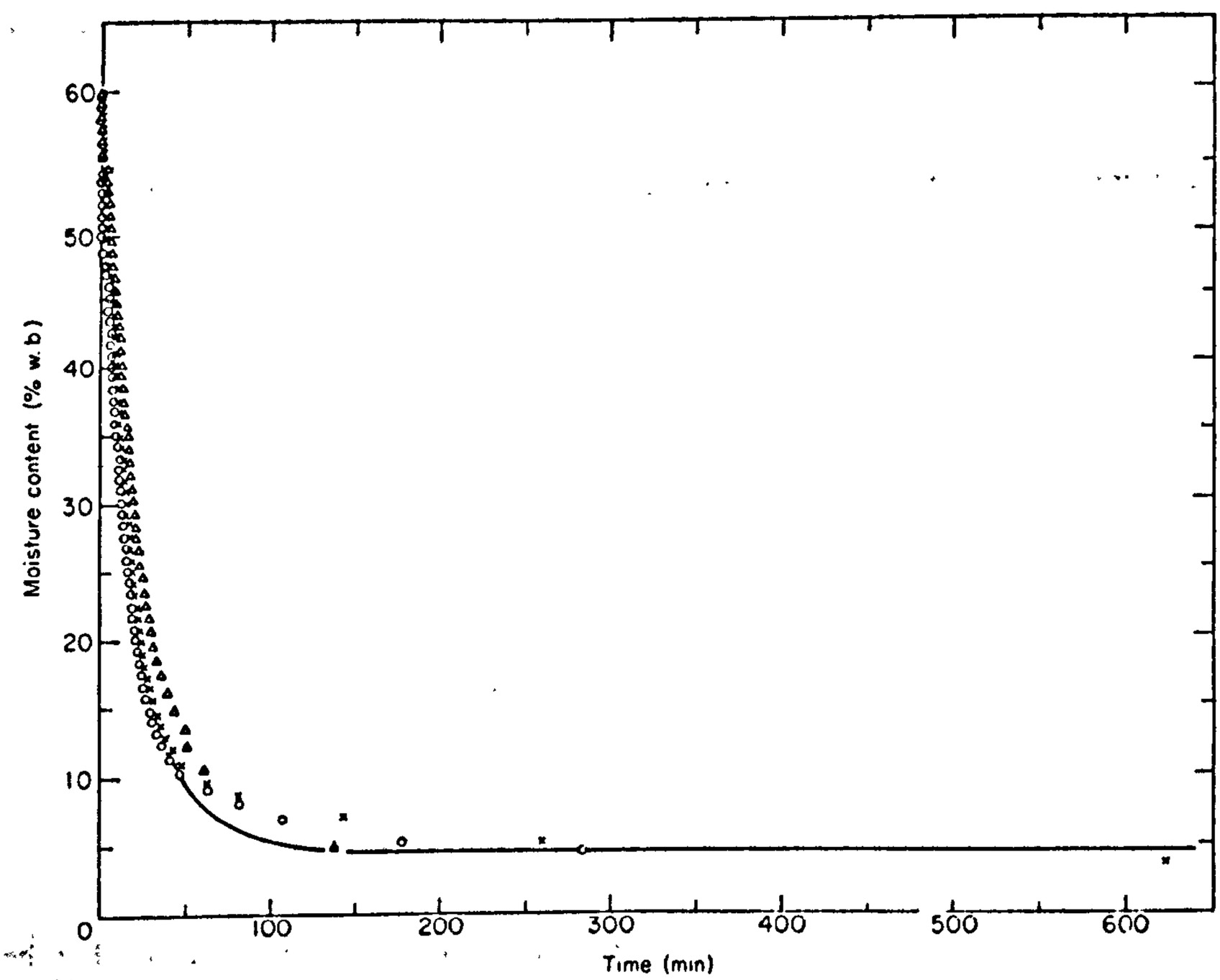

*Fig.*310 *Replicate drying curves for 61·7°C. Solid line = curve predicted by Eqn* 3.38 (1970 data)

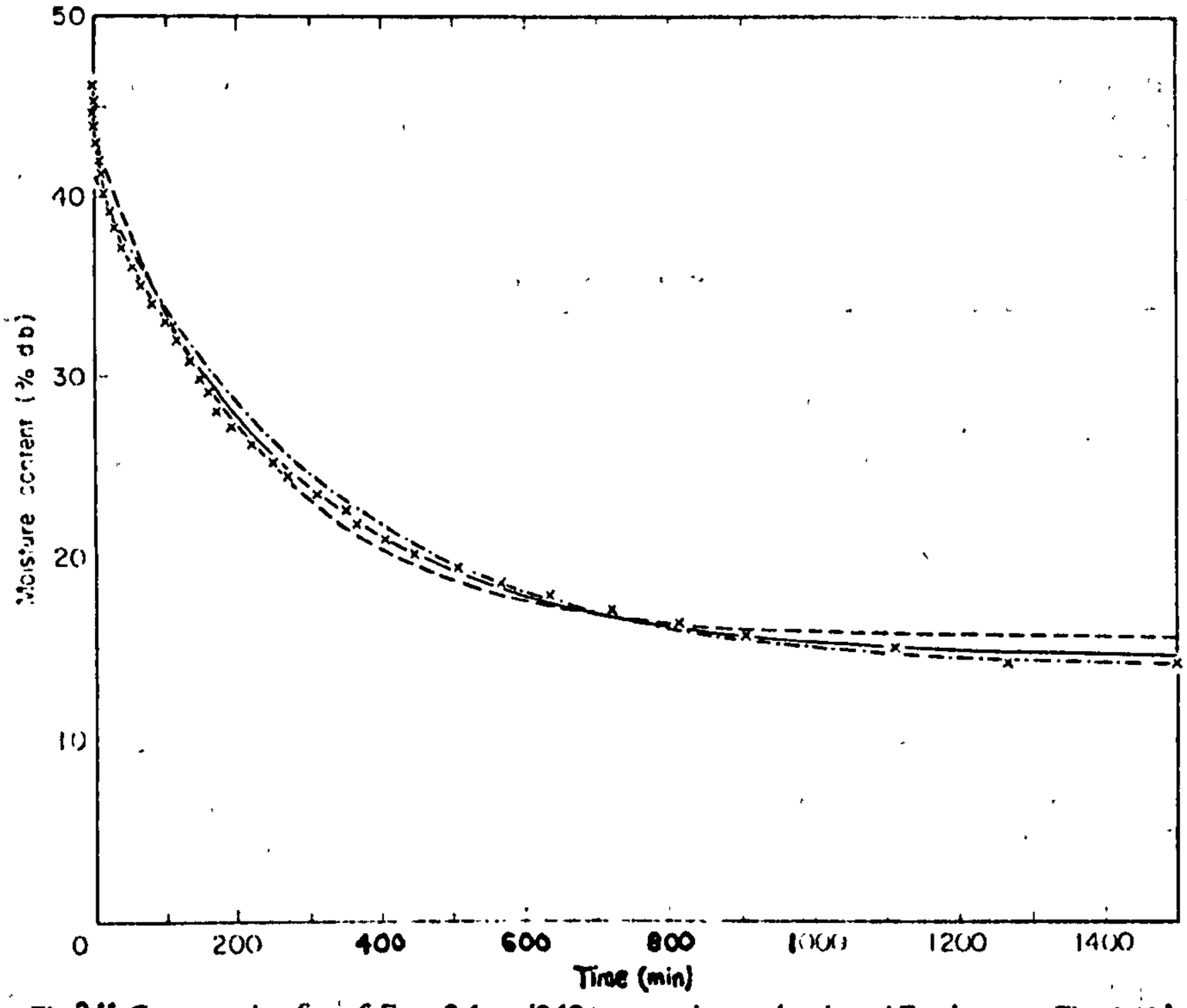

Fig 3.11 *Comparative fits of Eqns* 3.1 *and* 3.10 *to experimental points.* (*For key see Fig.* 3.12)

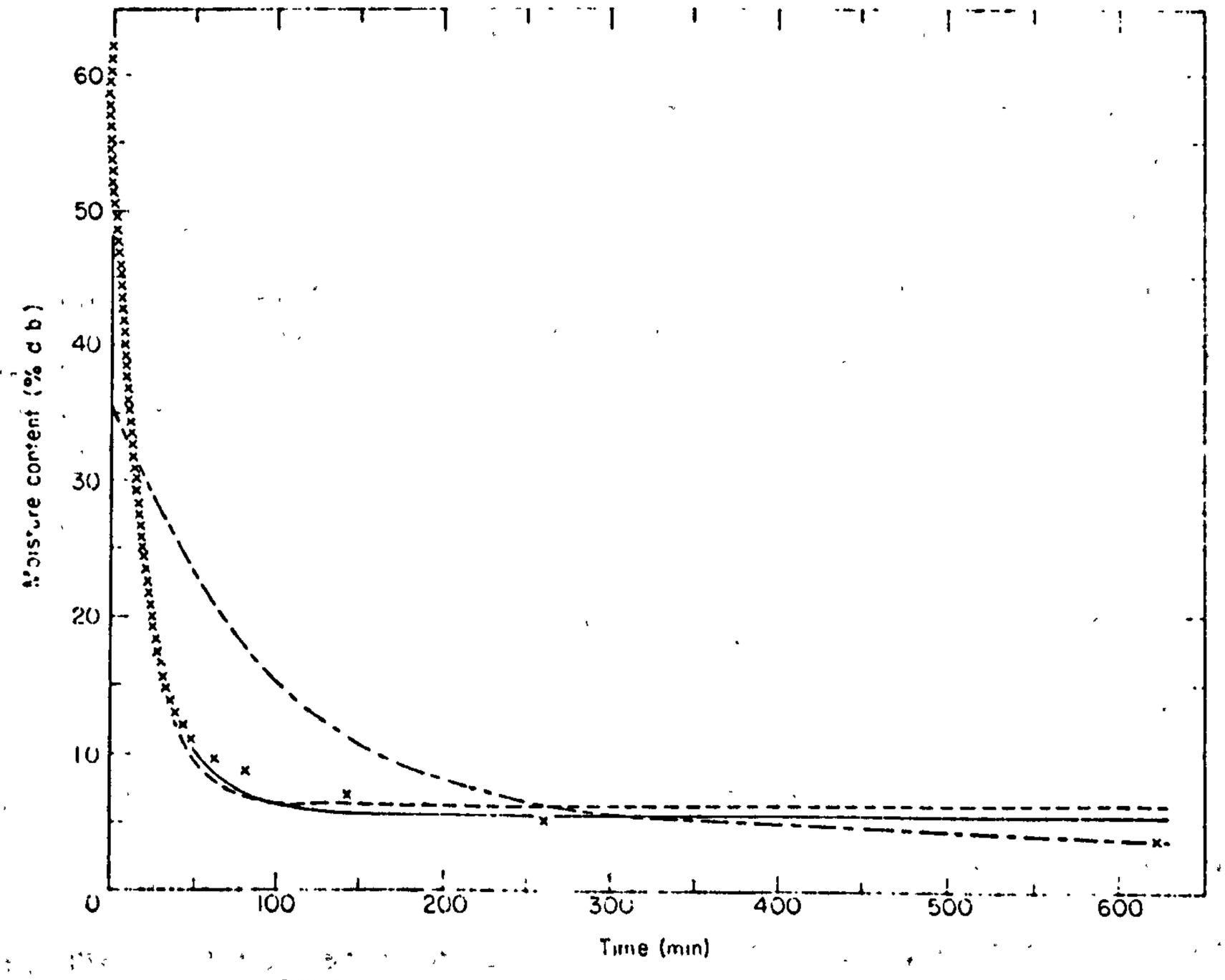

Fig. 3.12 *Comparative fits of Eqns* 3.1 *and* 3.10 *to experimental points*

———— *log least squares Eqn* 3.1

– – – – – – *direct least squares Eqn* 3.1

———— *direct least squares Eqn* 3.10

asymptotic value appreciably higher than the final moisture content. Eqn 3.10 provides a further improvement and falls roughly between the 2 single exponential curves. The constants of these fits are given in Table 3.2 together with the variance of the observed data from the calculated lines.

TABLE 3.2

Values of constant in fitted curves of *Figs* 3.11 & 3.12

Curve	*Fit*	*A*	*k or* k_1	*B*	k_2	M_e	*Variance*
A	Eqn (1) Logarithmic	27·4	0·00308			13·7	2·197
	Direct	27·9	0 00428			15·4	1·058
	Eqn (3)	25·9	0·00331	5·19	0·08613	14·3	0·153
F	Eqn (1) Logarithmic	32·1	0·01036			3·60	347·8
	Direct	53·7	0·05533			6·09	0·65
	Eqn (3)	23·8	0·03541	31·2	0·07516	5·28	0·51

The k values derived from the 2 fits of Eqn 3.1 and from the more slowly decaying term of Eqn 3.10 were clearly a function of drying air temperature and were fitted to the relationship

$$k = Ae^{BT} \qquad \ldots 3.41$$

where T = temperature, °C

and A and B are constants. The numerical values of these constants are given in Table 3.3 and the experimental data plotted in *Fig.* 3.13 & 3.14

TABLE 3.3

Values of the constants A and B in Eqn 3.41

Source of K	A	B	*No. of values*	*Variance*
Single exponential—logarithmic	0·0003673	0 05326	117	0·00335
—direct	0·0001535	0·09432	116	0·00369
Double exponential	0·0001707	0·08754	92	0·00306

The k values given by the more rapidly decaying term of the double exponential were not obviously related to either drying air temperature or initial moisture content.

Other factors which may have influenced the values of k are the variation in purity and 1000 seed weights of the samples. Although no attempt was made to relate these 2 parameters to the value of the constant, it should be noted that at the start of harvest the purity of the seed was low and ranged between 65 and 88%, only rising to 90% after the first 23 runs. Thereafter, it was commonly of the order of 94%. The 1000 seed weights followed a similar pattern to that of the controls.

Values of the asymptotic constant, Me, were plotted against relative humidity in Fig. 3.15. Since variation in relative humidity caused by variations in inlet absolute humidity were small in relation to those caused by the range in drying air temperature, the data contain a strong temperature effect and were fitted by the equation

$$Me = a - b \ln T - c \ln (1 - rh) \qquad \ldots\ldots\ldots\ldots 3.42$$

where the values of the constants were a = 34.75, b = 7.76 and c = 11.53. Fitted curves for 30 and 60°C are plotted in Fig. 3.15.

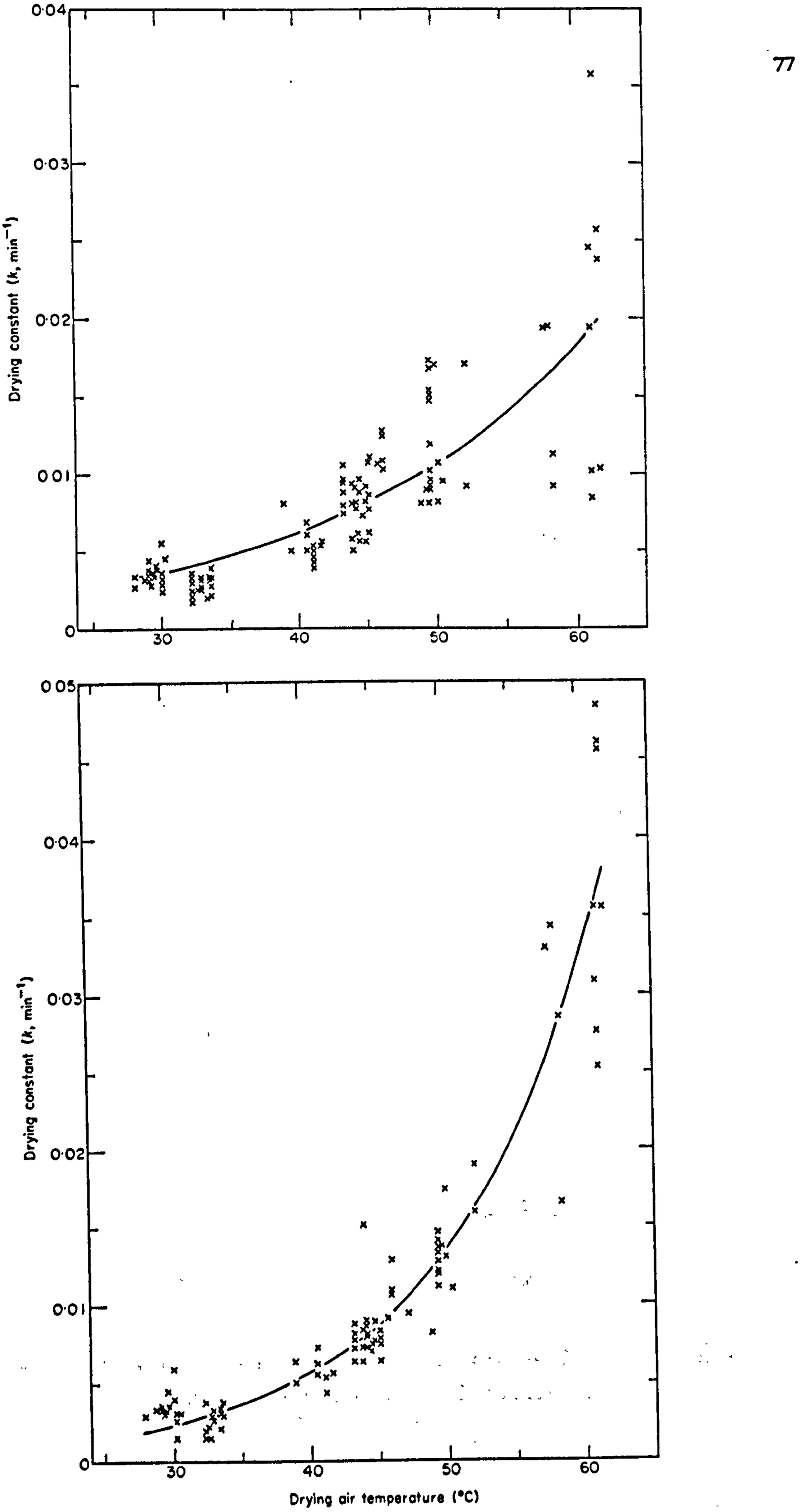

Fig. 3.13 Plots of drying constant k against drying air temperature for logarithmic least squares fit of Eqn. 3.1 (top) and direct least squares fit of Eqn. 3.10 (bottom)

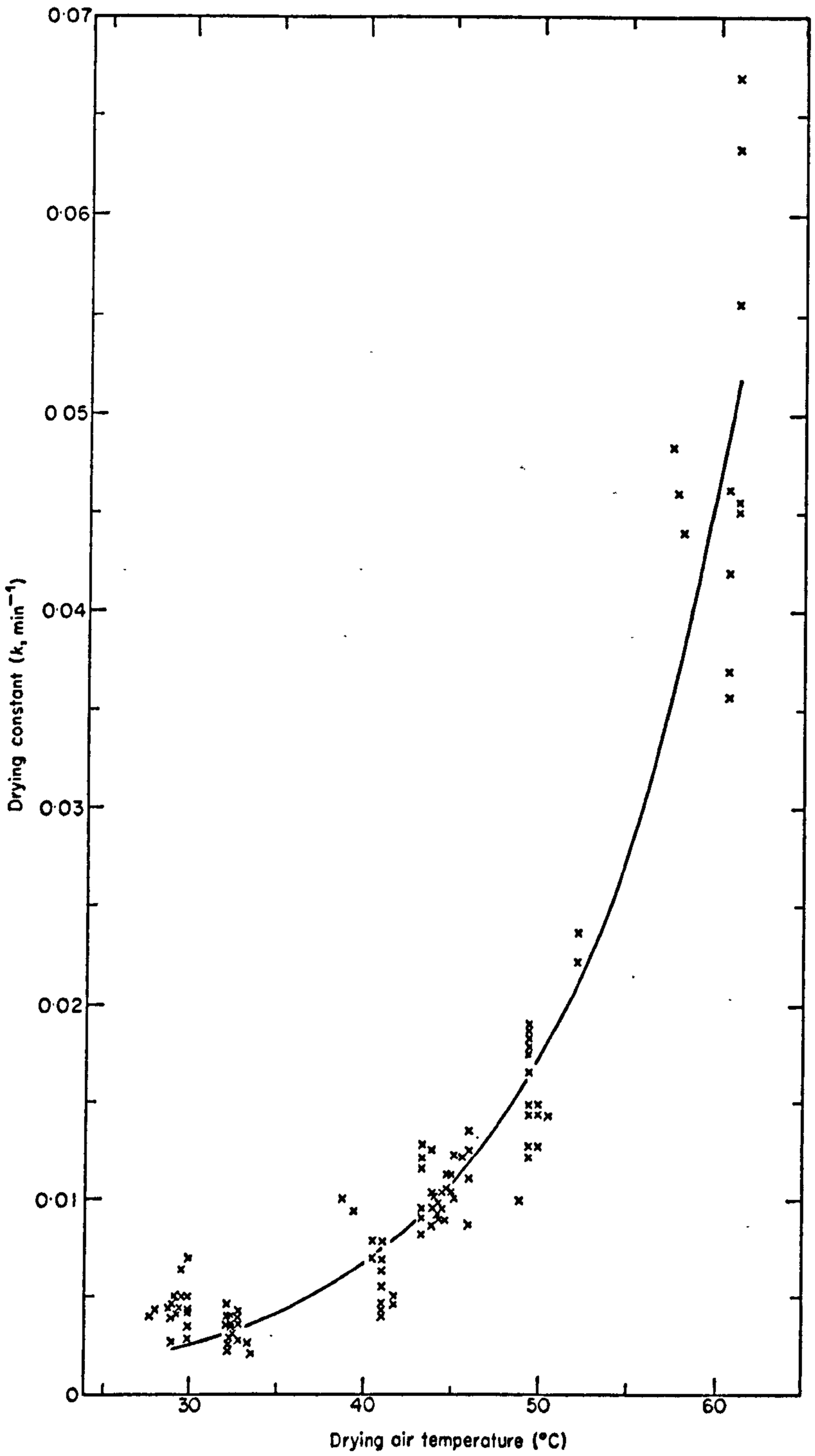

Fig. 3.14 Plot of drying constant k against drying air temperature for direct least squares fit of Eqn. 3.1

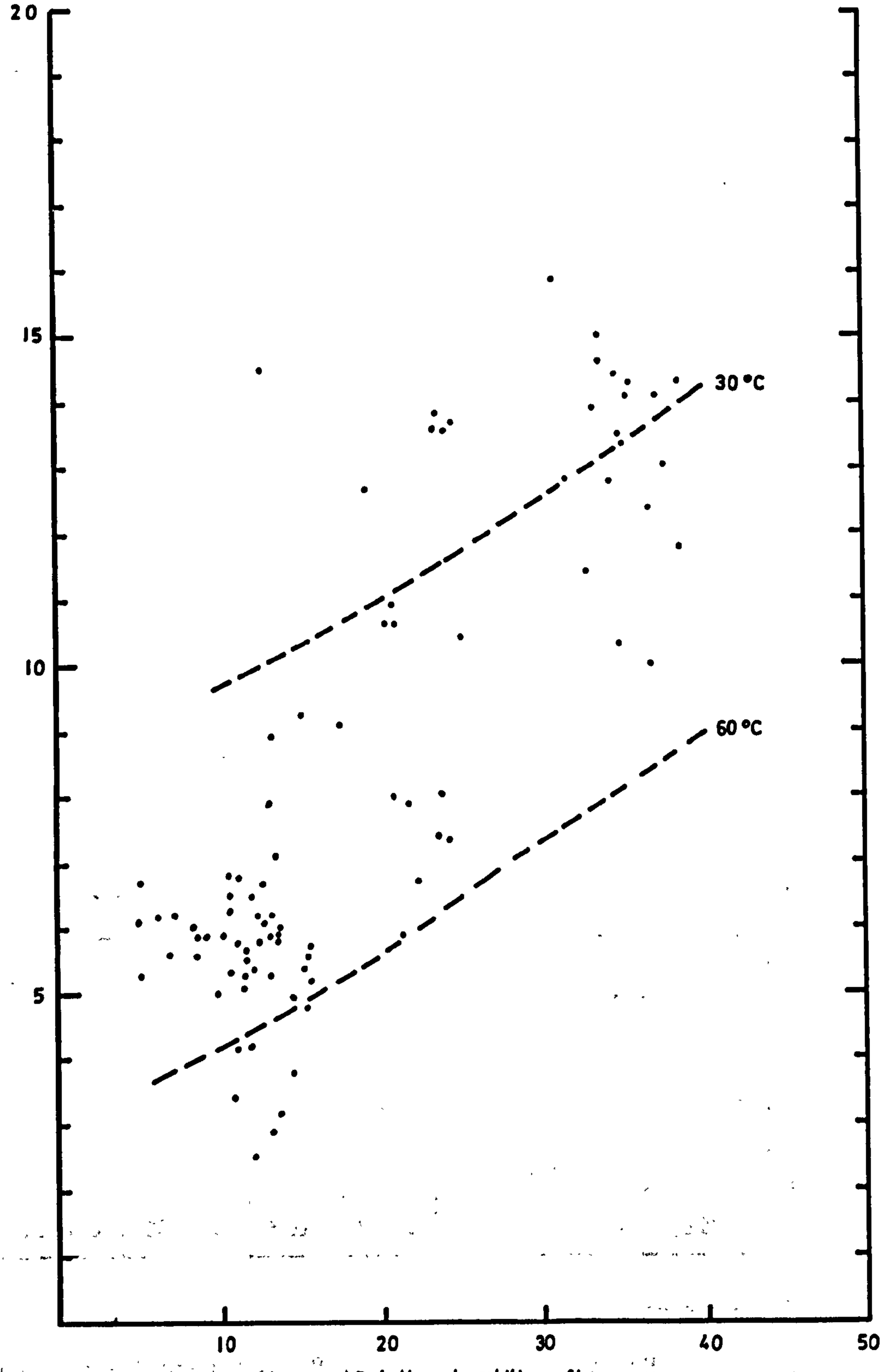

Fig. 3.15 Plot of eqiulibrium moisture contents against relative humidity with fitted lines of equation 3.42 at 30°C and 60°C (1970 data).

3.4.1.2. 1971 Experiments

The drying conditions in this series of tests are summarised for each variety in Table 3.4. The main difference between the varieties was the range of initial moisture contents; for Sabel the range was wide, 23.2 - 99.9% d.b. compared to 62.1 - 75.4% d.b. for S.23 but the mean values, 67.8 and 69.8% respectively, were comparable. The range for S.23 was less than it was in 1970. For the other variables the improvements made to the apparatus made a greater range possible. The temperature range was extended downwards by the use of the cooling unit on drier 6 and relative humidities up to 93.6% were achieved using the packed tower on drier 8.

Table 3.4

Drying conditions in 1971 thin-layer experiments

Condition	Crop			
	Sabel		S.23	
	Mean	Range	Mean	Range
Initial moisture, % d.b.	67.8	23.2 - 99.9	69.8	62.1 - 75.4
Final moisture, % d.b.	10.5	4.6 - 45.9	10.3	3.5 - 31.1
Temperature, °C	37.7	15.5 - 62.6	37.2	12.9 - 63.4
Relative humidity, %.	31.0	7.4 - 93.6	34.2	6.8 - 92.5
Humidity, kg/kg.	0.0105	0.0044-0.0235	0.0109	0.0061-0.0255

Goodness of fit

Equations 3.1, 3.10, 3.38, 3.39 were fitted to the data by the improved versions of SINGEX, DOUBEX and SEREX. Initial starting values were calculated within the subroutines but most of the curves were also fitted using externally supplied estimates. Where the original fit had been poor it was usually much improved

by the second attempt. In cases where the original fit had been good, the second attempt would normally converge to the same solution. All the subroutines worked by minimisation of the sums of squares of the deviations and for comparisons of goodness of fit this quantity was converted to the variance and hence the mean standard deviation, σ , (% d.b.) of predicted values of moisture content.

$$\sigma = \sqrt{\frac{\sum \left(M_{observed} - M_{predicted} \right)^2}{\text{No of data points}}} \qquad \ldots\ldots 3.43$$

By this measure the fits obtained from DOUBEX of the 2 term-exponential equation, 3.10, were superior to the others (Table 3.5). The mean σ , 0.41, is no greater (and for higher moisture contents is certainly less) than the error involved in determining moisture content in the laboratory. The exponential series for a plane sheet, gave the next lowest σ , 1.31% followed by the similar equation for a sphere, 1.81% and finally the single exponential equation, 2.20%. The worst range in σ was given by the fits of equation 3.38 for a sphere and this was the equation which was the most sensitive to starting values.

Table 3.5

Standard deviations of predicted from observed values derived from fits of 4 alternative diffusion equations.

Equation	Standard deviation σ	
	Mean	Range
Single exponential (3.1)	2.20	0.3 - 3.86
2 term-exponential (3.10)	0.41	0.07 - 1.40
Plate (3.39)	1.31	0.16 - 2.59
Sphere (3.38)	1.81	0.26 - 5.21

Visual comparisons of the fits given by the 4 equations are provided by the 3 examples drawn in Fig.3.16 and defined by Table 3.6. In the first case, Run 66, the best overall fit (i.e. lowest σ) is given by the 2-term exponential but the final data points are better fitted by the single exponential. The lines for the sphere and for the plate are approaching asymptotes greater than and less than respectively, the data points but the line for the plate has a much lower overall σ . In Run 106, the 2-term exponential is again the best fit and approaches a lower asymptote than the data. In this example, the line for the plate is better than that for the single exponential which now overestimates the final data values. So does the line for the sphere and this is the worst fit by a considerable margin. The final example, Run 207, a run carried out at high humidity, demonstrates the ability of the 2-term exponential to adapt to the shape of the drying curve to an extent the other 3 expressions cannot. Of these 3, the deviations are best minimised by the sphere and the single exponential is the worst.

Table 3.6

Drying conditions and standard deviations of the fitted curves for Runs 66, 106 and 207 drawn in Fig 3.16.

Condition	Run No		
	66	106	207
Initial moisture content, % d.b.	82.2	73.5	73.6
Final moisture content, % d.b.	5.2	6.9	19.6
Drying air temperature, °C	62.3	40.3	32.8
Humidity, kg/kg	0.0103	0.0104	0.0249
Relative humidity, %	7.6	21.0	79.5
No. of data points	84	71	51
Standard deviations (% d.b.) of-fitted curves:-			
Single exponential	1.17	1.61	2.77
2 term exponential	0.61	0.31	0.37
Exponential series - plate	1.36	0.91	1.81
- sphere	3.13	2.43	1.43

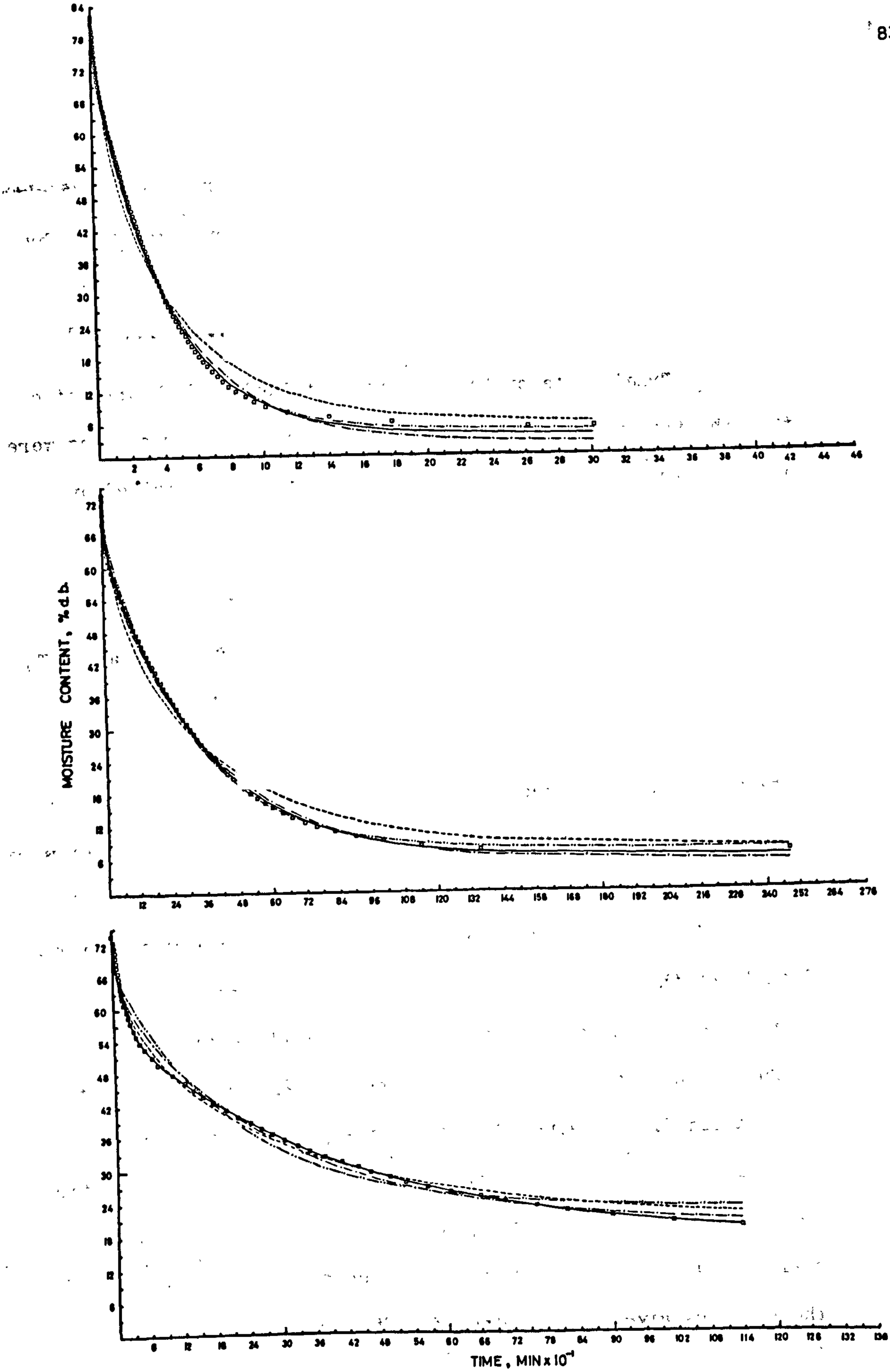

Fig. 3.16 Comparative fits given by equations 3.1(- - - - -),3.10(———),
3.38(-·-·-·-) and 3.39(-·-·-) for Runs 66(top),106(middle)
and 207(bottom). 1971 data.

Comparison of drying rate constants

In 1970 the k values generated by the fits obtained with SINGEX and DOUBEX were expressed as a function of temperature by the equation

$$k = A \exp (bT) \quad \ldots\ldots\ldots\ldots\ldots 3.41$$

Trial plots of the k values obtained in 1971 indicated that the two variables, humidity and initial moisture content were also influencing the results and a better fit was obtained by fitting the equation

$$k = A \exp (bT + cH + dMo) \quad \ldots\ldots\ldots\ldots\ldots 3.44$$

This was done by multiple regression of ln k against T, H and Mo using the computer statistical package GENSTAT [74]. For each set of k values the analysis was carried out on all the data and on the data separated into varieties. The correlations with the variables obtained by analysing all the data together were inferior to those obtained by separate analysis of each varietal set and significant differences in varietal response were proven. Details of the regression analyses including the statistical comparisons of the coefficients between varieties and between diffusion equations are given in Appendix 3.2. The coefficients in equation 3.44 obtained for each variety and each diffusion equation are summarised in Table 3.7. Of the 2 sets of coefficients given for the 2-term exponential it is the second and smaller value of k, k_2, which can be regarded as comparable with the k values given by the other 3 diffusion equations.

Table 3.7

Values of coefficients in equation 3.44 expressing drying constant, k, as a function of temperature, initial moisture content and absolute humidity

Source of k	Crop	Coefficient			
		A	b	c	d
Single exponential	Sabel	0.000490	0.0797	-55.07	-0.00778
	S.23	0.001193	0.0660	-23.02	-0.00799
2 term exponential	Sabel	.0628	0.0601	-10.75	-0.01384
k_1	S.23	.008998	0.0609	-77.01	+0.02527
k_2	Sabel	.000322	0.0888	-73.20	-0.00709
	S.23	.000624	0.0758	-31.16	-0.00756
Exp.series -sphere	Sabel	.000282	0.0809	-46.40	-0.00815
	S.23	.000433	0.0756	-24.80	-0.00586
Exp.series -plate	Sabel	0.000342	0.0830	-46.48	-0.00877
	S.23	0.000682	0.0725	-25.31	-0.00742

The k values derived from the fits of equation 3.39 (the plate) are plotted in Fig.3.17. The fitted lines represent the fits of equation 3.44 evaluated at the mean H and Mo for each data set. Similar plots of the k values derived for equations 3.1, 3.10 and 3.38 are given in the Appendix3.2.

The statistical comparisons of the coefficients in Table 3.7 indicated that the varietal difference was most marked for the k_2 term of the 2-term exponential equation, where the differences between the coefficients of T and H were both significant at the 0.001% level. The effect of the temperature difference is illustrated in Fig. 3.18. The drying rate constant for Sabel is less than that for S.23 over the whole temperature range but the difference decreases with increasing temperature. Since this is a logarithmic difference, the ratio k_{S23}/k_{Sabel} is decreasing.

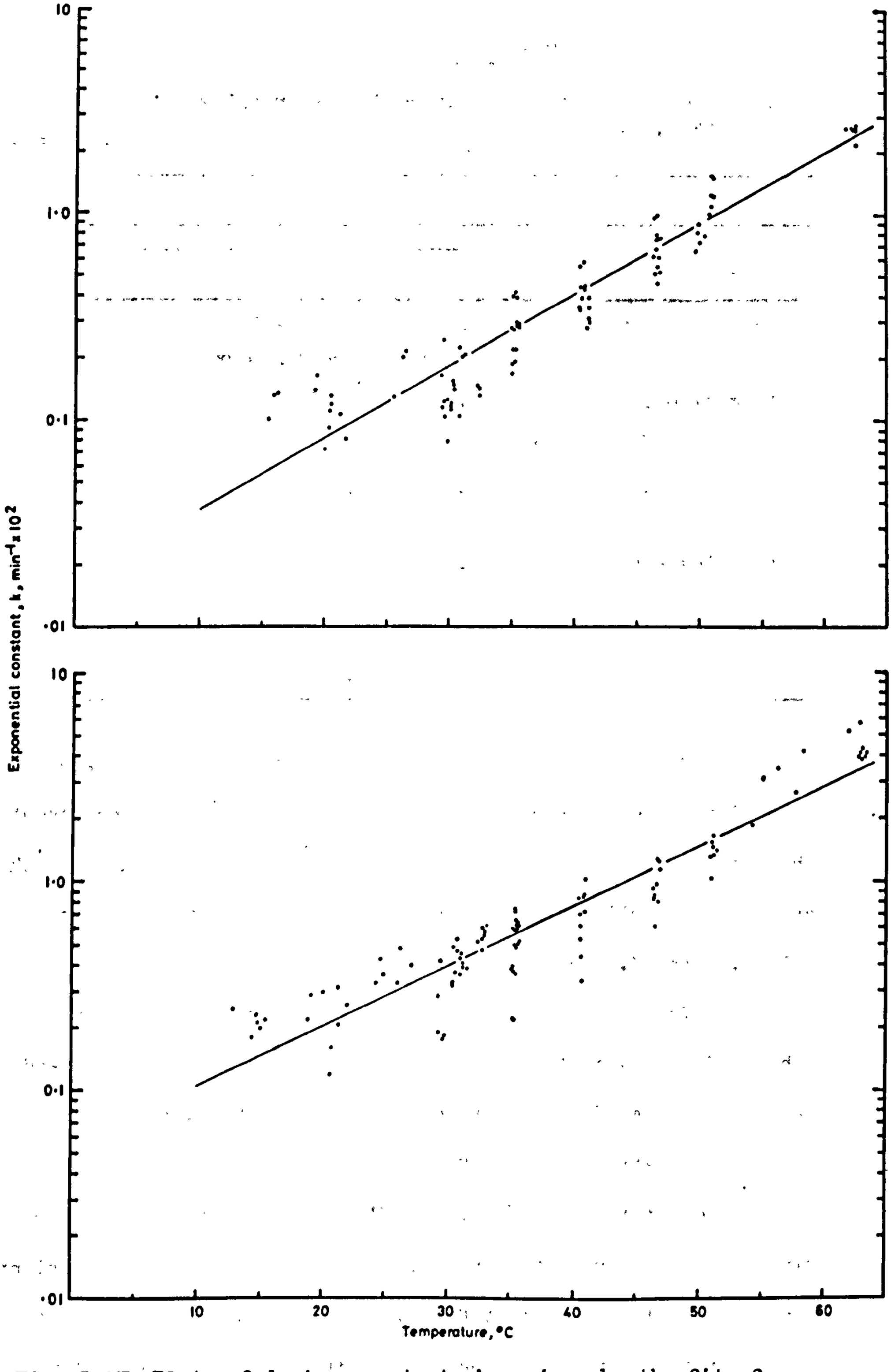

Fig. 3.17 Plots of drying constant, k , given by the fit of equation 3.39 to 1971 data for Sabel (top) and S23 (bottom) Fitted line plotted at mean humidity and initial moisture content for each data set.

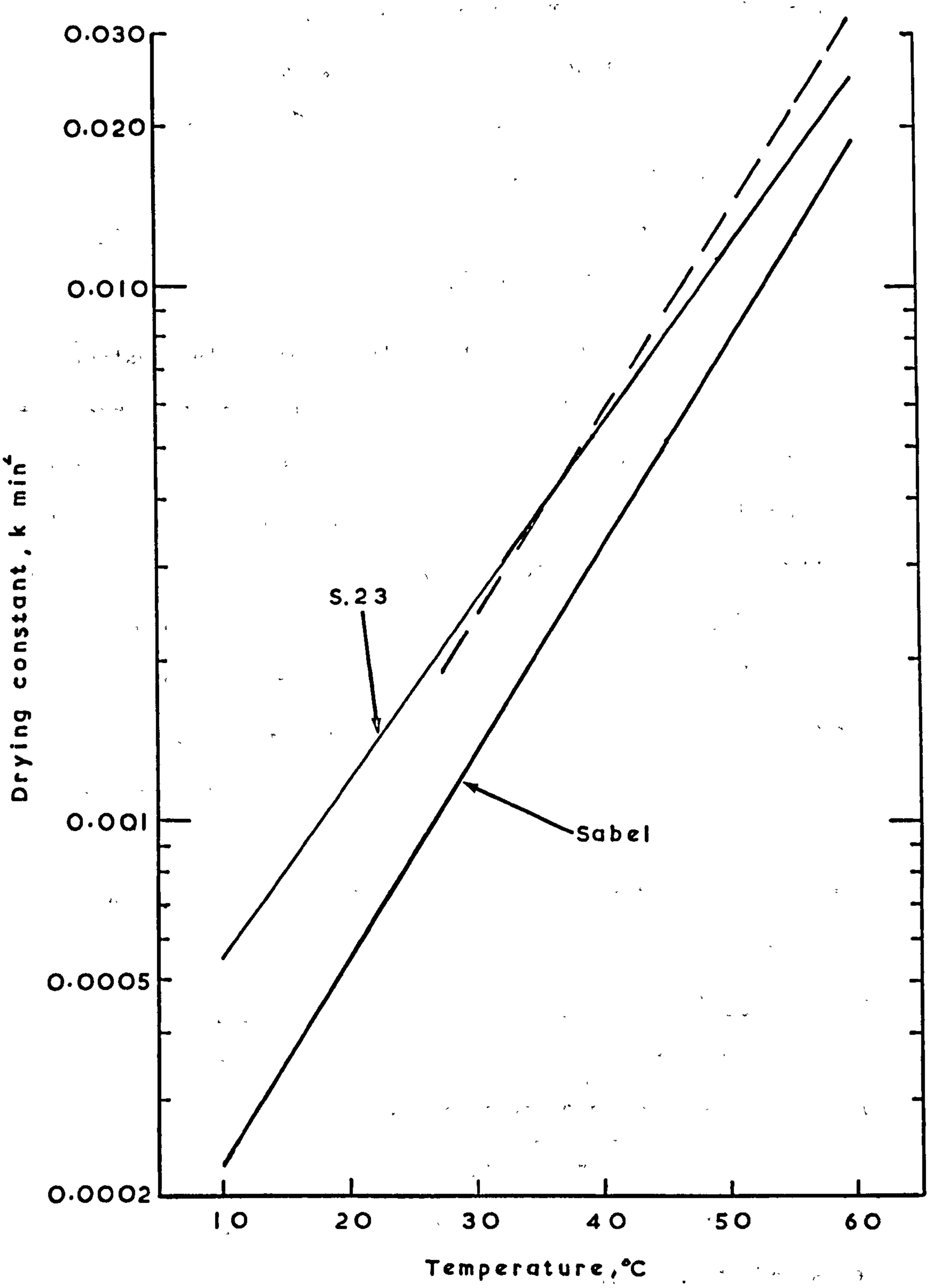

Fig. 3.18 Drying constarts, k_2 , of equation 3.10 as a function of temperature for Sabel and S23. —— 1971 data. – – – 1970 data.

The effect of air humidity is illustrated in Fig.3.19 by plots of k values derived from drying curves in the temperature range 29.2-32.9°C. The fitted lines for Sabel and S.23 were evaluated at the mean temperatures, 30.2 and 31.1°C and mean initial moisture contents, 65.9 and 70.5% d.b. respectively of the data subsets plotted. The value of k is reduced by increasing humidity and the effect is greater for Sabel than for S.23 (i.e. $k_{S.23}/k_{Sabel}$ increases).

The differences between the drying rate constants given by the alternative diffusion equations are less than those between varieties. Where they existed, significant differences were most frequently associated with temperature. Fig. 3.20 compares the regression equations obtained for the 4 sets of k values for S.23. As in 1970, the values of k given by the direct iterative fit of the single exponential (eqn. 3.1) were larger than those from the 2-term exponential (eqn.3.10). The plate(eq3.39) gave values very similar to those of 3.10 whilst the lowest values were given by the sphere. This order reflects the contribution to describing the early part of the drying curve made by the extra term in the equations.

Comparison of 1971 and 1970 drying rate constants

For several reasons statistical comparison of the k values obtained for S.23 in 1971 with those obtained in the previous year could not be carried out. A visual comparison of values for the 2 term exponential is made in Fig.3.18. The agreement between years is very good indeed.

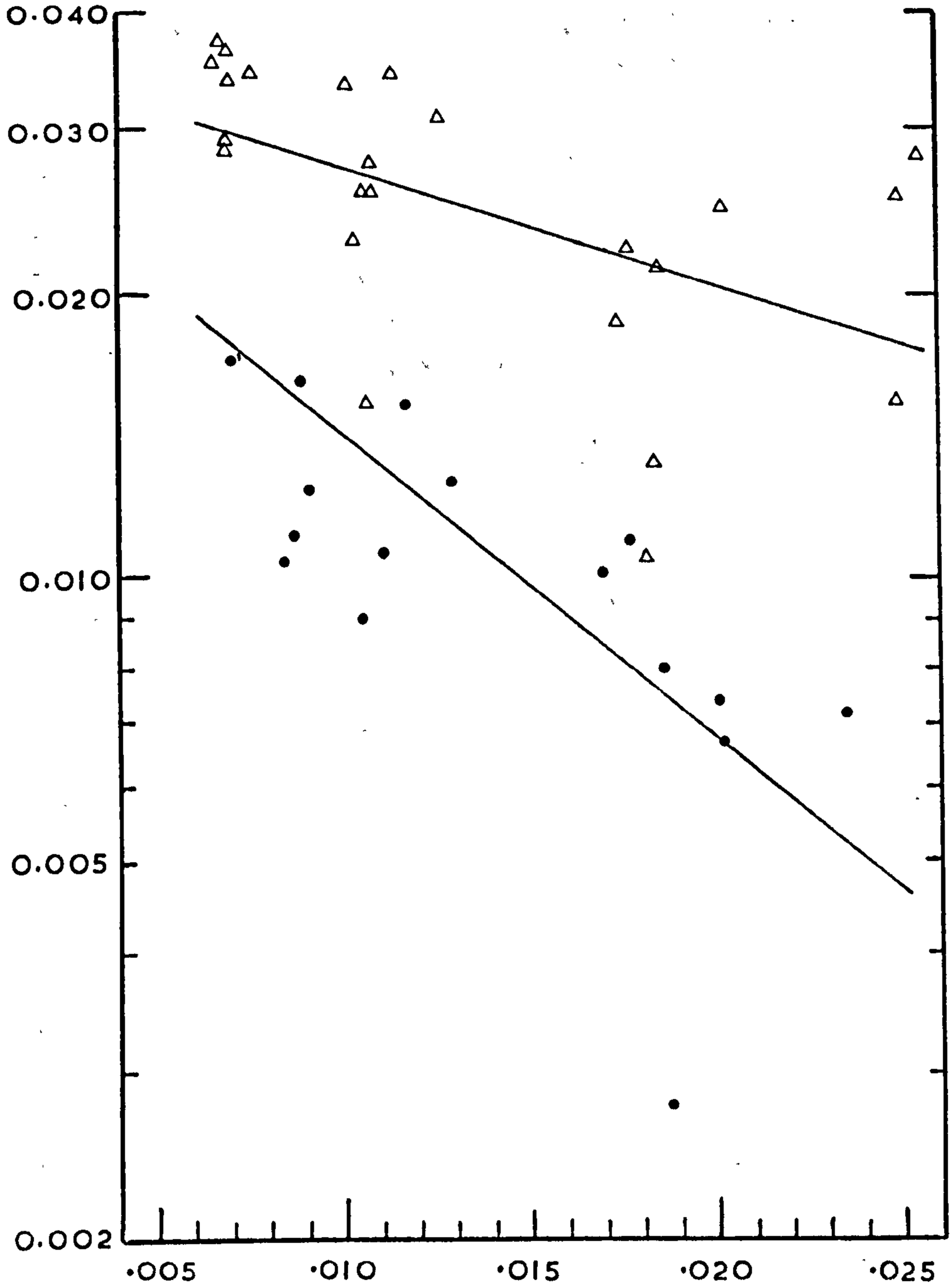

Fig. 3.19 Drying constant, k_2 ,of equation 3.10 as a function of air humidity for Sabel(•) and S23(Δ). 1971 data.

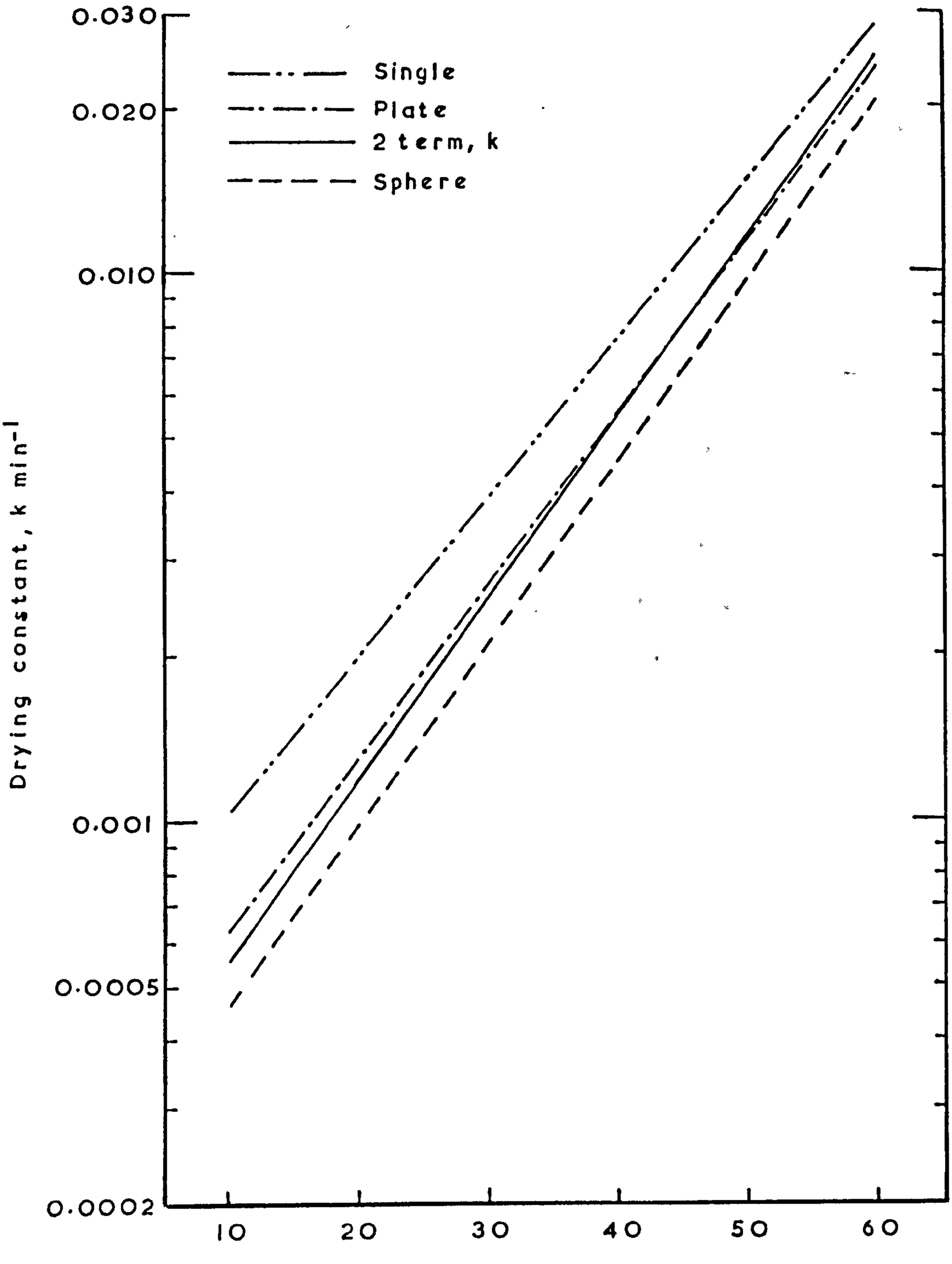

Fig. 3.20 Drying constant ,k, as a function of temperature for 4 alternative drying curve equations fitted to 1971 data for S23

Comparison of asymptotic moisture values

Values of Me given by the fits of equations 3.10 are plotted in Fig.3.21 and similar plots of the values given by the other three fits are in Appendix 3.2 . Equation 3.42 was fitted to each set of values and the constants obtained are tabulated in Table 3.8. Because of significant differences in the residual variances, statistical comparison of the coefficients between varieties and in the case of S.23, between years, was not valid.

Table 3.8

Values of the constants a, b, c in equation 3.42 for asymptotic moisture content classified by variety and source of values

$$Me = a - b \ln T - c \ln (1 - rh)$$

Source of asymptotic values	Crop	Constant		
		a	b	c
Single exponential	(Sabel	15.09	2.83	12.93
	(S.23	25.67	4.85	8.90
2 term exponential	(Sabel	7.77	1.15	9.56
	(S.23	18.84	3.66	8.64
Exponential series plate	(Sabel	5.06	0.63	13.18
	(S.23	15.70	2.82	9.11
sphere	(Sabel	11.71	2.14	12.85
	(S.23	12.41	1.80	9.11
Final moisture	(Sabel	13.18	2.29	10.71 *
	(S.23	16.50	3.05	9.02

* 4 values deleted from data set.

However, there is a difference of practical significance which is illustrated in Fig.3.22. The values of Me are greater for S.23 than Sabel; the difference is very small at 60°C but increases with reducing temperature and is of the order of several % d.b. at 10°C. The temperature effect in Sabel is clearly small and in the case of the values derived from fitting

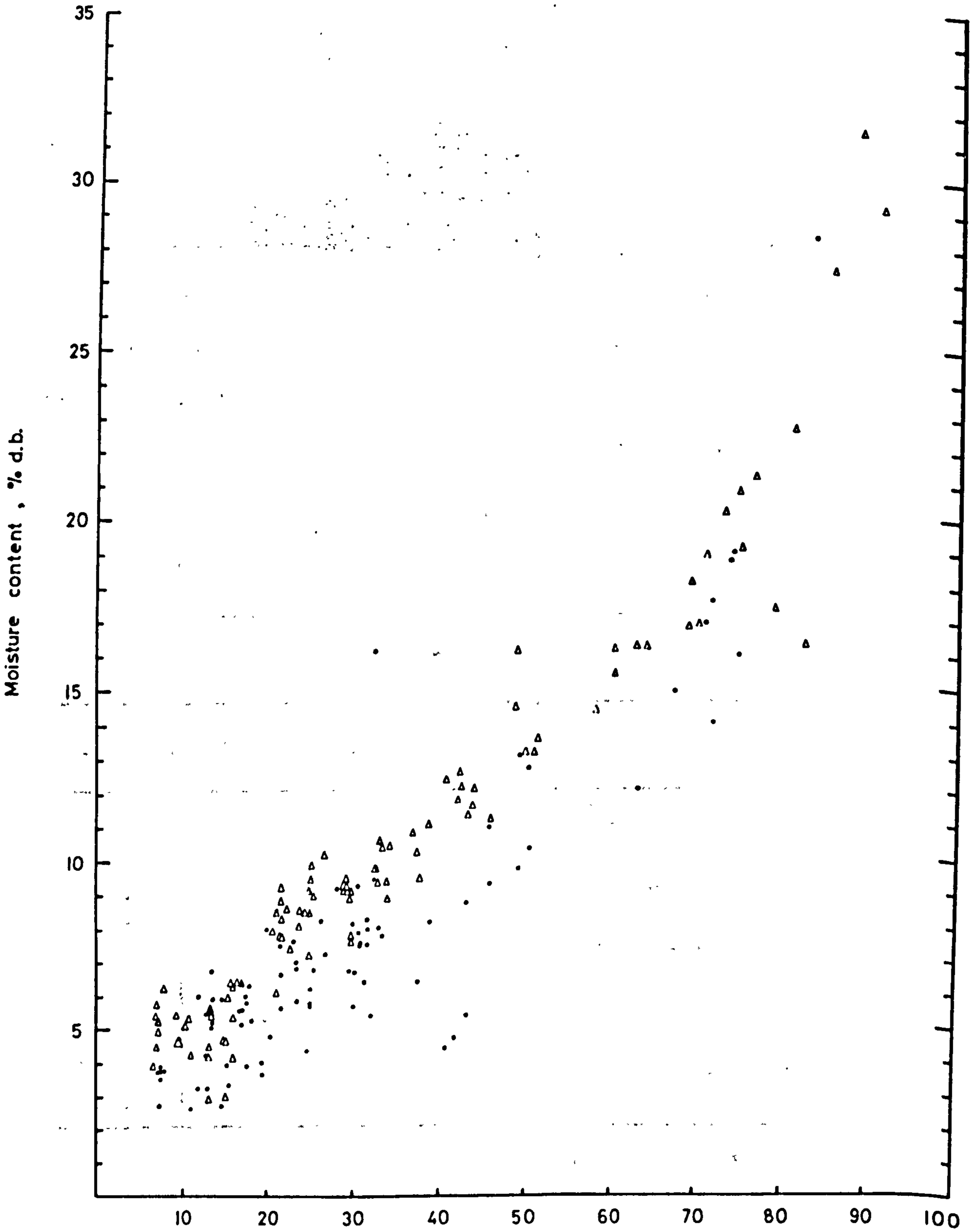

Fig. 3.21 Asymptotic constants, Me, derived from fits of equation 3.10 plotted against relative humidity for Sabel(•) and S23(Δ). 1971 data.

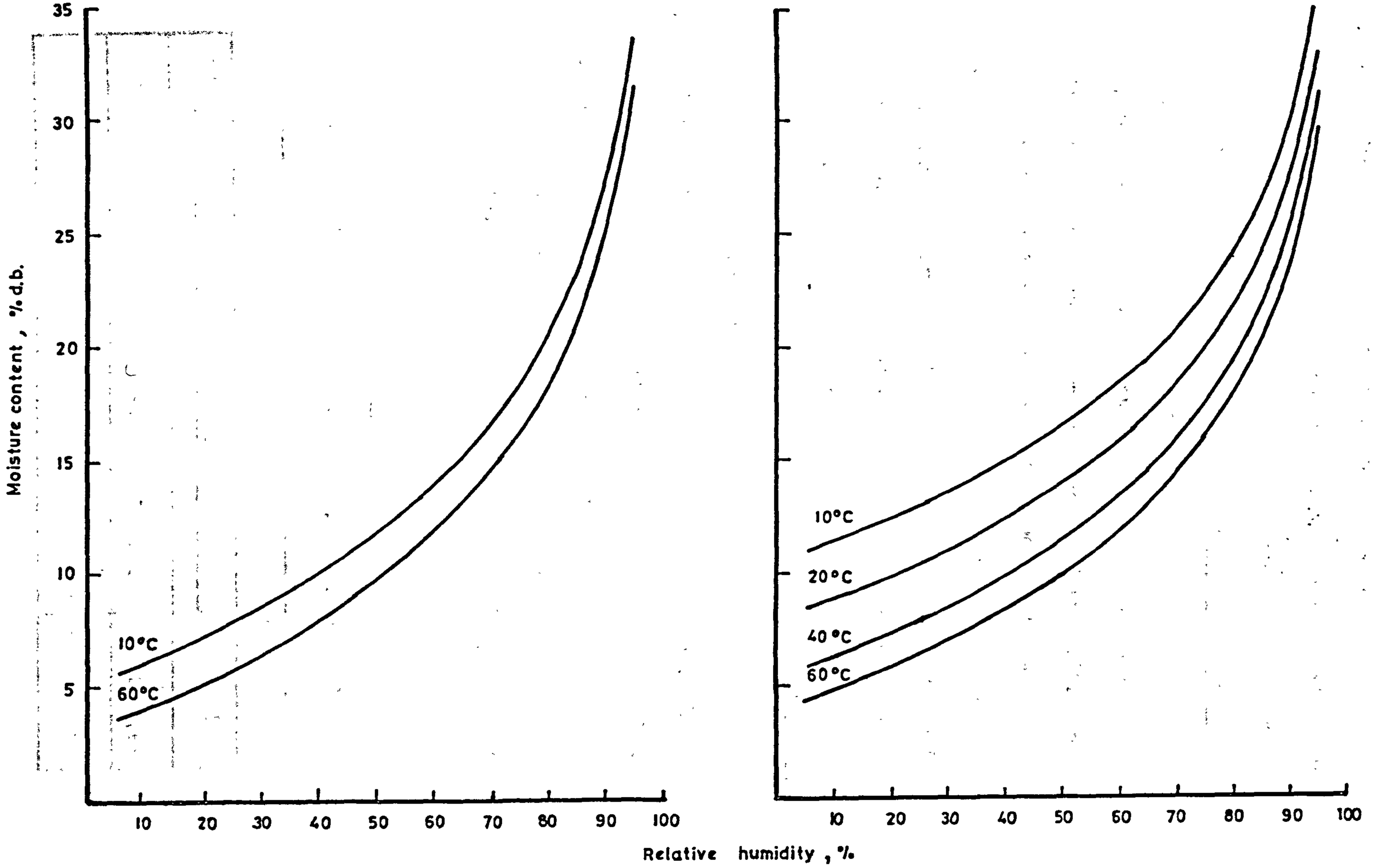

Fig.3.22 Correlation of asymptotic moisture contents, M_e, with temperature and humidity given by equation 3.42 for values of M_e obtained for the 2 term exponential equation for Sabel (left) and S.23 (right).

the plate equation, the effect was not significant although the coefficients have been included in Table 3.8. The temperature effect for S.23 also appears to be less than it was in the equivalent 1970 data.

Final moisture values

With the exception of a few of the data points, a plot of final moisture values, Mf, against relative humidity (Fig. 3.23) reveals a more uniform picture than plots of the derived asymptotes, Me. The inclusion in Fig. 3.23 of the final moisture contents from the 1972 germination experiment illustrates the sigmoid nature of this curve . Equation 3.42 was fitted to the 1971 data and values of the constants for Sabel and S.23 separately are included in Table 3.8. The fit to the Sabel data was made after 4 of the values had been deleted. Fits were also made to the combined data from 1971 only and from both 1971 and 1972. The latter produced an equation valid up to 78.5°C with very little change in the values of the coefficients. (Table 3.9). Predicted values for a constant absolute humidity (H = 0.01 kg/kg) and over the temperature range 20-78.5°C (rh range = 3.5 - 68%) are represented by the continuous curve in Fig.3.23.

Table 3.9

Constants in equation 3.42 for all 1971 data and for 1971 plus 1972 data

Data	Constant			No. of data values
	a	b	c	
1971 all	16.05	2.96	9.34	186
1971 + 1972	16.25	3.00	9.28	216

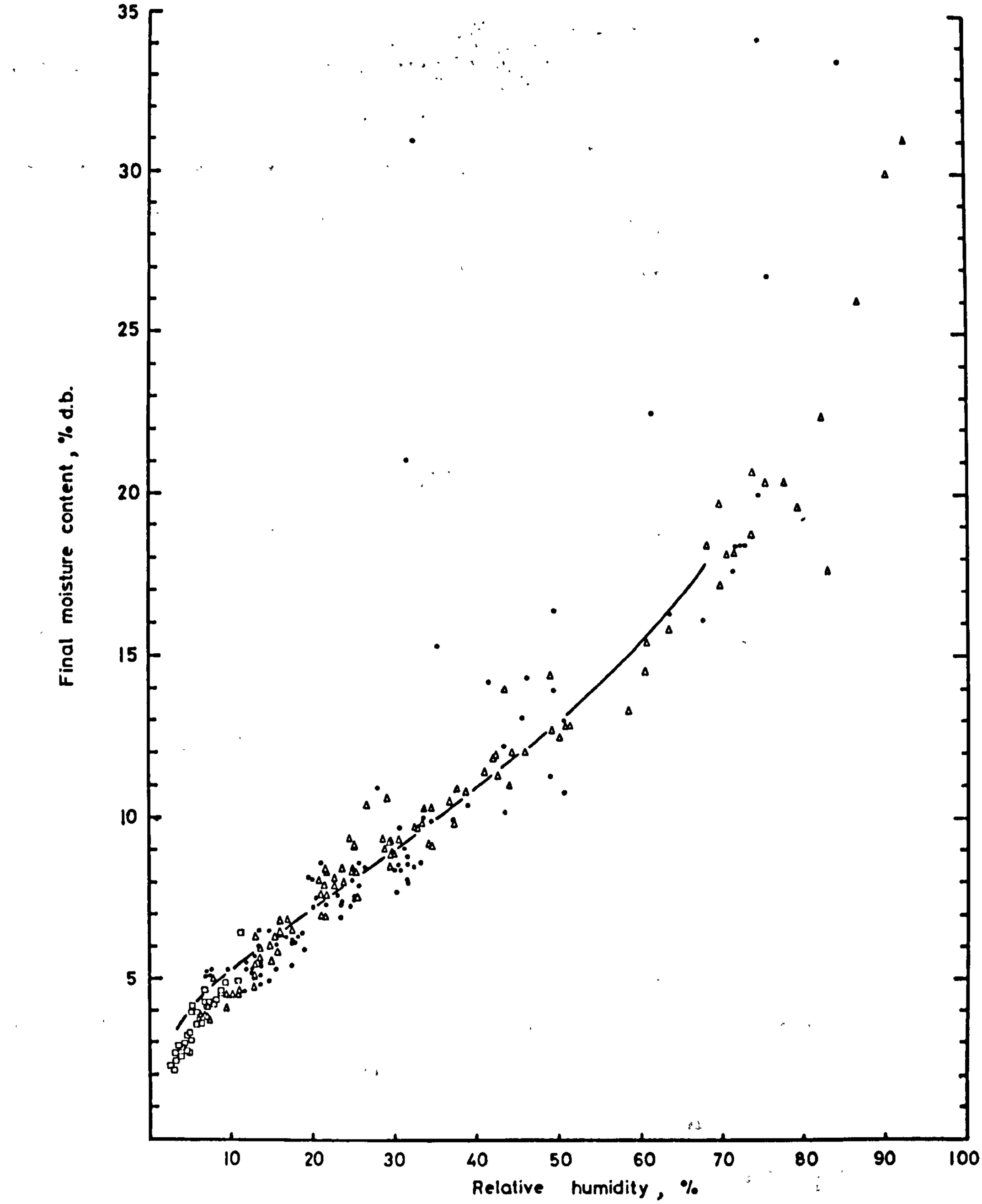

Fig. 3.23 Final moisture contents, M_f, plotted against relative humidity for 1971 results for Sabel (•) and S23 (△) and for results from both varieties in the 1972 germination experiment (□).

—— = Plot of equation 3.42 for constant absolute humidity.

3.4.2. Germination

The germination results are divisible into 2 classes.

(a) Those originating mainly from the thin-layer rate tests and representing the effect of exposure to a constant drying air temperature for many hours.* The 10 hour exposure treatments in the 1972 germination experiment are also included in this class (3.4.2.1)

(b) The full results from the 1972 tests and representing the effect of exposure time over a limited range of high temperatures (3.4.2.2)

3.4.2.1 Effect of long-term exposure to drying air temperatures

A preliminary analysis of the class (a) results obtained for S.23 seeds in 1970 was included in the paper describing that year's work.(81) Results from 125 runs at initial moisture contents <84% d.b. were represented by a third-order polynomial in T

$$G = 263.3 - 13.09T + 0.3297T^2 - 0.002797T^3 \quad \ldots\ldots\ldots\ldots \quad 3.45$$

Excluded from this analysis were samples which were thought to have deteriorated during storage at m.c.'s >13% m.c.w.b. and those which had had initial moisture contents greater than 84% d.b. The base germination of the latter were clearly a function of their initial moisture content and at that time the data was not sufficient to quantify the effect. In the plot of the data and fitted curve in Fig. 3.2 4 the results from these high moisture samples are represented by triangles.

* Separation of the results from 1971 into freshly-harvested, cold-stored and deep-frozen seed did not reveal any differences between freshly-harvested and cold-stored seed but all the deep-frozen seed had been severely damaged. These results were excluded from subsequent analyses.

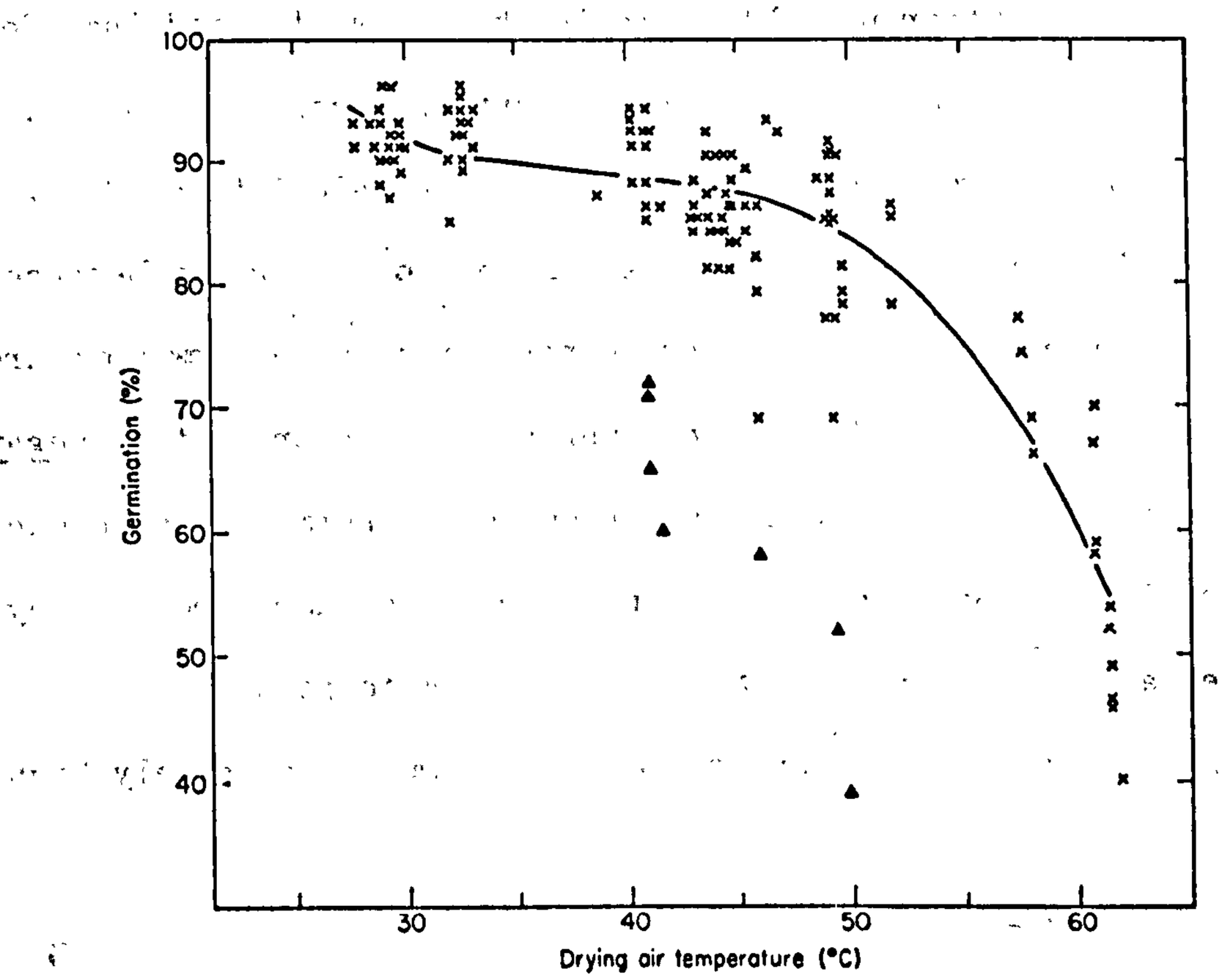

Fig. 3.2 4. Germination results from 1970 tests on S.23 seed with fitted curve of equation. 3.45

With the accumulation of 3 year's results and the establishment in Section 2 of a relationship between initial moisture content and the germination of control samples dried with ambient air, a more rigorous analysis of the data was possible. The initial moisture content effect was eliminated by defining the germination <u>depression</u>, G_D, as the difference between the germination at ambient temperature predicted by equation 2.1 (Sabel) or 2.3(S.23) and the germination at temperature, T. A third order polynomical in T was then fitted to the depression, G_D and gave the following relationships.

For Sabel (all 1971 results + 1972 10 hour exposures)

$$G_D = 38.11 - 2.681T + 0.04691T^2 - 0.0001075T^3 \quad \ldots\ldots 3.46$$

For S.23 (all 1970 and 1971 results + 1972 10 hour exposures)

$$G_D = 51.74 - 3.808T + 0.08127T^2 - 0.0004121T^3 \quad \ldots\ldots\ldots 3.47$$

Other possible relationships investigated included introducing initial moisture content as a separate factor, although it was, of course, used in the calculation of G_D. The inclusion reduced the overall variance slightly because of the improved fit at high temperatures but at low moistures and temperatures the fit was unrealistic in predicting negative depressions which would have resulted in germination in excess of 100%. Small negative depressions are also predicted by equations 3.46 and 3.47 over the medium temperature range, peaking about 30°C, but these do not imply excessively high

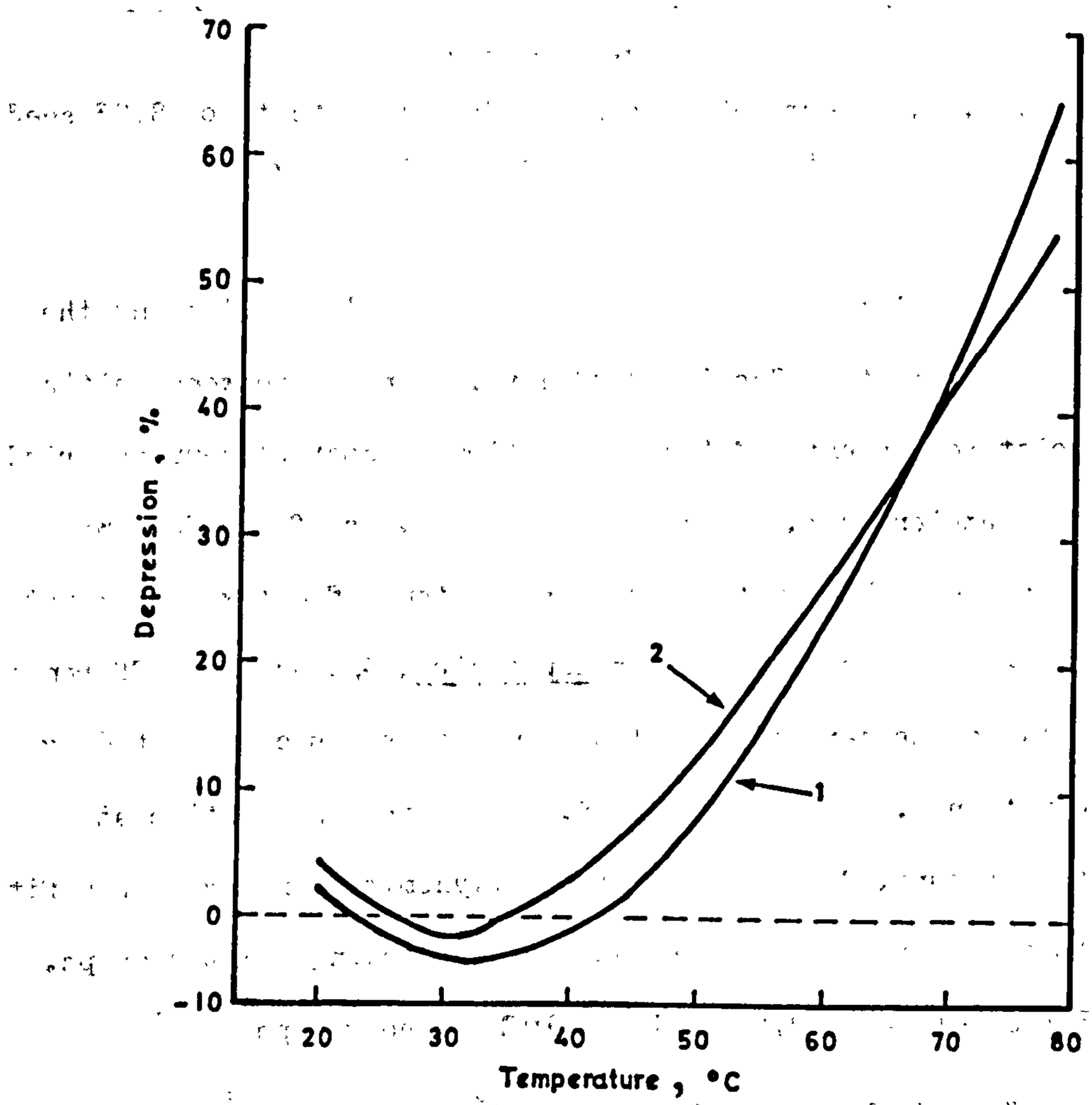

Fig.3.25. Effect of drying air temperature in depressing germination of Sabel (1) and S.23 (2)

germinations. Equations 3.46 and 3.47 are illustrated in Fig.3.25 which shows the slight negative depressions and the rapid increase in depression which occurs above about 40°C. The two equations produce very similar curves and there were no significant differences between the coefficients (see Appendix 3.2) That is, the response to drying air temperature of both the diploid and tetraploid seeds was similar. The difference between them was mainly one of germination potential.

The germination results are plotted in Figs. 3.26 and 3.27. The fitted curves were obtained by subtracting the depressions given by equations 3.46 and 3.47 from the potential germination predicted by equation 2.1 and 2.3 at the mean, maximum and minimum initial moisture contents of the respective data sets. The extreme variability characteristic of the germination results is clear from both of these plots.

Heat damage during drying not only caused germination reduction but also reduced the speed or vigour, with which the surviving seeds germinated. A quantitative measure of vigour, the ratio of the number of seeds germinating in 7 days to the total germination in 14 days, is represented by the plots of Figs. 3.28 and 3.29. This is a crude measure, not so much by definition, but because 7 day counts are very variable between operators. The basic purpose is to ease the counting at 14 days by removing obviously germinated seedlings and any critical decisions as to whether or not proper germination has taken place are deferred until the final count. At low germinations a difference of a single seedling may count for several percent vigour. Nevertheless the data clearly exhibit a temperature effect and were also found to contain a moisture content effect. The following equations gave a reasonable description of the data.

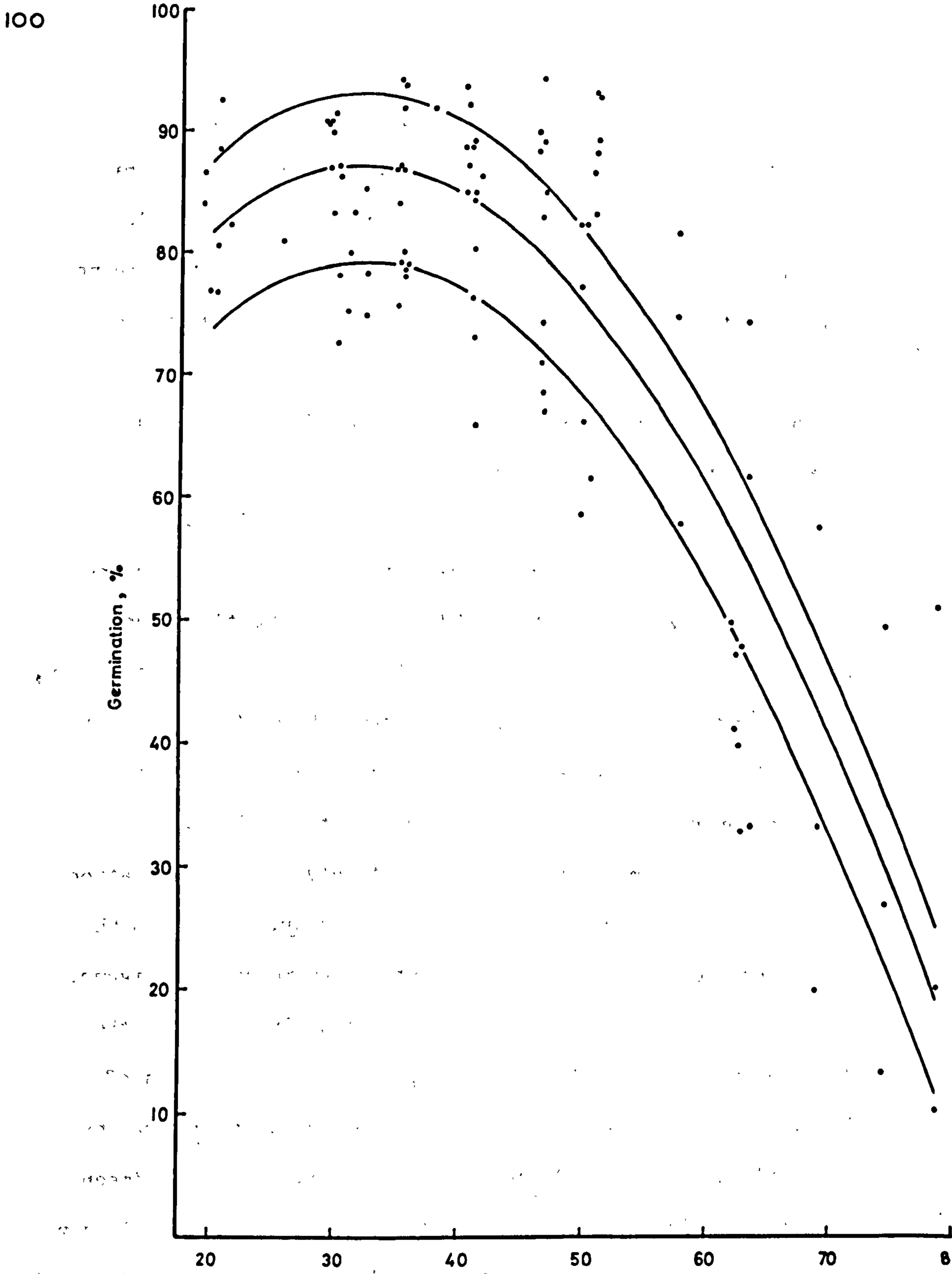

Fig. 3.26 Effect of long-term exposure to temperature on germination of Sabel. Fitted curves at 23.2 (top) 68.2 (centre) and 99.9 (bottom) % dry basis moisture content.

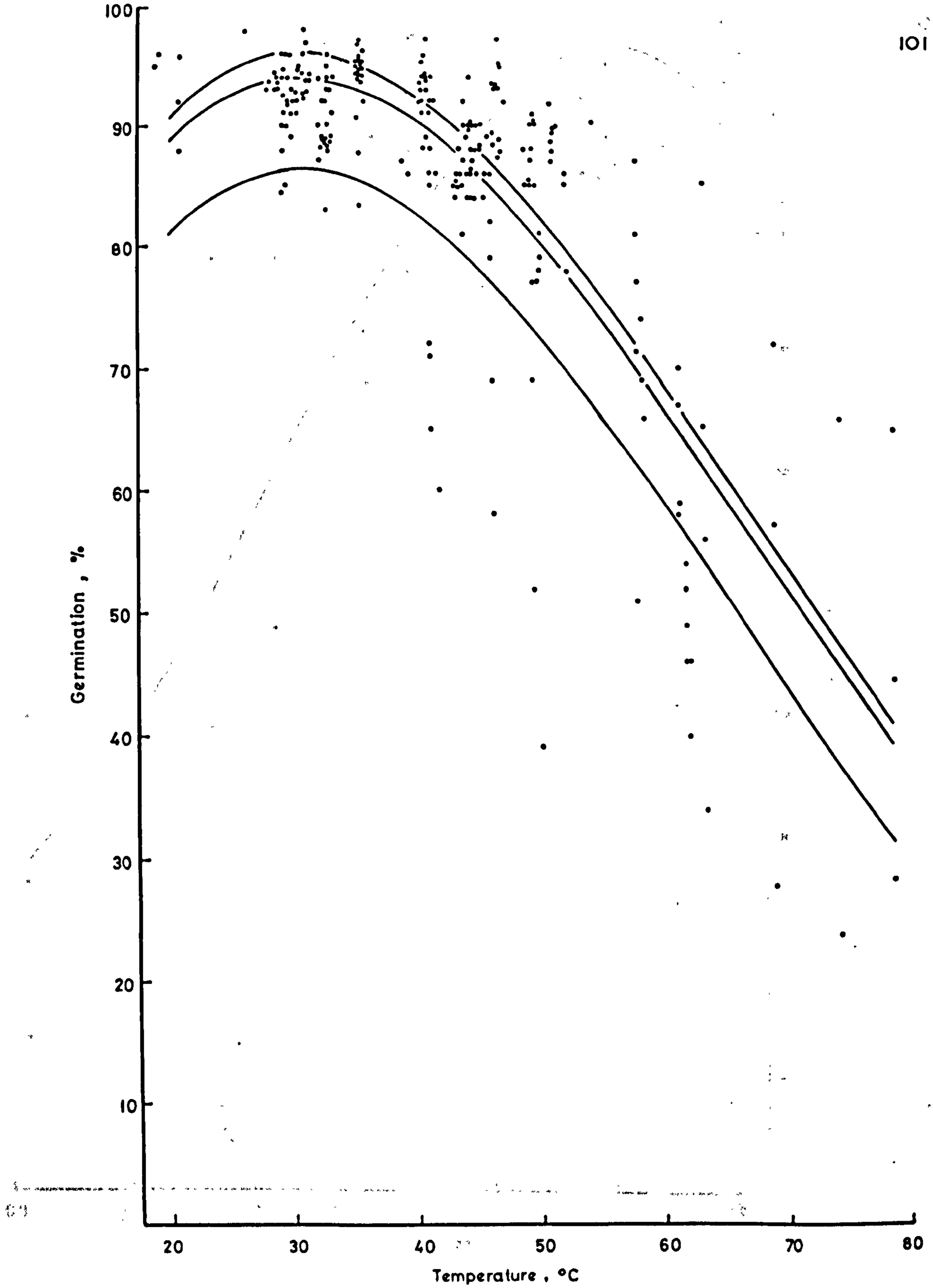

Fig. 3.27 Effect of long-term exposure to temperature on the germination of S23. Fitted curves at 31.1(top),62.3(centre) and 93.9(bottom) % dry basis moisture content.

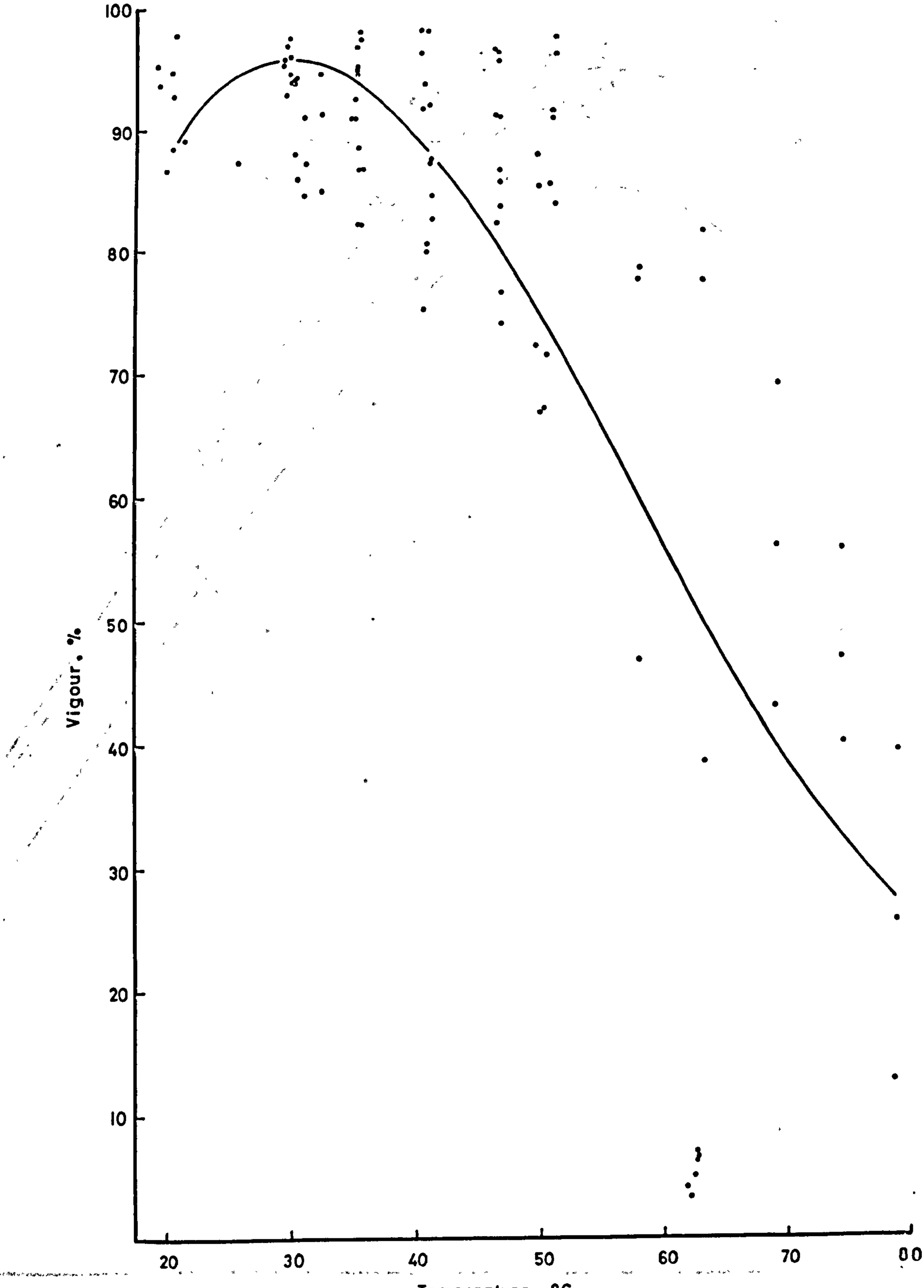

Fig. 3 28 Effect of long-term exposure to temperature on the vigour of Sabel with fitted curve of equation 3.48.

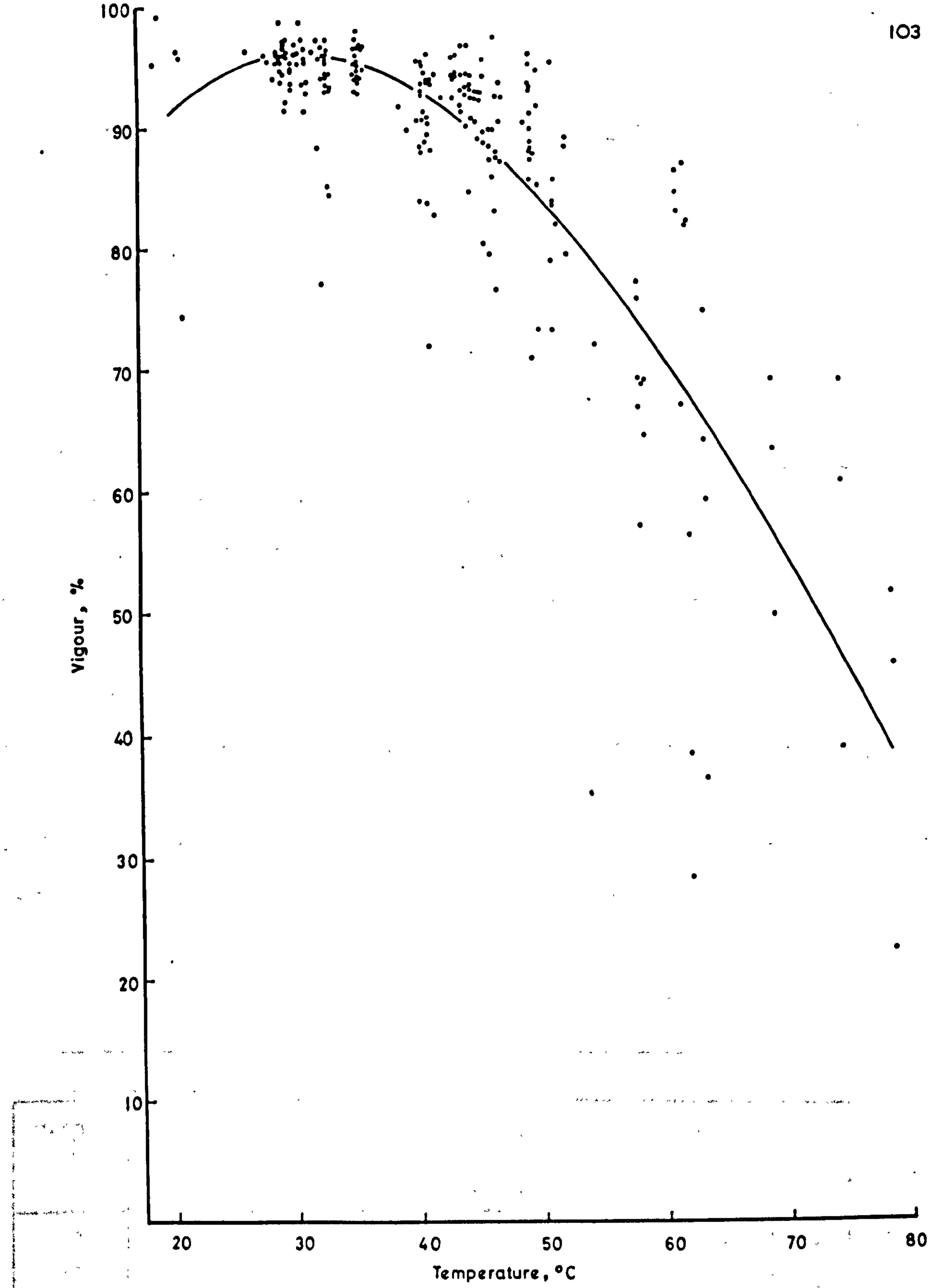

Fig. 3.29 Effect of long-term exposure to temperature on the vigour of S23 with fitted curve of equation 3.49.

For Sabel

$$\text{Vigour} = 34.24 - 0.3329Md + 6.371T - 0.1440T^2 + 0.0008348T^3 \quad \ldots\ldots\ldots 3.48$$

For S.23

$$\text{Vigour} = 68.74 - 0.2408Md + 2.93T - 0.05794T^2 + 0.0002312T^3 \quad \ldots\ldots\ldots 3.49$$

3.4.2.2. Results of 1972 experiment

3.4.2.2.a. Controls The dates of harvest, initial moisture contents, potential germination and vigour of the seed used in the 1972 experiments are summarised in Table 3.10. The moisture range for both crops was similar but slightly higher for the Sabel (44.4 - 31.8% w.b.) than for the S.23 (41.7 - 26.5% w.b.). With the exception of the germination of the S.23 seed harvested on August 8th, which had a low germination, the germinations of the samples was in line with the more comprehensive control data of Section 2. Thus at these moisture contents none of the tetraploid seeds reached 90% germination whereas even the 71.5% d.b. control for S.23 exceeded 90%. In all cases the vigour is over 90%.

Table 3.10

Dates of harvest, initial moisture contents and properties of control samples

Run	Crop	Date	Initial m.c. % w.b. (% d.b.)	1000 seed weight, g	Germination %	Vigour %
1	Sabel	18.7.72	44.4(80.0)	3.92	82	93
2	"	20.7.72	39.1(64.1)	3.92	86	94
3	"	25.7.72	31.8(46.5)	3.92	85	95
4	S.23	3.8.72	41.7(71.5)	1.53	93	92
5	"	8.8.72	34.8(53.4)	1.53	86	91
6	"	10.8.72	26.5(31.1)	1.53	96	94

3.4.2.2.(b) Air temperature & humidity

From the temperature records (Table 3.11) it can be seen that at every level the mean temperatures exceeded the nominal settings by 2-3°C, but that once these settings had been fixed, the accuracy of control was very high. Within any one series of exposures, the standard deviations of the mean values (usually a period of about 30 h) ranged between 0.1 and 0.6 with a mean of 0.4 degrees. From run to run the mean temperature varied very little and the final means at each level, 57.7, 63.2, 68.8, 74.2 and 78.5°C had standard deviations of 0.2 degrees or less.

Table 3.11

Means and standard deviations of drying air temperatures with grand mean at each level and standard deviation of that mean.

		Nominal temperatures, °C ± σ				
Crop	Run	55	65	65	70	75
Sabel	1	57.8±0.2	63.2±0.3	68.8±0.2	74.5±0.2	78.5±0.2
	2	57.6±0.5	63.2±0.6	68.8±0.5	74.1±0.4	78.6±0.4
	3	57.3±0.4	62.8±0.4	68.6±0.3	73.9±0.4	78.4±0.4
S.23	4	57.7±0.4	63.1±0.4	68.8±0.5	74.0±0.5	78.3±0.6
	5	57.9±0.2	63.2±0.4	69.0±0.1	74.2±0.3	78.5±0.3
	6	57.9±0.3	63.4±0.6	69.0±0.3	74.4±0.5	78.7±0.4
Mean		57.7	63.2	68.8	74.2	78.5
S.D. of mean		±0.2	±0.2	±0.1	±0.2	±0.1

Air humidities for the six runs were 0.0125, 0.0128, 0.0093, 0.0107, 0.0092 and 0.0083, and depending upon temperature gave values of relative humidity in the range 11.4 to 3.0%.

3.4.2.2. (c) Final moisture contents

Final moisture contents (% d.b.) are presented in Table 3.12. For any one series of exposure times these results represent points on a drying curve but are inadequate for use in determining drying rate constants. (There are not enough observations and the errors in each

Table 3.12

Final moisture contents, % d.b.

Crop	Run No.	Initial m.c. % d.b.	Temp °C	Exposure time, h					
				0.25	0.5	1	2	4	10
Sabel	1	80.0	57.3	61.5	49.3	34.7	16.3	16.2	5.0
			62.8	54.0	40.0	20.9	8.3	6.2	4.7
			68.6	47.1	20.2	9.6	7.0	5.0	4.3
			73.9	39.0	18.4	7.6	5.9	5.0	4.2
			78.5	32.4	15.2	7.6	5.7	4.2	2.7
	2	64.2	57.6	47.0	37.0	24.7	11.7	7.5	6.4
			63.2	46.4	29.9	16.6	8.2	6.8	4.6
			68.8	34.6	21.7	9.8	6.8	5.9	4.6
			74.1	29.1	14.3	7.5	5.6	5.1	4.0
			78.6	21.6	11.1	7.1	5.3	4.2	2.7
	3	46.6	57.7	31.9	22.9	13.3	8.0	5.8	4.8
			63.1	25.7	17.7	10.2	6.9	5.2	4.2
			68.8	21.0	12.4	7.3	5.4	4.9	4.0
			74.0	16.5	9.6	6.3	5.2	5.0	3.2
			78.3	14.0	8.1	5.8	4.4	3.7	2.8
S.23	4	71.5	57.8	43.3	81.3	15.3	7.5	5.6	4.3
			63.2	39.4	24.2	9.2	5.8	4.0	3.7
			68.8	28.3	12.6	5.9	5.1	4.2	3.3
			74.5	20.3	7.2	4.6	4.2	3.8	2.5
			78.4	16.4	7.1	5.6	5.1	3.1	2.2
	5	53.4	57.9	29.4	22.6	11.4	6.4	5.3	4.2
			63.2	28.2	15.3	7.7	5.5	4.7	3.6
			69.0	18.4	8.6	5.8	4.7	3.7	3.1
			74.2	15.8	8.0	5.2	4.3	3.4	2.9
			78.5	11.2	6.3	4.6	3.7	3.1	2.4
	6	36.1	57.9	22.2	16.7	9.1	6.0	4.9	4.2
			63.4	19.0	12.1	5.8	5.1	4.4	3.6
			69.0	14.3	7.4	5.6	4.2	3.8	3.0
			74.4	10.5	6.9	5.0	4.2	3.5	2.6
			78.7	10.3	6.2	4.7	3.6	3.0	2.3

point are greater than in a drying curve determined by weight loss from a single sample). An attempt was made to compare drying curves at any one temperature level by evaluating the relation $(M - M_e)/(M_o - M_e)$ using the moisture content at 10 hours as Me. The results indicated that the drying rate increased in inverse proportion to initial moisture content and seed size (variety). In those curves (the majority) for which little drying took place in the last 8 hours, a second falling rate period was indicated.

Plots of the drying curves revealed one anomaly in that in Run 1 in the 57.5°C treatment virtually the same moisture content (16.2%) was recorded at 4 hours as at 2 hours when a substantial fall would have been expected. There are no grounds for discarding either value but that at 4 hours looks the most suspect.

With the exception of the lowest temperature, 57.5°C in Runs 1 and 2 all of the seed was reduced to below 10% d.b. within the first 2 hours and very little drying took place in the remaining 8 hours. At 78.5°C in Runs 3, 5 and 6, at 74.0°C in Runs 5 and 6 and 68.8°C in Run 6, the moisture contents were reduced below the safe storage level (15.6% d.b.) within 15 minutes, the minimum exposure time.

The final moisture contents at 10 hours were used in Section 3.4.1.2 to extend the fit of the equilibrium moisture content equation 3.42, to lower relative humidities and higher temperatures. A large scale plot of the data (Fig. 3.30) in which the individual runs are identified suggests that the equilibrium moisture contents of both varieties are similar. The apparently lower values for S.23 in Table 3.12 can now be seen to be associated with lower values of relative humidity.

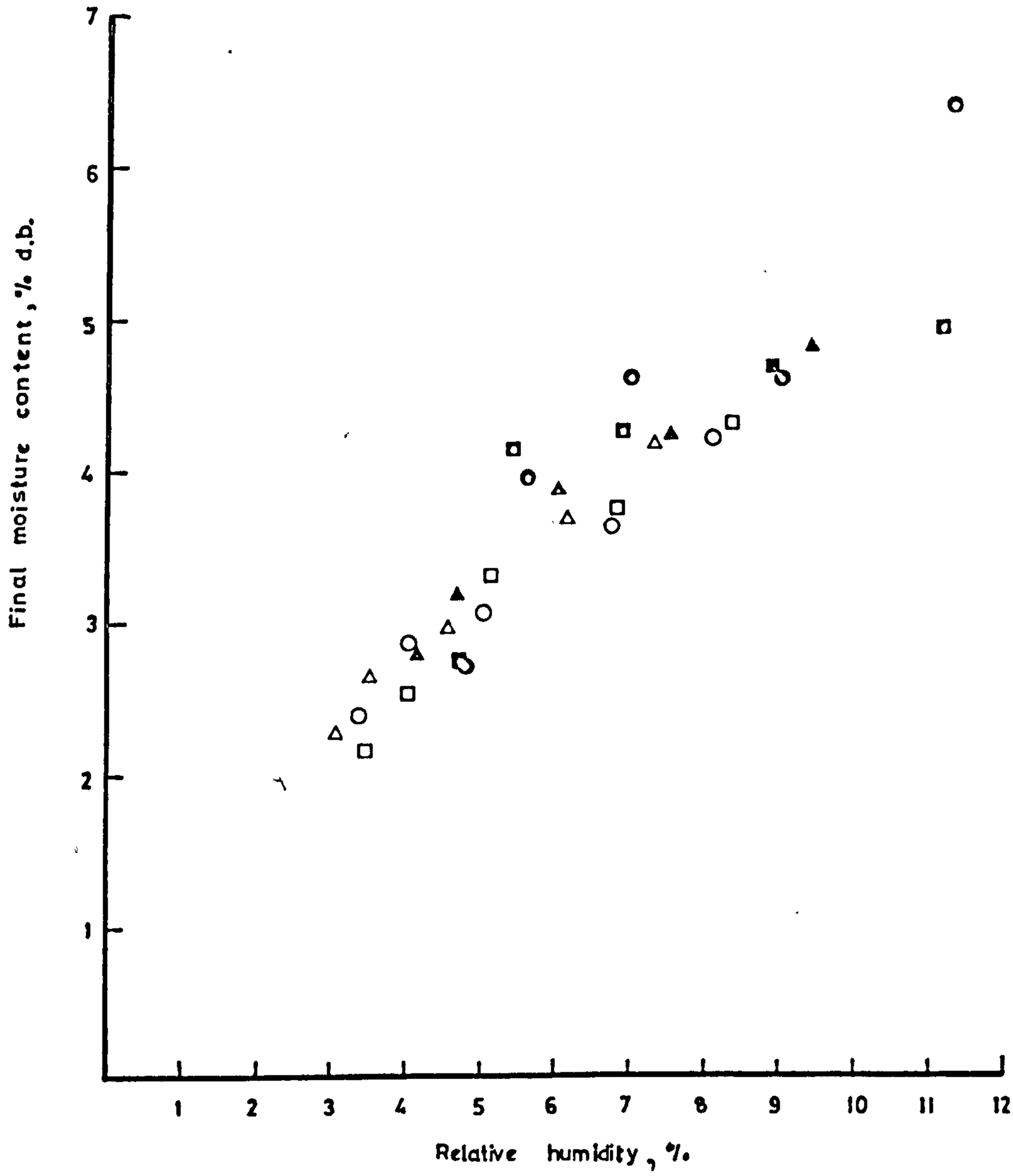

Fig. 3.30 Final moisture contents after 10 hours exposure to temperatures in the range 57.3 - 78.7°C plotted against corresponding relative humidities for Sabel, Runs 1 (■), 2 (●) and 3 (▲) and S.23, Runs 4 (□), 5 (○) and 6 (△).

3.4.2.2. (d) Germination

Results for the 7, 14 and 21 day count are all presented in the Appendix 3.2 but only the 14 day count and the 14 day vigour results are presented here. This is because very few extra seeds germinated after 14 days which meant that germination and vigour comparisons were similar and it is the 14 day count which is the commercially important value. The results in Table 3.13 are based on 3 replicate 100 germinations per treatment. In view of the findings of Thomson (117) discussed in section 3.2.3 the standard deviation of each of these tests was calculated and compared with the mean values and with the drying treatments. The standard deviations varied between 0.58 and 11.72% and appeared to follow a random distribution independent of either mean germination or the treatment variables. (Appendix table 3.2.37).

A defect of the experimental design is that there is no replication of moisture content. This was a deliberate omission for two reasons. Firstly it is almost impossible to achieve replication of moisture levels when harvesting seed from a crop which passes through the whole mature moisture range in about a fortnight. Even if synchronous harvests from two separate crops are used, equivalent moisture levels may not be obtained. Secondly it was known that the moisture effect was a strong one and would prove significant if replication were possible. For this reason in analysis of variance of the results the moisture level interactions were not assigned to error but were tested for significance and a study of the differences between means was used to indicate the important trends in treatment effects. These detailed comparisons are tabulated in Appendix 3.2.1 . Tables of variance for both germination counts and vigour results are given in Table 3.14. Since the three initial moisture levels obtained for each crop

Table 3.13

Mean 14 day germination counts

Crop	Run No.	M.C. % d.b.	Temp, °C	Exposure time, h					
				0.25	0.5	1	2	4	10
Sabel	1	80.0	57.7	74.3	75.0	62.0	55.0	58.0	58.0
			63.2	58.3	49.3	38.3	61.0	37.0	33.3
			68.8	21.0	22.3	21.7	14.7	20.7	20.0
			74.2	18.3	16.7	10.7	17.7	14.7	13.3
			78.5	9.3	14.0	12.7	12.0	9.3	10.3
	2	64.1	57.7	81.7	80.7	77.0	80.3	71.3	75.0
			63.2	72.7	61.3	58.7	58.7	53.7	61.7
			68.8	40.7	33.0	33.0	33.7	38.3	33.3
			74.2	27.0	26.7	27.7	25.3	30.0	27.0
			78.5	23.7	18.0	17.3	25.0	18.3	20.3
	3	46.5	57.7	87.3	83.3	91.0	85.7	80.3	81.7
			63.2	84.0	78.0	80.0	77.3	74.3	74.7
			68.8	60.0	57.0	69.7	64.0	59.3	57.7
			74.2	53.3	52.3	51.3	51.7	53.3	49.7
			78.5	42.0	39.7	44.7	49.3	46.3	51.3
S.23	4	71.5	57.7	71.3	64.0	58.7	49.0	49.0	51.0
			63.2	45.3	37.3	36.3	37.7	34.7	34.0
			68.8	34.3	30.7	27.3	25.3	30.0	27.7
			74.2	16.7	17.7	19.7	26.3	19.0	23.7
			78.5	16.0	20.0	17.7	16.3	27.0	28.3
	5	53.4	57.7	78.0	82.3	75.3	75.7	73.0	71.3
			63.2	58.3	79.0	56.7	68.3	68.3	63.7
			68.8	51.0	59.3	55.0	47.0	51.3	57.3
			74.2	41.7	46.7	47.0	42.0	47.0	50.3
			78.5	46.0	40.3	40.0	42.7	40.3	44.7
	6	31.1	57.7	96.0	92.3	88.3	88.0	87.7	87.0
			63.2	85.7	95.3	81.0	82.0	85.0	85.3
			68.8	75.0	74.0	72.7	66.0	69.7	72.0
			74.2	67.7	67.3	76.0	69.0	70.0	66.0
			78.5	68.0	58.7	58.3	67.0	67.3	65.0

Table 3.14

Analysis of variance of 14 day germination counts (transformed to angles) and percent vigour of Sabel and S.23 seeds

Source of variation	d.f.	Germinations			
		Sabel		S.23	
		M.S.	F	M.S	F
Moisture (M)	2	10067.91	978.56	15951.11	1333.21
Temperature (T)	4	9432.88	81.84***	3880.36	100.04***
Moisture (M) x T (error a)	8	115.26	6.20***	38.79	2.087*
Exposure (E)	5	88.85	2.51*	43.91	2.362 NS
M x E	10	35.34	1.90NS	18.95	1.019 NS
T x E	20	38.61	2.08*	47.78	2.570**
M x T x E (error b)	40	18.60	1.808*	18.59	1.554*
Residual	180	10.29		11.96	

Source of variation	d.f.	Vigour			
		Sabel		S.23	
		M.S.	F	M.S.	F
Moisture (M)	2	11652.4	130.164	5692.15	76.753
Temperature (T)	4	6609.97	3.200 NS	2966.07	3.796 NS
Moisture (M) x T (error a)	8	2064.72	7.186***	781.30	4.213***
Exposure time (E)	5	4649.93	16.184***	2292.51	12.363***
M x E	10	376.20	1.309NS	443.21	2.390*
T x E	20	627.96	2.186*	359.84	1.941*
M x T x E (error b)	40	287.32	4.478***	185.43	2.498***
Residual	180	89.52		74.16	

could not be regarded as equivalent, a separate analysis of variance was carried out for each variety. The analyses of the germination percentages were carried out on the angular transformation of the values. Parallel analyses of the untransformed percentages gave similar results but with rather higher levels of significance.

The results of the analyses were similar for both varieties but provide an interesting contrast between germination and vigour. For germination, the effect of temperature was highly significant and time of exposure relatively unimportant. In the case of S.23, in particular, exposure was not a significant effect except in its interaction with temperature. But for germination vigour, exposure time had a highly significant effect whilst temperature was relatively unimportant and, as an independant factor, was not significant for either variety. The reasons for this are explained shortly.

Effects on germination

Since the effect of exposure on germination was relatively weak, the main effects are illustrated by plots of germination against temperature for each moisture level for the shortest (15 minutes) and the longest (10h) exposure times only (Figs.3.31 and 3.32). The strong interaction between moisture content and temperature is clear. At any moisture level increasing temperature from 57.7 to 78.5°C causes an approximately similar depression, the effect being most pronounced between 60 and 70°C and decreasing thereafter. Differences between germination resulting from the two highest temperatures, 74.2 and 78.5°C, were seldom significant.

The lowest temperature, 57.7°C, was the only one which failed to cause damage in all treatment combinations. For Sabel there was no reduction at 46.6% m.c.d.b. after $\frac{1}{4}$h exposure and reductions at

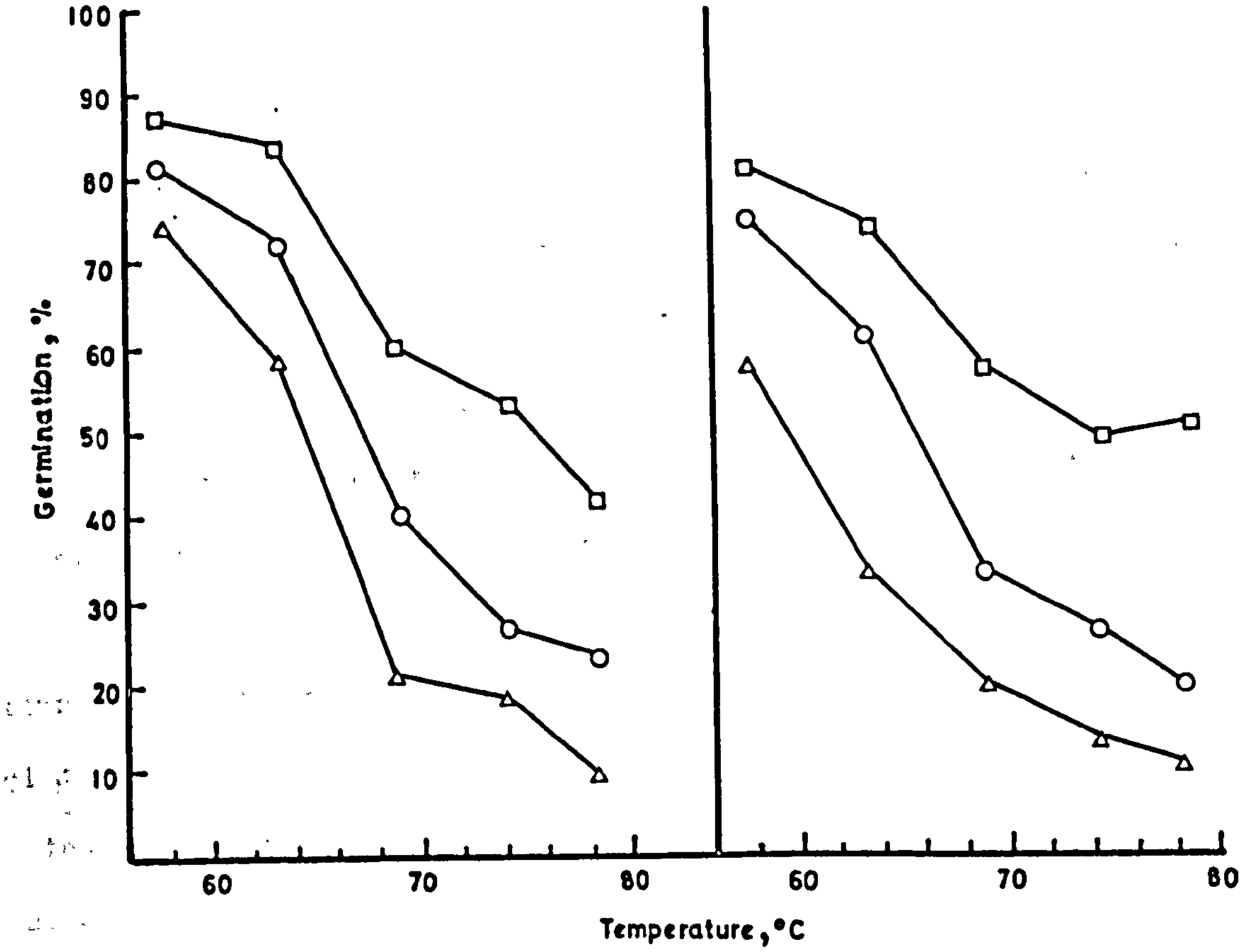

Fig. 3.31 Effect of temperature on germination of Sabel seeds after 15 min (left) and 10h (right) exposure from initial moisture contents of 80.0 (△), 64.2 (○) and 46.6 (□) % dry basis.

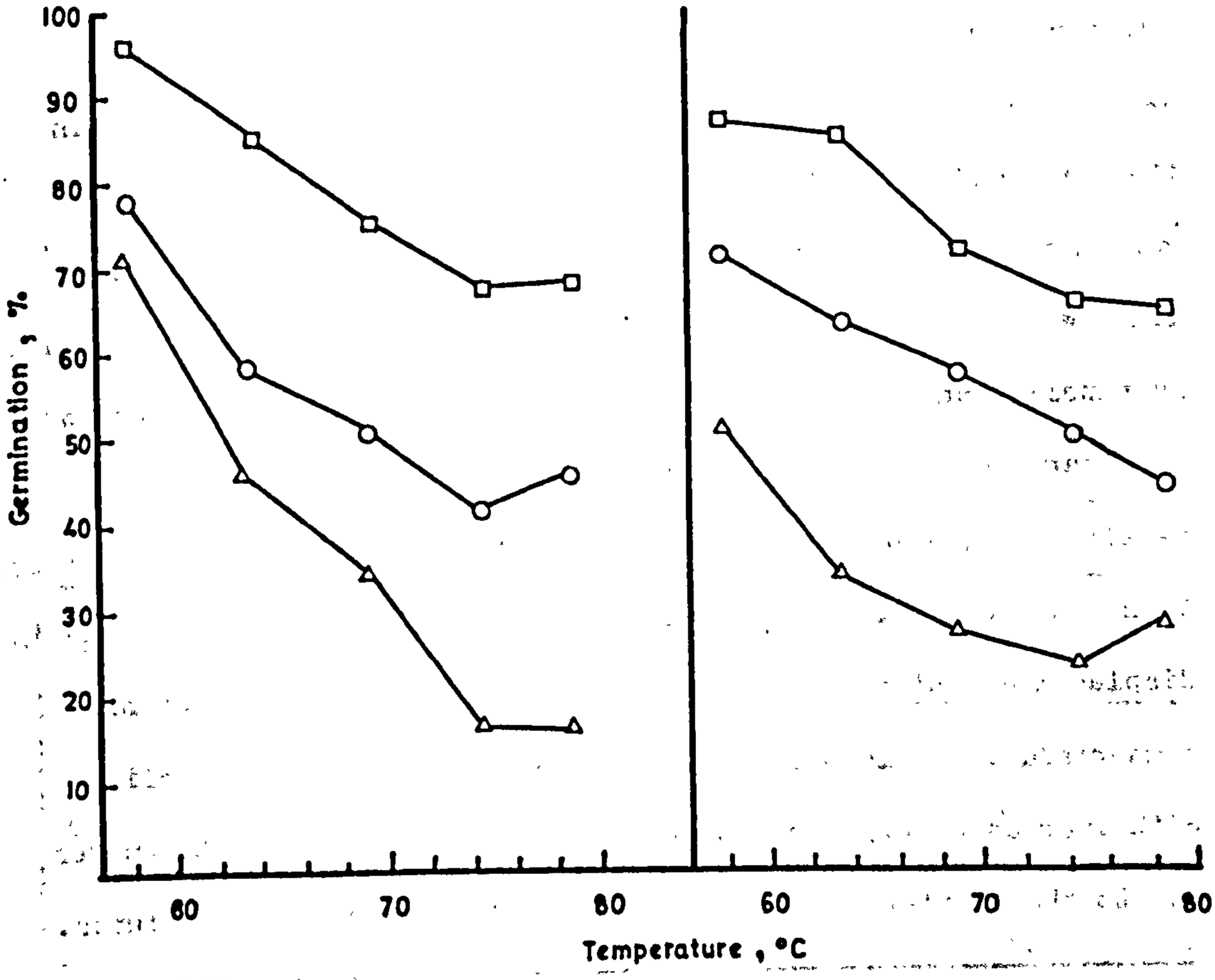

Fig. 3.32 Effect of temperature on germination of S.23 seeds after 15 min (left) and 10h (right) exposure from initial moisture contents of 71.5 (△), 53.4 (○) and 36.1 (□) % dry basis.

the higher moisture levels were modest. For S.23 there was no reduction at 36.1% d.b. but rather greater reductions at the 2 higher moisture levels than with the Sabel.

For both varieties, additional reduction caused by further exposure up to 10 hours were only significant at the 2 lower temperatures and then most strongly at the highest moisture contents. i.e. in general those treatments for which appreciable moisture loss continued at exposures greater than 15 min. Exposure time was not significant at the three highest temperatures because the maximum depression had been induced within the first 15 minutes of exposure. A general consideration of the significant effects in the interaction tables suggests that critical exposures for S.23 are shorter than those for Sabel.

Because the use of analysis of variance to test the moisture content interactions was theoretically suspect, the moisture content/temperature interaction at each exposure time was also examined by a parallel curve analysis available within the MLP* package on the ICL 470. To each set of 3 curves of germination against temperature at each exposure time, straight lines were fitted (a) to the individual curves, (b) to the 3 curves in parallel and (c) a common curve. An analysis of variance was then carried out in which curve displacement (intercept) and parallelism (slope) were tested against the within curve variance. With but one minor exception significant differences were found in displacement but not in slope. The intercepts and slopes are summarised in Table 3.15. Both intercepts and slopes decline with increasing exposure reflecting the flattening of the curves due to the greater effect of exposure at the lower temperatures.

---

* MLP = Maximum likelihood programme - a self contained system for fitting models to data. Written by G.J.S. Ross, R.D. Jones, R.A. Kempton and F.B. Lauckner, Statistics Department, Rothamsted Experimental Station, Harpenden, Herts.

Table 3.15

Germination as a straight line function of temperature at each exposure time and moisture content

Crop	Coefficients	M.C. % d.b.	Exposure time h					
			¼	½	1	2	3	10
	Slope	all	-2.89	-2.73	-2.54	-2.38	-2.15	-2.21
		80.0	234.1	222.4	203.0	195.1	175.4	178.3
Sabel	Intercept	64.1	247.0	230.9	216.7	207.6	189.8	194.8
		46.5	263.2	249.0	241.3	228.6	210.2	214.3
	Slope	all	-1.89	-1.97	-1.55	-1.43	1.30	1.19
		71.5	165.9	168.9	137.9	124.1	120.6	114.4
S.23	Intercept	53.4	184.2	196.5	160.8	153.3	144.7	138.9
		36.1	207.7	210.5	181.2	172.6	164.6	156.5

Over the range investigated the germinationof Sabel declines at a greater rate with temperature than that of S.23. The constants in Table 3.15 have been used to calculate the values in Table 3.16 of temperatures at which 90% germination is predicted. Where the extrapolation goes very far outside the experimental temperature range, as for example the results for the high moisture S.23 at exposures greater than ½h, the results are unrealistic but otherwise a good indication of safe temperatures is given.

Table 3.16

Drying temperatures, °C giving 90% germination predicted by the linear equations of the parallel curve analysis, Table 3.15

Crop	M.C. % d.b.	Exposure time, h					
		¼	½	1	2	4	10
	80.0	49.9	48.5	44.5	44.1	39.6	40.0
Sabel	64.1	54.3	51.6	49.9	49.4	46.3	47.4
	46.5	59.9	58.2	59.6	58.2	55.8	56.2
	71.5	40.2	40.0	30.9	27.3	23.6	20.5
S.23	53.4	49.9	54.0	45.7	44.2	42.2	41.1
	36.1	62.4	61.1	58.9	57.6	57.6	55.9

Effect on vigour

As noted in section 3.4.2.1. vigour results tend to be even more variable than the germinations from which they are derived. One reflection of this is the higher residual variance of the vigour analysis of variance compared with those of the germinations. (Analysis of the germinations as percentages produced residual σ^2 approximately twice those of the angular transformations but this is still only $\frac{1}{4}$ of the vigour residual σ^2). In this analysis the temperature effect was weak and the exposure effect strong. Inspection of the data in Table 3.17. confirms that there was considerably more variability between temperature levels than between exposure levels at one temperature. Consider Run 3 for example. The vigour of the 68.8°C treatment for exposures up to 2h is over 90% and stands out as not being part of/a uniform pattern. There are a number of other similar examples. Hence perhaps the most that should be said is that the general conclusion of the analysis was that continuing exposure tends to cause a continuing decline in vigour and this effect is strongest at the higher temperatures. In particular, the vigour of seed exposed for 10 hours to 78.5°C was consistently low for both varieties at all moisture contents.

Table 3.17

Mean vigour percentages (7/14 day)

Crop	Run No.	M.C. % d.b.	Temp °C	Exposure time, h					
				0.25	0.5	1	2	4	10
Sabel	1	80.0	57.7	91.2	77.7	77.4	63.2	45.6	46.7
			63.2	38.0	42.6	39.8	57.9	46.7	38.6
			68.8	57.0	53.0	46.9	64.0	32.3	43.1
			74.2	68.9	76.5	28.1	42.0	15.1	40.3
			78.5	61.5	80.6	69.7	50.1	26.7	12.8
	2	64.1	57.7	96.7	91.0	84.4	82.3	79.5	78.6
			63.2	87.2	83.4	69.7	79.1	73.9	77.7
			68.8	65.6	72.9	65.1	50.1	45.4	56.2
			74.2	85.2	88.5	88.1	68.5	61.7	47.1
			78.5	72.5	84.4	36.3	56.4	13.9	25.8
	3	46.5	57.7	86.3	85.2	82.4	80.6	86.4	77.6
			63.2	79.6	70.6	78.7	86.3	85.9	81.7
			68.8	92.8	91.2	94.7	93.4	74.5	69.4
			74.2	76.6	83.8	64.2	64.9	57.0	56.0
			78.5	49.8	48.8	59.5	45.3	27.3	39.7
S.23	4	71.5	57.7	77.1	70.5	82.1	83.1	83.9	77.2
			63.2	64.2	66.8	77.8	66.8	63.1	59.4
			68.8	70.5	69.6	63.9	79.7	52.3	63.5
			74.2	69.2	53.3	41.9	69.9	35.8	38.8
			78.5	39.9	61.2	70.5	61.6	54.7	22.4
	5	53.4	57.7	77.2	73.6	78.8	68.0	67.5	66.9
			63.2	56.0	76.3	75.9	73.2	77.2	74.8
			68.8	87.5	74.6	73.4	79.2	70.3	69.2
			74.2	93.7	83.0	76.8	79.3	76.7	60.7
			78.5	47.4	49.3	74.4	74.5	42.4	45.8
	6	31.1	57.7	81.4	88.9	93.2	84.5	79.5	75.8
			63.2	90.2	91.0	89.0	87.3	82.4	64.2
			68.8	91.6	92.8	88.1	76.1	63.6	49.9
			74.2	97.0	95.5	75.3	66.6	64.4	69.2
			78.5	86.2	84.5	75.6	65.7	56.5	51.7

3.5. DISCUSSION

3.5.1. Drying rate

In 1971 the general improvement in operating technique, which included the reduction in the weight loss discrepancies by the use of lower air velocities and more precise control of air temperature, produced drying curves which were more reliable than those obtained in 1970. In addition, the improvements and extensions in the curve-fitting routines reduced the random variation in the drying constants derived. Nevertheless the agreement between the 2 years results was very good and very few of the conclusions reached in 1970 [81] have had to be revised as a result of the extra insight gained in 1971.

3.5.1.a 1970 results

The 1970 results showed that the 2 term exponential fitted the curves better than the single term equation commonly used for cereal grains [16,88,110,69,70,49]. The original reason for attempting to fit an extra-term to equation 3.1 as in equation 3.10 was as a device to approximate the higher order terms of the exponential series of equation 3.38. It was felt that this would obviate the need to make an arbitrary selection of the point at which these higher order terms faded on any particular curve and beyond which a fit of equation 3.1 would have given a realistic value of k for use in the series. This approach was successful and in those cases for which DOUBEX found a reasonable solution, the difference between the constants of exponentiation was always such that the one term faded very rapidly compared to the other.

The improved fits given by DOUBEX tended to occur over the whole length of the curve. In most cases it was markedly better than either of the alternative fits of Eq. 3.1 by SINGEX as in the example of Fig.3.11 where the variance was

reduced to 1/10th of that from the direct least squares fit of equation 3.1 (see Table 3.2). Sometimes the improvement was less marked as in the example of Fig. 3.12 but some improvement was always gained. From a comparison of Figs. 3.11 and 3.12 with Figs. 3.9 and 3.10 it can be seen that the fits of equation 3.10 are at least as good as if not better than, the agreement between replicate curves.

Equation 3.1 would predict that plots of drying rate, $\frac{dM}{d\theta}$ against moisture content, M, would be linear but such plots for drying curves A-E of Fig. 3.9 (Fig.3.33) exhibit a steep rise away from linearity at high moisture contents. This is the sort of pattern to be expected from plots of the differential

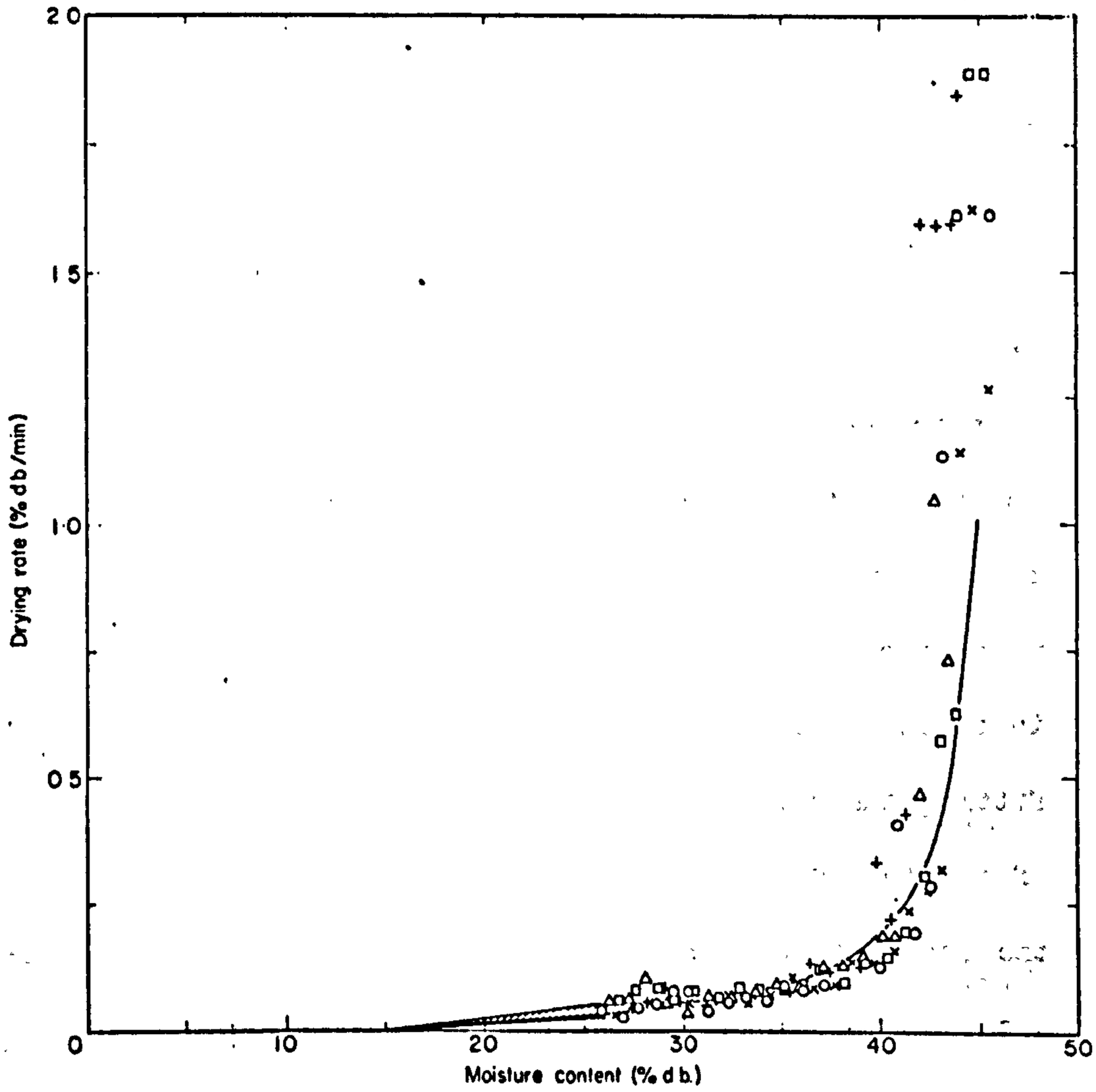

Fig. 3.33 Comparison of experimental and predicted drying rates given by data in Fig. 3.9.

of either of the series equations 3.38 and 3.39 and in 1970 the possible use of Eqn. 3.38 was investigated using k values derived from the 3 equations for k given by Table 3.3 . Drying curves and drying rates were generated from the exponential series equation for a number of initial moisture contents and using a number of arbitrarily chosen asymptotic values. Those were then compared with the experimental curves. The best fits were obtained when using the 'k' values derived by DOUBEX and example predictions are plotted in Figs. 3.9 and 3.10. Comparing those with the experimental variation between replicate curves the agreement must be regarded as good. The predicted differential curve for the curves of Fig. 3.9 is plotted in Fig. 3.33 . Here again agreement is reasonable although for many of the data sets the increased variation caused by the simple differentiation precludes any real critical comparison.

3.5.1.b. 1971 Results

In 1970 the wide variation in the values of k for the rapidly decaying term of the 2 term exponential suggested that the equation did nothing more than accouht empirically for the initial part of the drying curve where theory and measurement predicted that the drying rate was not directly proportional to moisture content. It was expected therefore that comparable, or even better, fits would be obtained by fitting the series equations direct using SEREX. But analysis of the 1971 data showed that the 2 term-exponential was still the most satisfactory. To a certain extent this is probably because in DOUBEX, the two exponent terms are adjusted independently of each other and therefore provide more flexibility than in the series where all the component terms are related by the particular progression. Nevertheless, the

values of $\underline{k}_1$ obtained for the rapidly decaying term of eqn. 3.10 in 1971 bore a clear relationship to temperature in a similar manner to the values of k_2 (see Table 3.7 and Appendix Figures 3.2.2&3). This prompted a closer examination of equation 3.10 and the realisation that it is the solution of a second order linear differential equation

$$\frac{d^2M}{d\theta^2} + p\frac{dM}{d\theta} = -q(M-Me) \qquad \ldots\ldots\ldots 3.50$$

where the constants p and q are defined by the quadratic equation

$$k^2 + pk + q = 0 \qquad \ldots\ldots\ldots 3.51$$

and the constants k_1 and k_2 in equation 3.10 are the roots of this quadratic. From which it follows that $k_1 + k_2 = p$ and $k_1 k_2 = q$ and if equation 3.50 is at all applicable then it would be expected that p and q would prove to be functions of the drying variables. The sums and products of k_1 and k_2 were evaluated and expressed as exponential functions of temperature. The coefficient of the equations are given in Table 3.18 and the functions and data points are plotted in Fig.3.34. The correlation is sufficiently good to suggest that equation 3.10 is not just an empirical description of the drying curve. It is of interest to note that there is hardly any difference between varieties in the values of p and that there is a difference in the logarithmic intercept of q, significant at the 5% level.

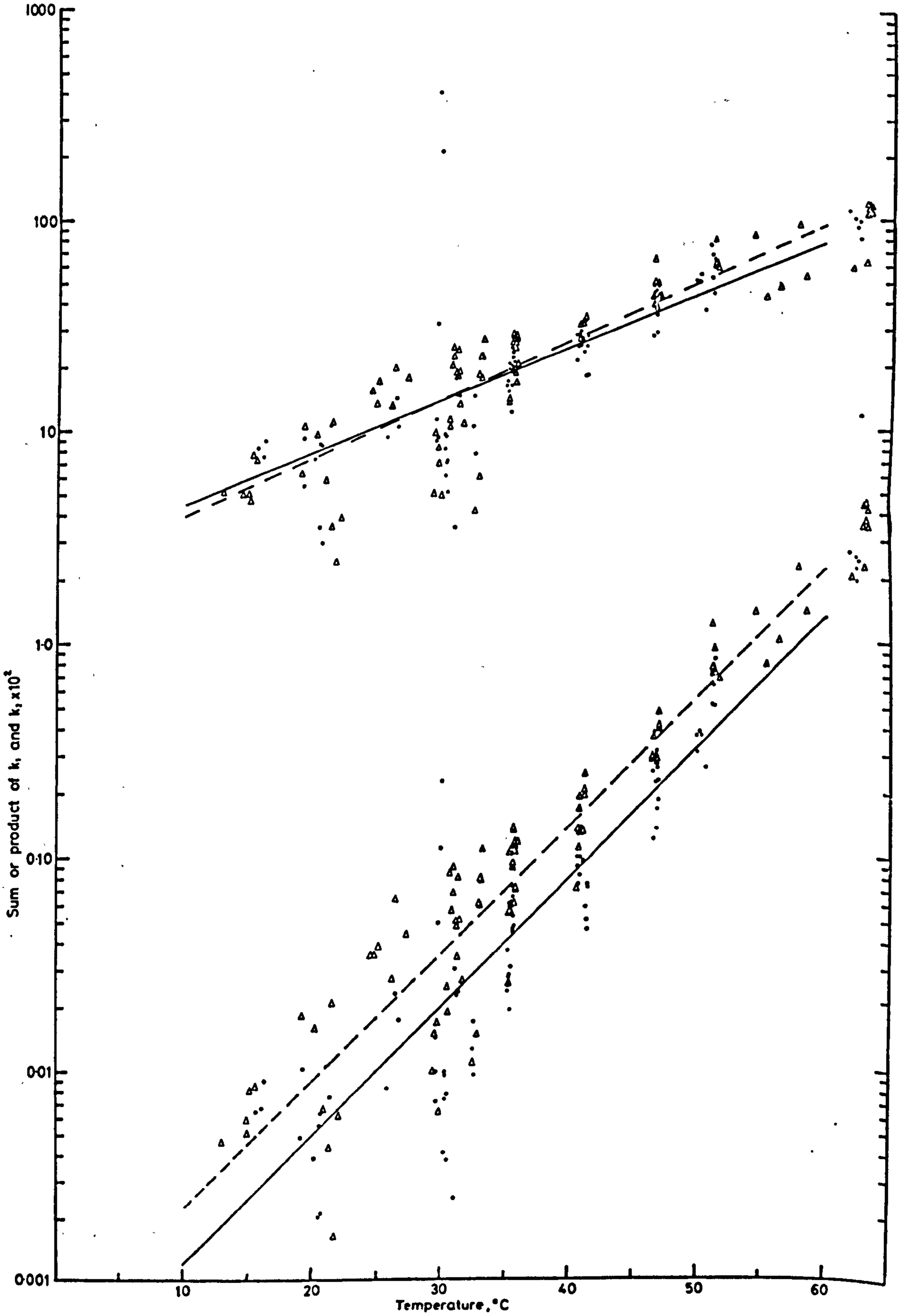

Fig. 3.34 Sum(top) and product (bottom) of the constants, k_1 and k_2 in equation 3.10 for Sabel (•) and S23 (Δ) with fitted lines represented by continuous and dotted lines for Sabel and S23 respectively.

Table 3.18

Coefficients in the expression y = A exp (bT) where y = p or q of equations 3.50 or 3.51

Constant	Sabel		S23	
	A	b	A	b
p	2.480×10^{-2}	0.0574	2.065×10^{-2}	0.06393
q	2.717×10^{-6}	0.1415	5.647×10^{-6}	0.1380

Comparison of k values between diffusion equations and between strains

For the purposes of comparison of 'k' values from the alternative equations and from the two different strains, the 'k' values were expressed as exponential functions of the three variables, drying air temperature, initial moisture content and humidity. Diffusivity is commonly accepted to be related to temperature by the Arrhenius relation

$$D = D_o \exp (E/(R(T + 273))) \quad \ldots\ldots\ldots\ldots \quad 3.52$$

and since the drying constant, k, is directly proportional to diffusivity it would be reasonable to expect that an equation of this form could be used for describing k. It has been used by several authors [16, 27, 46, 10], some of whom have attempted to evaluate D_o and the activation energy, E. But what is apparent from the attempts is that the range of absolute temperature covered by most data sets is very small and experimental variations causing what are in practice, only slight differences in slope, cause large differences in D_o and the value of E. It was felt therefore that equation 3.41

$$k = A \exp (bT) \quad \ldots\ldots\ldots\ldots \quad 3.41$$

was more convenient. There is precedent for its use [96, 69, 110, 49]

and, over the temperature range covered by the data, differences in k values predicted by the two equations fitted to the same data are very small.

Inclusion of the initial moisture content, M_o, and air humidity, H, as additional exponent terms (equation 3.44) was convenient because of the ease with which they be included in the least squares fit. Relative humidity could have been used instead of absolute humidity but the latter was preferred because of its independence from temperature. Neither of the two factors, M_o or H, was as important as temperature but their inclusion did improve the fit and their regression coefficients were significant. Although dependence of 'k' values on humidity has been doubted (46, 25, 118) positive evidence has also been presented (1, 34, 132, 130) and Troeger and Hukill (124) include dependence on initial moisture content.

There was very little difference between the k values given by the 2 term exponential and those given by the equation for the plane sheet over the whole temperature range (Fig.3.20). These two equations gave the best fits and clearly represent a reasonable compromise between the under-compensation of initial drying rate given by the single exponential, with a slightly larger k, and the over-compensation given by the sphere equation with the smallest k values. Although not giving as good a fit as 2 term exponential, the equation for the plane sheet is easier to use

since it only involves the 2 constants, k and Me. This result also suggests that the ryegrass seed is better approximated as a plane sheet than as a sphere.

There is some advantage here in that for the purpose of calculating diffusivity, thickness is a readily definable quantity whereas the choice of an appropriate characteristic 'diameter' is largely subjective (see Section 2.23).

The comparison of varieties proved that the smaller seeded S.23 dried faster than the larger seeded tetraploid, Sabel, although the difference decreased with increasing temperature. Since in theory, k is proportional to the square of some characteristic dimension (see Equations 3.6, 3.7) the square roots of the ratio of the k values for the two varieties are compared in Table 3.19.

Table 3.19

Values of the quantity, $\sqrt{(k_{S23}/k_{Sabel})}$ at 5 temperatures for the 4 alternative diffusion equations.

Temperature, °C	Diffusion equation				Mean
	Single	2 term	Slab	Single	
10	1.69	1.58	1.55	1.44	1.57
20	1.58	1.48	1.47	1.41	1.49
30	1.47	1.39	1.39	1.37	1.41
40	1.38	1.30	1.32	1.33	1.33
50	1.29	1.22	1.25	1.30	1.27
60	1.20	1.14	1.19	1.27	1.20
Mean	1.44	1.35	1.36	1.35	1.38

Clearly similar ratios are given by all 4 diffusion equations at any one temperature and the mean range 1.57 - 1.20 from 10°C to 60°C is representative of them all. It is of interest to note that the mean ratio is 1.38 which is in very good agreement with the ratios of dimensions, and in particular thickness, tabulated in Table 2.3 of Section 2.2.3. The implication here is that the

difference in drying rate between the varieties is due to the size difference rather than a difference in diffusivity. However the comparison is affected by temperature and humidity to an extent which procludes combining the k values from the two varieties by correcting for relative size alone. From a practical point of view the difference is important because it means a difference of from $1\frac{1}{2}$ to $2\frac{1}{2}$ times in the drying rate depending on temperature and humidity and supports the view of those growers who maintain that tetraploid ryegrass seeds are more difficult to dry than the diploids.

Comparison with other seeds

Fig. 3.35 compares the drying constants for S.23 and Sabel obtained from the 1971 data with published data for barley (16) and wheat (69). At low temperature the drying rate of the grass seed is less than that of wheat or barley but it increases at a greater rate until at higher temperatures it is greater. Since wheat and barley belong to the Graminae it might have been expected that differences between them and grass seed would have resulted from differences in size, but this would have meant drying rates in grass seed 9 times higher than in wheat or barley. This is clearly not the case and it follows that the diffusivity of grass seeds must be less than that of cereal grains. Comparative diffusivities over the range 30-60°C are plotted in Fig.3.36. The data from Pabis(96) were taken direct from his paper, that of Boyce(16) for barley and M'Ewen & O'Callaghan(69) for wheat were calculated from estimated diameters based on equation 2.7 whilst that for the grass seeds is based on equation 3.6 using the mean values for thickness, z, given in Table 2.3, Section 2.2.3. The lower diffusivity of grass seed is confirmed. The most probable explanation for it would seem to be the variation in diffusivity of moisture through individual seed tissues and the varying ratios

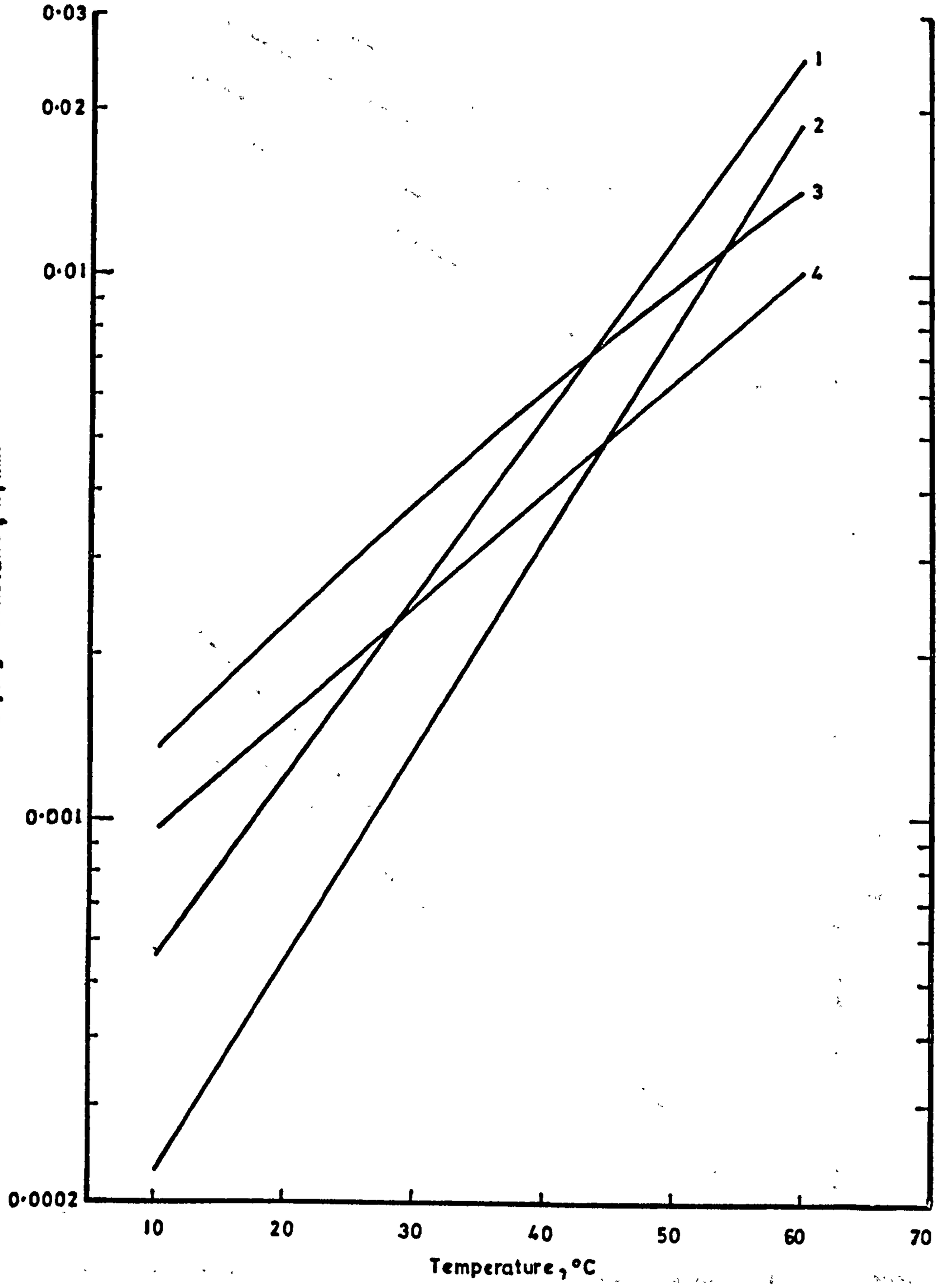

Fig. 3.35 Comparative drying rate constants, k, for S.23 (1) and Sabel (2) ryegrasses (equation 3.10), barley (3) (Boyce, ref. 16) and wheat (4) (McEwen and O'Callaghan, ref. 69).

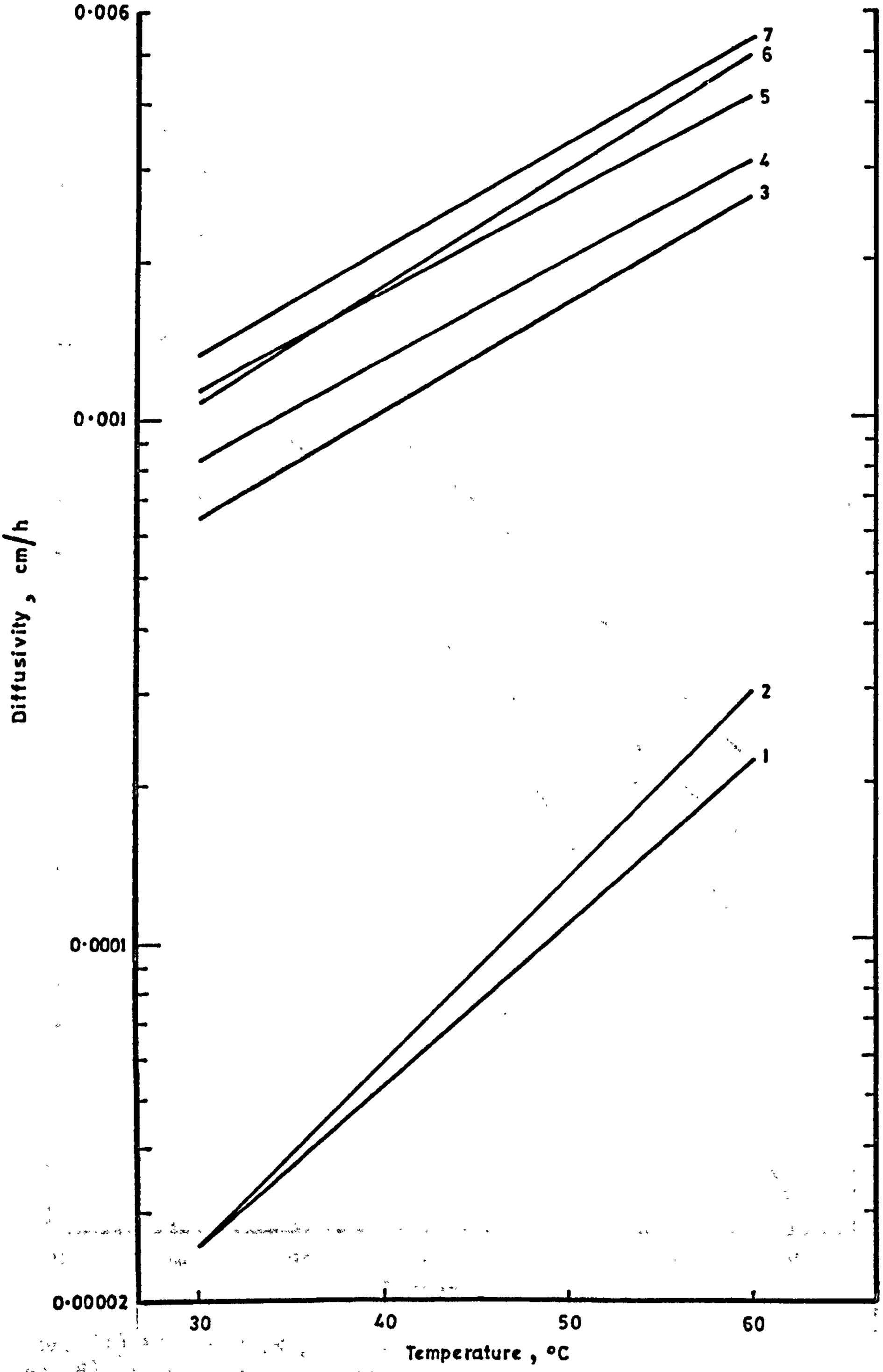

Fig. 3.36 Comparative diffusivities of S.23 (1) and Sabel (2) ryegrass, with other grains
3 = Wheat - McEwen & O'Callaghan (69)
4 = Barley - Boyce (16)
5 = Maize)
6 = Wheat)- Pabis (96)
7 = Beans)

of such tissues in cereal grains compared to grass seeds.

3.5.2. Equilibrium moisture content

The data were in general very well correlated by equation 3.42 and given the variation inherent in the data it is unlikely that a more complex expression would have given significantly better predicted values of M_e. Equation 3.42 is simple, it is easily fitted to the experimental data and it has the correct shape over the entire practical range. This point requires amplification. Plots of the equation for constant temperature as in Fig. 3.22 produce sets of lines which do not have the sigmoid shape evident from the data plot of Fig.3.23. However it must be remembered that the variation in relative humidity in that plot is mainly achieved by changing the temperature of air of ambient absolute humidity. Thus if a series of predicted data points are generated using a constant absolute humidity, the resultant line has the same sigmoid shape as the data (Fig.3.23) and fits it extremely well. The equation was suggested by that of Smith

$$M = Mo - c\ln(1 - rh) \qquad \ldots 3.11$$

in which Mo represents the bound water fraction and is the asymptote at zero relative humidity. It was realised that this asymptote must be dependent on temperature and would, in fact, become zero at the temperature (130°C) and humidity (rh = 0.6% at 0.01 kg/kg absolute humidity) at which the oven moisture test is determined. An examination of the correlation of the values of Me with t suggested that this function might be logarithmic hence Mo was replaced by the term a - b ln T. The various experimentally determined constants of equation 3.42 predict somewhat higher temperatures (1) than 130°C for the

---

(1) The correlation of all 1971 and 1972 data predicts zero M_f at 225°C.

attainment of zero moisture, but it is reasonable to suppose that the logarithmic function for T is only a coarse approximation.

The generally greater variability of the derived asymptotic constants, M_e, compared with the actual final moisture contents, M_f, supports the view that the derived values are more specific to the individual curve fits than to the true asymptotic value. Because of this it could be argued that for predicting drying rates, the values of M_e should be those derived from the same diffusion equation as the k values. But the use of the correlation of final moisture might be expected to give more realistic values of the moisture content to which the seed will tend at equilibrium. This point can only be resolved by trial and error within a simulation, but predicted values of M_e and M_f are of a similar order.

In fact the differences between the M_e values predicted for S23 by the correlation of the values from the 2 term exponential equation in 1971 and those predicted by all 216 data points for both varieties in 1971 and 1972 are of no practical significance. Values of M_e for Sabel predicted by the diffusion equations are generally less by the order of 1% m.c.d.b. than those for S.23 although the differences between the actual final moisture contents were much less than this. It seems probable that the lower derived M_e values of Sabel reflect a slight difference in the shape of the drying curve for which the curve-fitting procedures compensate by adjustment of both the k and M_e values.

Precise comparison with data from other sources is not possible, but predicted values are in reasonable agreement with static equilibrium values given for ryegrass by other workers (59, 109, 61). Comparison with published results for other seed species is also difficult but there seems little doubt that the M_e values for ryegrass seed are lower at low humidities than those

for wheat (69) or barley (16). This accords with the authors experience that the ease with which the seed is overdried is the main problem in using heated air driers for grass seed. At relative humidities within and above the normal ambient range the differences are much less. Static equilibrium data for wheat and barley presented by Pixton & Warburton(97). correspond at relative humidities > 30% with the ryegrass data and exhibit a temperature effect similar to that of Sabel.

3.5.3. Germination

The dominant feature of the germination results was the amount of variation which could not be attributed to, or quantified by, the treatment variables. Since the drying conditions were controlled within narrow limits it seems reasonable to suppose that the variation must be a result of other factors. It is unlikely that there were marked differences in mechanical damage at harvest since drum speed and concave setting were standardised. Storage prior to drying might have been expected to affect response but there were no apparent differences between freshly-harvested and cold-stored seed from the 1971 tests. Frozen seed was severely damaged, of course, but this was excluded from the analysis. It seems most likely that, for the reasons put forward by Thomson (117) and discussed in section 3.2.4, the variation lies within the germination test itself. This view is supported by the wide range and random distribution of the standard deviations given by the tests in the 1972 experiment. Nevertheless the standard test is more repeatable than any field test yet devised, it is the important commercial criterion and the one by which the results of the work must be judged.

The bulk of the germination results originated from the thin-layer rate test and, with the inclusion of the 10h data from 1972, represented the effect of long-term exposure to temperatures from near-ambient up to 78.5°C. The expression of the results as depressions from a base level calculated from the ripening equations did not entirely remove the effect of initial moisture content and, in particular, differences in response due to maturity were greater at the higher temperatures. However, within the range of depressions which might be tolerated in practice, the effect was much smaller. The use of the depression values was useful because

it did separate out the temperature effect and showed that this was similar for both varieties even though their base germinations were quite different (Fig.3.25). An interesting feature of this response was the tendency for the depression to become negative at temperatures slightly above ambient i.e. germination was improved. Two explanations can be put forward for this. Drying at slightly elevated temperatures means that the relative humidity of the air to which the seeds are exposed is below that which would encourage the growth of micro-organisms and ensures that the seeds reach a safe storage moisture content in a reasonably short period. In contrast, control seeds dried with ambient air may be exposed to comparatively high relative humidity, their moisture content may fluctuate about the safe storage moisture content for some days and pathogenic organisms may cause some deterioration before the safe storage moisture content is reached. The second explanation for the effect may be that some dormancy is being broken; drying at 30°C is a recommended way of breaking seed dormancy (55).

Under these conditions of prolonged exposure positive depression of germination began to occur between 35 and 40°C and had reached unacceptable levels by 50°C. Thereafter, further depression was very rapid. Using the maturity equation 2.4 and the depression equation 3.47 it can be shown that S.23 seed in the moisture range 66.7 to 33.3% d.b. (40 - 25% w.b.) will be depressed to 90% germination by temperatures from 40 to 43°C. This is a narrower range than inspection of the data would suggest, partly because not all the variation in response due to moisture content is accounted for in 3.47, and partly because of seemingly random variation in the data. It does, however, provide some useful guide lines, the values of which are in general agreement with results from experiments by a number of authors with different

types of seed[82]. The range of 40-43°C is also much narrower than that indicated by the author's previous results for 6 inch layers of S.24 ryegrass seed [79]. This is to be expected since in a 6 inch layer being dried to an average moisture content, safe for storage, only a relatively small proportion of the seed ever reaches the inlet air temperature and that which does may not do so for very long. The factors which are important in this situation are time of exposure to a changing temperature regime which in turn reflects a complex relation to changing moisture content. The aim of the 1972 experiment was to try and quantify the effect of exposure under conditions of constant temperature. Drying was allowed to continue and since air of ambient humidity was used, the drying rates were at or near the maximum which would be encountered in practice at the temperatures used. Whether this increased or decreased the damage to quality is difficult to say. It may be argued that the rapid dehydration subjects the seed to greater stress but there is the evidence of sealed heating experiments[129,134,64] to show that, where drying is inhibited, as it might be under conditions of high humidity, the greater heat capacity of the moist seeds may result in worse damage. In retrospect it is clear that the combinations of exposure and temperature chosen were not ideal since so much of the damage was done within the first 15 minutes, although it should be noted that so great was the variation in response that for seed at the lowest moisture contents and temperatures it took nearly 10h for the exposure effect to become significant. But shorter exposure times for the higher temperature treatments would have been useful. From the many hours exposure needed to cause depression at 40°C (the long-term exposure results), there is clearly a rapid decline in critical exposure times as temperatures are increased and above 68°C they are a matter of minutes only. The decline is of the exponential order

suggested by the equations of Hutchinson [54] and Ptitsyn [98] derived from sealed heating experiments. A correlation of the present data in a similar manner to that of Hutchinson [54] or Ptitsyn [98] was not attempted mainly because it was felt that these equations were not suitable for use within a computer simulation of the drying process of the type described in Section 5. For this purpose an equation is needed which can be used to calculate cumulative changes in germination throughout the bed in order to further calculate the overall mean germination at any point in time.

A study of the results of the 1972 experiment suggested a correspondence between germination reduction and moisture reduction with time but a correlation between the two was not established. Germination reduction did not parallel moisture loss and maximum damage was normally sustained before the seed was dry. However, both phenomenona exhibit an exponential decay asymptotic to a value greater than zero. For germination it seemed reasonable to assume that both rate of decay and the asymptotic value were a function of temperature.

As a first step plots of germination against exposure time for Sabel were used to draw by eye smoothed curves from which a series of revised germination values, G and asymptotic germinations, G_e, could be read. These were then used to derive graphically values of k_g in the equation

$$G = (G_o - G_e)\, e^{-k_g \theta} + G_e \quad \ldots\ldots\ldots\ldots\ldots\ldots 3.53$$

which is, of course, analogous to the drying curve equation , 3.1. G_o is the value predicted for a given initial moisture content, M_o, by ripening equation 2.1 or 2.3. For simplicity, G_e, was expressed as a linear function of temperature and initial moisture content and k_g as an exponential function of temperature.

$$G_e = 331.0 - 3.24T - 1.14M \quad \ldots\ldots\ldots\ldots\ldots\ldots 3.54$$

$$\ln (k_g) = 0.1475T - 12.8114 \quad \ldots\ldots\ldots\ldots\ldots\ldots 3.55$$

Both these equations are gross simplifications which lead to unrealistic results if extrapolated too far. In particular G_e may exceed a sensible value of G_o at low temperatures and/or moistures and may become negative at high temperatures. However, in a computer programme an upper limit of G_o and a lower limit of say 10% can be set to override predicted values. The function for k_g ignores the moisture content effect which although small in relation to the effect of T was consistent at each value of T. The agreement between the experimental and predicted values is illustrated by Fig. 3.37. For the three lowest temperatures, the agreement is good but at the two highest, predicted values are less than the observed. As mentioned above, the setting of a lower limit to G_e alleviates this to some extent and if it does result in a weighting of the calculated results for a deep bed, the weighting will produce a conservative, and hence 'safe' estimate. A similar exercise was carried out on the S.23 results and gave the following equations for the constants G_e and k_g

$$G_e = 222.3 - 1.65T - 1.03\,M \quad \ldots\ldots\ldots\ldots 3.56$$

$$\ln (k_g) = 0.123T - 10.531 \quad \ldots\ldots\ldots\ldots 3.57$$

Predicted values are compared with the observed values in Fig.3.38. Agreement is slightly better than for Sabel and the overestimation of the depression at the highest temperatures is not so severe. The slopes of the temperature and moisture content effects are less steep in equation 3.56 than in equation 3.54 and extrapolation to the extremes of these two factors does not yield such unrealistic values as it does for Sabel. Nevertheless the remarks concerning the use of limits inside a computer programme still apply.

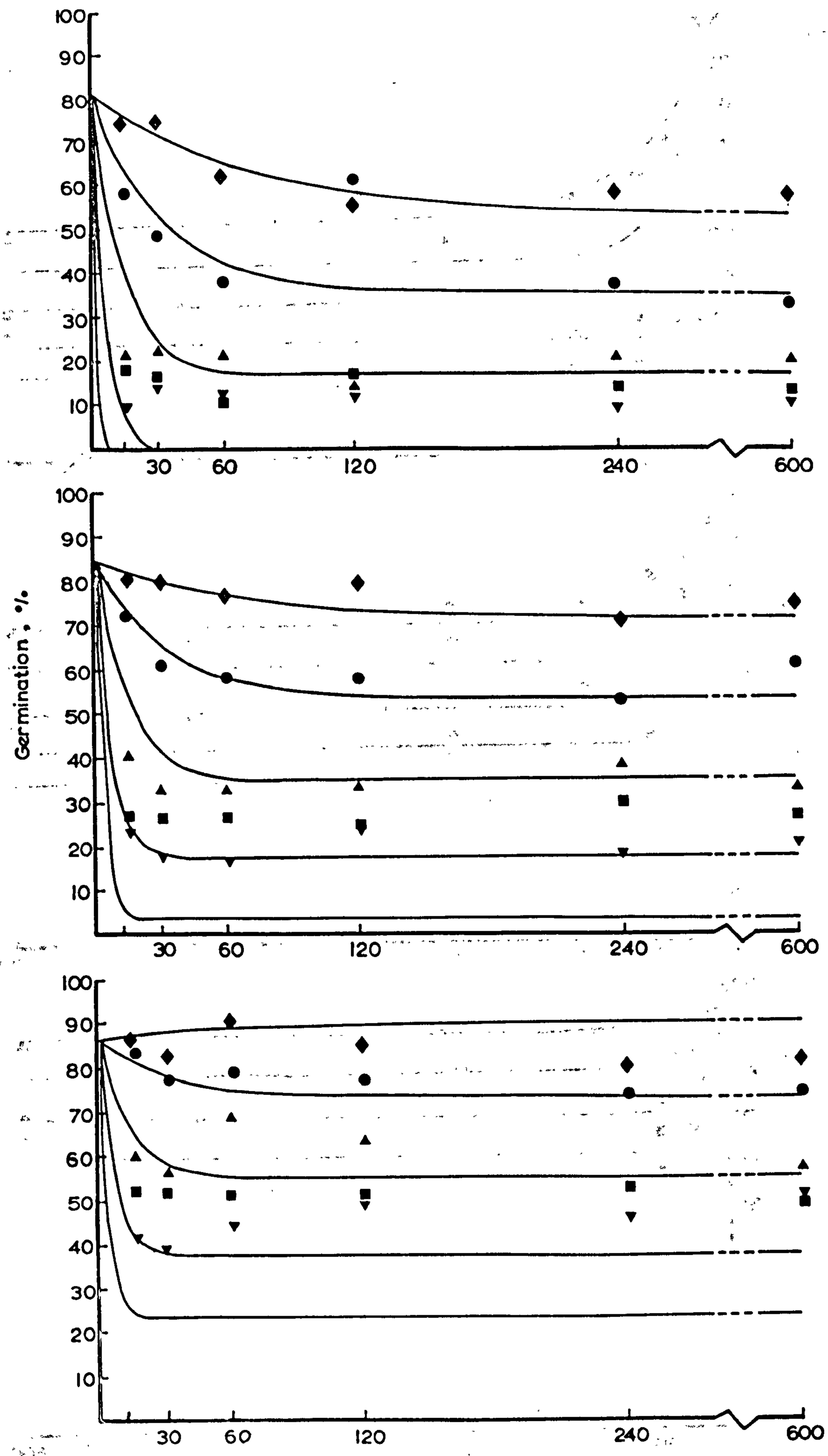

Fig. 3.37 Comparison of experimental and predicted germinations of Sabel as a function of exposure time, Eqn. 3.55, at 57.7(♦), 63.2(●),68.8(▲),74.2(■)and 78.5 °C(▼) at moisture levels of 80.0(top),64.1(middle) and 46.5(bottom) % d.b.

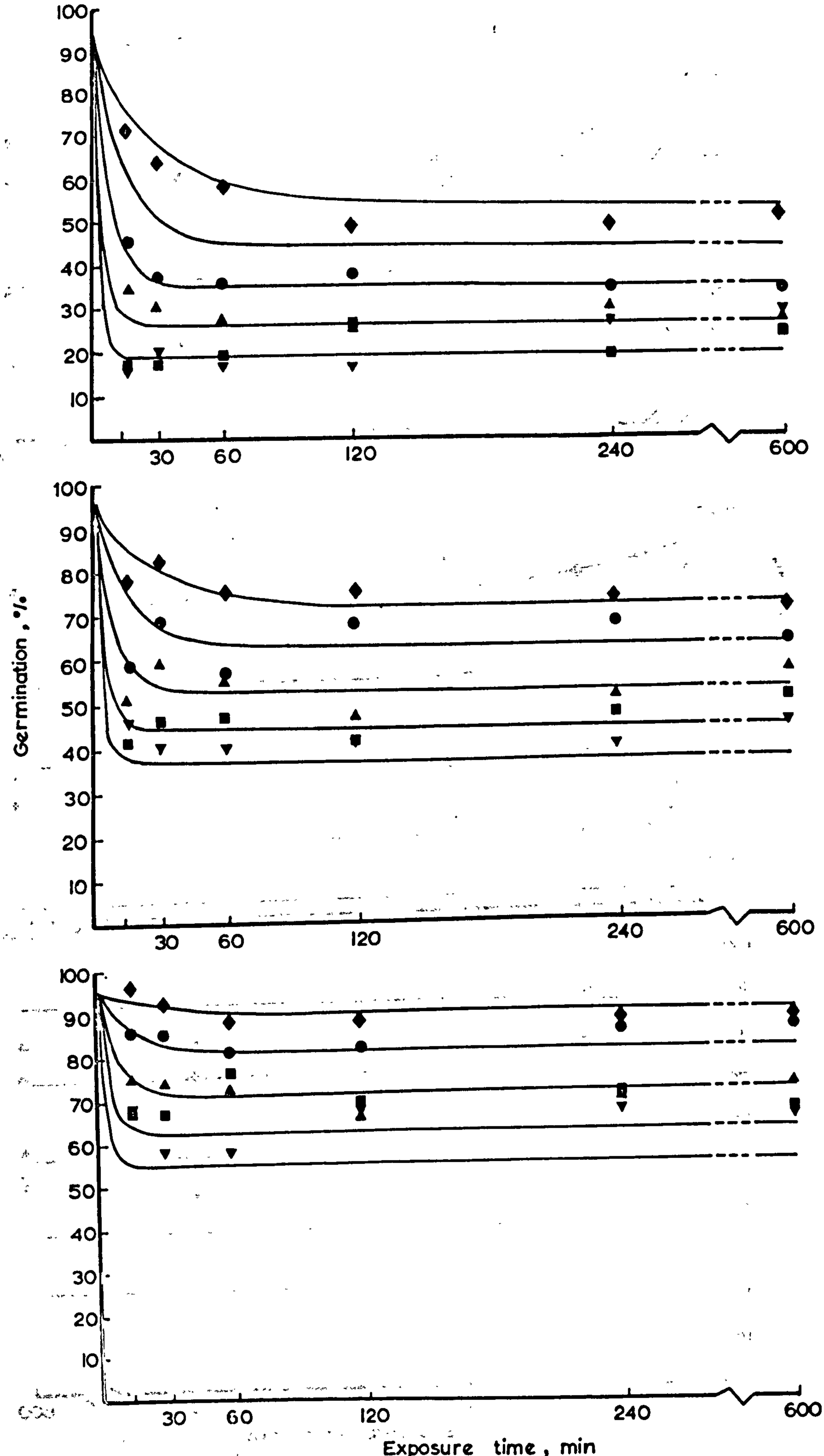

Fig. 3.38 Comparison of experimental and predicted germinations of S23 as a function of exposure time, Eqn. 3.53, at 57.7(♦), 63.2(●), 68.8(▲), 74.2(■) and 78.5 °C(▼), at moisture levels of 71.5(top), 53.4(middle) and 31.1(bottom) % d.b.

It will be evident that for the prediction of G_e equations 3.46 or 3.47 derived from all the long-term exposure results together with the ripening equation could have been used but the aim of the exercise which led to equations 3.53 to 3.57 was to try and obtain a simple description of the 1972 data only. There is clearly scope for further analysis of the whole three year's results. An interesting point about the existence of an asymptotic value of germination, particularly when this is a considerable percentage as it is with S.23, is that in a deep bed a considerable contribution to the mean germination of the whole bed may be made by layers which have sustained maximum damage. It also prompts the thought that resistance to drying damage has a wide statistical distribution within a seed population and might perhaps be selected for in a breeding programme.

It should be noted, however, that continuing exposure did appear to reduce germination vigour or speed of germination so that even viable seeds had sustained some damage which may reduce the ability of the seed to withstand long-term storage. Reduction in speed of germination had been anticipated and had led to counts being continued up to 21 days. Although some extra germinations did occur between the 14th and 21st days they were not specifically associated with the most damaging treatments and made very little difference to the results.

The estimations of mould growth which were also made during this period also gave inconclusive results. Undamaged diploid ryegrass seed normally germinates with a vigour well over 90% and Kahre [59] has suggested that the present 14 day test period should be shortened. If this were done the conclusions of this work would need revision.

3.6. SUMMARY AND CONCLUSIONS

3.6.1. Experimental

An eight-unit experimental drier was modifed for the determination of weight loss during drying of thin-layers of seed exposed to an excess of air of controlled temperature and humidity. Weight loss and temperature data were automatically recorded.

One unit of the drier was fitted with a refrigerated condensing unit which enabled the use of air temperatures and humidities less than ambient. During the period of study two other units were fitted with packed towers through which air could be conditioned to dew points in the approximate range 4 to 36°C.

Experiments to determine thin-layer drying curves were carried out in the 1970 and 1971 harvests. In 1970, data was analysed from 140 runs with S.23 obtained at air temperatures from 27.7°C to 61.7°C and initial moisture contents from 40 to 117% d.b. In 1971, data was analysed from 91 runs with Sabel and 102 runs with S.23. The initial moisture contents varied between 23.2 and 99.9% d.b. for the Sabel samples and between 62.1 and 75.4% for the S.23 samples. The drying season was slightly extended by the use of cold-stored and deep-frozen seed. Drying air temperatures from 12.9°C to 63.4°C were used.

Experiments to determine the effect of time of exposure to drying air temperature on seed germination were carried out in 1972. At 3 moisture levels for each variety, seeds of Sabel and S.23 were exposed to temperatures from 57 to 79°C for periods of $\frac{1}{4}$, $\frac{1}{2}$, 1, 2,4 and 10h.

3.6.2. Data processing

A set of computer programmes were written to analyse the weight loss and temperature data. These included procedures for fitting the drying curves to 4 alternative diffusion equations by an iterative least squares method. The equations were:-

$$M = (M_o - M_e).\exp(-k\theta) + M_e \qquad 3.1.$$

$$M = A\exp(-k_1\theta) + B\exp(-k_2\theta) + M_e \qquad 3.10.$$

$$M = (M_o - M_e)\frac{6}{\pi^2}\sum_{n=1}^{\alpha}\frac{1}{n^2}\cdot\exp(-n^2k\theta) + M_e \qquad 3.38$$

$$M = (M_o - M_e)\frac{8}{\pi^2}\sum_{n=1}^{\alpha}\frac{1}{(2n-1)^2}\cdot\exp(-(2n-1)^2k\theta) + M_e \qquad 3.39$$

Each of these equations defines the drying curve by an exponential constant, k and an asymptotic value, Me. Equation 3.10 is a special case with 2 constants k_1 and k_2 determined independently of each other. Provided k_1 is much greater than k_2 it can be regarded as representing the higher order terms of a series such as equation 3.38 and k_2 is then analogous to the k of the other equations.

3.6.3. Drying rate constant:

Similar values of k were given by the fits of all 4 equations but the closest agreement was obtained between those given by equations 3.39 and k_2 of 3.10. These two equations and especially 3.10 also gave the best fits of the drying curves. Equation 3.10 was shown to be the solution of a second-order differential equation. Equation 3.39 is the solution for a plane sheet of Fick's equation for the rate of change of concentration of diffusion substance with time.

Differences between k values of Sabel and S.23 were shown to be in proportion to their size although diminished by increasing temperature. Hence the two ryegrasses have similar diffusivities.

Differences between k values for ryegrasses and cereal seeds were not a function of size and indicated lower diffusivities in the former which are probably due to differences in tissue ratios.

The constant k was expressed as a function of drying air temperature and humidity and seed initial moisture content.

$$k = A \exp(bT + cH + dM_o) \qquad ...3.44$$

Values of the coefficients A,b,c and d are given in Table 3.7, Page 85.

3.6.4. Asymptotic moisture content:

The asymptotic moisture contents, Me and the actual final moisture contents, Mf were expressed as a function of drying air temperature and relative humidity by equation 3.42.

$$M_e = a - b.\ln T - c.\ln(1- rh) \qquad ...3.42$$

Values of the coefficients a,b and c are given in Table 3.8, Page 91 and Table 3.9, Page 94 for Me and Mf respectively.

Differences in Me between varieties were small. In general under similar conditions values for Sahel were 1% d.b. less than those for S.23. Differences between Me and Mf were less than this.

3.6.5. Germination:

Germination depression was defined as the difference between the potential germination predicted by the ripening equations derived in Section 2, and the actual value. Under conditions of prolonged exposure, depression began to occur between 35 and 40°C and had reached unacceptable levels by 50°C. It was described by cubic functions of drying air temperature (Equations 3.46 and 3.47, Page 97). Similar depressions occurred in both varieties even though their potential germinations were different. For S.23, the only variety to exceed 90% germination, the fitted equations predict that germination will be depressed to 90% by temperatures from 40 to 43°C in the initial moisture range 66.7 to 33.3% d.b.

The 1972 experiments showed that as temperatures are increased above 40°C there is a rapid decline in critical exposure times and above 68°C they are a matter of minutes only. An empirical exponential function, equation 3.53, was developed to describe the decline in germination with drying air temperature and exposure time.

$$G = (G_o - G_e) \exp(-kg\theta) + G_e \qquad \ldots 3.53.$$

The constants kg and G_e were described as linear functions of temperature and of temperature and initial moisture content respectively (equations 3.54 - 3.57, Page 136). In its differential form, equation 3.53, which is analogous to equation 3.1. for moisture loss, is suitable for use within a deep bed simulation programme.

4. DEEP BED EXPERIMENTS

4. DEEP BED EXPERIMENTS

4.1. INTRODUCTION

This section describes experiments to record the progress of drying in deep layers of seed subjected to either parallel- or radial- airflow. The records were required to provide a yardstick by which to assess the accuracy or validity of similar records generated artificially by means of the thin layer data of Section 3 and the computer programme described in Section 5.

Compared with the thin-layer experiments, the time, seed and labour required to obtain results for one run was very great and it was not possible to carry out more than 2 or 3 runs with each variety in any one season. This inherent limitation of large scale drying experiments has already been recognised as one justification for the thin layer/numerical integration approach to the solution of seed drying problems.

The apparatus was designed and built and the measuring and recording equipment was scaled in Imperial units and for convenience these are adhered to in this chapter although SI equivalents are given either as supplementarics in the text or in Appendix tables.

4.2. APPARATUS

4.2.1. General description

The drier used for the deep bed tests is described by reference to Fig. 4.1 and is illustrated in Fig.4.2.

Air was drawn in by a centrifugal fan, C, through a bank of heaters, A, and an air control valve, B, and blown along an insulated pipe, D, containing an orifice plate E. It then passed via a flexible coupling, F, into a plenum chamber, G, from where it enters the drying bin, H, and exhausted to atmosphere. The plenum chamber and drying bin were supported by a platform, I, which formed

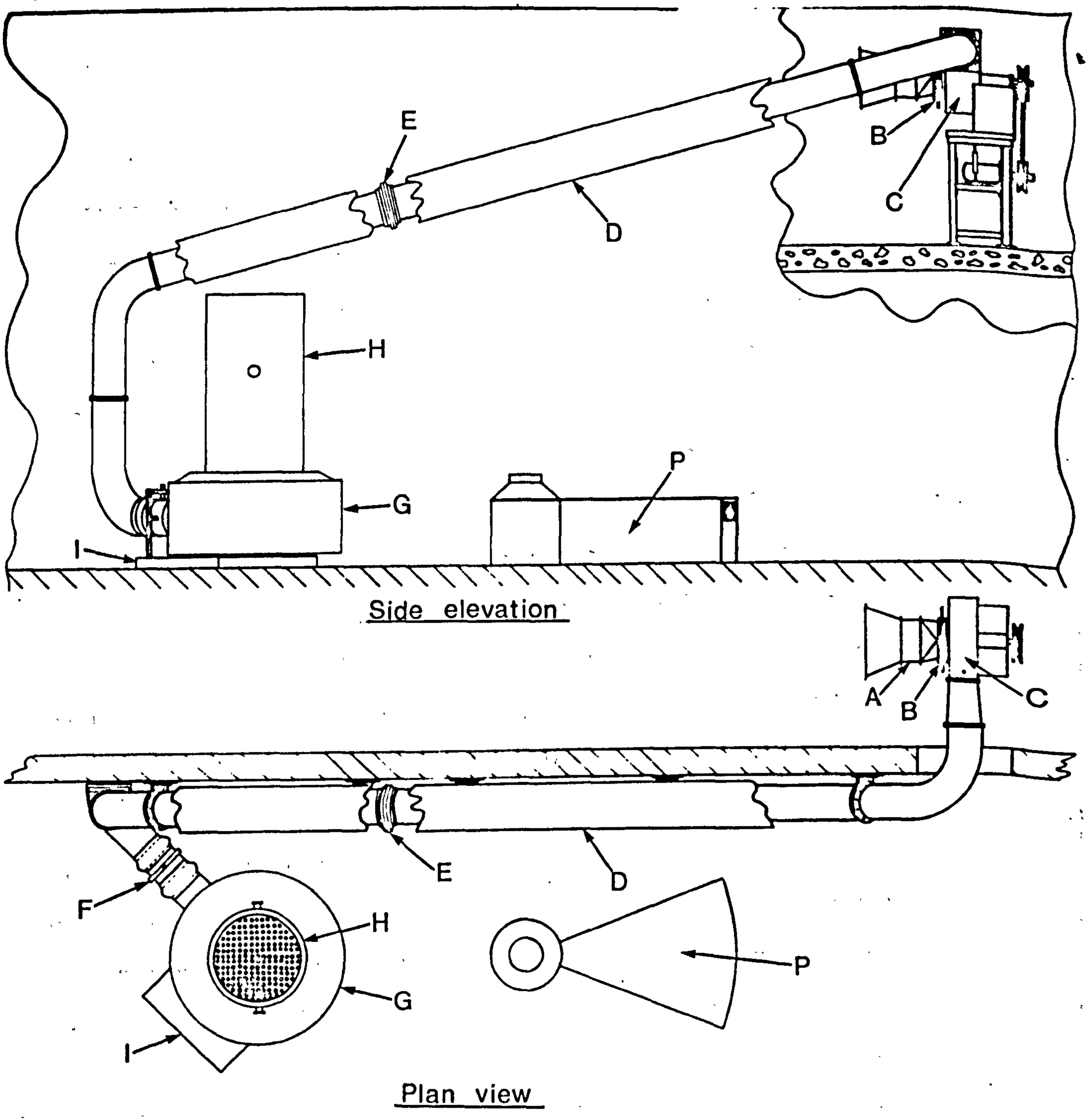

Fig.4.1. Apparatus for parallel- and radial-flow deep bed tests.

part of an automatic weighing system. Since it was not possible to use this system for any of the tests reported here, it is not described.

4.2.2. Drying bins

The drier was designed to cope with the drying of a wide range of product densities, drying air temperatures and flows and, for parallel flow drying, was equipped with 2 drying bins of 5 and

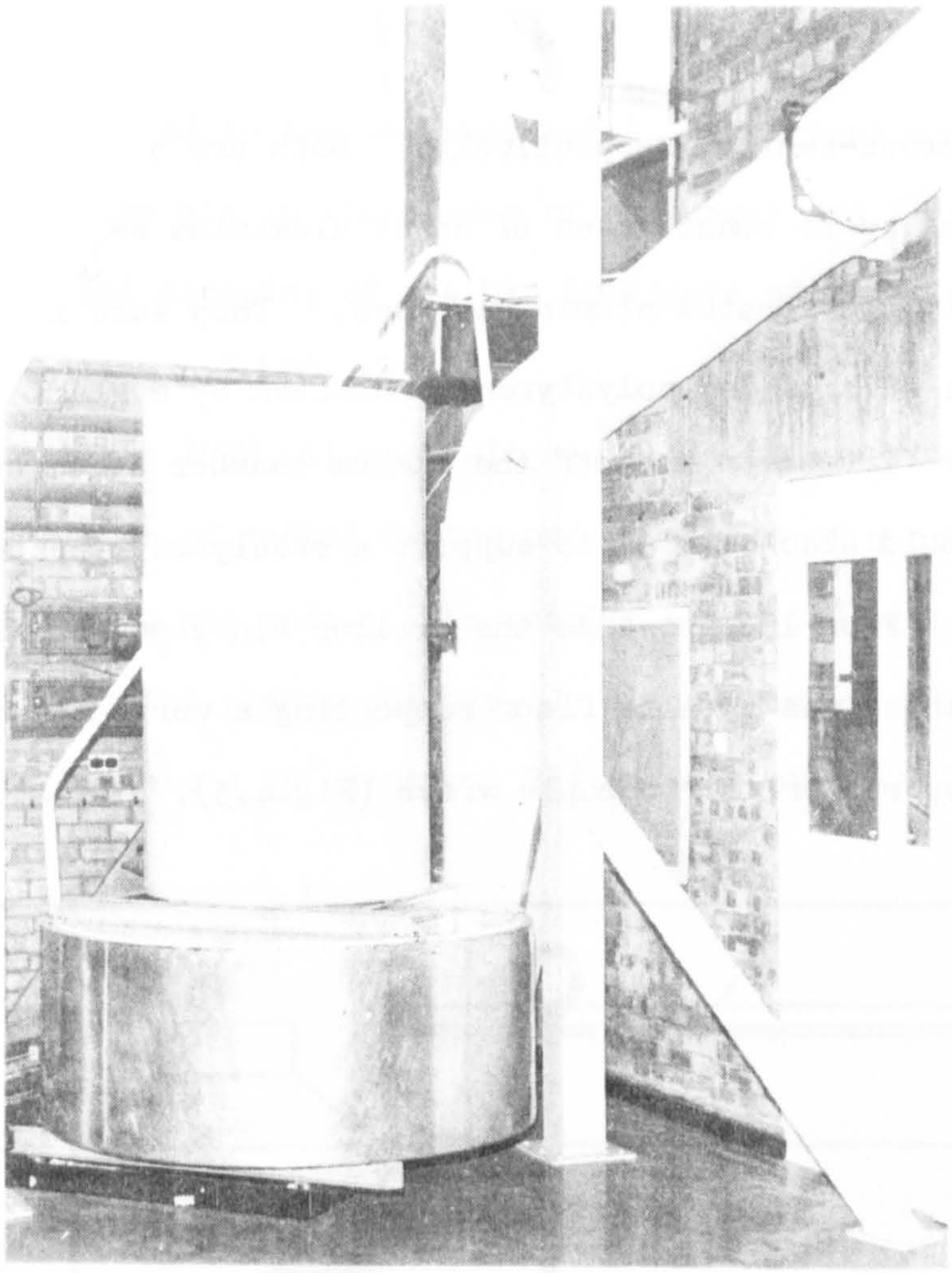

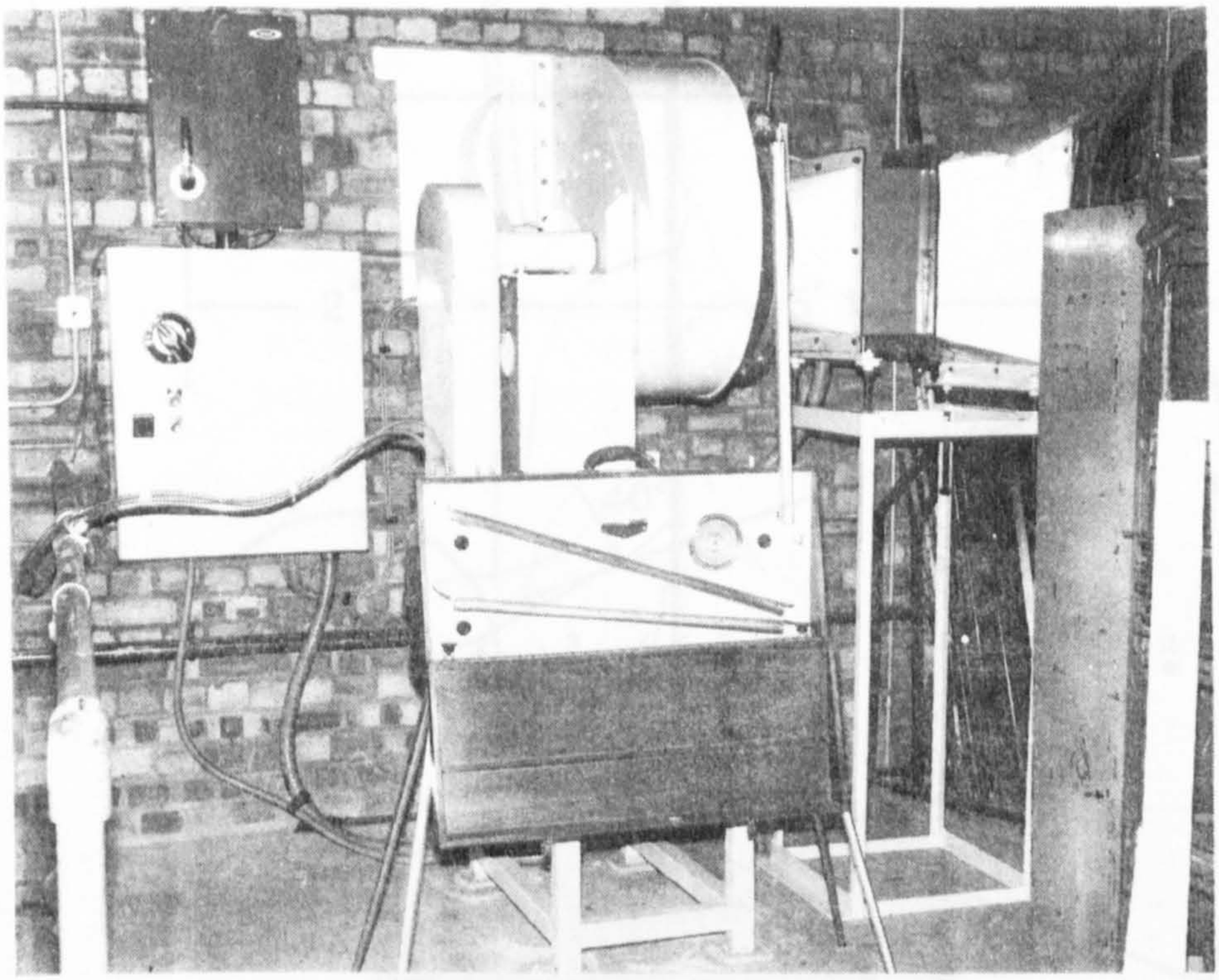

Fig.4.2. Deep bin drier. Air duct, plenum chamber and drying bin (Top) and fan, heater, electrical and inclined tube gauges (Bottom)

15 ft^2 cross-section respectively. Both are 5 ft deep and, for lightness, were constructed of sheet aluminium welded to aluminium rings with perforated aluminium bases. They were insulated with 2 inches of expanded polystyrene protected by a glass-fibre coat. They were lifted on and off the plenum chamber by an overhead hoist which could also be used to support a steelyard type of weighing unit.

From 1971 onwards the smaller bin was used with a special insert which was a false floor supporting a vertical rod which acted as a support for thermocouple wires (Fig.4.3). By attaching the

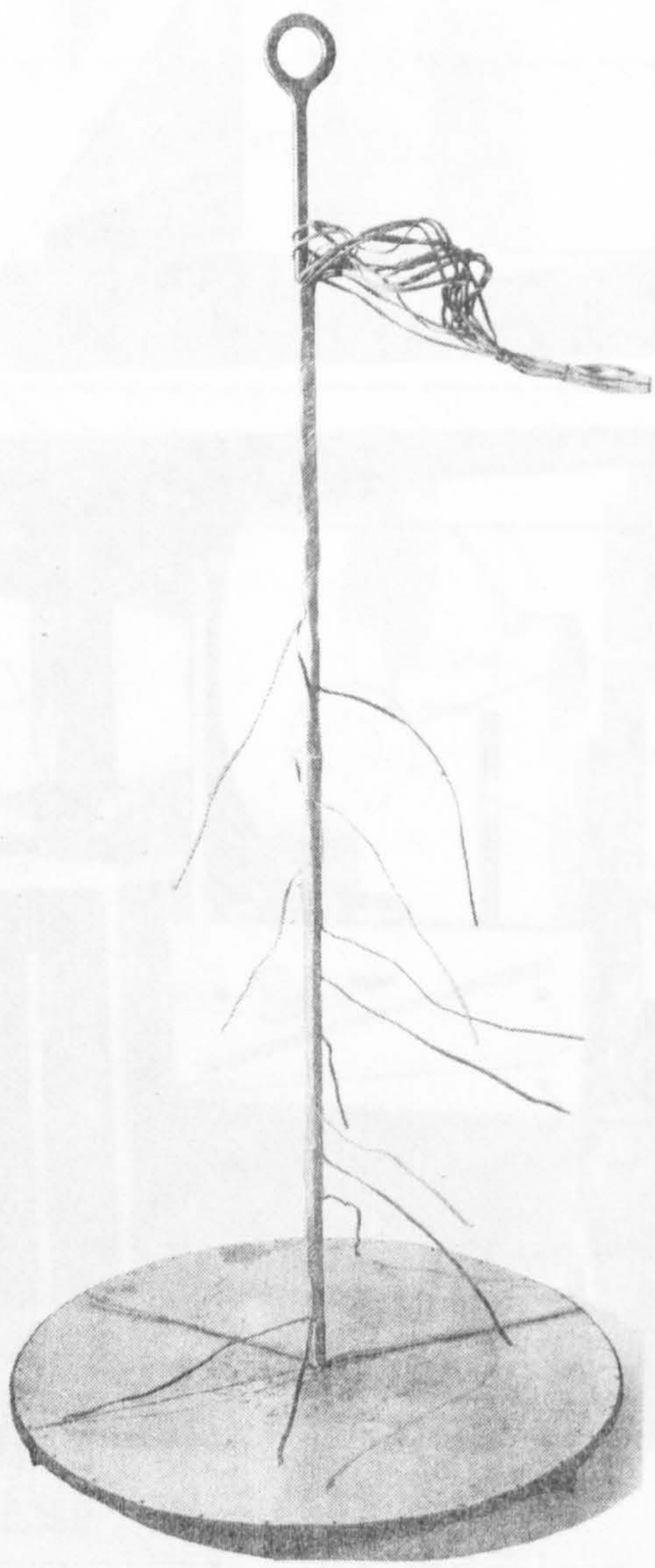

Fig.4.3. False floor insert for small drying bin with thermocouple leads fastened to central stalk at 3 in. intervals.

top of the rod to the overhead hoist, the insert could be moved up and down the bin in the manner of a plunger and facilitated the filling and emptying of the bin in layers of measured depth. (See Section 4.3.1.6)

In 1972, it was felt desirable to make some practical observations of radial drying and a section of a commercial (Simplex) radial drier was made. The section (Fig.4.4) consisted of a 2 ft. diameter metal plenum chamber, J, discharging air through a perforated sheet, K, into a 40° section, 21¾ in deep of a 12' 2" diameter bin, L.

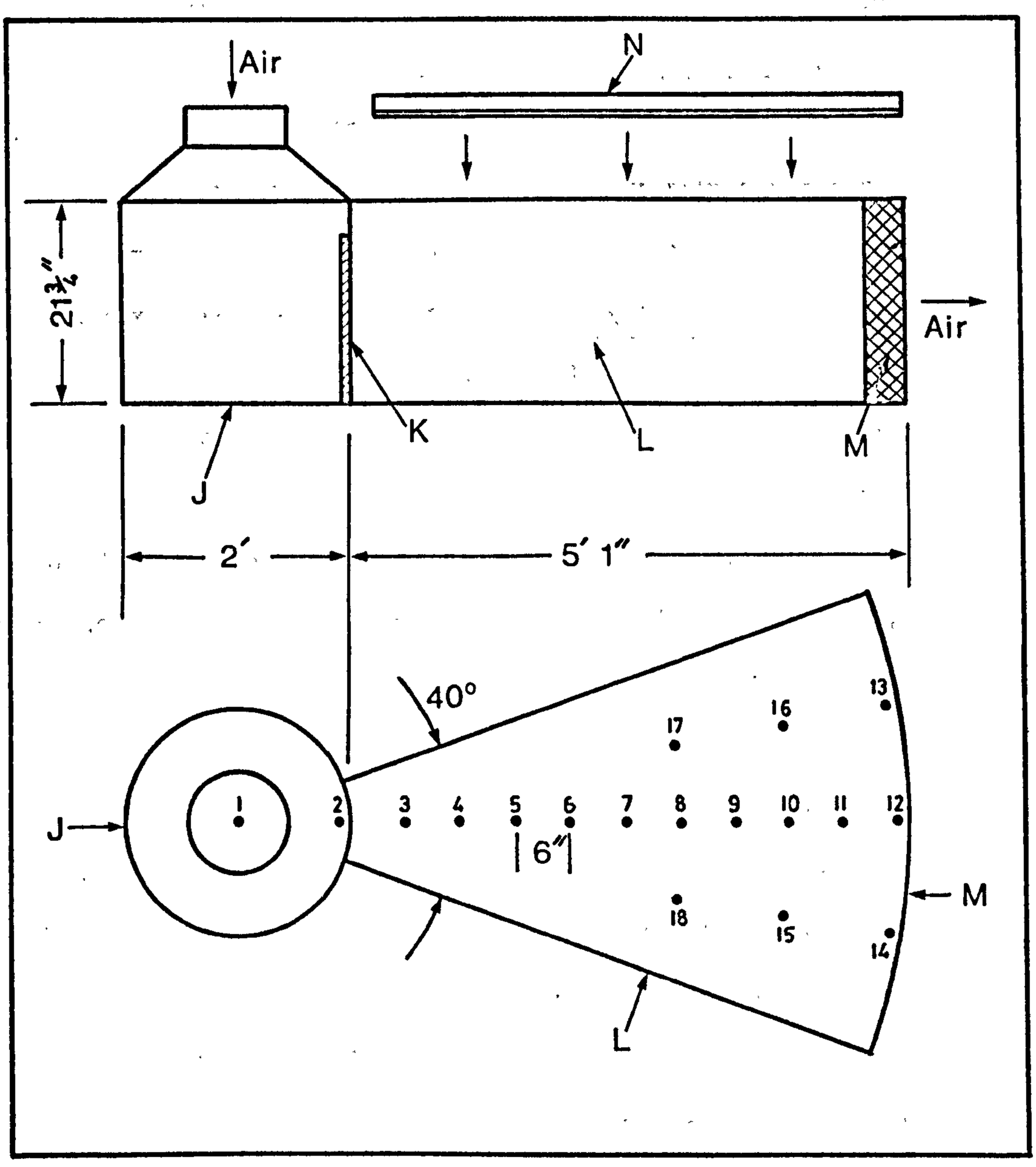

Fig.4.4. Section of radial bin drier. Thermocouple locations indicated by numbered dots.

The floor and side of the section were made of hardboard and the outer wall,M, of fine nylon mesh supported by 1" weldmesh. A continuous plastic sheet was fastened around the sides in such a way that it could be folded across the top to act as a seal beneath the hardboard lid,N. The horizontal cross-sectional area was 12.58 sq.ft and hence a maximum capacity of 22.8 cu.ft. The drying air was supplied to the top of the plenum chamber through a flexible plastic tube, 11" diameter, connected to the flexible coupling, F, in Fig.4.1. The outline diagram of the unit, P, included in Fig.4.1. illustrates its relationship to the rest of the deep-bed apparatus.

4.2.3. Fan and heater bank

A 5 h.p. 3 phase electric motor running at 2800 r.p.m. drove the centrifugal fan through a belt and variable speed pulley which allowed impeller speeds of 2800 to 3700 r.p.m. Maximum fan output was 2000 ft^3/min at 12 in w.g. (see Appendix Figure 4.1.2). Further control of airflow was given by the air control valve which was of the iris diaphragm type, variable between 0.5 and 12.75 in. diameter.

The 15.5 kW heater contained 5 separate banks of 0.5, 1, 2, 4, and 8 kW each of which could be switched independently onto either manual or automatic control. The control circuit for fan and heaters is given in Appendix figure 4.1.1. . The thermistor sensor for temperature control was positioned in the duct almost immediately downstream of the fan. This gave a quick control response but adequate insulation of the rest of the duct and plenum chamber was necessary to prevent the final air temperature being influenced by ambient conditions. Both were insulated with 2 in. thickness of expanded polystyrene.

4.2.4. Flow measurement

The internal diameter of the ducting was 11.5 in.; the diameters of the 3 British Standard orifices [19] used within it were 3.0, 4.4 and 7.8 in. respectively. The orifice plate equation simplified to

$$G = A\sqrt{\frac{P_{at}}{(460 + t)}}\sqrt{h} \qquad \text{lb/h} \qquad \ldots.4.1$$

$$Q = B\sqrt{\frac{460 + t}{P_{at}}}\sqrt{h} \qquad \text{ft}^3/\text{min} \qquad \ldots.4.2$$

where A and B have the following values.

	Orifice size		
	3.0"	4.4"	7.8"
A	3189	6942	24432
B	19.69	42.85	150.82

Plots of equation 4.2 for the 3 orifice sizes are given in Appendix 4.1. Linear flows for the parallel bins are obtained by dividing by the appropriate cross-sectional area.

Calculation of linear velocities in the radial bin has to take account of the radial geometry and possible variations in the depth of seed being ventilated. It can be shown (see Appendix 4.1) that for the experimental rig the following relationships applied:-

Velocity flow at bin wall = $1.4324\ Q/D_R$ ft/min

Velocity flow at outer wall = $0.2355\ Q/D_R$ ft/min

Mean velocity = $0.50878\ Q/D_R$

where Q = flow evaluated by equations above and D_R = vertical depth of seed in feet.

4.2.5. Temperature measurement

Temperatures were measured by means of chromel-constantan thermocouples connected to a multi-point Honeywell-Brown potentiometric recorder. In 1970 the thermocouples were placed in the seed and plenum chamber only. In 1971 and 1972 the wet and dry bulb temperatures of the air at inlet to the fan were also recorded. In all but two of the parallel flow runs the vertical interval between thermocouples was 3 inches; in Runs 2 and 3 it was 6 inches. In Runs 1-3 a further thermocouple was placed 1 inch below the seed surface. For runs 1-3 further details of thermocouple position are given in the Appendix. For runs 4-12 the thermocouple positions were numbered as follows:-

Thermocouple	Distance from air inlet, in
2	0
3	3
4	6
5	9
6	12
7	15
8	18
9	21
10	24
11	27
12	30
13	33
14	36
15	39

In the radial flow bin, thermocouples were inserted through the floor at 6 inch intervals along the centre radius and at 36, 48 and 60 inches from the inlet on 2 other radii (fig.4.4) The couple leads extended approximately 6 inches above the base of the bin.

4.3. EXPERIMENTAL

In the 3 seasons, 1970-72, a total of 12 parallel and 3 radial flow runs were carried out and are defined briefly by Table 4.1. The smaller drying bin (5 ft^2 cross-section) was used for all the parallel flow runs.

Table 4.1

Summary of deep bin runs

Run No.	Date of start	Seed	Initial m.c. % d.b.	Depth ft (m)	Drying time h	Nominal drying conditions	
						Airflow ft/min. (m/min)	Temperature °C (°F)
Parallel flow							
1	10/7/70	Sabrina	82.1	2(0.61)	52	40(12)	32(90)
2	28/7/70	S.23	69.5	3(0.91)	48	43(13)	32(90)
3	4/8/70	S.23	56.0	3(0.91)	43	36(11)	49(121)
4	12/7/71	Sabel	104.5	$\frac{2}{3}$(0.20)	23	28(9)	Ambient
*5	14/7/71	Sabel	92.7	$3\frac{1}{4}$(0.99)	115	28(9)	Ambient
*6	19/7/71	Sabel	63.1	$3\frac{1}{4}$(0.99)	65	26(8)	Ambient
7	22/7/71	Sabel	49.0	$3\frac{1}{4}$(0.99)	$21\frac{1}{2}$	23(7)	55.4(132)
*8	26/7/71	Sabel	23.5	$3\frac{1}{4}$(0.99)	69	16(5)	Ambient
*9	30/7/71	S.23	72.4	$3\frac{1}{8}$(0.95)	89	23(7)	Ambient
*10	4/8/71	S.23	64.2	$3\frac{1}{8}$(0.95)	136	16(5)	Ambient
11	16/8/71	S.23	35.8	2(0.61)	16	24(7)	49(120)
12	17/7/72	Sabel	80.2	4(1.22)	$46\frac{1}{2}$	16(5)	Ambient
Radial flow							
13	25/7/72	Sabel	46.9	0.93(0.28)	71	35(11)	Ambient
*14	3/8/72	S.23	75.1	1.67(0.51)	$160\frac{1}{2}$	17(5)	Ambient
*15	10/8/72	S.23	36.7	1.46(0.45)	88	20(6)	Ambient

* Pressure resistance determined.

Seven of the parallel-, and all of the radial-, flow runs were carried out at ambient temperature without the addition of any supplemental heat beyond that due to frictional heating through the fan. Runs 1 and 2 were carried out at controlled temperatures of 32°C, Runs 3 and 11 at 49°C and Run 7 at 55.4°C. Difficulties with the heater unit prevented any runs being carried out at temperatures higher than this. Eight of the parallel-flow runs were carried out with a seed depth of the order of 3 ft; shortage

of seed limited the depth to 2 ft in Runs 1 and 11 and to only $\frac{2}{3}$ ft in Run 4. A depth of 4 ft was used in Run 12. Drying times varied from 16 to 160h.

4.3.1. Procedure for parallel flow runs

4.3.1. (a) 1970 (Runs 1,2,3)

Because of the heavy contamination of both crops with barley it was necessary to clean all the seed before loading the drier. As this job took over 6 hours on a small laboratory cleaner, it was not possible to start any of the runs until the day after harvest. The seed was therefore stored overnight in half-filled hessian sacks which were laid out as thinly as possible on a cold concrete floor. This prevented any heating taking place.

In order to fill the drier bin, the required depth of seed was divided into a convenient number of layers and the weight of a single layer calculated from a bulk density determination. Aliquots of seed of this weight were then filled into the bin, each layer being separated from the next by a disc of nylon mesh. A thermocouple was inserted between each layer, in the surface of the final layer, and in the plenum chamber. A cumulative sample of seed was taken during this filling operation to be used for moisture content determination.

The drying container and seed were weighed before and after drying on a steelyard type of balance. In addition in Run 1, the bin was weighed 3 times during drying. Weight loss recordings during drying were not made on Runs 2 and 3.
In each case drying was continued until it could be seen from the temperature recorder chart that the drying zone had passed through the bed.

After drying had been completed, the seed in Run 1 was left overnight in the drying chamber. By morning some heating had

taken place and the fan was run for about 1½ hours to cool the mass down. For Run 2, the heat only was switched off after 48 hours and the fan used to cool the seed for about 2½ hours. A 6 hour cooling period was used in Run 3. At the end of these operations, the seed was emptied from the drying container layer by layer by means of an industrial vacuum cleaner. Each layer was weighed separately and a sample taken for determination of moisture content and subsequent seed analysis.

Separate determinations of the bulk density and porosity of the wet seed were made in the case of Runs 2 and 3 and of the dry seed from all 3 runs.

The temperature charts were converted into the temperature profile of Figs. 4.7, 4.8and 4.10 by manual reading and plotting.

4.3.1. (b) 1971/72 (Runs 4-12)

In these two subsequent years the crops were much cleaner and it was possible to start the runs on the same day as harvesting using the seed as-harvested by the combine-harvester.

Significant improvements were made to the experimental procedure. For filling the bin, the false floor insert described in Section 4.2.2. and Fig. 4.3 was raised to within 1 layer depth of the top of the bin, the first layer filled into it and carefully levelled. The floor and seed were then lowered by the thickness of another layer, which was then added. Thus as each successive layer was added the false floor was gradually lowered towards the bottom of the bin. At appropriate intervals, the thermocouples, which were already fastened to the centre support rod, were laid out radially between the layers.

For emptying, the false floor was raised up again layer by layer so that each layer in turn stood proud of the top of the bin. A broad flat scoop (Fig.4.5) was used to slice off the layer and transfer it into a container in which it could be weighed and then sampled. The advantages of this system over that of 1971 were:-

(a) The elimination of the need to reach to the bottom of a 5 ft. deep bin. Thus each layer was within easy reach for careful levelling during filling.

Fig. 4.5 Flat sampling pan for the deep bin drier.

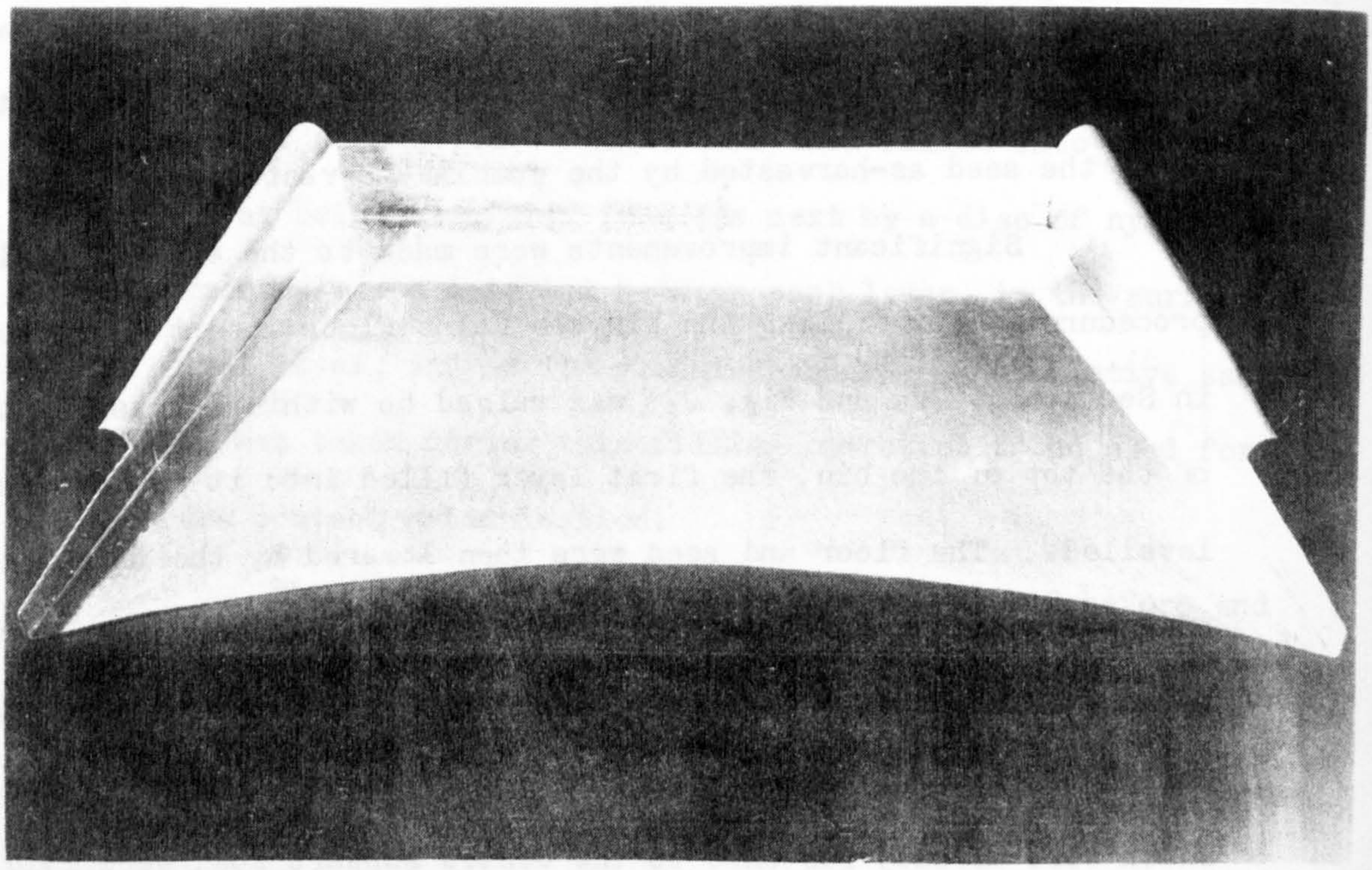

(b) The elimination of the nylon mesh layer separators together with the original system of laying in the thermocouples down the side of the bin greatly reduced air leaks resulting from shrinkage during drying but did not entirely eliminate them as some loss of air could occur from around the central rod. This was easier to rectify however.

(c) Sampling the final profile was very accurate because the seed could be removed, if desired, in layers only 1 inch deep.

(d) Filling and emptying were quicker and less exhausting physically.

The temperature charts from Runs 4 and 5 were read and plotted manually as in 1970. The remaining charts were read by chart reader direct onto punched tape in the Computer Department of Rothamsted Experimental Station. The data was then processed in the ICL 470 computer using the FORTRAN programme, DEEP. This programme, which is described in detail in the Appendix output the data

(a) as tables of results, including the means and standard deviations of the inlet conditions.

(b) as a line file suitable for input to

(i) a graph plotting programme, SIMPLT, which was used to plot temperature/time profiles. This programme is also listed and described in the Appendix.

(ii) the simulation programme STATIC (see Section 5).

4.3.2. Procedure for radial flow runs (Runs 13, 14, 15)

The wet seed was simply put into the section in weighed amounts and carefully spread by hand. Care was taken to see that the thermocoupleleads were held vertically by the seed. When the section was full the plastic sheeting was folded back over the seed and the lid placed on and weighed down with iron weights. Before starting the run proper, the air supply was switched on for a test

to be made for leaks and if necessary the lid readjusted. At sometime during the run, the drier would be stopped and samples for moisture content determination taken by means of a vacuum tube inserted at appropriate intervals along a radius. It was found possible to remove a thin column of seed down to about 10 inches from the surface, extract a small sample and return the surplus back into the hole created by the original removal. In this way a minimum of disturbance was caused. The same method was also used at the end of the run after which the drier was emptied and the seed weighed.

The temperature charts were read direct onto punched tape and processed by the programme RDEEP. This was a modified version of DEEP which produced similar output including a line file suitable for input to a graph plotting programme RADPLT and the radial-flow simulation programme RADIAL (Section 5).

4.3.3. Pressure resistance to airflow

Whenever possible series of measurements of pressure resistance in the plenum chamber were made for a series of airflows obtained by adjusting the iris in convenient steps. Differential pressures across the orifice plate were read by an inclined tube gauge and static pressures in the plenum chamber were read from the pressure recorder chart.

For the parallel flow bins it was assumed that the resistance was a linear function of depth and results were brought to a common scale by dividing by bed depth. These values were then fitted by linear least squares to the equation

$$\frac{P_P}{D_P} = a\,(V)^n \qquad \ldots\ldots\ldots\ldots\ldots\ldots 4.6.$$

If this relationship is true for parallel flow then it is shown in Appendix 4.1.22 that the total pressure drop through a radial bin is given by

$$P_R = \left(\frac{a}{1-n}\right)\left(\frac{Q}{2\pi}\right)^n \left(\frac{(\phi^{n-1} - 1)}{(R_2\,\phi)^{n-1}}\right) \qquad \ldots\ldots\ldots\ldots\ldots 4.7.$$

which for the experimental rig, simplifies to

$$P_R = \left(\frac{a}{1-n}\right)\left(\frac{Q}{0.69813\ D_R}\right)^{n} (0.1644^{n-1} - 1) \qquad \ldots\ldots\ldots\ldots 4.8.$$

Hence values of the constants a and n were determined from the radial flow data by linear regression of ln(P) on ln (Q/0.69813D) which has as its intercept $\ln\left[\frac{a}{1-n}(0.1644^{n-1} - 1)\right]$ and from which a was determined by the substitution of the value of n.

4.4. RESULTS AND DISCUSSION

4.4.1. Drying runs

The most important variables affecting the moisture and temperature gradients established across a deep bed of seed are the initial moisture content of the seed and the temperature and flow of the drying air. In addition the depth of the bed and the required final moisture content affect the drying time and final moisture and temperature profiles. The interaction of all these factors can be seen in the results of the deep bed tests. However, the conditions, both chosen and met with,in each run, varied so much that neat comparisons between runs are not possible. The best that can be done is to describe briefly the effect of the most important variables and to indicate the main features of individual runs.

The main characteristics of each run are summarised in Tables 4.2, 4.3, 4.4, 4.5 and initial and final moisture profiles and temperature-time profiles are plotted in Figs. 4.6 - 4.30. The quality of the original computer plots from which the temperature time profile were reduced photographically was poor so that in some cases their legilibility is bad. However they do provide a reasonable visual guide to temperature changes occurring with depth during the runs. Where individual lines can be distinguished they have been numbered with the number of the thermocouple location defined in Section 4.2. The same numbers are used to classify the tabulated data in the Appendix 4.2 .

Table 4.2

Summary data for parallel-flow deep-bed runs, 1-6. Imperial units

	Run No					
	1	2	3	4	5	6
Initial conditions						
Moisture content, % d.b.	82.0	69.4	56.0	104.5	92.7	63.1
Grain temperature, °F	-	-	-	84.9	-	82.2
Weight, lb	248	300	330	86	447	388
Depth, ft	2.0	3.0	3.0	0.67	3.25	3.25
Bulk density, A, lb/ft^3	-	21.3	23.2	-	23,5	21.7
B, lb/ft^3	24.8	20.0	22.0	25.8	27.5	23.9
Final conditions						
Moisture content, % d.b.	9.32	12.1	9.6	43.1	16.2	26.5
Moisture range, % d.b.	8.6-11.1	12.0-12.5	9.1-10.4	36.6-48.6	10.9-43.3	13.1-50.6
Weight, lb	144	203	241	60	257	294
Depth, ft	-	2.5	-	0.58	2.5	2.75
Shrinkage, %	-	16.7	-	12.5	23	15.
Bulk density, lb/ft^3	20.6	17.4	20.0	20.6	17.7	21.4
Mean germination, %	78	91	92	-	7.6	85
Mean 1000 seed wt, g	3.72	1.43	1.70	-	3.44	3.83
Drying air						
Temperature, °F	90.5	90.6	120.7	77.3	75.6	75.7
±	2.5	3.4	3.2	1.7	4.0	2.3
Humidity, ratio	-	-	-	-	0.00850	0.00931
Relative humidity, %	-	-	-	-	-	49.7
Velocity, ft^3 min^{-1} ft^{-2}	40	43	36	28.3	28.3	25.9
Mass flow, lb. h^{-1}, ft^{-2}	174	179	147	125.8	126.0	115.0
Static pressure, in W.G.	-	3.6	3.5	0.4	2.5	2.25
Range, in W.G.	-	-	-	0.45-0.4	2.83-2.2	2.3-2.2
Total drying time, h.	52.4	48	43.5	23	115	65

A = measured in 2 cu,ft. container.

B = calculated from weight and depth in bulk bin.

Table 4.3

Summary data for parallel-flow deep-bed runs, 7-12. Imperial units

	Run No					
	7	8	9	10	11	12
Initial conditions						
Moisture content, % d.b.	49.0	23.5	72.4	64.2	35.8	80.2
Grain temperature, °F	84.2	77.0	91.9	73.8	75.0	88.5
Weight, lb	345	334	283	325	180	459
Depth, ft	3.25	3.25	3.13	3.17	2.08	4.04
Bulk density, A, lb/ft^3	20.1	-	16.5	18.5	15.4	20.8
B, lb/ft^3	21.2	20.6	18.1	20.5	17.1	21.8
Final conditions						
Moisture content, % d.b.	16.9	13.0	14.6	17.1	5.5	60.0
Moisture range, % d.b.	4.5-45.3	12.1-14.2	12.6-21.4	12.1-33.7	4.8-6.8	30.3-72.7
Weight, lb	291	302	190	232	144	398
Depth, ft	2.75	2.96	2.67	2.75	1.88	3.83
Shrinkage, %	15.4	8.9	14.7	13.2	9.6	5.2
Bulk density, lb/ft^3	21.1	20.2	14.3	16.8	15.3	20.8
Mean germination, %	86	89	93	96	95	84
Mean 1000 seed wt, g	3.93	3.71	1.25	1.39	1.48	3.88
Drying air						
Temperature, °F	131.7	79.5	78.8	78.8	119.5	78.3
±	5.0	2.2	3.0	2.4	0.8	2.5
Humidity ratio	0.01078	0.01128*	0.0114	0.01044	0.00719	0.010709
Relative humidity, %	11.1	57.7	48.6	50.4	10.2	52.5
Velocity, $ft^3 min^{-1} ft^{-2}$	22.8	16.4	23.0	16.3	24.0	16.4
Mass flow, lb. $h^{-1} ft^{-2}$	92.8	72.5	102.6	72.5	98.9	72.6
Static pressure, in W.G.	1.8	1.2	2.2	1.85	1.55	2.45
Range, in W.G.	-	-	2.3-2.1	1.9-1.8	-	2.2-2.75
Total drying time, h.	21.75	69	89	136	16	46.5

A = measured in separate container.

B = calculated from weight and depth in bulk bin.

* = estimated value (wick ran dry on aspirated hygrometer).

Table 4.4

Summary data for radial-flow deep bed runs, 13-15. Imperial units

	Run No		
	13	14	15
Initial conditions			
Moisture content, % d.b.	46.9	75.1	36.7
Grain temperature, °F	76.5	73.0	75.9
Weight, lb	214.5	335.0	305.0
Depth, ft[1]	0.93	1.67	1.46
Bulk density, A, lb/ft^3	-	-	13.6-15.6
B, lb/ft^3	18.4	16.0	16.6
Final conditions			
Moisture content, % d.b.	15.3	25.1	10.8
Moisture range, % d.b.	12.4-21.5	11.0-53.4	9.4-15.5
Weight, lb	168.5	239.5	241.0
Depth, ft	-	1.46	1.29
Shrinkage, %	-	12.5	11.4
Bulk density, lb/ft^3	-	13.1	14.8
Mean germination, %	86.0	93.0	94.0
Mean 1000 seed weight, g	3.97	1.39	1.46
Drying air			
Temperature, $\pm$ °F	72.0	75.6	81.3
	2.8	1.8	2.8
Humidity ratio	0.007719	0.008613	0.007514
Relative humidity, %	47.0	46.5	33.4
Velocity, ft^3 min^{-1} ft^2			
(a) at bin wall	97.5	43.7-52.2	51.7-59.2
(b) mean	34.6	16.2-18.5	18.4-21.0
(c) at periphery	16.0	7.5-8.6	8.5-9.7
Volume flow, ft^3/min	63.1	53.2	53.4
Mass flow, lb air/h	282.6	236.0	235.0
Static pressure, in W.G.	3.1	3.3-4.2	3.1-3.6
Total drying time, h	70.9	160.5	87.8

1) Depth normal to flow along duct axis.

Table 4.5

Some approximate measures of air utilisation

Run No	Mass water removed/unit mass air, ratio	Column 1 as % of adiabatic pick up, %	Vol.of air/unit mass water removed		Vol.of air/unit mass of dry seed		Vol.of air/unit of time and per unit of dry seed	
			ft^3/lb	m^3/kg	ft^3/lb	m^3/kg	$ft^3\ min^{-1}\ ton^{-1}$	$m^3/h/tonne$
1	0.00228	-	6071	379	4790	299	3423	5724
2	0.00226	-	6327	395	3428	214	2668	4461
3	0.00278	-	5222	326	2162	135	1857	3105
4	0.00178	-	7853	473	4645	290	7539	12607
5	0.00262	81	5142	321	4405	275	1432	2395
6	0.00252	84	5366	335	2179	136	1248	2087
7	0.00540	43	2739	171	593	37	1027	1718
8	0.00128	44	10609	663	1265	79	688	1150
9	0.00203	73	6616	415	3700	231	1551	2595
10	0.00190	61	7112	444	3363	210	924	1545
11	0.00457	63	3188	199	849	53	1974	3301
12	0.00385	124	3748	234	920	57	738	1234
13	0.00230	77	5831	364	1826	114	968	1619
14	0.00253	79	5350	334	2675	167	623	1041
15	0.00310	70	4400	274	1265	79	536	897

Run 1 (Table 4.2, Figs. 4.6 and 4.7)

This was the only deep bed test to be carried out with Sabrina. At a depth of only 2 ft (0.61 m) and air velocity of 40 ft/min (12.2 m/min) the amount of air used per unit of dry seed and per unit of time was high (3423 ft^3 min^{-1} ton^{-1}). In spite of additional heat supplied to maintain a constant temperature of 90°F (32.5°C), a relatively high volume of air/unit of water removed was used and the temperature profile would suggest that the diffusional drying rate was a severely limiting factor for at least one-third of the total drying time. In addition the final moisture gradient, 8.5 - 11.1 % d.b, is shallow and indicates that the bed was approaching equilibrium conditions. It should be noted that even at these low moisture contents some heating occurred overnight in the seed left at 90°F (32.2°C).

Run 2 (Table 4.2, Figs 4.6 and 4.8)

The first run with S.23 seed. Its moisture content, 69.4% d.b, was less than that of the Sabrina in Run 1 and the depth was increased to 3 ft (0.91 m). Otherwise it was a similar run with a slightly higher airflow controlled at 90°F (32.2°C). The run was shorter and surprisingly, had a higher final moisture content, 12.1%, and a much shallower gradient. This run was blown with cool air for $2\frac{1}{2}$ h at the end of the run and this may have resulted in rewetting of the seed. This may also explain the greater volume of air used per unit weight of water removed although the greater depth has improved the ratios of air to dry seed compared with Run 1.

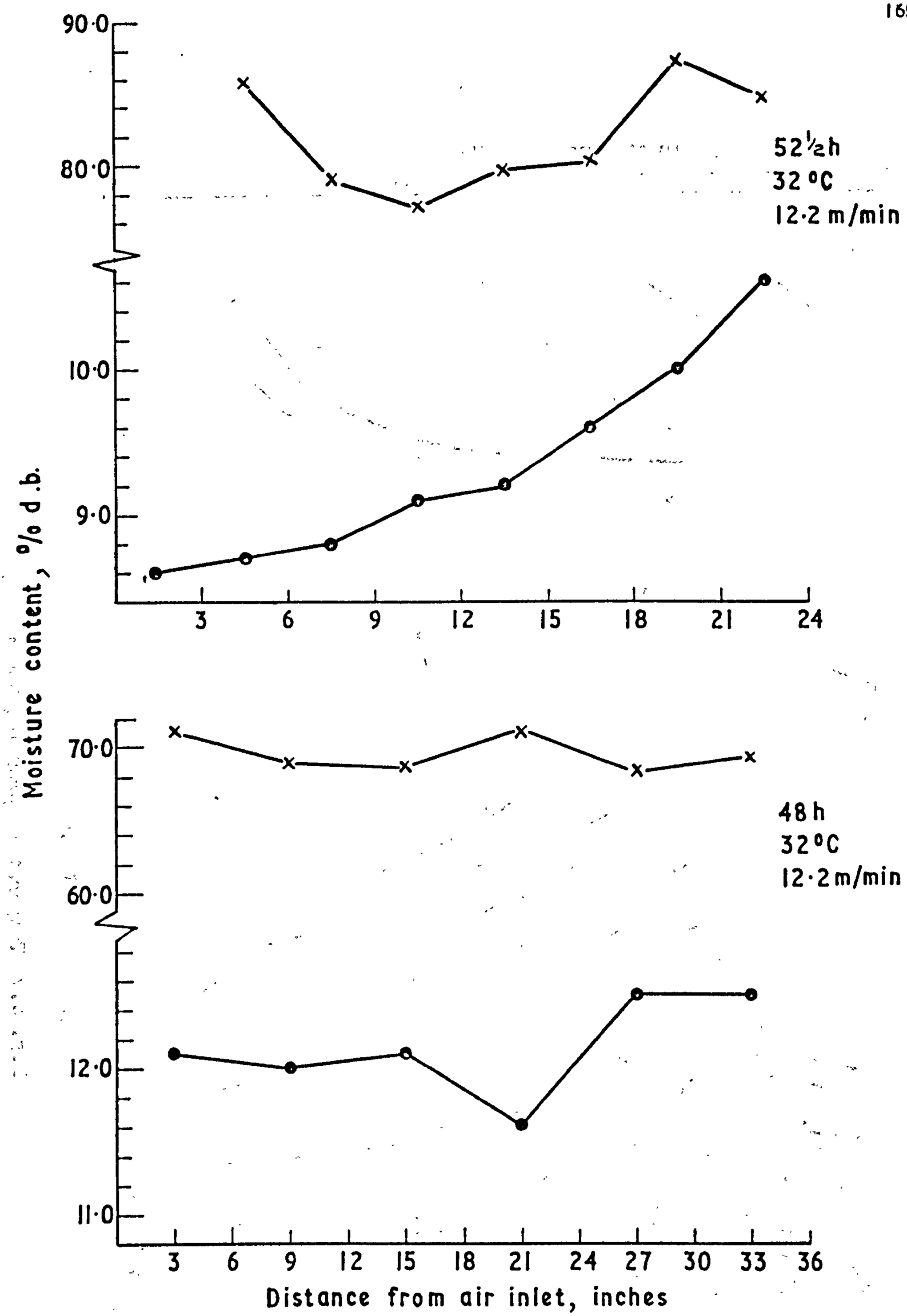

Fig.4.6 Initial (x) and Final (•) Moisture Gradients for Parallel–Flow Runs 1 (Top) and 2 (Bottom)

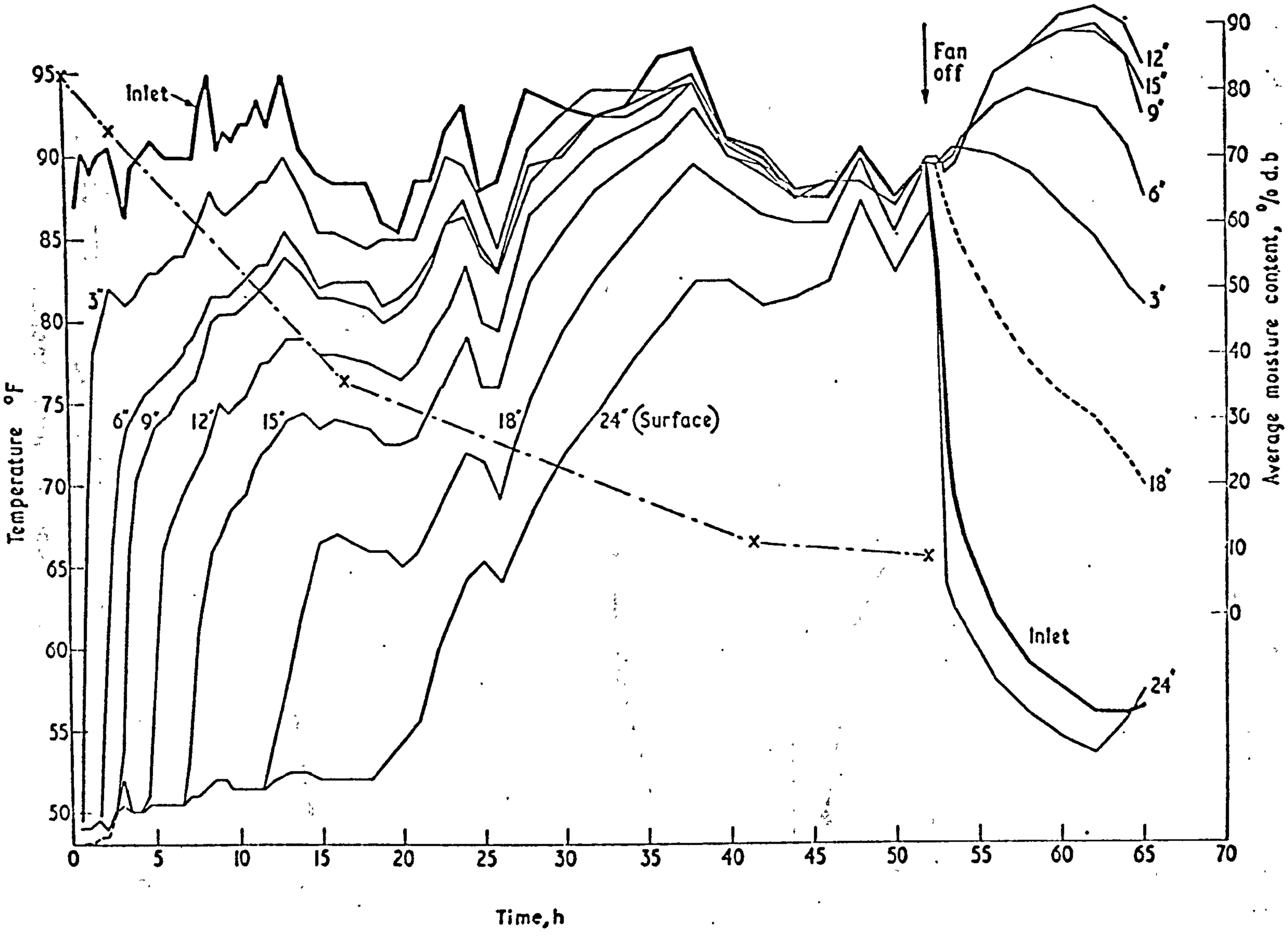

Fig. 4.7 Temperature profile, Run 1 10.7.70.

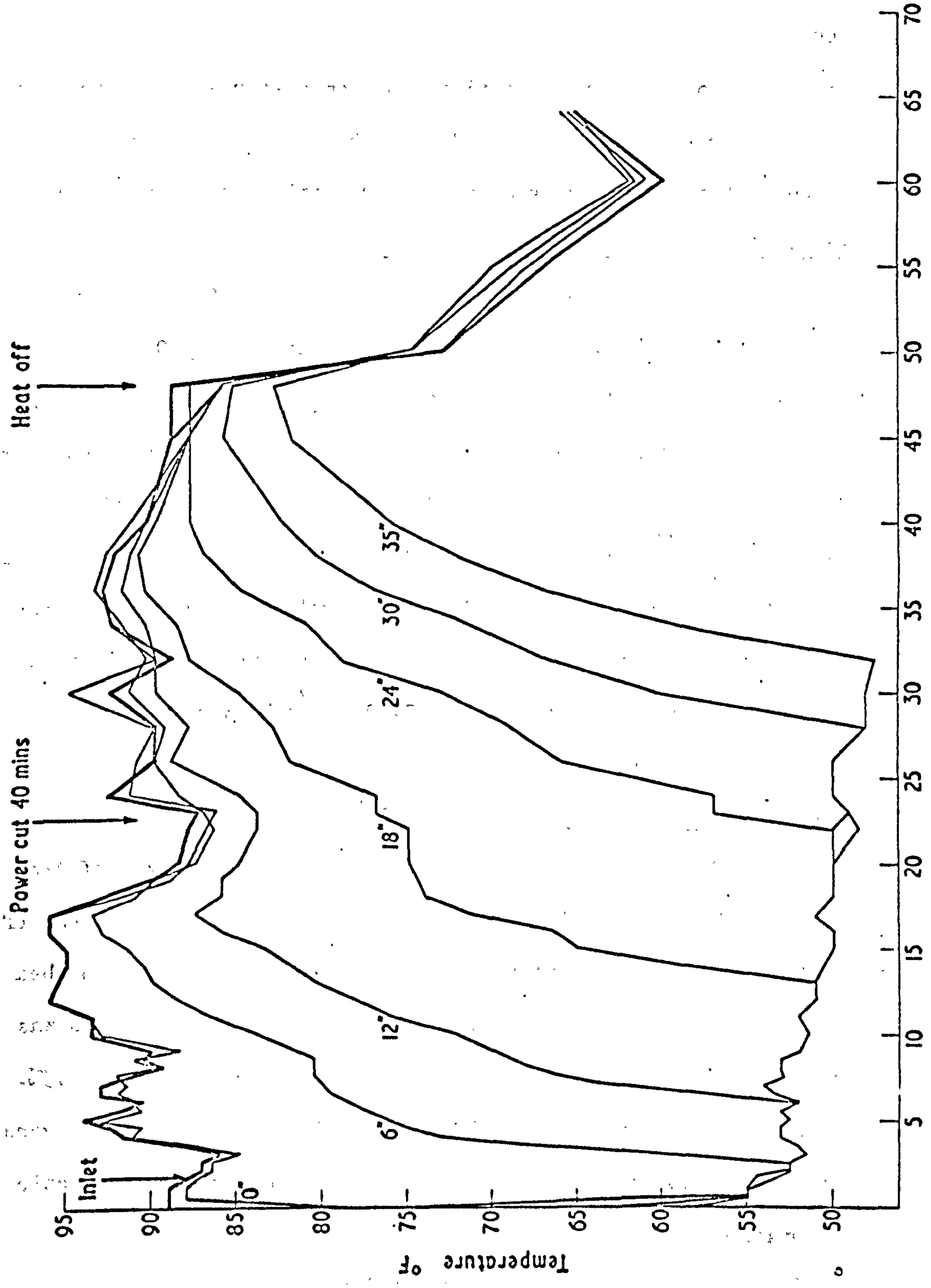

Fig. 4.8 Temperature profile, Run 2 28.7.70.

Run 3 (Table 4.2, Figs. 4.9 and 4.10)

A second 3 ft (0.91 m) layer of S.23 at lower moisture content, 56.0% d.b. than Run 2, at a higher temperature 120°F (49.1°C), and lower airflow, 36 ft/min (11.0 m/min). The run was continued for 43½h by which time, the temperature-profile indicates that the drying zone had passed through the bed. It then received 6 hours of cooling during which some rewetting probably occurred.

Run 4 (Table 4.2, Figs. 4.9 and 4.11)

The first run in 1971 and in which the false floor and thermocouple stalk were used was carried out on only 9" (0.2 m) of very wet (104.5%) Sabel seed ventilated with ambient air for just 23 hours. The seed was not dry at the end of this period varying from 36.6% at the bottom to 48.6% at the top. Because of the shallowness of the layer and in spite of the high moisture content of the seed, the drying rate was diffusion controlled and much less than the carrying capacity of the air. Hence the volume of air used to evaporate one pound of water (7583 ft^3/lb) was the second highest of all the runs.

Run 5 (Table 4.2, Figs. 4.12 and 4.13)

The same airflow was used in this run which was of the same seed but at a depth of 3¼ ft (0.99 m) and moisture content of 92.7%. The run was continued for 114 h by which time a mean bed moisture content of 16.2% d.b. had been reached although this was associated with a steep moisture gradient of from 10.9% to 43.3%. The increase occurred mainly in the top 9" of the bed. The overall drying rate was about 81% of the possible rate based on adiabatic evaporation

Run 6 (Table 4.2, Figs. 4.12 and 4.14)

This was a similar run to Run 5 with slightly less air and an almost 30% reduction in initial moisture content. Mean bed moisture content after 65 hours was 26.5% d.b. with a range of 13.1

to 50.6% d.b. 84% of the adiabatic pick-up was achieved but the greater humidity of the air meant that more of it was required per unit weight of water removed than in Run 6. Conversely the lower initial moisture content led to better air utilisation per unit of dry seed.

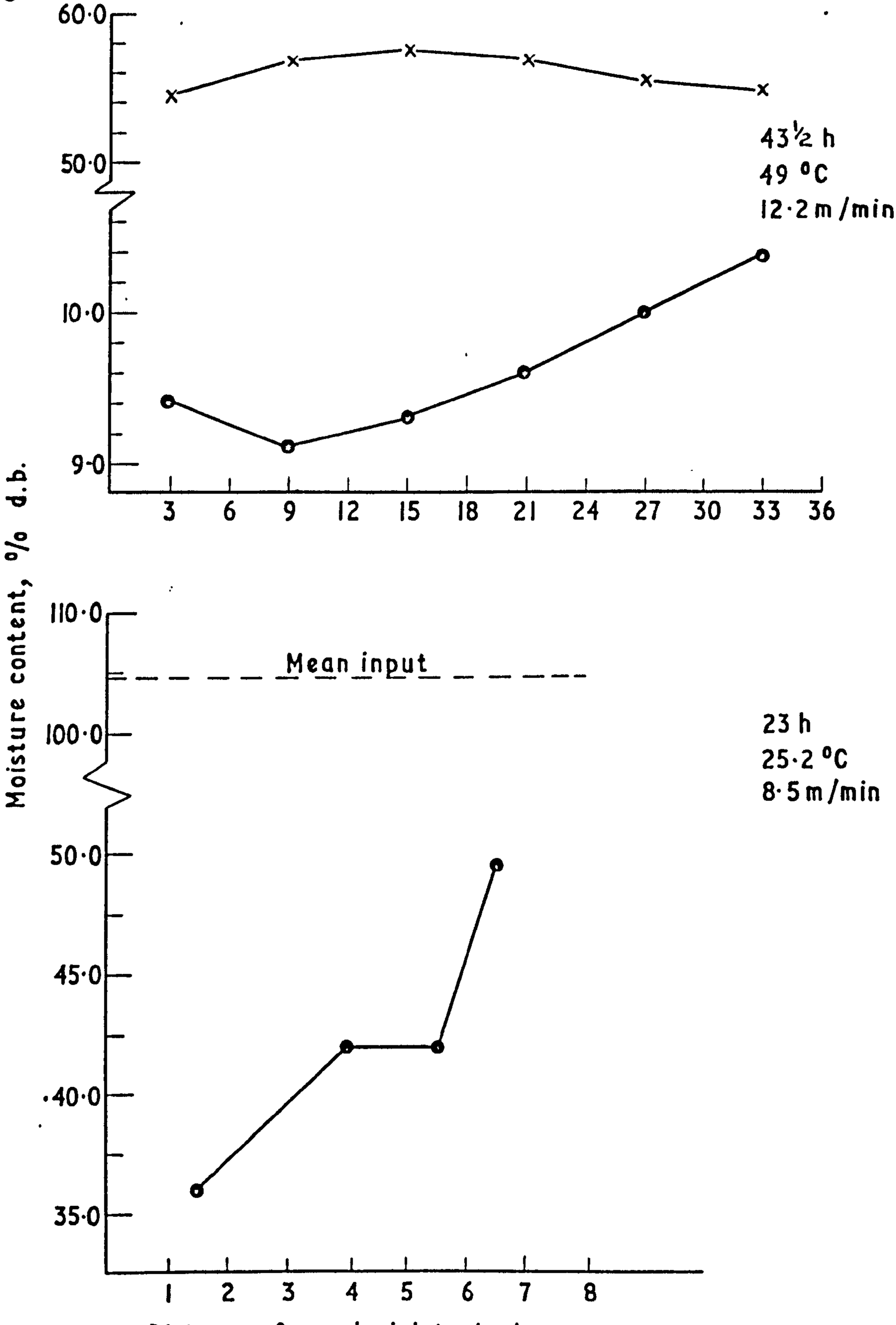

Fig. 4.9 Initial (x) and Final (•) Moisture Gradients for Parallel—Flow Runs 3 (Top) and 4 (Bottom)

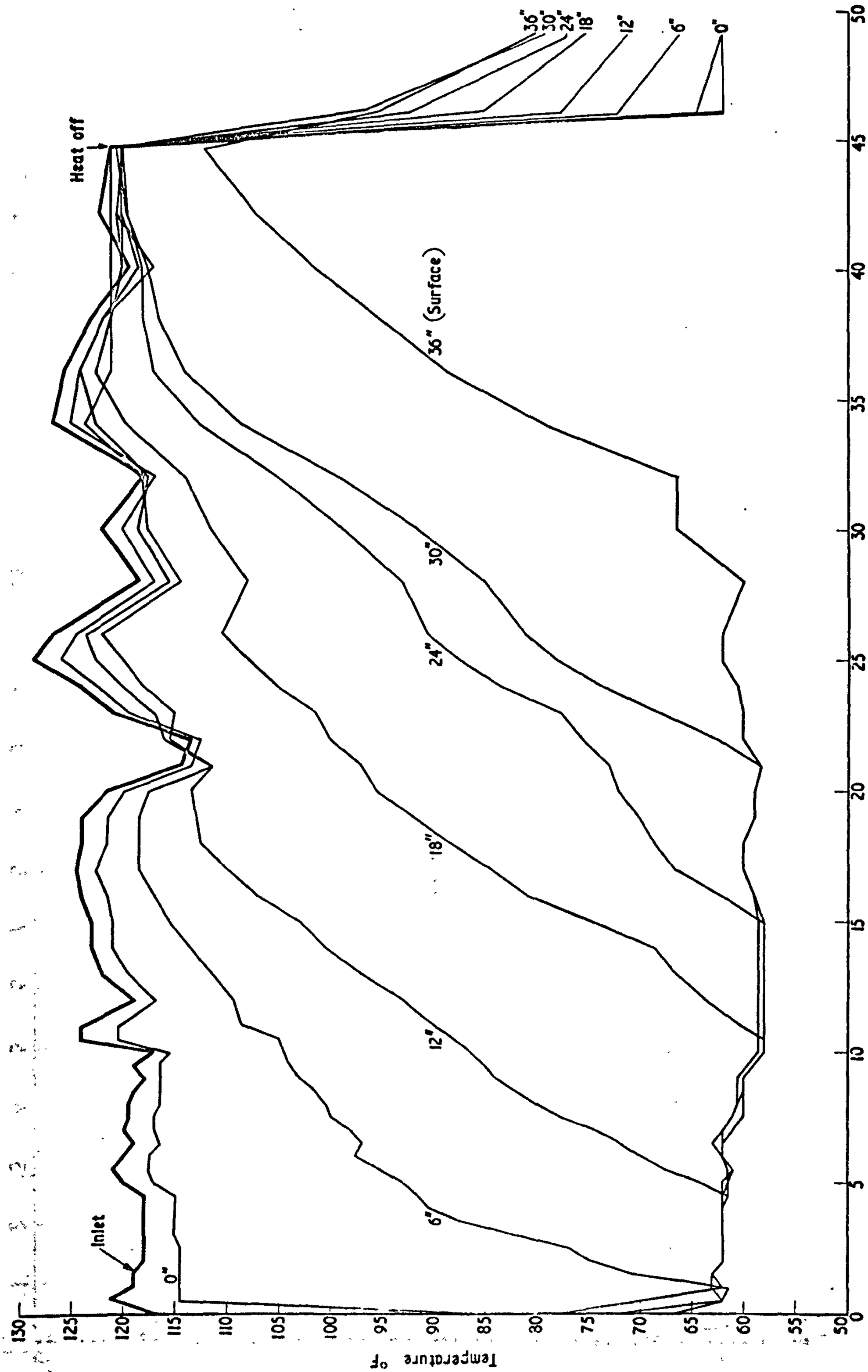

Fig. 4.10 Temperature profile, Run 3 4.8.70.

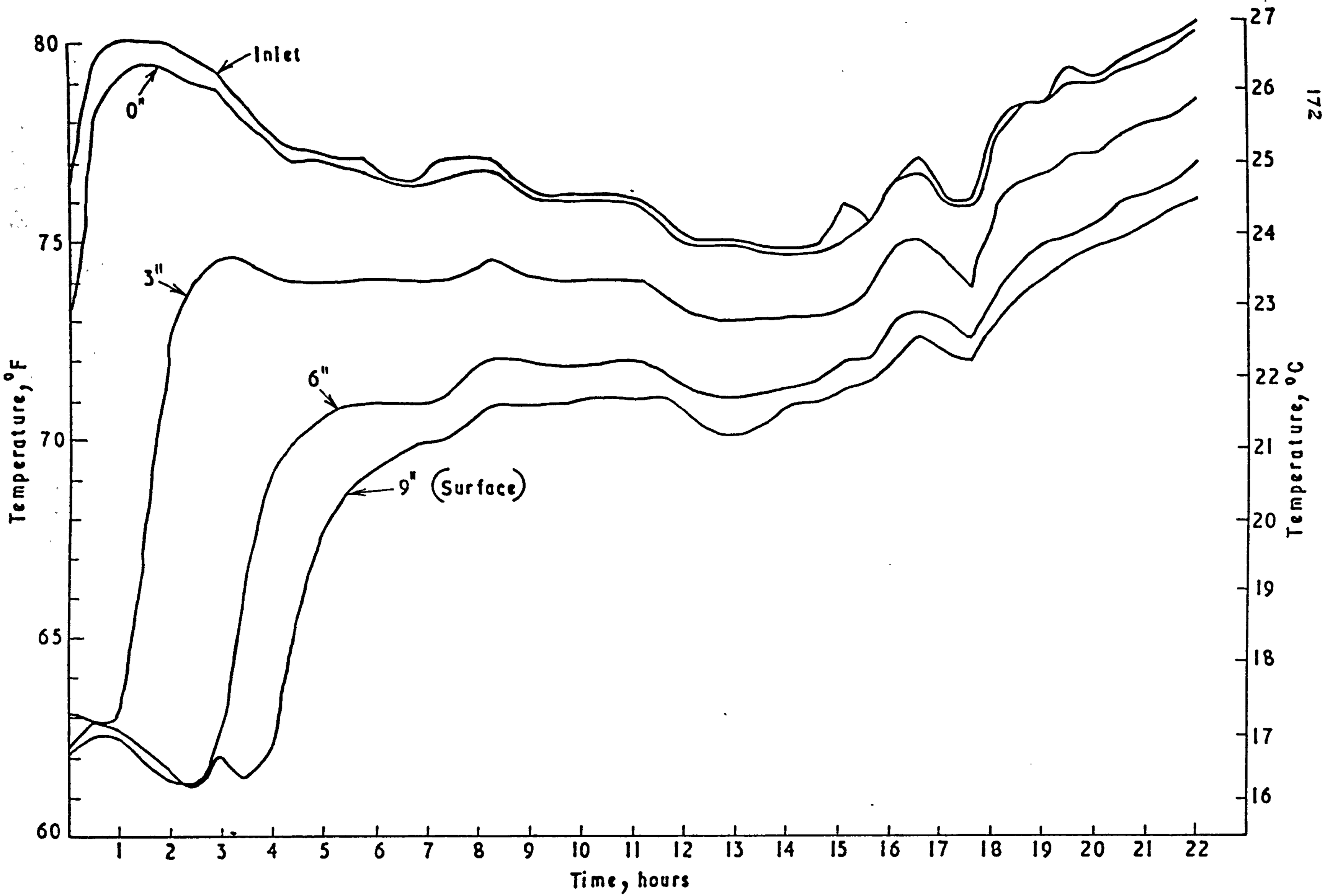

Fig. 4.11 Temperature profile, Run 4 12.7.71.

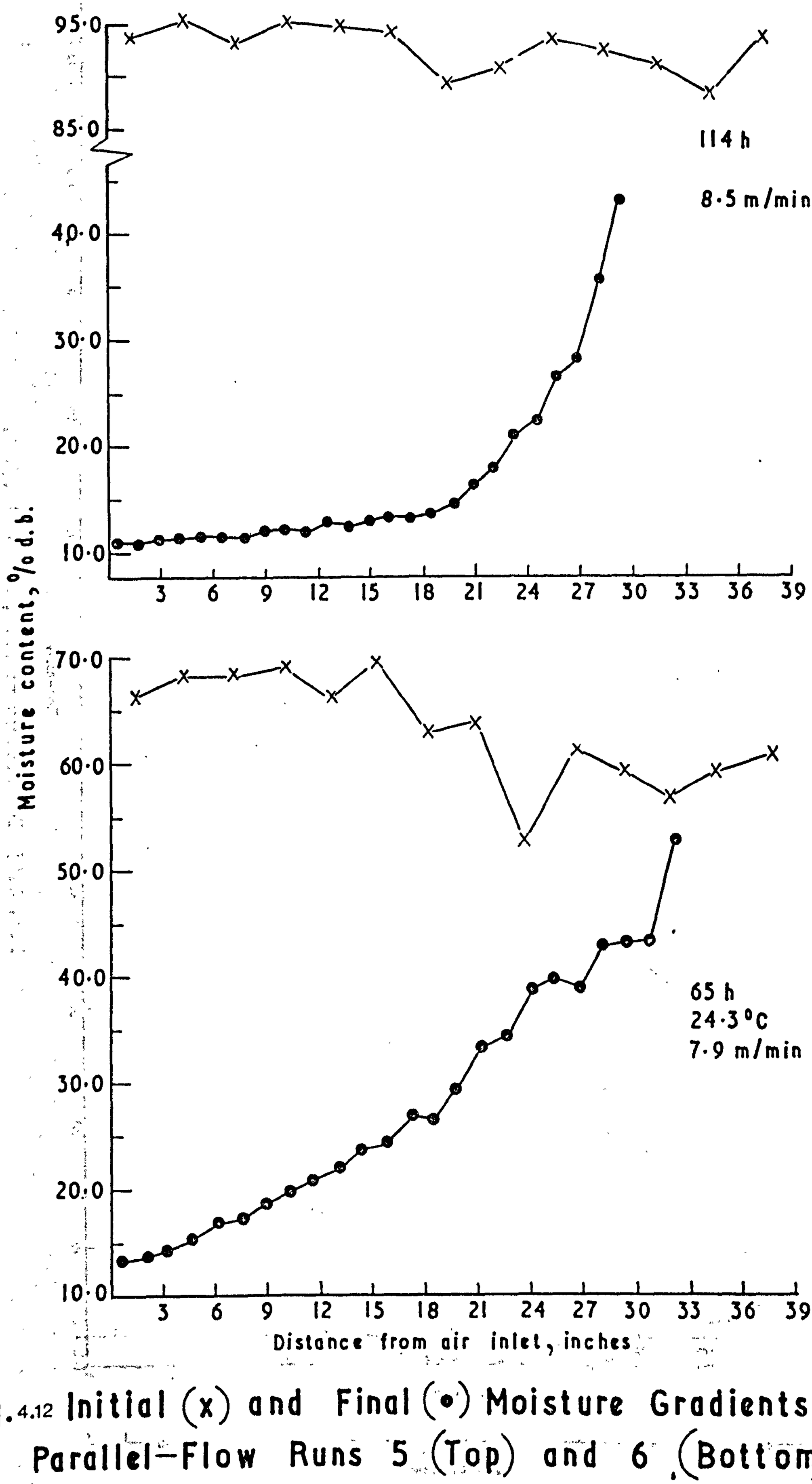

Fig. 4.12 Initial (x) and Final (•) Moisture Gradients for Parallel-Flow Runs 5 (Top) and 6 (Bottom)

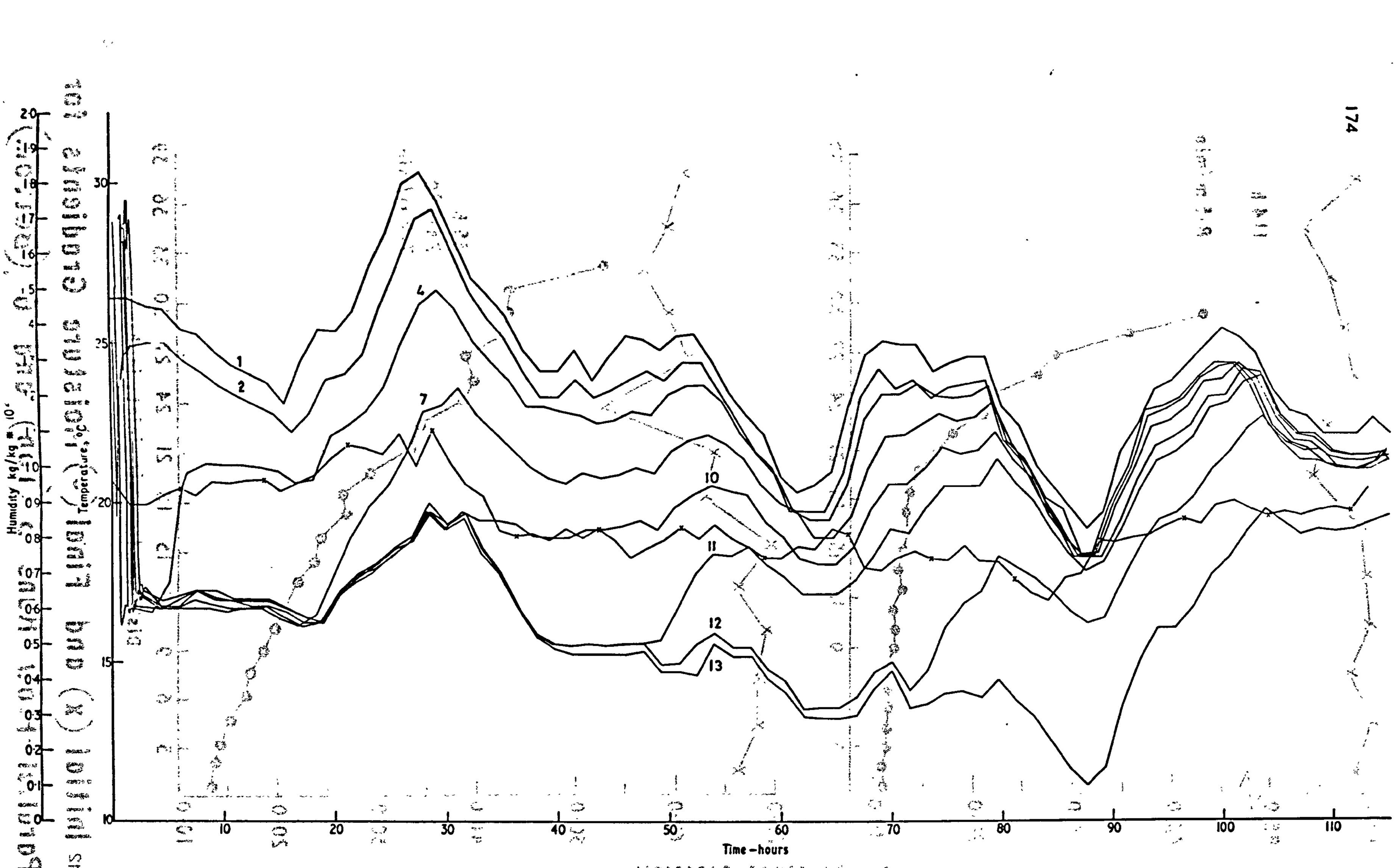

Fig. 4.13 Temperature profile, Run 5 14.7.71.

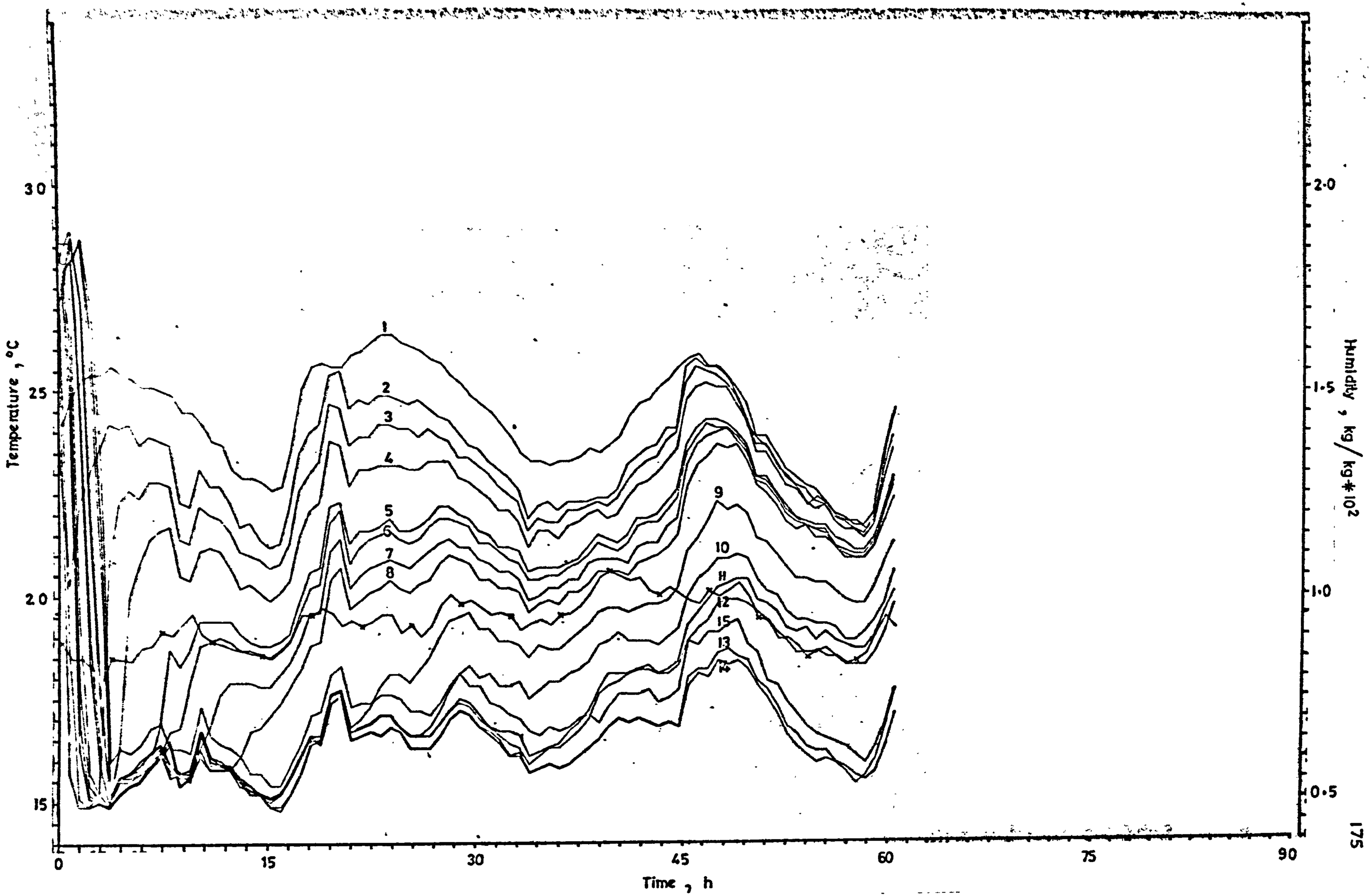

Fig. 4.14 Temperature profile, Run 6 19.7.71.

Run 7 (Table 4.3, Figs.4.15 and 4.16)

This run was carried out at 131.7°F (55.4°C), the highest temperature of all the deep bed tests. From an initial moisture content of 49% d.b, the Sahel seed was dried to a mean of 16.9% d.b. in 21¾h. The final moisture gradient was steep (4.5 to 45.3% d.b.) contrasting sharply with that of Run 3 which, even if allowance is made for the difference in drying times, would support the conclusion that there was moisture interchange between the seed and the cooling air at the end of Run 3. The effect of the high temperature in Run 7 was to produce an average evaporation rate of 0.00540 lb/lb which, although about twice the pick-up to be obtained under ambient conditions represented only 45% of the possible adiabatic pick-up. In volume terms this was 2739 ft^3 of air per lb water removed and 593 ft^3 per lb of dry seed.

Run 8 (Table 4.3, Figs.4.15 and 4.17)

The Sahel seed used in this run had the lowest initial moisture content (23.3% d.b.) of all the runs. It was dried for 67h with ambient air to a mean moisture content of 13.0% d.b. The final moisture gradient was very small. Compared with other runs the progression of temperature from wet bulb towards inlet temperature began throughout the whole bed very soon after the start of drying. It seems likely that a complete drying zone was never established, and more air per lb water evaporated(10609 ft^3/lb) was used than in any other run. Conversley, but also because of the low initial moisture content, less air per lb of dry seed(1265 ft^3/lb) was used than in all the other runs at ambient temperatures. The absolute humidity plotted in Fig. 4.17 is unnaturally uniform because estimated mean values were used to replace known faulty recordings.

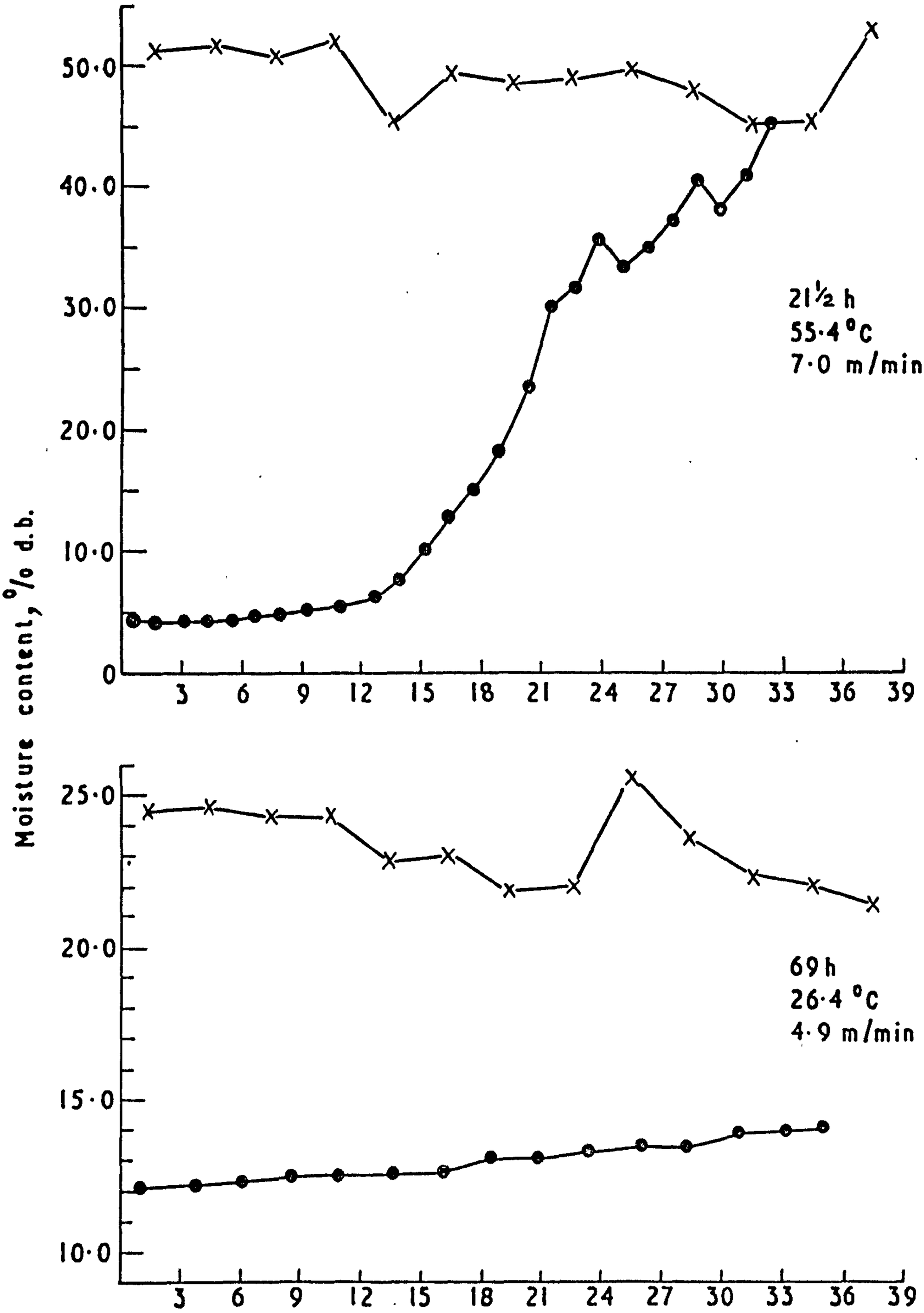

Fig. 4.15 Initial (x) and Final (•) Moisture Gradients for Parallel-Flow Runs 7 (Top) and 8 (Bottom)

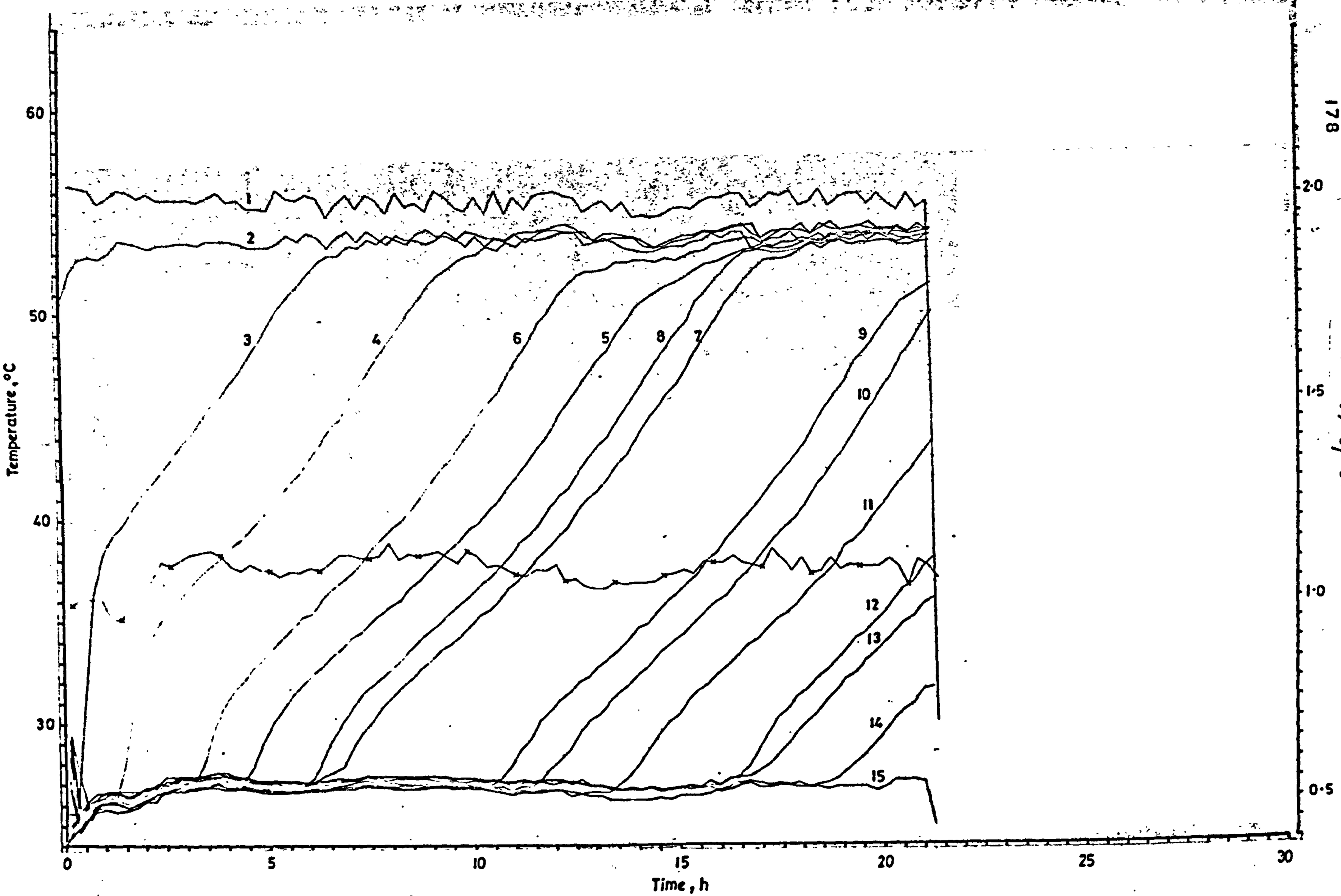

Fig. 4.16 Temperature profile, Run 7. 22.7.71.

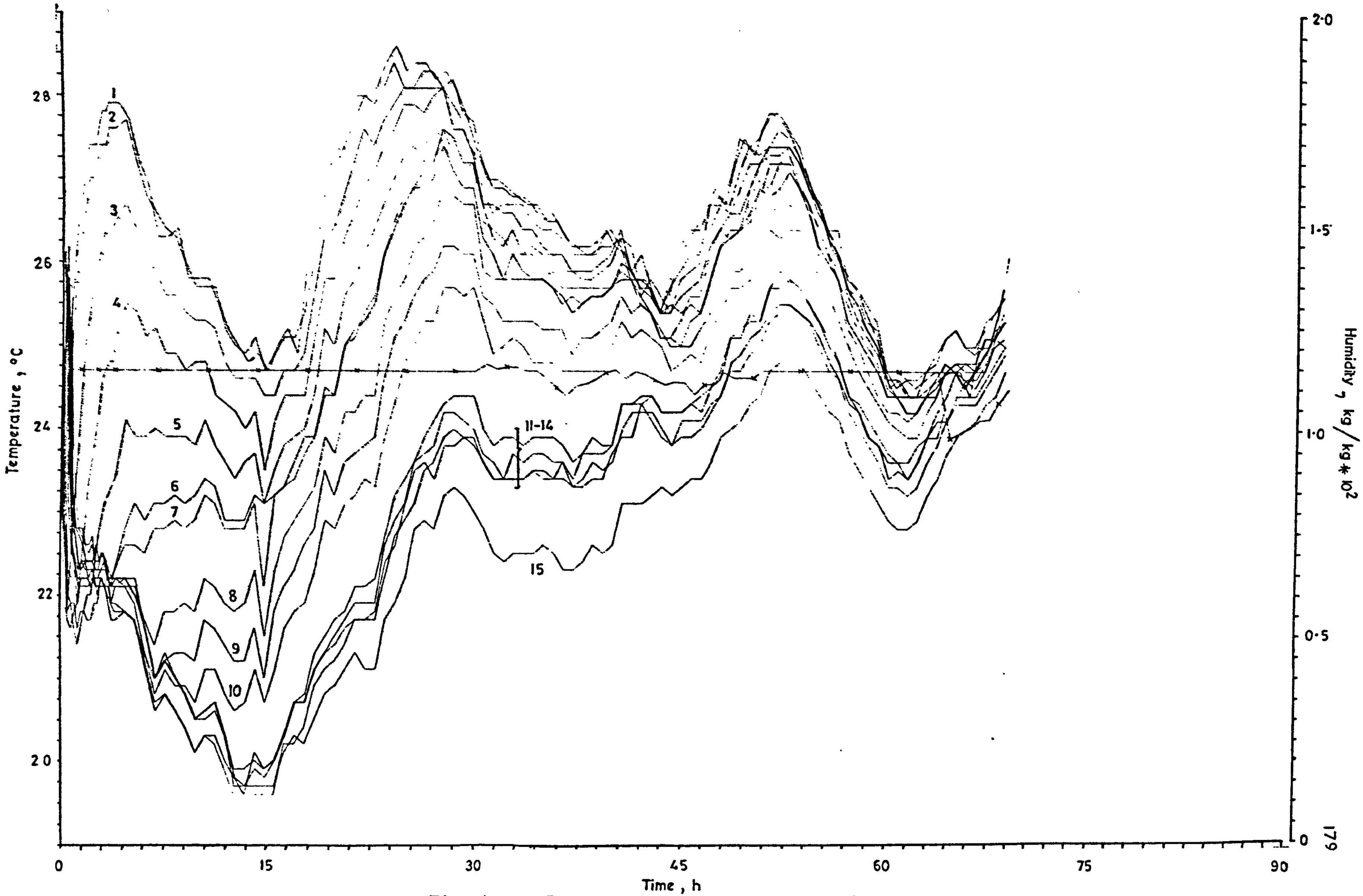

Fig. 4.17 Temperature profile, Run 8 26.7.71.

Run 9 (Table 4.3. Figs. 4.18 and 4.19)

This was the first run in 1971 with S.23 seed and consequently had a high initial moisture content, 72.4%. A drying time of 89 hours produced a mean bed moisture content of 14.6% d.b. with a gradient of from 12.6 to 21.4%. This was a removal of 58% moisture compared to only 10% in Run 8. However the drying time was not proportionately longer because the air velocity had been increased by 1.4 and the wetter seed clearly released its moisture more readily for the temperature profile suggests that in the initial stages of drying a complete drying zone existed. The apparent evaporation was 73% of the possible adiabatic pick-up.

Run 10 (Table 4.3, Figs. 4.18 and 4.20

This was a similar run to Run 9 but with slightly drier seed (64.2%). The airflow was reduced back to the Run 8 value and 136 hours were needed to reach a final moisture content of 17.1% d.b. with a gradient of from 12.1% to 33.7% d.b. More air per unit of water evaporated (7112 ft^3/lb) was used than in Run 9 but not as much as with the drier seed of Run 8 or with the much shallower layer (9 in) of Run 4. The apparent evaporation was only 61% of the possible adiabatic pick-up.

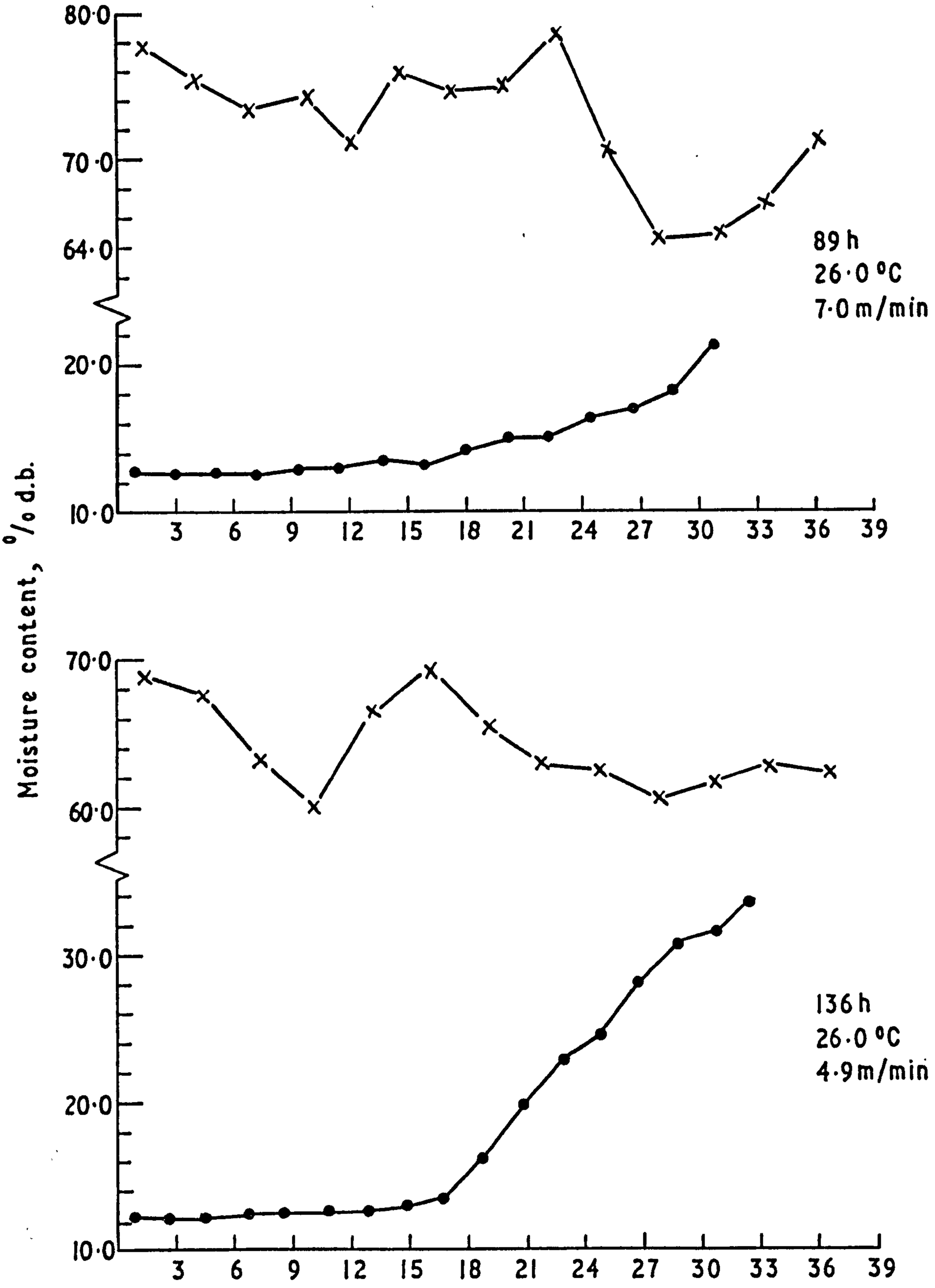

Fig. 4.18 Initial (x) and Final (•) Moisture Gradients for Parallel–Flow Runs 9 (Top) and 10 (Bottom)

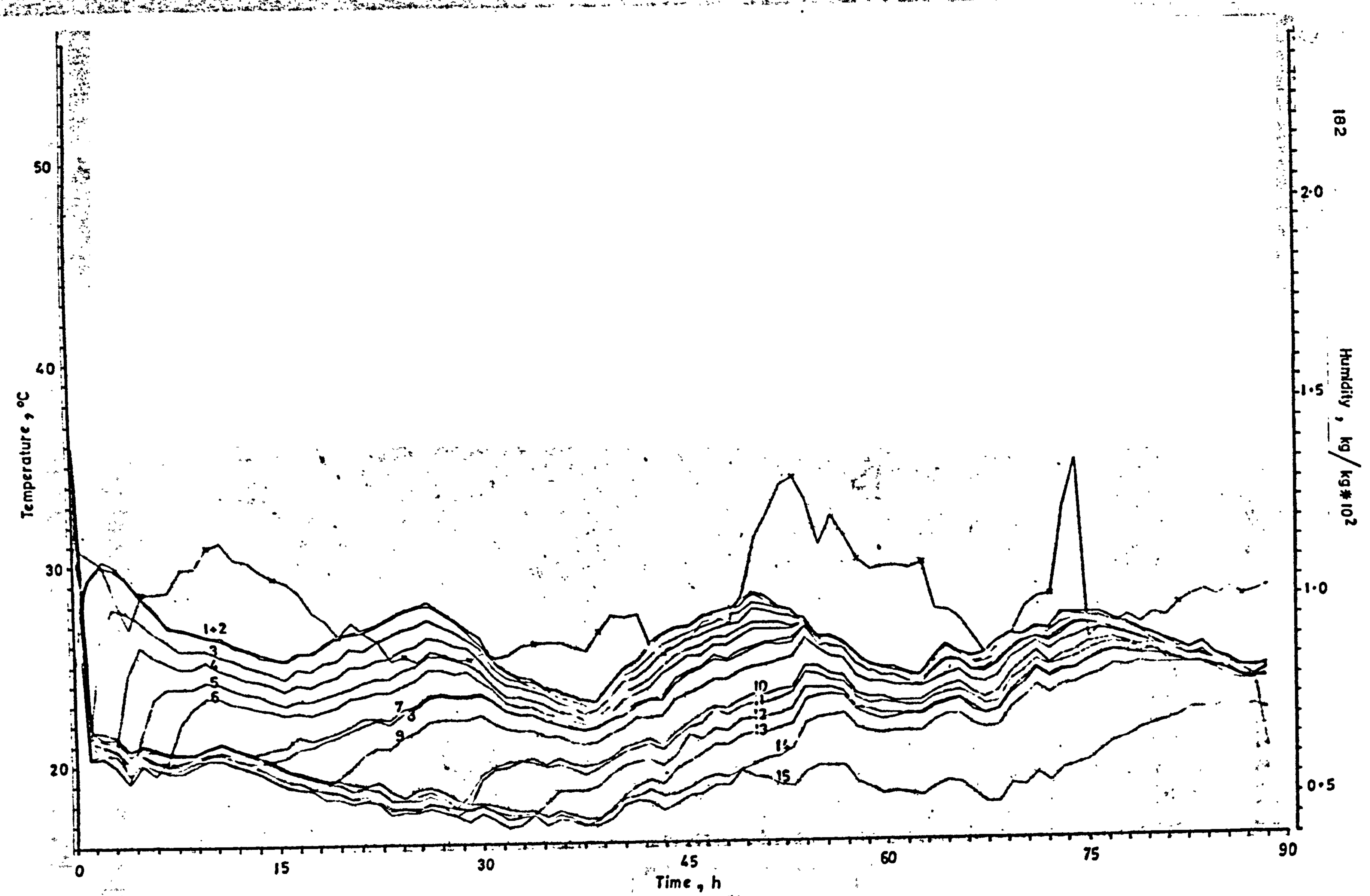

Fig. 4.19 Temperature profile, Run 9 30.7.71.

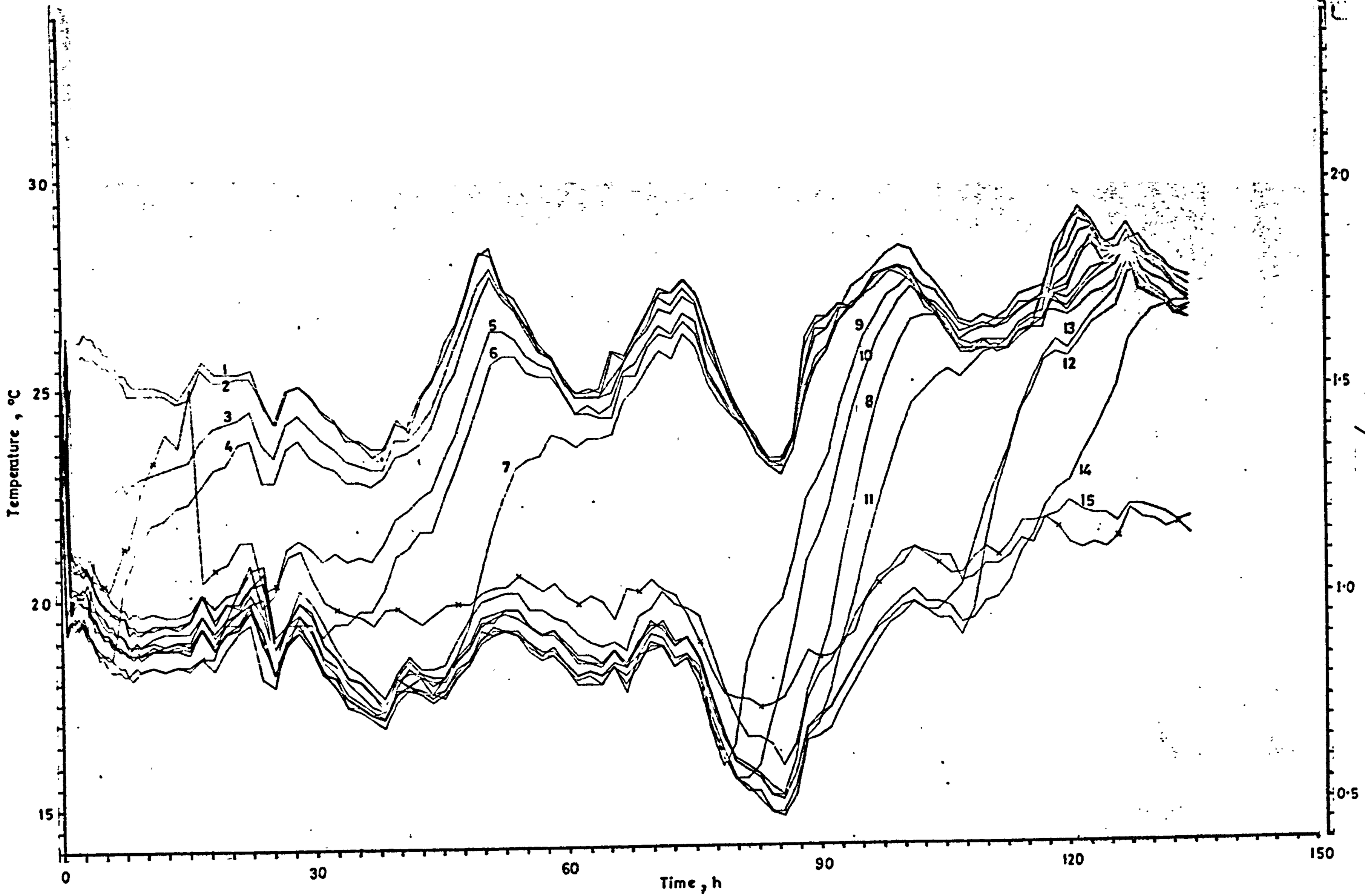

Fig. 4.20 Temperature profile, Run 10 4.8.71.

Run 11 (Table 4.3, Figs. 4.21 and 4.22)

A high temperature, 120°F (48.6°C) run with relatively dry seed (35.8% d.b.) and a shallower layer, 2.08 ft (0.63 m). In only 16 hours at a velocity of 24 ft/min (7.32 m/min) the seed had been dried to 5.5% m.c.d.b. with a shallow gradient of 4.8 to 6.8% d.b. The moisture pick-up was only 43% of adiabatic but this represented about twice that possible at ambient temperature and was nearly as good as was achieved in Run 7 which had a higher temperature and a much higher final moisture content because of a steeper gradient in a deeper layer.

Run 12 (Table 4.3, Figs. 4.21 and 4.23)

This was the only parallel flow run carried out in 1972 and at a depth of 4 ft (1.23 m) was the deepest of all the beds dried by parallel flow. The run was of particular interest because it was stopped after 46½h at a very early stage of drying and provided some interesting insight into initial drying rate. The initial moisture content was 80.2% and was only reduced to a mean of 60% d.b. This represented a definite gradient of from 30.3 to 65% in the bottom 16 inches with the remainder of the bed varying within the range 66.7 to 72.7% d.b.

These top layers may be considered to be above the drying zone and yet they exhibit a considerable reduction in moisture content over the initial value. This is because part of the drying occurred during cooling phases. When the seed bed temperature is above that of the incoming air the bed will be cooled but in the process the air will be warmed and the moisture carrying capacity of the air increased. Hence, provided the seed is above the moisture content equilibrium of the air, moisture will be transferred to it. Such transfer will precede the cooling zone throughout the entire bed and in front of the normal drying zone which moves much more slowly(108)

Because its passage is rapid the drying done in the wet layers by the cooling zone may be a small proportion of the total but is very important in that it cools and dries a little closer to a safe moisture level, that seed which is most likely to deteriorate in quality. Thus daily temperature fluctuations perform a useful function in the low temperature drying of high-moisture seeds. In this present Run the greater part of the seed had lost moisture only in the cooling phases and as a result this type of drying formed a significant part of the total evaporation. The overall ratio of moisture removed to air used was 1.24 times the possible adiabatic pick-up. It is probable that some, at least, of this discrepancy may be attributable to weighing errors and to error introduced by calculating an average adiabatic pick-up for air of fluctuating ambient humidity. If the initial and final moisture content determinations were correct and the final weighing of individual layers was more accurate than the initial weighing of the loaded bin, then the amount of moisture removed was not 61 lb but 50 lb. But it can also be shown that during the initial cooling phase at the start of the run when the temperature of the seed was cooled from 90°F (32.2°C) down to 72°F (22.2°C) in just under 2 hours, another 5 lb of moisture could have been removed in excess of that possible by adiabatic pick-up alone. Thus perhaps only 45 lb were removed by adiabatic evaporation alone and this would then have formed about 91% of the possible pick-up; a more realistic figure. Had the run been allowed to continue until the seed had been dry then the possible weighing errors would have formed a much smaller proportion of the total weight loss and the lower drying rate over the later stages of drying would have masked the effect of the cooling phases.

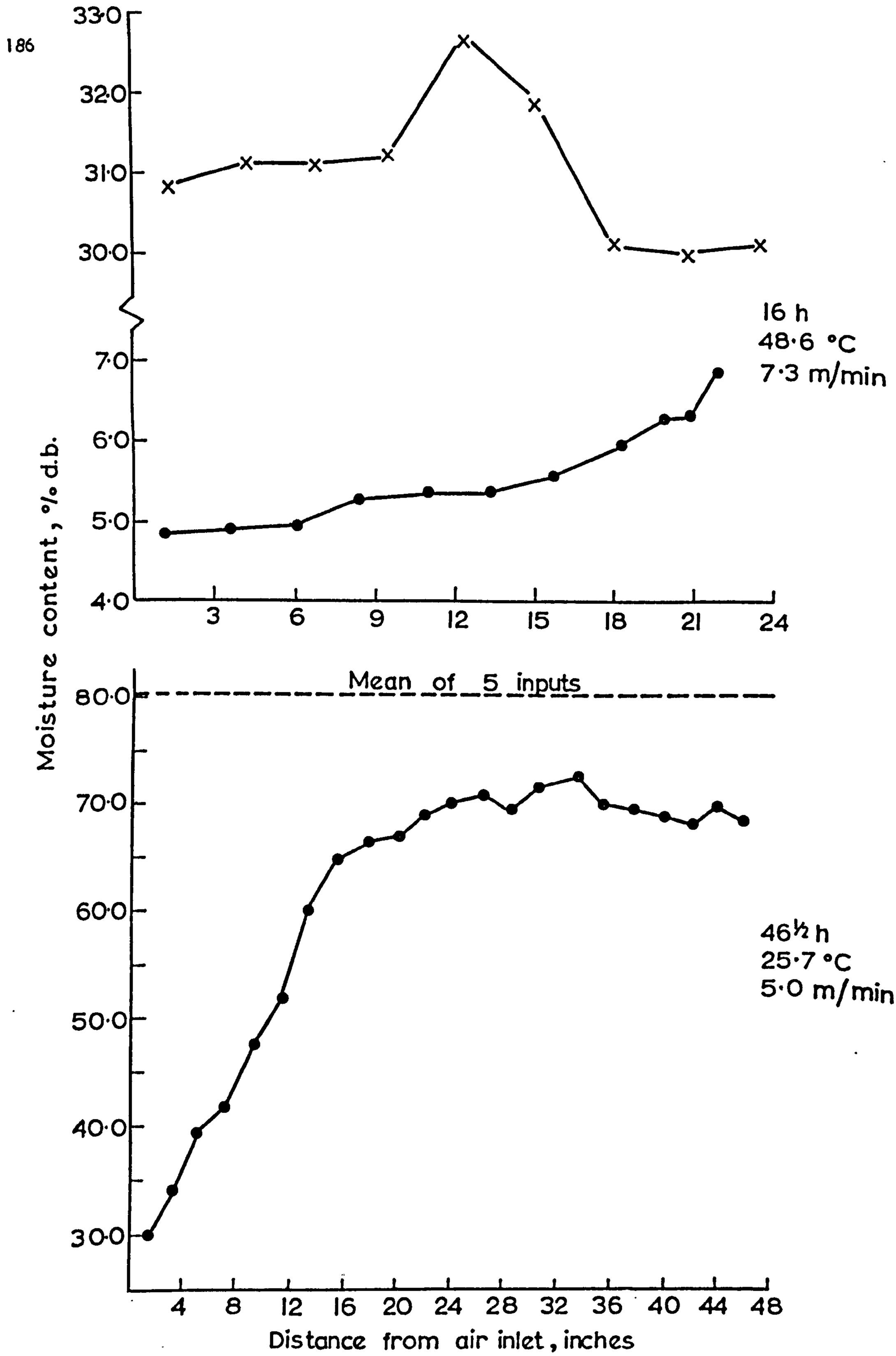

Fig. 4.21 Initial (x) and Final (•) Moisture Gradients for Parallel Flow Runs 11 (Top) and 12 (Bottom)

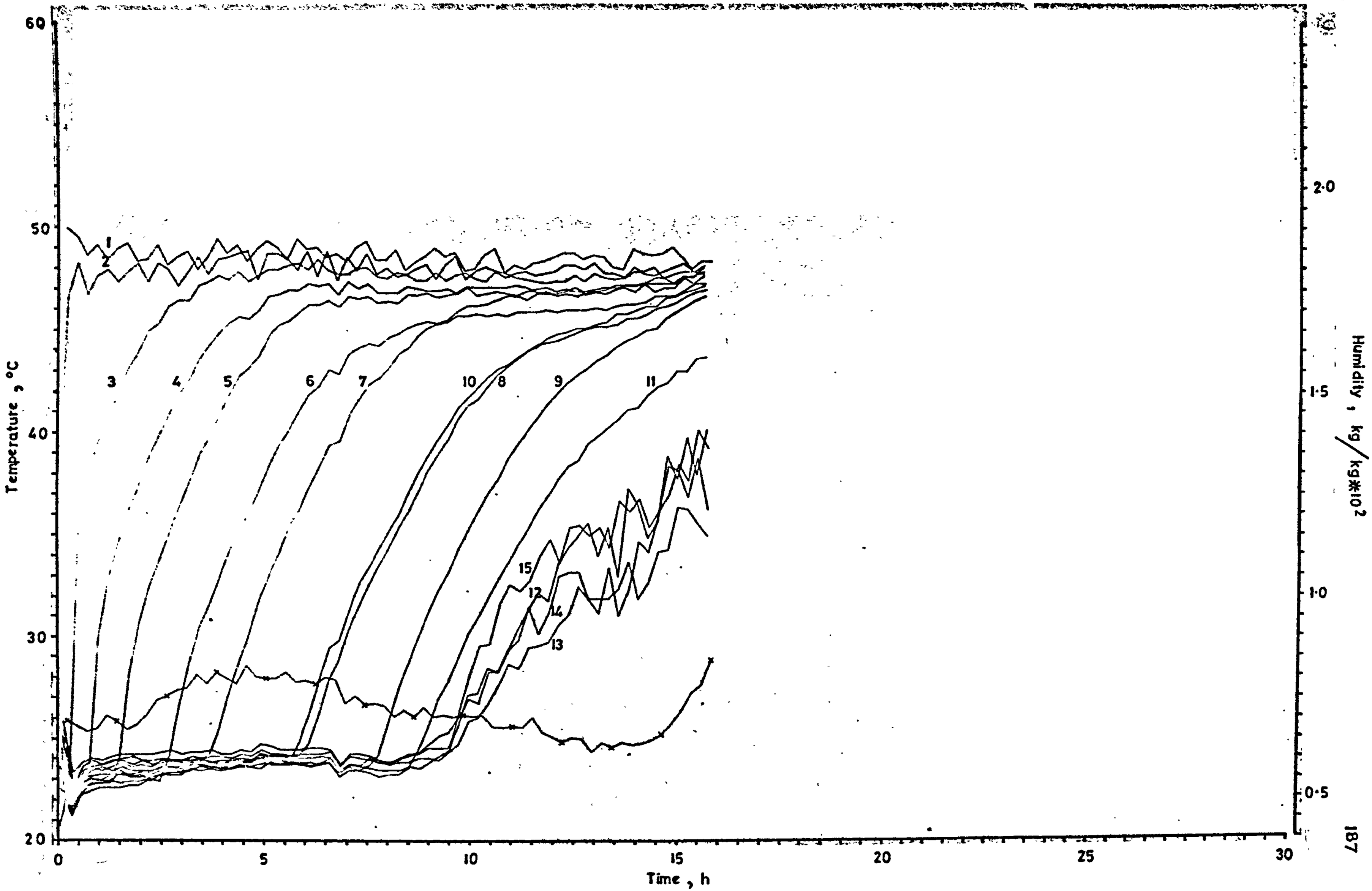

Fig. 4.22 Temperature profile, Run 11 16.8.71.

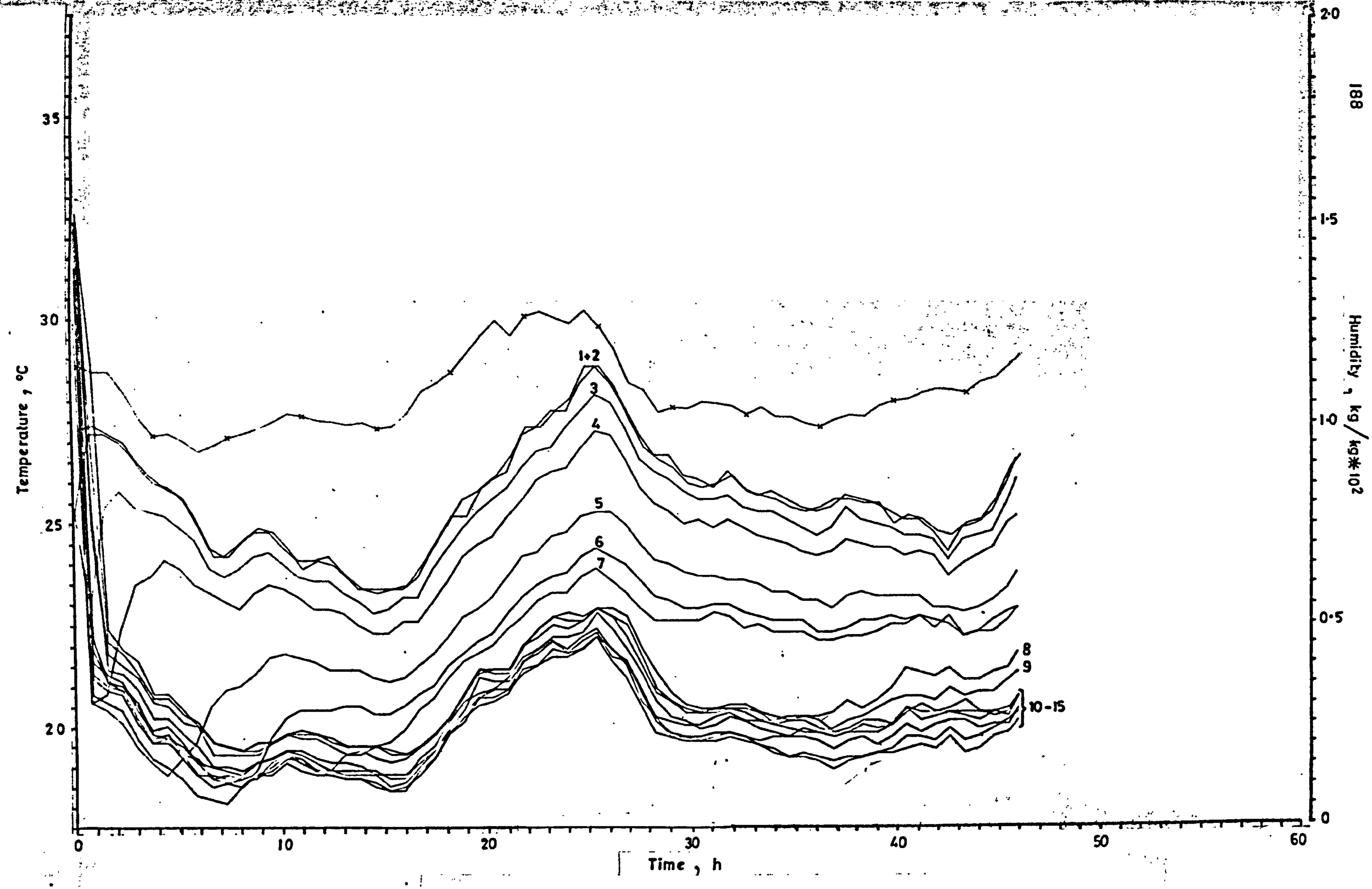

Fig. 4.23 Temperature profile, Run 12 17.7.72.

Run 13 (Table 4.4, Figs. 4.24, 4.25 & 4.26)

This was the first of the radial flow runs. Sabel seed at 46.9% d.b. was dried to 15.3% d.b. after 71h. Apart from the change in air velocity with distance from the air inlet the run was similar to the parallel flow runs at ambient temperatures and the results present a similar picture. The mean air velocity was 34.6 ft/min (10.5 m/min)/and represented 97.5 ft/min (29.7 m/min) at the inlet declining to 16.0 ft/min (4.9 m/min) at the outlet. In sympathy with this velocity pattern, the rise in temperature to near that of the inlet was very rapid in the 15 inches of seed nearest to the inlet (Thermocouples 3, 4, 5 in Fig. 4.4).

Run 14 (Table 4.4, Figs. 4.24, 4.25 & 4.27)

This run took 160½ h to reach a mean moisture content of 25.1% from an initial value of 75.1% d.b. Compared to the previous run the airflow had been halved and there was more moisture to remove so that a similar volume of air was used per unit of moisture removed. The final mean m.c. conceals a steep gradient from 11 to 50% in the outer 15 ins of the section.

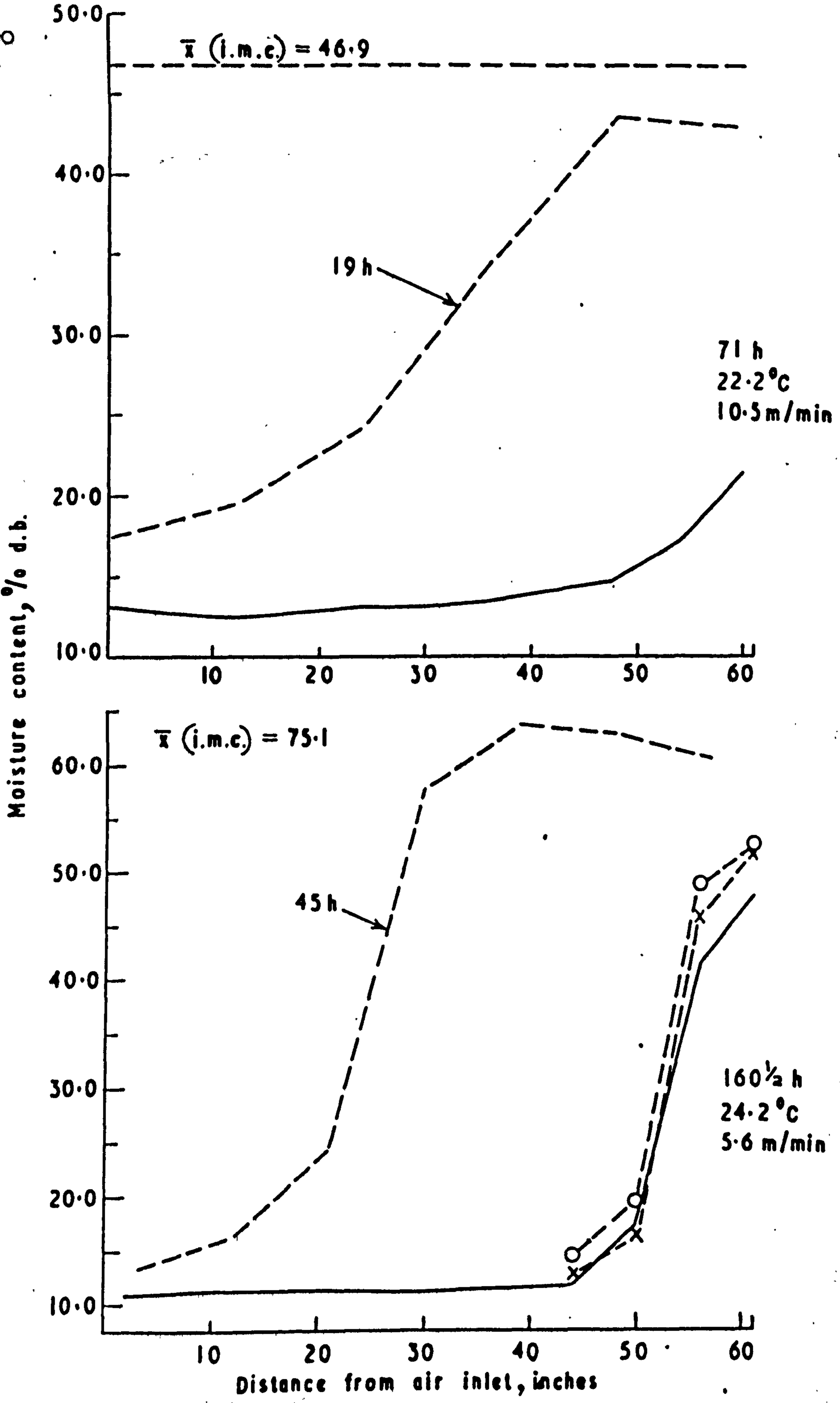

Fig. 4.24 Intermediate and Final Moisture Gradients for Radial Flow Runs 13 (Top) and 14 (Bottom)

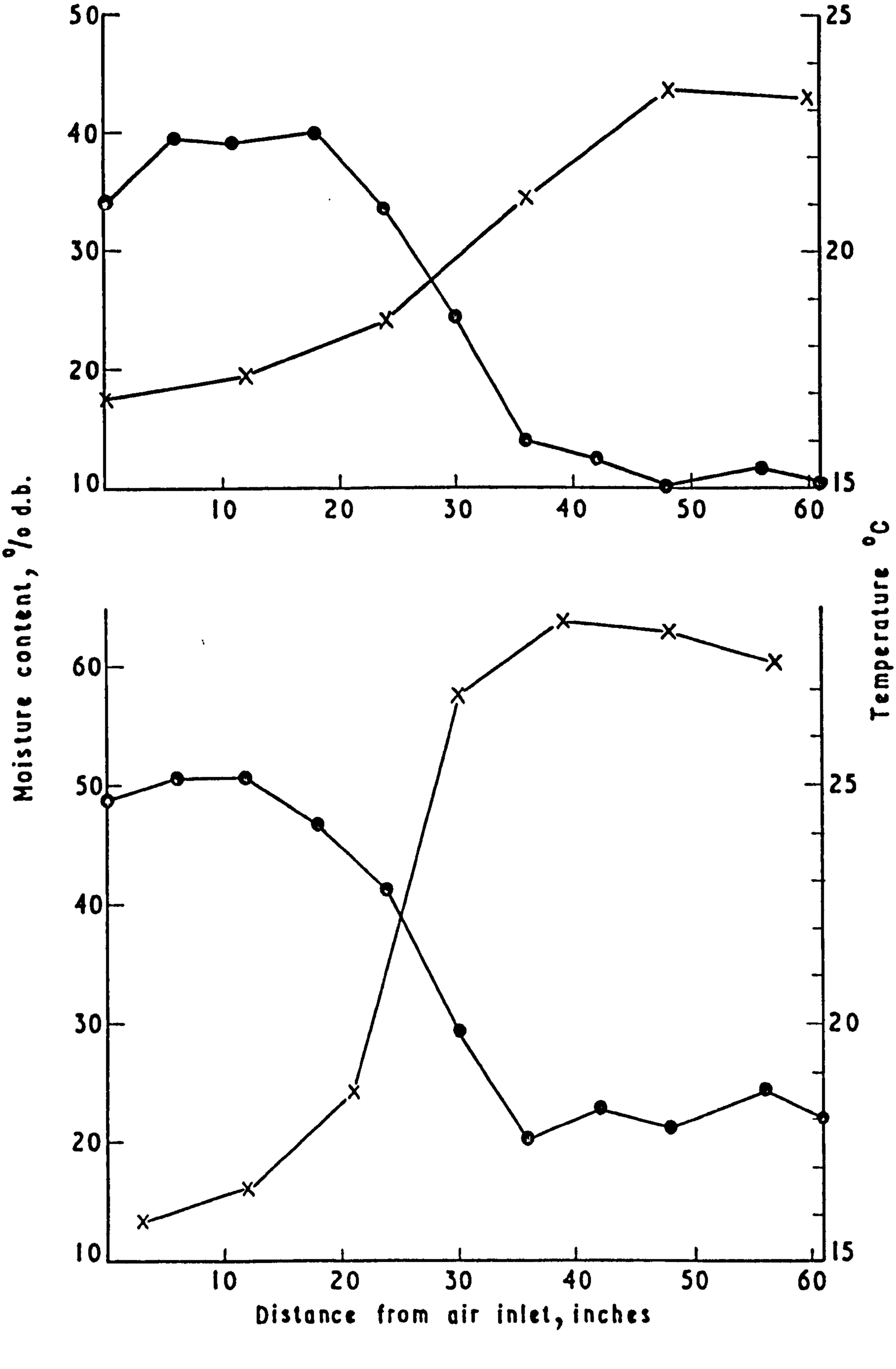

Fig.4.25 Temperature (•) and Moisture (x) Gradients Sampled at 19h in Run 13 (Top) and 45h in Run 14 (Bottom)

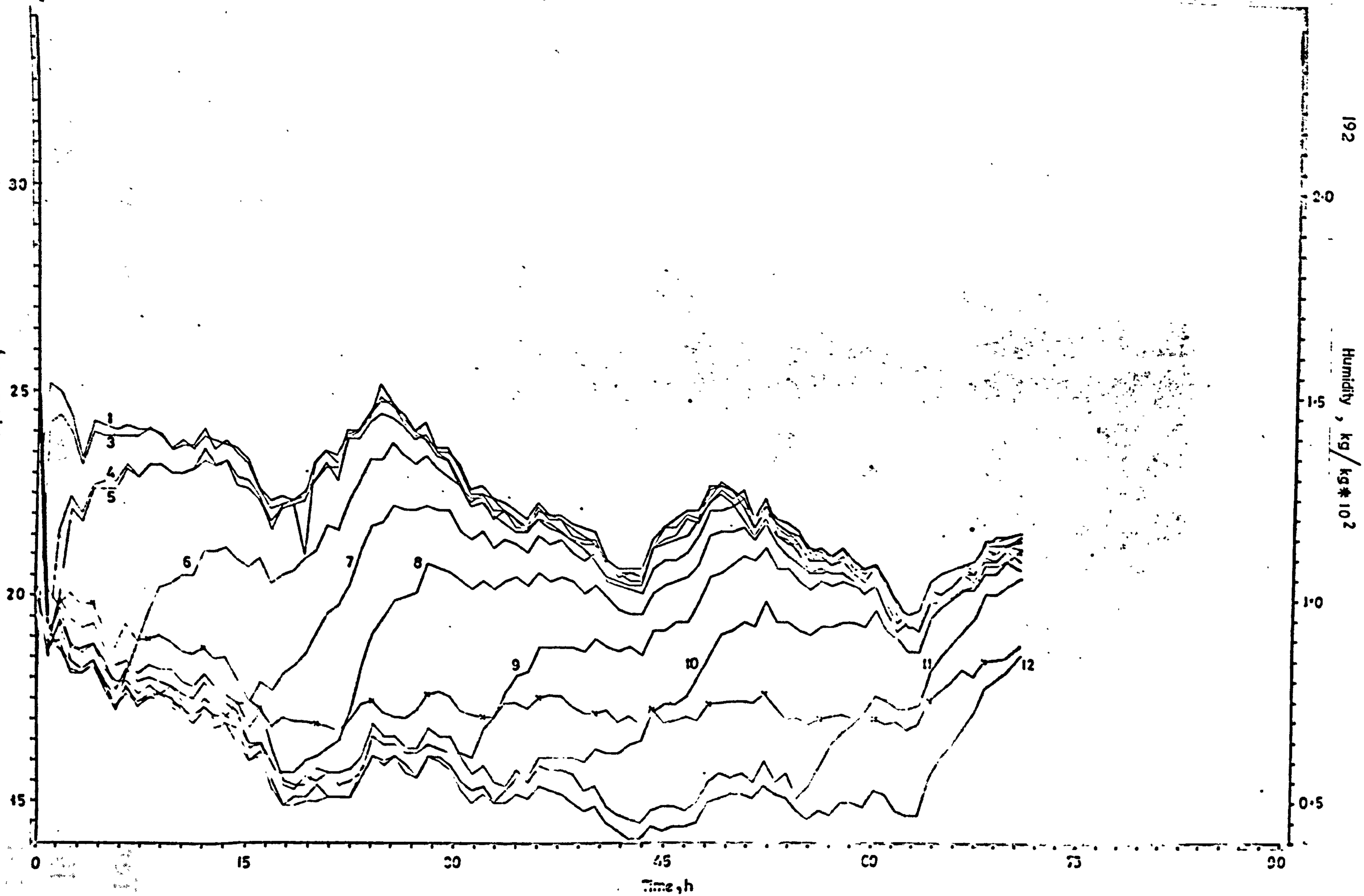

Fig. 4.26 Temperature profile, Run 13 25.7.72.

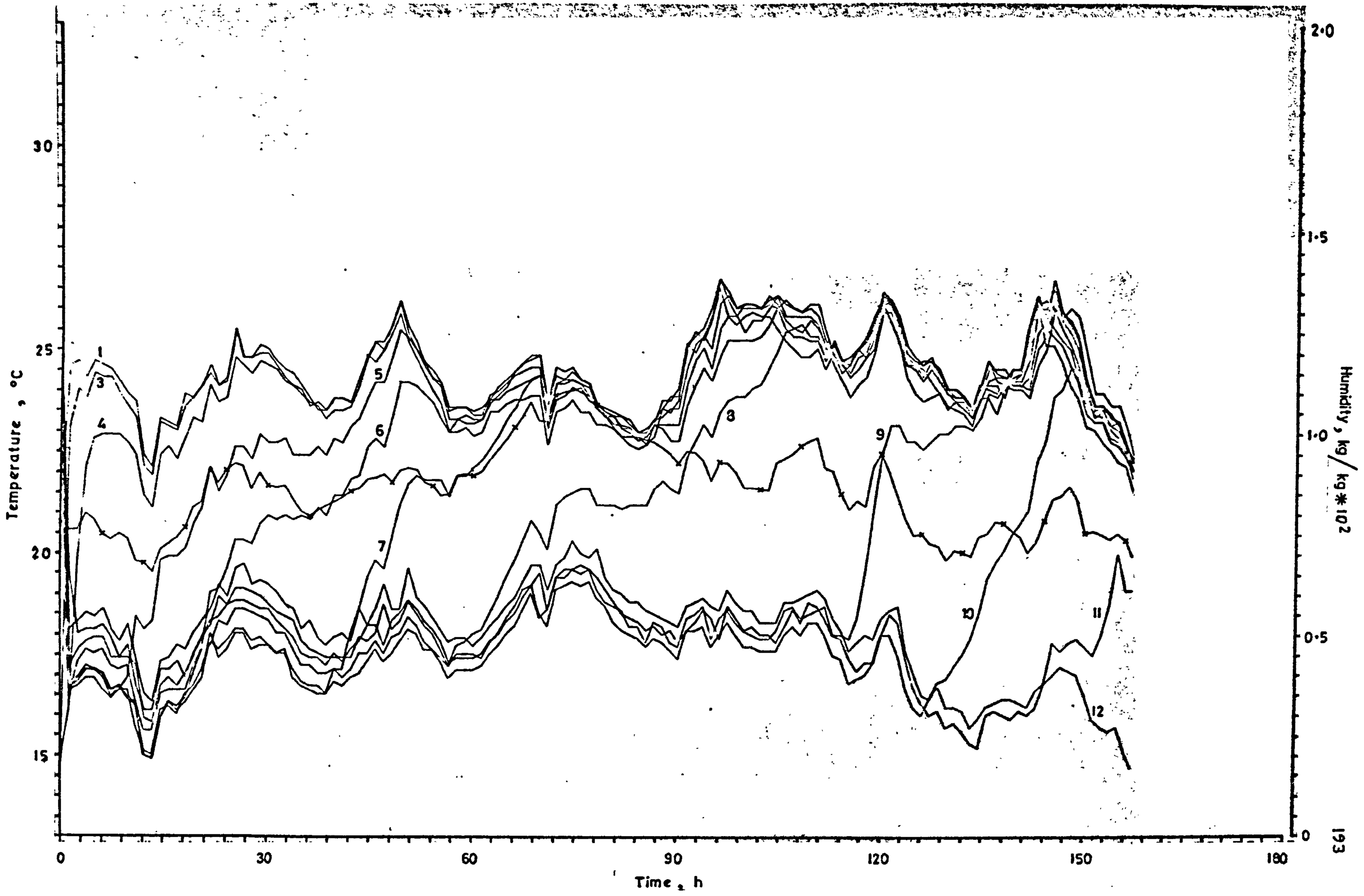

Fig. 4.27 Temperature profile, Run 14 3.8.72.

Run 15 (Table 4.4, Figs. 4.28, 4.29 & 4.30)

The initial moisture content in this run was 36.7% and a mean moisture content of 10.8 was achieved in 87.8h. Once again the rise in m.c. with increasing radius was confined to the extremity of the bin. The lowest moistures reached were lower than those in Runs 13 and 14 because of the higher mean temperature, 81.3°F (27.4°C) and low absolute humidity, 0.00751 lb/lb. This greater drying capacity also reduced the volume of air used to evaporate unit weight of water compared with Runs 13 and 14. Conversely the drier seed released its moisture less readily and the drying rate was a smaller proportion of the possible adiabatic pick-up.

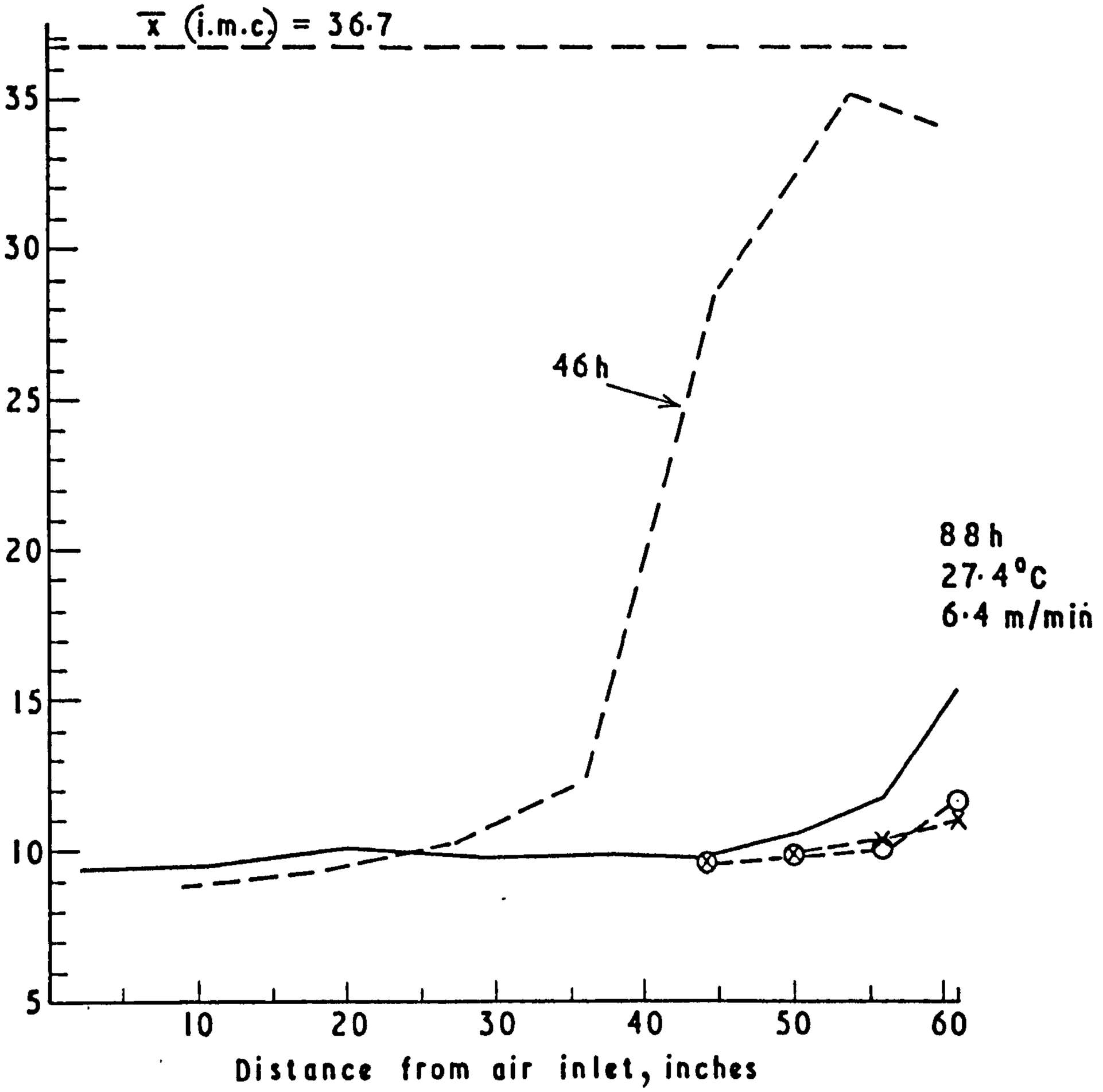

Fig.4.28 Intermediate and Final Moisture Gradients for Radial Flow Run 15

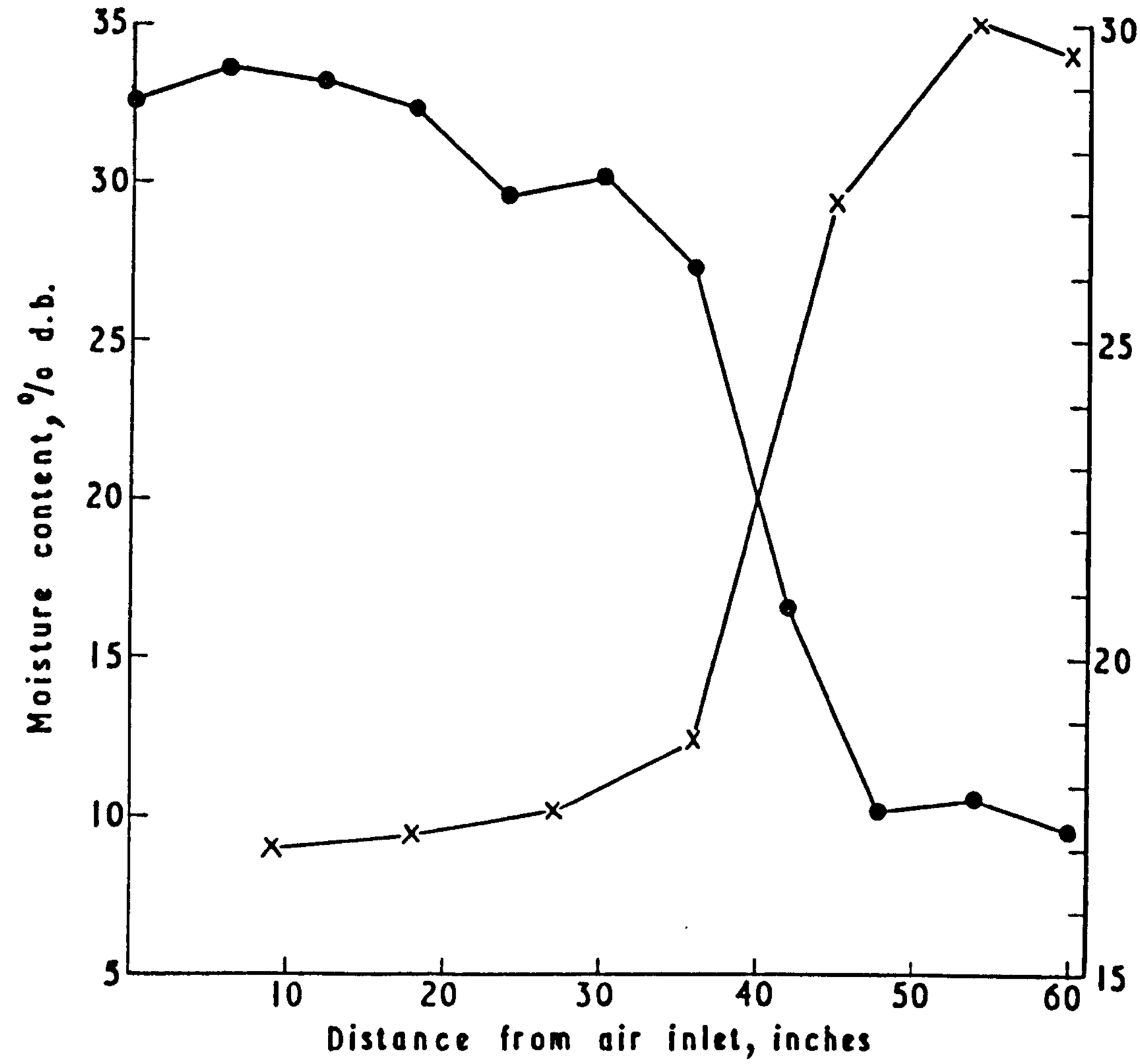

Fig.4.29 Temperature (•) and Moisture (x) Gradients Sampled at 46h in Run 15

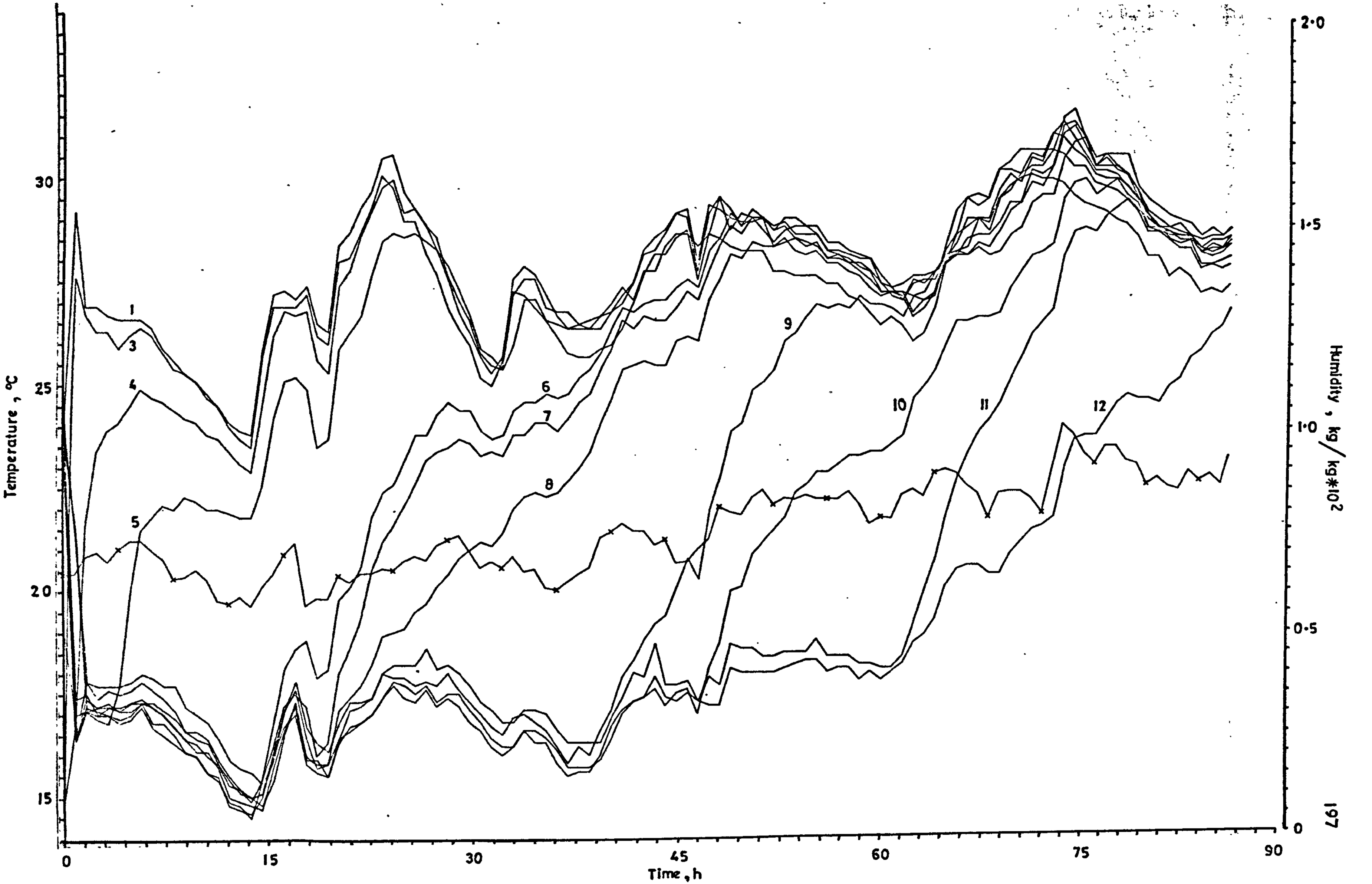

Fig. 4.30 Temperature profile, Run 15 10.8.72.

Germination means are given in Tables 4.2,4.3,4.4 and results for individual layers are tabulated in the Appendix. Although there were differences between layers these appeared to be unrelated to the pattern of drying and were not conspicuously greater than differences normally given between tests on different samples of the same population. Without replication of the runs nothing could be proved. Slight moulding was either indicated by smell or by caking of the seed in several of the low temperature runs. The worst case was in the second radial-bin run in which after 160½ h drying the outer layers were still over 40% m.c.d.b. and were both caked and smelly. But after final drying in shallow layers on a sample drier, the germination was unaffected.

It will be apparent from the preceding paragraphs that the results vary greatly from run to run and are not easily fitted into any simplified framework describing the interaction of the factors involved. It has to be admitted that a significant source of variation lies with the experimental method. Variation in the initial moisture profile, for example, was sometimes greater than in the final profile and furthermore was of a random nature whereas the final moisture profiles were clearly a result of the progression of the dryingzone. Tnis sort of variation could possibly have been avoided by using less seed but to do so for the same bed depths would have meant a much narrower cross section and would have intensified the already severe problem of air leakage around the perimeter of the bed. Errors in weighing were also introduced by the quantities of seed used (a) because the balance available for weighing the seed and drying bin together was not very accurate (±1lb) and (b) because weighing the seed in a large number of aliquots was also unsatisfactory.

Weighing errors may also have contributed in some measure to the variation in bulk density. The mean bulk density for Sabel was 23.0 lb/ft^3 and ranged from between 27.5 and 18.4 lb/ft^3. For S.23 the mean was 18.6 lb/ft^3 and ranged between 16.0 and 22.0 lb/ft^3. So there was an apparent difference between varieties although with some overlap. Within varieties the bulk density appeared to be slightly correlated with initial m.c. and hence maturity but there was considerable variation here. Variation in shrinkage was more consistent and showed some correlation ($r = 0.79$) with the percentage of moisture removed, $M_o - M_f$ (Figure 30a). The data were fitted by equation 4.9 in which ΔD = shrinkage as a percentage of original depth.

$$\Delta D = 5.34 + 0.1889\ (M_o - M_f) \qquad \ldots(4.9)$$

The exact value of the intercept is specific to these data but a positive value is consistent with the probability that part of the shrinkage is due to settling which would occur even in an undried bed.

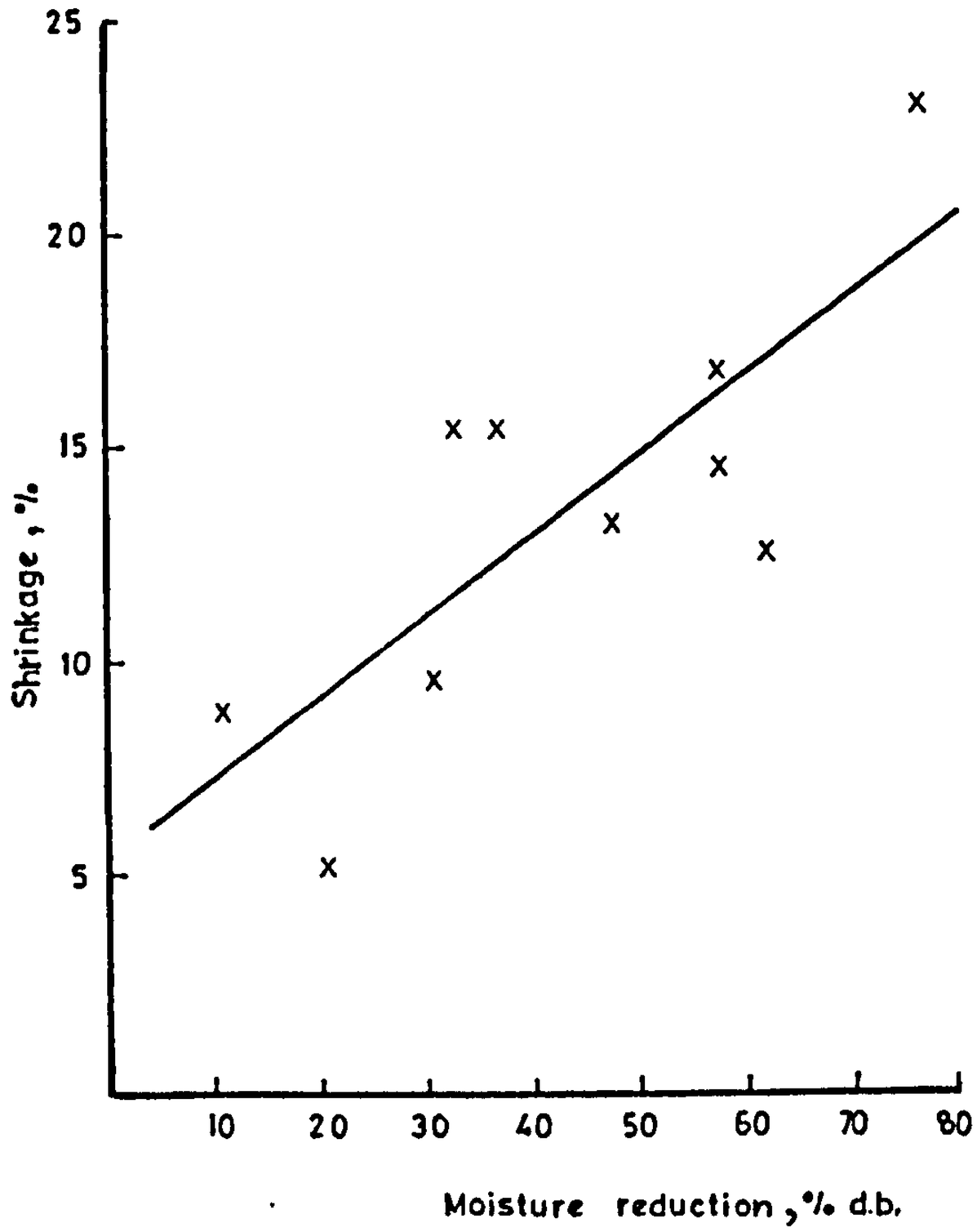

Fig 4.30a. Effect of moisture reduction upon shrinkage.

Clearly even if allowance is made for some of the experimental errors there still remains a good deal of unexplained variation which must result from the complexity of the interaction between all the factors, known and unknown involved in the experiments. In this respect one of the most important factors was the diurnal fluctuation in inlet corditions. It could be argued that more comprehensible information would be obtained from deep bed runs carried out with constant inlet conditions. The necessary resources to do this were not available but even if they had been it would have been an unrealistic approach since the whole point of low temperature drying on the farm is the low cost of circulating ambient air only. And as has been seen for wet seed cyclic temperatures are an advantage.

These results confirm that a few high-cost large scale experimental runs cannot, by themselves, provide sufficient insight upon which to base advisory recommendations. In Section 5 it will be shown how the results can be used in conjunction with a mathematical model of the deep bed process (a) to simulate the drying process under variable inlet conditions and (b) to check the validity of such predictions.

4.4.2. Pressure resistance to airflow

Least squares fits of equation 4.6 were carried out on groups of data defined in Table 4.6 and illustrated by Figures 4.31 and 4.32. The dotted lines in Fig.4.32 are derived from the radial flow readings, Fig.4.33 by the fitting of equation 4.8.

Table 4.6

Coefficients a and n in equation 4.6, $p = aV^n$ derived from various groups of data

Crop	Origin of data	n	a	
			Imperial units in w.g./ft depth	S.I. Units kN/m3/m depth
Sabel	From parallel flow Runs 5, 6 and end of Run 8.	1.186	.01628	.05439
	Start of Run 8	1.184	.01432	.04775
	End of Run 12	1.012	.04384	.11920
S.23	Run 9 plus start Run 10	1.137	.02178	.06870
	End of Run 10	1.127	.02771	.08639
	Radial bin Run 14	1.211	.02257	.07772
	Radial bin Run 15	1.091	.02579	.07707

The groups were selected because they were markedly different to other readings within the same variety. Variations between sets of readings obtained from independent harvests of seed of field purities of the order of 80-85% would be expected, but two sets gave noticeably higher pressures than the remainder. These were, for Sabel, the set of readings taken at the end of Run 12 and, for S.23, the readings taken at the end of Run 10.

No definite explanation of the higher resistance encountered in these two runs can be given. In the case of Run 10 which after

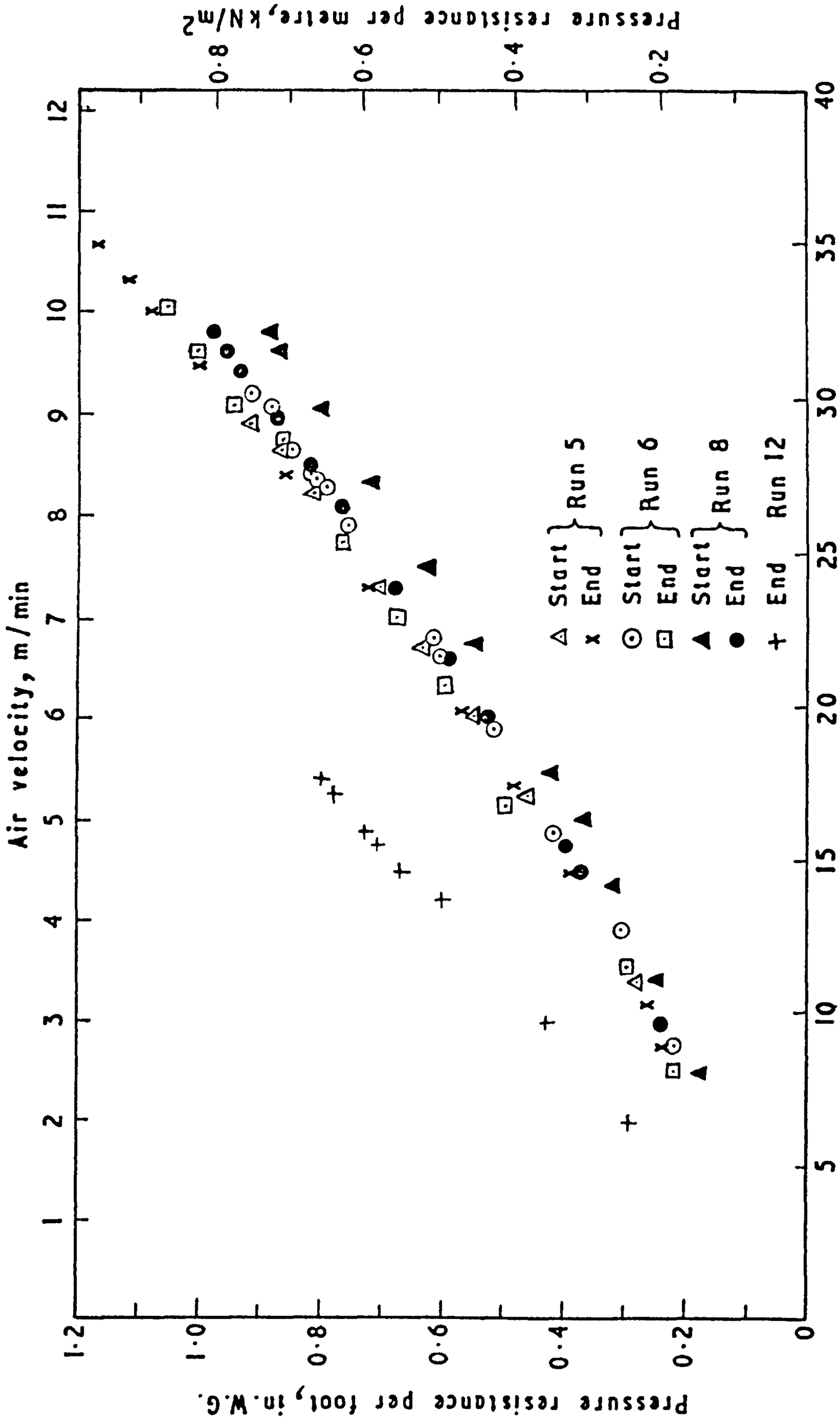

Fig. 4.31 Pressure Resistance for Sabel, Parallel Flow Runs 5,6,8 and 12

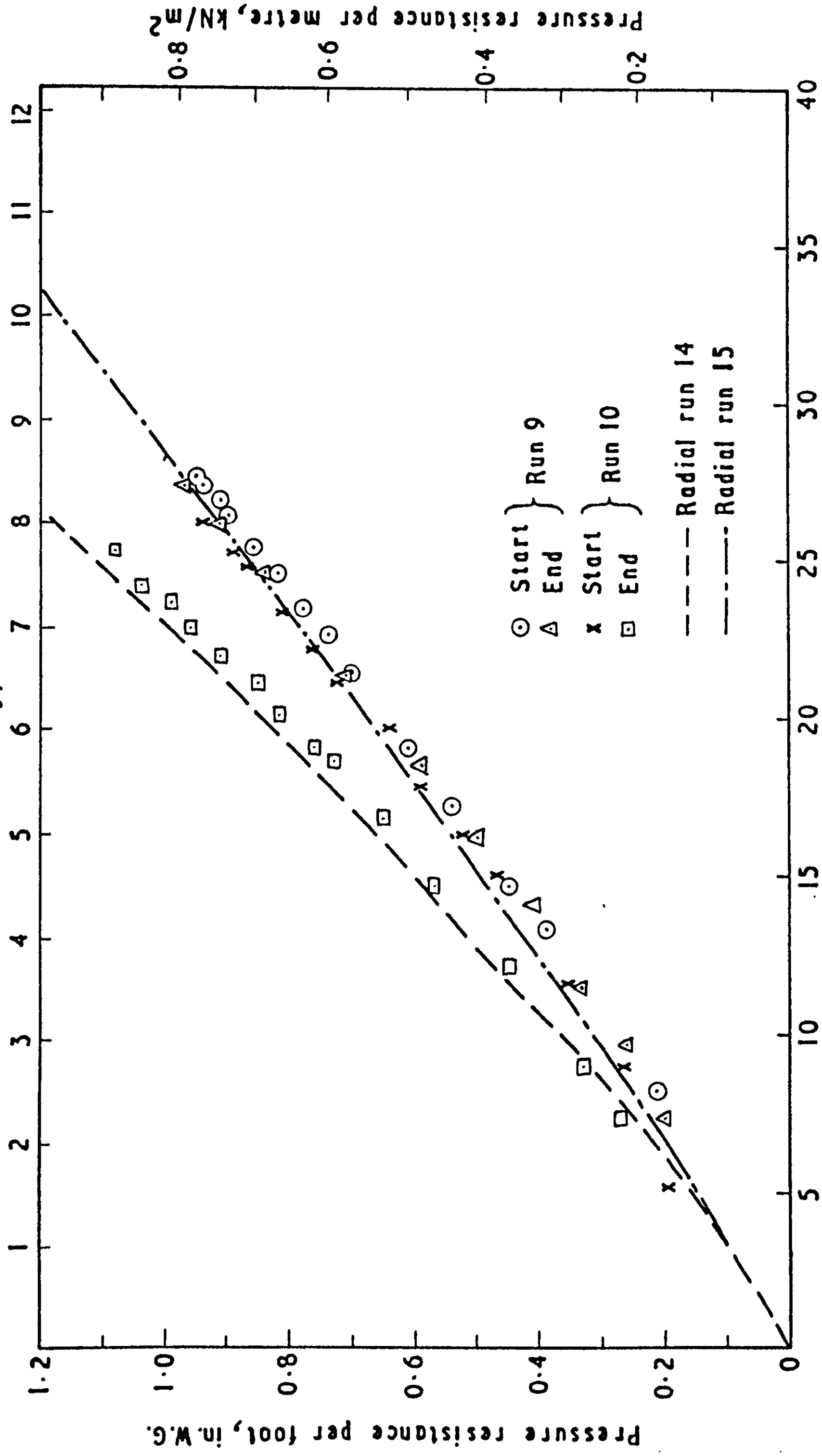

Fig. 4.32 Pressure Resistance for S.23 Parallel Flow Runs 9 and 10 and Flow Runs 14 and 15 Derived from Radial Flow Curves

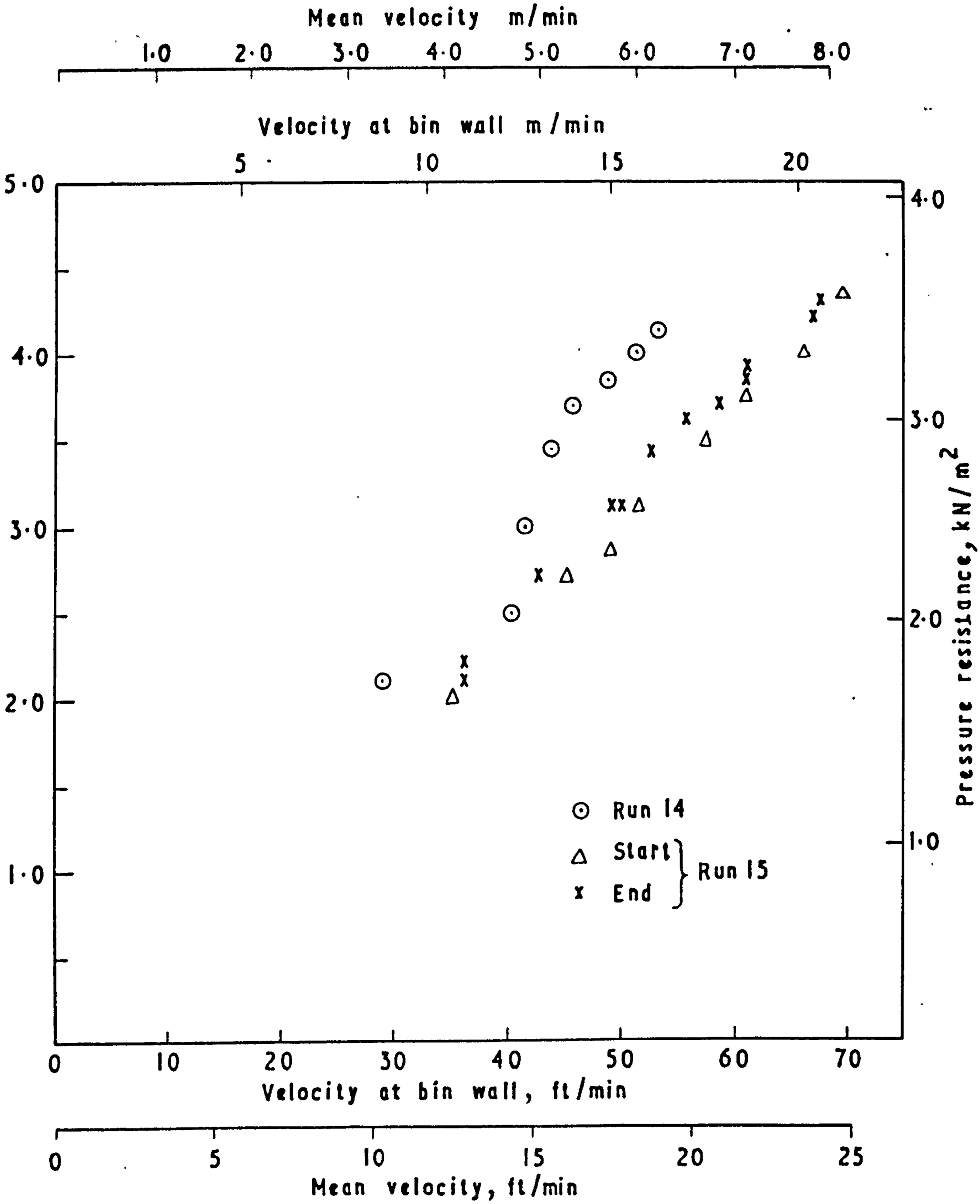

Fig. 4.33 Pressure Resistance for S.23, Radial Flow Runs 14 and 15

136h was still above safe storage moisture content in the top layers, it is possible that the seed had both compacted and begun to be bound together by bacterial or fungal growth. 'Clotting' of the seed surface in this way in on-floor driers is a common phenomenon in grass-seed drying and is usually remedied by mechanical disturbance of the surface. Run 12 was a much shorter run and although the top 30 inches of seed were clearly damp and a little caked, all the indications were that this was as a result of compaction rather than 'clotting'. It may be that at a depth of 4 ft and at high moisture content the increasing compaction caused a more than linear increase of pressure resistance with depth.

The results from the radial-flow Run 15 for S.23 agree with those from Run 9 and the start of Run 10, but those from Run 14 agree with those from the end of Run 10. Here again no definite explanation of these differences can be given.

These apparent anomalies apart, the values in Table 4.6 and the plots of Figs 4.31 and 4.32 suggest that Sabel produced a lower resistance to airflow than S.23; a reflection of the smaller seed size of the latter and an associated larger proportion of fine rubbish. In general the results also support the measurements of Osborne [91] on S101 perennial ryegrass seed and the data of Run 9 fit his curve very closely.

Compared with cereal grains [91] the resistances are high and the anomalous results suggest that differences in seed condition and compaction are more important than varietal differences of size in producing a wide range of resistance at any one airflow. This underlines the importance of obtaining an even distribution of seed in on-floor driers and of avoiding any form of localised compaction such as is caused by walking on the bed. Clearly also, by its effect in reducing airflow, the growth of mould is self-accelerating and results in a delicate balance between drying regimes which are safe and those which are not.

4.5. SUMMARY AND CONCLUSIONS.

1. Detailed results of 12 parallel-flow and 3 radial flow deep bed drying runs have been given. Each run was a unique combination of several variables - the main variables were as follows:-

Seed

Initial moisture content - 23.5 to 104.5% d.b.

Final mean moisture content - 5.5 to 60% d.b.

Depths, normal to flow: Parallel - 9 in to 4 ft

Radial - 5 ft

Bulk density: Sabel 23.9 (18.4 - 27.5) lb/ft^3

S.23 18.6 (16.0 - 22.0) lb/ft^3

Shrinkage: 13.5 (5.2 - 23.0) %

Drying air

Temperatures: Ambient (10), 90°F (2), 121°F (2), 132°F (1)

Flows: Parallel 16 - 43 ft/min

Radial 16 - 35 ft/min

2. The runs were primarily intended for the validation of a mathematical model of the deep bed drying process. To this end, changes in inlet air condition with time were recorded and processed to a form suitable for input to the model. For eventual comparison with predicted values, temperature-time profiles were plotted by computer.

3. Partly because of the priority given to the thin-layer tests, the problems of working with relatively large quantities of seed were not completely solved.

In particular there were (a) weighing discrepancies between total bin weights and accumulated aliquot weights and (b) shrinkage of the seed away from the thermocouple leads led to air leakage.

4. These experiments confirmed that attempts to understand the deep-bed drying process by purely empirical experimentation of this type would be prohibitively costly in equipment, seed and labour and the results would, in any case, be almost impossible to interpret in more than very general terms.

5. The quantity of air needed to remove 1 lb of water varied from 10609 ft^3 in Run 8 to 2739 ft^3 in Run 7. Run 8 had the lowest initial moisture content(23.5%) and a complete drying zone was never established within the bed. The good evaporation rate in Run 7 was undoubtedly associated with use of heated (132°F) air. The volume of air required per unit mass of dry seed was also lowest (593 ft^3/lb) in Run 7. It was highest (4790 ft^3/lb) in Run 1 in which one of the highest airflows was used with a 2 ft layer and the seed was allowed to approach equilibrium throughout its depth.

6. Run 12 was unusual in exhibiting a drying rate greater than predicted by adiabatic pick-up. This phenomenon was not entirely explained by extra drying during cooling phases nor by weight discrepancies.

7. The mean bulk density of Sabel was greater than that of S.23 but there was some overlap between the ranges for each variety. There was no firm correlation between bulk density and moisture content. Shrinkage was expressed as a linear function of moisture removed.

8. There was no detectable impairment of seed germination even in seed which had moulded sufficiently to be caked and smelly.

9. Pressure resistance to airflow in the parallel flow runs was adequately described by the equation $P = aV^n$. Values of $\underline{a}$ and $\underline{n}$ were also derived from measurements made with the radial flow rig using 4.8.

$$P_R = \frac{a}{1-n}\left(\frac{Q}{0{\cdot}69813.D}\right)^n\left(0{\cdot}1644^{n-1} - 1\right) \qquad \ldots 4.8$$

Values of a and n appeared to be affected more by differences in seed condition and compaction than by varietal differences of size but the values describing the majority of the data for each variety were:-

	a in w.g./ft depth	n
Sahel	.01628	1.186
S.23	.02178	1.137

5. SIMULATION OF DRYING IN DEEP BEDS.

5. SIMULATION OF DRYING IN DEEP BEDS

5.1. INTRODUCTION

The results of the thin-layer tests represent the behaviour of seeds exposed throughout the duration of drying to constant drying conditions. In contrast the results of the deep bed tests represent the behaviour of seeds exposed to drying conditions which are continually varying with both time and depth. Thin-layer data can be used to predict these deep bed changes if the deep bed is visualised as a series of thin layers. In any small increment of time, each layer is subject to constant drying conditions and, hence during that increment, can be visualised as following a small section of the thin-layer drying curve. This is the basis of the workdescribed in this section.

5.1.1. Review of previous work

For at least a decade the application of thin-layer drying theory to the drying of deep beds was hindered by the difficulties of integrating the equations by conventional mathematical methods. In 1955 M'Ewen and O'Callaghan[69] made a significant contribution by suggesting a graphical method of integration. The graphical construction was based on a psychrometric chart and made the basic assumption that the change in temperature of the air passing through the bed would follow the constant heat line. Unfortunately the method was still too laborious for general use. At about the same time, Van Arsdel[126] proposed a mathematical model which in most respects is very similar to contemporary models and which was based on the solution of a set of simultaneous heat and mass transfer equations. A numerical method of integration was employed but at that time such techniques were beyond the resources of most interested organisations and the work lapsed. It is significant also that Van Arsdel had no experimentally determined thin-layer constants and had to invent them

in order to provide a worked example.

In 1960, Nelson [83] published a dimensional analysis of batch-type drying and a similar exercise was recently carried out for the drying of rice [24]. Morris-Thomas [73] correlated rate of airflow, temperature rise and drying time for a fixed moisture loss from shallow (4-12") beds of wheat and his equation forms the basis of a method for correcting evaporation rate to standard conditions prescribed in BS 3986:1966 [20]. None of these studies have provided more than a limited insight into the drying process.

The most significant advance came in 1965 when Boyce [16,17] published a model in which the equations were solved by electronic digital computer. In some respects the model was less advanced than Van Arsdel's but it had two significant advantages. The first was that the publication had coincided with the growing availability of the electronic computer as a research and adviscry tool. And secondly the model had more impact because Boyce used real thin-layer drying data to predict the behaviour of deep beds for which he had experimental results. The comparisons were not good but the point was made and since that time there has been renewed interest in the grain drying problem on both sides of the Atlantic.

At Newcastle, Boyce's original model was developed further, first by Menzies [66] and later by Bailey [3] and applied to 4 types of heated air drier. [88] The basis of the Newcastle model is the solution of 4 heat and mass balances by the simple Euler method of integration. Bakker-Arkema [6] appears to have experimented with various numerical integration procedures for the solution of the Michigan State University model, [5] the full version of which contains an equation describing the moisture and temperature gradients within the kernel. Spencer [113] used a Runge Kutta method of integration. Baughmann et al [9] used

CSMP (continuous system modelling program) but do not state which of the alternative integration methods they used. Hamdy and Barre [41,42] solved the equations on a hybrid digital/analogue computer. Bakker-Arkema [6] defines the heat and mass equations as 'stiff', by which he means that they contain constants with greatly different values. The effect is that in conventional integration procedures the step size has to be small for convergence and stability and this increases computing time. Menzies[65] and more recently Spencer in association with Bailey [4] concluded that the saving in time given by the simple Euler integration far outweighed any improvement in accuracy achieved with the Runge Kutta method.

Because of the computing time required, the more sophisticated techniques have been confined to models of heated air driers with short drying periods. A number of simpler models have been proposed for low temperature situations. In that of Thompson [118], the moisture and temperature changes within each thin layer are calculated by means of a sensible heat balance which assumes that during each time increment the grain and air temperature will equalise. This model is economical in computing time and has been found useful in

(a) optimisation studies [119,72,71] where the optimisation routine may call for a number of repeat simulations to be carried out and

(b) low temperature drying [121] where the real time periods to be simulated are long. An even simpler model was proposed by Bloome [14] for the natural-air drying of maize. For this purpose it was assumed that the grain was always close to equilibrium with the air and that, in the time increments chosen, it would reach such equilibrium. Hence rates of heat and mass transfer could be neglected but diurnal fluctuations in inlet air became important and recorded

The most recent developments have been in the use of such models for predicting grain quality. For the high temperature drying of wheat and barley, Bailey [3] has introduced the critical temperature equations of Hutchinson [54] and Ptitsyn [98] into the Newcastle model. Flood et al [34] used the dry matter loss curves of Saul [105] as a failure criterion in a study of natural-air drying of maize based on the model of Thompson [118]. Thompson [122] also used similar data updated by Steele et al [115] and Saul [104]. Bloome [15] also used this data within an optimisation study.

As far as the author is aware all of the models referred to are still regarded as being in an experimental state and are not yet available for general advisory work.

5.2. DEVELOPMENT OF A MODEL FOR GRASS SEED

The simulation developed in this present work is very similar to that of the Newcastle model.[88] It differs from it in being developed independently in FORTRAN as opposed to ALGOL and in a number of other features which are elaborated further in the text.

The following notation is used.

Symbol	Definition	Units
z	Depth of deep layer (thickness of thin-layer dz)	L
θ	Elapsed drying time	θ
M	Seed moisture content (db)	Ratio
H	Moisture content of air (absolute humidity)	Ratio
T_a	Temperature of the drying air	T
T_g	Seed temperature	T
ρ	Bulk density of dry matter	M/L^3
h	Heat transfer coefficient	$H/\theta.T.L^2$
S	Surface area/unit volume	1/L
hS	Combination of h & S to give volumetric heat transfer coefficient	$H/\theta.T.L^3$
La	Latent heat of vapourisation of water at 0^oC	H/M
Lg	Latent heat of vapourisation of water from seed	H/M
Cpa	Specific heat capacity of air	H/M.T
Cpg	Specific heat capacity of dry seed	H/M.T
Cpw	Specific heat capacity of water vapour	H/M.T
Cpl	Specific heat capacity of water liquid	H/M.T
G	Mass flow of air per unit area	$M/\theta L^2$

5.2.1. Heat and mass transfer equations

The first step in the development of the model is to derive a set of equations to describe the heat and mass transfer within a thin layer during a small time increment. Consider an elemental layer dz, of unit cross section and average moisture content M ventilated in the direction of z with a flow of air G, of air temperature T_a and humidity H. (Fig. 5.1)

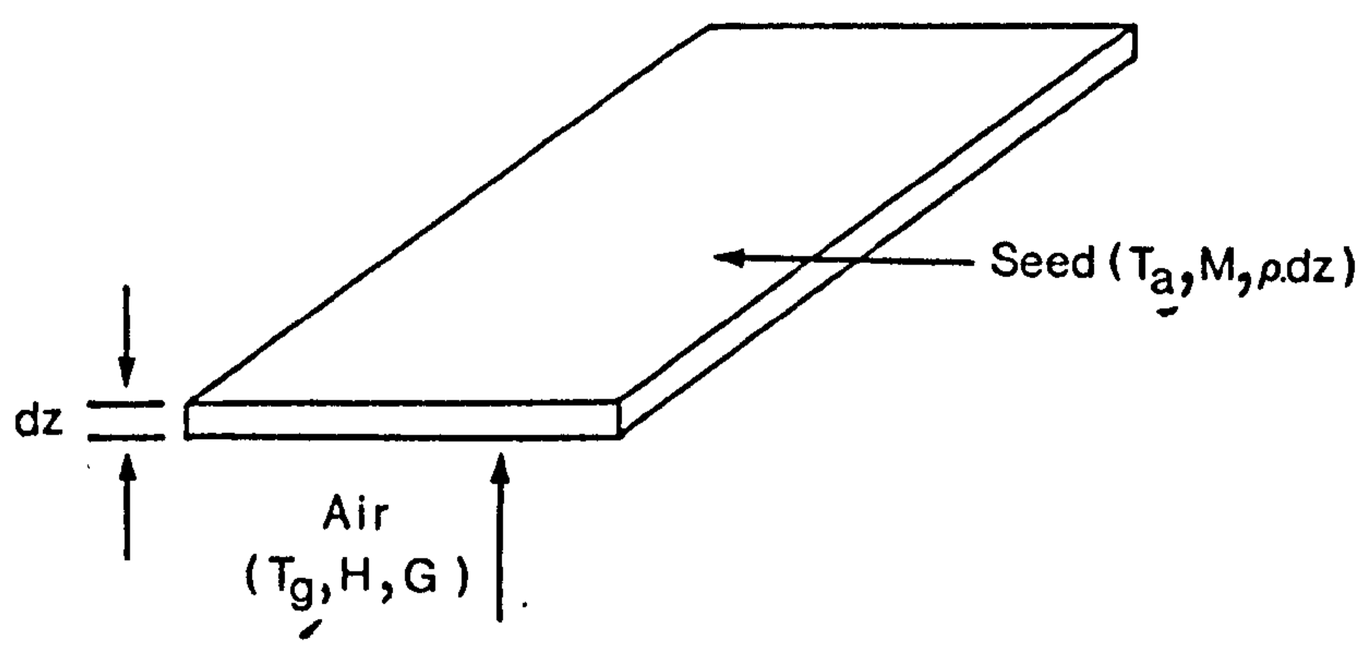

Fig. 5.1. Interacting variables in the thin-layer

Assuming that the air either gains or loses heat only in the direction of flow, the differential rate of change in air temperature during an elemental time $d\theta$ will be

$$\Delta T_a = \left(\frac{\delta T_a}{\delta \theta}\right) d\theta + \left(\frac{\delta T_a}{\delta z}\right) dz \qquad \ldots\ldots\ldots 5.1$$

However, in a short time interval the change of temperature with respect to depth will be much greater than with respect to time. Hence the change may be approximated by the partial component

$$\left(\frac{\delta T_a}{\delta z}\right) dz$$

Similarly the change in seed temperature will be greater with respect to time than it will be with respect to depth so that ΔT_g may be approximated by $\left(\frac{\delta T_g}{\delta \theta}\right) d\theta$

Likewise the differential rates of change of seed moisture

content ΔM and air humidity ΔH are approximated by $\left(\frac{\delta M}{\delta \theta}\right) d\theta$ and $\left(\frac{\delta H}{\delta z}\right) dz$.

The relationship between these four changes of state can be represented by 4 equations.

5.2.1.1. Moisture balance

The change in moisture of the seed must equal the change in humidity of the air

$$\rho . dz \left(-\frac{\delta M}{\delta \theta}\right) d\theta = G \, d\theta \left(\frac{\delta H}{\delta z}\right) dz$$

$$-\left(\frac{\delta H}{\delta z}\right) dz = \rho . \frac{dz}{G} \left(\frac{\delta M}{\delta \theta}\right)$$

which can be written in finite difference notation

$$\Delta H = -\rho . \frac{\Delta z}{G} . \frac{\Delta M}{\Delta \theta} \qquad \ldots\ldots\ldots 5.2$$

5.2.1.2. Heat transfer equation

Heat transferred between air and seed	=	Change in heat of seed	+	Enthalpy in evaporated moisture	-	Enthalpy of moisture prior to evaporation

$$hS \, \Delta z \left[\left(T_a + \tfrac{1}{2}\Delta T_a\right) - \left(T_g + \tfrac{1}{2}\Delta T_g\right)\right] \Delta \theta$$

$$= \rho . \Delta z . \Delta T_g \, (Cpg + Cpl . M) + \rho . \Delta z (-\Delta M)(Lg + Cpw . T_a - Cpl . T_g)$$

$$2 (T_a - T_g) + \Delta T_a - \Delta T_g$$

$$= \rho . \frac{2}{hS} \frac{\Delta T_g}{\Delta \theta} (Cpg + Cpl . M) - \rho \frac{2}{hS} . \frac{\Delta M}{\Delta \theta} (Lg + Cpw . T_a - Cpl . T_g)$$

Let $A = 2 (T_a - T_g)$ $\qquad B = (Cpg + Cpl . M)$

$Y = (Lg + Cpw . T_a - Cpl . T_g)$

$$\Delta T_a = -A + \Delta T_g \left(1 + \rho . \frac{2}{hS} . \frac{B}{\Delta \theta}\right) - \rho . \frac{2}{hS} . \frac{\Delta M}{\Delta \theta} . Y \qquad \ldots\ldots 5.3$$

5.2.1.3. Heat balance equation

Change in enthalpy of air = Change in enthalpy of seed

(a) the change in the air enthalpy is given by

$$G.\Delta\theta\left[(Cpa.T_a + Cpw.H.T_a + La.H) - (Cpa\,(T_a + \Delta Ta) + Cpw\,(H + \Delta H)\,(T_a + \Delta T_a) + La\,(H + \Delta H))\right]$$

Reducing and substituting for ΔH from equation 5.2

$$G\,\Delta\theta\left[-\Delta T_a\left(Cpa + Cpw\left(H - \rho.\frac{\Delta z}{G}.\frac{\Delta M}{\Delta\theta}\right)\right) + \rho.\frac{\Delta z}{G}.\frac{\Delta M}{\Delta\theta}\left(Cpw.T_a + La\right)\right]$$

(b) the change in the enthalpy of the seed is given by

$$\rho\Delta z.T_g\,(Cpg + Cpl.M) - \rho.\Delta z\left((T_g + \Delta T_g)\,(Cpg + Cpl\,(M + \Delta M))\right)$$

which reduces to

$$-\rho.\Delta z.\Delta T_g\,(Cpg + Cpl\,(M + \Delta M)) - \rho.\Delta z.\Delta M.Cpl.T_g$$

Equating both sides and dividing through by $G.\Delta\theta$ and letting

$$E = (Cpa + Cpw\,(H - \rho\frac{\Delta z}{G}.\frac{\Delta M}{\Delta\theta}))$$

$$\Delta T_a = -\frac{\rho.\Delta z}{G.E}.\frac{\Delta T_g}{\Delta\theta}.(B + Cpl.\Delta M) + \frac{\rho.\Delta z}{G.E}.\frac{\Delta M}{\Delta\theta}\,(Cpw.T_a + La - Cpl.T_g)$$

Let $F = (Cpw.T_a + La - Cpl.T)$

$$\Delta T = -\frac{\rho.\Delta z}{G.E\,\Delta\theta}\,(\Delta T_g\,(B + Cpl\Delta M) - \Delta M.F) \qquad \ldots\ldots\ldots\ 5.4$$

Combining equation 5.3 with 5.4

$$-A + \Delta T_g\left(1 + \frac{\rho.2}{hS}.\frac{B}{\Delta\theta}\right) - \frac{\rho.2}{hS}.\frac{\Delta M}{\Delta\theta}.Y = -\frac{\rho.\Delta z}{G.E\Delta\theta}\left(\Delta T_g\left(B + Cpl\Delta M\right) - \Delta M.F\right)$$

gives

$$\Delta T_g = \frac{A + \frac{\rho.\Delta M}{\Delta\theta}\left[\frac{2}{hS}.Y + \frac{\Delta z}{G.E}.F\right]}{1 + \frac{\rho}{\Delta\theta}\left[\frac{2}{hS}.B + \frac{\Delta z}{G.E}\left(B + Cpl.\Delta M\right)\right]} \qquad \ldots\ldots\ldots\ 5.5$$

5.2.1.4 Drying Rate

The expression of the differential moisture loss ΔM as a function of the other three factors Ta, Tg and H is based on the relationships developed in section 3. The simplest of these, equation 3.1. was used by Boyce[16,17] and Henderson and Henderson[47] in its simple differential form.

$$\frac{M - Me}{M_o - M_e} = e^{-k\theta} \quad \ldots\ldots\ldots\ldots 3.1$$

becomes $\Delta M = -k\,(M - M_e)\Delta\theta$ 5.6

Menzies[66] modified this equation by adjusting M by the half-increment $\frac{\Delta M}{2}$ to compensate for the change in M during the time interval.

Equation 5.6 then becomes

$$\Delta M = \frac{-k\,(M - M_e)\Delta\theta}{(1 + \frac{1}{2}\,k.\Delta\theta)} \quad \ldots\ldots\ldots\ldots 5.7$$

This is a very small adjustment provided the value of $(k.\Delta\theta)$ remains below .01. (Table 5.1). Above this level ΔM becomes sensitive to $\Delta\theta$

Table 5.1

Effect on ΔM of modifying equation 5.6 to form 5.7

$k.\Delta\theta$	$(k\Delta\theta/1+\frac{1}{2}\,k\Delta\theta)$	% reduction in ΔM
.001	.0009995	99.95
.01	.00995	99.5
.1	.09524	95.2
.2	.1818	90.9
.5	.400	80.0
1.0	.6667	66.7
2.0	1.0	50

In section 3 it was shown that the exponential series equations gave a better description of the drying curve than equation 3.1.

Differentiation of equations 3.38 or 3.37 give the general form

$$\Delta M = -k\,(M - Me)\,\frac{E_2}{E_1}\,.\,\Delta\theta \qquad \ldots\ldots\ldots\ldots\ldots\ldots\ldots\ldots 5.8$$

where $E_1 = \sum_{j=1}^{\alpha} \frac{1}{2} \exp(-n^2.k\theta)$

and $E_2 = \sum_{j=1}^{\alpha} \exp(-n^2.k\theta)$

where n = j for the exponential series for the sphere

and n = (2j-1) for the exponential series for the plate

Both E_2 and E_1 are dependent on the total drying time θ. This has the effect of increasing the estimates of ΔM during the first few iterations while $k.\theta$ remains small. (Table 5.2)

Table 5.2

Values of E_2, E_1 and E_2/E_1 as affected by $k.\theta$

$k\theta$	Series equation					
	Plate			Sphere		
	E_1	E_2	E_2/E_1	E_1	E_2	E_2/E_1
0.0002	1.221	31.332	25.66	1.620	62.00	38.27
0.0004	1.216	22.155	18.22	1.610	43.81	27.22
0.0006	1.212	18.090	14.93	1.602	35.68	22.27
0.0008	1.209	15.666	12.96	1.595	30.83	19.33
0.0010	1.206	14.012	11.62	1.589	27.52	17.32
0.0050	1.171	6.266	5.35	1.522	12.03	7.91
0.01	1.145	4.431	3.87	1.473	8.36	5.68
0.02	1.108	3.133	2.82	1.404	5.77	4.11
0.03	1.080	2.558	2.37	1.353	4.62	3.41
0.04	1.056	2.216	2.10	1.310	3.93	3.01
0.10	0.953	1.401	1.40	1.134	2.30	2.03
0.15	0.891	1.043	1.17	1.034	1.79	1.73
0.20	0.837	0.991	1.18	0.952	1.482	1.56
0.60	0.554	0.549	1.01	0.572	0.644	1.13
1.00	0.368	0.368	1.00	0.3725	0.386	1.04

If the correction of equation 5.7 is applied to equation 5.8 it becomes

$$\Delta M = \frac{-k(M - Me) \frac{E_2}{E_1} . \Delta\theta}{(1 + \frac{1}{2} k \frac{E_2}{E_1} . \Delta\theta)} \qquad \ldots\ldots\ldots 5.9$$

The sensitivity of ΔM to the size of $\Delta\theta$ at low values of $k\theta$ is obviously greater than with equation 5.7 although the increase in the numerator caused by the multiplier E_2/E_1 will still result in a larger value of ΔM.

From Section 3 values of k can be represented by the equation

$$k = a \exp (bT + cMo + dH) \qquad \ldots\ldots\ldots\ldots 3.44$$

or alternatively by $k = a \exp (b/(T + 273))$ $\ldots\ldots\ldots$ 3.52

and Me by the equation

$$Me = a - b.\ln(T) - c.\ln(1 - rh) \qquad \ldots\ldots\ldots 3.42$$

5.2.1.5. Method of solution

Ideally the equations 5.2, 5.4, 5.5. together with any one of the equations 5.6 to 5.9 should be solved simultaneously but this is extremely difficult if not impossible. The problem is simplified if it is assumed that ΔM can be evaluated at the inlet air condition T_a rather than at the average value $(T_a + \Delta T_a/2)$ for the depth increment, Δz. The estimated value of ΔM can then be used in equation 5.5 to evaluate ΔT_g and thence by substitution into equation 5.3, evaluate ΔT_a. The change in air humidity, ΔH is then given by equation 5.2. For the complete deep bed divided into a large number of thin layers of thickness Δz, this process is repeated layer by layer for a small time interval $\Delta\theta$. The quantity of air flowing in time $\Delta\theta$ is assumed to pass instantaneously through the whole bed and the air exhausting from the n/th layer is used as input to the $(n + 1)^{th}$ layer. Bailey [3] has shown that this is a justifiable assumption.

Clearly this is a simple integration procedure and only works well if the time and depth intervals produce small incremental changes in moisture and temperature. But for economy of computing time the largest intervals compatible with obtaining reliable results have to be used. The size of the intervals is largely determined by the difference between the grain and air temperatures. The assumption that ΔM can be evaluated at the air temperature, Ta, is a reasonable one since the thin-layer data were correlated with air temperature rather than grain temperature. However, in the thin layer tests, it was assumed that the thinness of the layer and relatively high air velocity would cause the seed to approach air temperature very rapidly. In the deep bed integration, the air velocity and hence heat transfer may be much lower and the incremental depth

several times thicker than was used in the thin-layer tests. Thus if Ta is much greater than Tg an over-estimate of ΔM will be made and may result in the calculation of unrealistic changes in Ta and Tg. For a static bed these initial fluctuations are not too serious since they will tend to be balanced by an opposite effect in adjacent layers and subsequent time iterations and will tend to disappear as Tg approaches close to Ta. Boyce [18] experimented with evaluating ΔM at both the air and grain temperatures and found that it made very little overall difference. A similar conclusion was also reached by Bailey [3] for the potentially more sensitive case of the concurrent flow drier where fresh cold grain is mixed with hot air in each time iteration. Thompson et al. [118] introduced a sensible compromise of evaluating ΔM at an equilibrium temperature between the grain and air calculated from an initial heat balance assuming no mass transfer.

It seems possible that the overestimation of ΔM which may result from the use of Ta during the first two or three iterations in the first two or three layers is offset by an underestimation of ΔM at small θ in those simulations using the simple differential drying rate equations 5.6 or 5.7.

5.2.1.6 Condensation and re-evaporation

Using the differential drying equations, ΔM will normally be negative unless $M_e > M$ when it will become positive and moisture will be condensed back into the seed. This assumes that the rate of rewetting (and of subsequent re-evaporation) will be the same as the rate of drying which is not necessarily true. Flood et al [34] used a rewetting equation in a maize drying simulation. However the speed of rewetting is only likely to be of importance when the term $(M-M_e)$ is a large negative value. This is not likely to be the case for normal drying since $(M-M_e)$ will tend to become negative

as a result of small and gradual changes in inlet condition. It could be more important for the cooling of hot dry grain. The rate of re-evaporation is likely to be underestimated by the normal drying rate equation.

This method of solution is only satisfactory while the moisture added to the air does not saturate it. Once this begins to occur the moisture change is no longer dependent on diffusion but becomes dependent on the psychrometric balance between the air and the now freely available water. An iterative procedure was developed to find this balance.

The principle is illustrated in Fig.5.2 which represents a small section of a psychrometric chart. Initially the air in the layer is at temperature, T_o and humidity, H_1 represented by point 1 on the chart. Under these conditions, the predicted value of moisture loss may be ΔM_o but the use of this value in the heat and mass transfer equations predicts a temperature change from T_o to T_1 and moves the state point to 2. Here the relative humidity would be in excess of saturation. ΔM_o may now be reduced to ΔM_1 the moisture loss which apparently would give 100% r.h. at T_1 (state point 3). But when substituted in the heat and mass transfer equations, ΔM_1 produces a new temperature T_2 and a corresponding r.h. less than saturation, represented by state point 4. By similar reasoning T_2 can now be used to obtain a new estimate ΔM_2 (state point 5) which will predict a temperature T_3, and new state point 6. By this path the value of ΔM which gives a temperature change predicting 100% saturation may be converged upon.

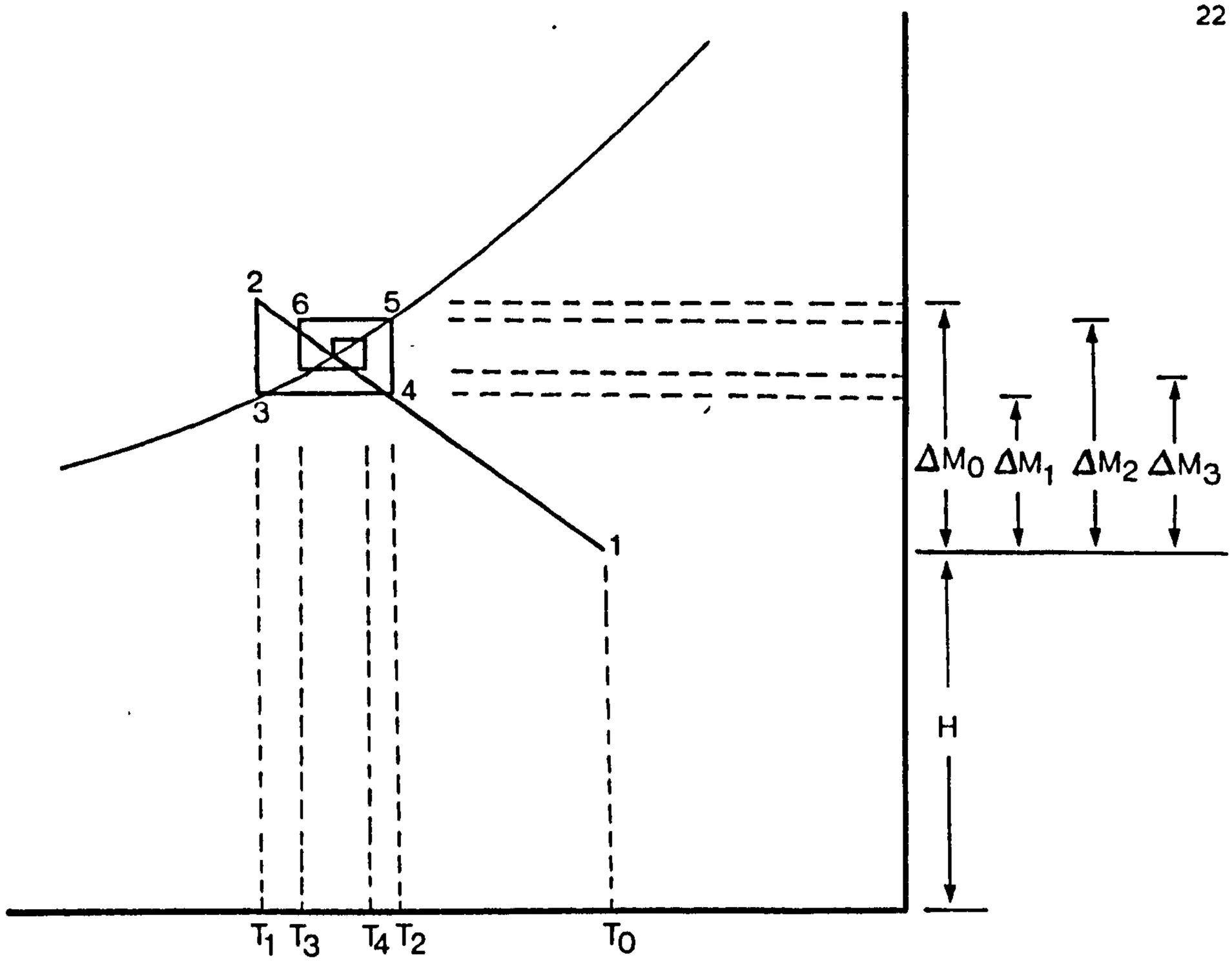

Fig. 5.2 Principle of adjusting ΔM to contain exhaust r.h. within the the feasible range(where the symbol ΔM represents $\Delta M\left[\frac{\rho \Delta z}{G \Delta \theta}\right]$).

Fig.5.2 could have been drawn such that the solution diverged. To ensure that the computer solution converged with a minimum number of iterations the required value of ΔM was found by using an interpolating polynomial to find the zero of the function $y = f(x)$ where y = (maximum permissible rh - predicted exhaust rh) and x = moisture loss, ΔM.[120] Given the 2 estimates of the variable x given by ΔM_0 and ΔM_1 (state points 2 and 3 of Fig. 5.2) successive estimates are calculated in the following way. The x and y values are re-arranged and re-indexed in ascending order of y and, letting $x_{ii} = x_i$ for i = 1,2,3 ..... n, a triangular matrix (Table 5.3) of values x_{ij} can be calculated according to the formula

$$x_{ij} = \left[(x_{j-1,\ j-1})\ (y_i) - (x_{i,j-1})\ (y_i - 1)\right] / (y_i - y_{i-1}) \qquad \ldots\ldots\ldots\ldots\ 5.10$$

for j = 2, 3 ..... n

and i = j, j + 1, ... n

Table 5.3

Triangular matrix of x_{ii} derived from values of x and y arranged in ascending order of y.

y	x					
y_1	x_1	x_{11}				
y_2	x_2	x_{21}	x_{22}			
y_3	x_3	x_{31}	x_{32}	x_{33}		
y_i	x_i	x_{i1}	x_{i2}	x_{i3} - - -	x_{ii}	
y_n	x_n	x_{n1}	x_{n2}	x_{n3} - - -	x_{ni} - - -	x_{nn}

x_{nn} is the new estimate of x and is accepted if $y = f(x_{nn}) < 0.1\%$ r.h.

In the first version of this routine a maximum permissible relative humidity of 98% was used. Some precedent for setting a limit at less than 100% saturation had been established by previous models in which condensation had not been attempted[17,88,113]. However it was also found that if a value much in excess of 98% was chosen it would cause the exhaust r.h. to oscillate from layer to layer. The reason for this oscillation was the steepness of the equilibrium moisture content curve in the region of 100% saturation. If the condensation procedure is used to ensure an exhaust r.h. close to 100%, then when this air is used as input to the next layer it will predict a very high value of the asymptotic moisture content, M_e and hence a positive value of ΔM. Moisture is now condensed back into the 2nd layer and the air exhausts from it at well below saturation. As the input to the 3rd layer it now overestimates the drying rate and the condensation procedure has to be entered to reduce the predicted r.h. back within the feasible range.

And so the process oscillates up through the layers. This oscillation can be prevented or controlled if some limit is set to the maximum relative humidity at which the asymptotic moisture content is evaluated. Later versions of the programme allowed the maximum permissible exhaust relative humidity and the maximum relative humidity for the evaluation of M_e to be set independently.

It should be noted that below approximately 98% the exponential form of the equilibrium moisture curve is important in ensuring a smooth transition to condensation conditions. Both Bailey [3] and Spencer [114] have found it necessary to introduce empirical modifications to their equilibrium relative humidity relationships to achieve the same end.

5.2.1.7. Heat transfer coefficient

The heat transfer coefficient, h, is normally defined as the quantity of heat transferred per unit of time, area and temperature difference between the gas stream and the interface with the solid surface. However, it is a complex function of the properties of the gas stream and experimental data is normally correlated by means of the j-factor developed by Colburn [29].

The dimensionless group

$$j_h = \frac{h}{Cpa.G}\left(\frac{Cpa.\mu}{k}\right)^{\frac{2}{3}} \qquad \ldots\ldots\ldots 5.11$$

is plotted against the modified Reynold's number for a granular bed, $\frac{DpG}{\mu}$

where j_h = Colburn heat transfer factor, ratio

h = heat transfer coefficient, kJ/min m^2 K

μ = dynamic viscosity of air, kg/m min.

k = thermal conductivity of air, kW/m K

D_p = average particle diameter, m.

Heat transfer data of this kind was reviewed by Barker[8] and from that review, the work of Gamson, Thodos and Hougen [36] was selected as being most relevant to this present study.

Spherical and cylindrical catalyst carrier pellets of diameters from 2.29 to 18.8 mm and cylindrical heights from 4.78 to 16.9 mm were investigated under conditions of constant drying rate at temperatures from 26.7 to 71.1°C at mass velocities of air from 0.54 to 3.12 kg/s m^2. The following equations correlated the results

(i) For Re > 350

$$h = 1.064\ Cpa.G \left(\frac{Dp\,G}{\mu}\right)^{-0.41} \left(\frac{Cpa\ \mu}{k}\right)^{-\frac{2}{3}} \quad \ldots\ldots\ldots 5.12$$

which if the Prandtl No. $\frac{Cpa\ \mu}{k}$ is taken as constant at 0.7 for air, simplifies to

$$h = 1.064\ Cpa \left(\frac{\mu}{Dp}\right)^{0.41} G^{0.59} \quad \ldots\ldots\ldots\ldots 5.13$$

(ii) For Re < 40

$$h = 18.1\ Cpa\ G \left(\frac{DpG}{\mu}\right)^{-1} \left(\frac{Cpa\ \mu}{k}\right)^{-\frac{2}{3}} \quad \ldots\ldots\ldots\ldots 5.14$$

which simplifies to

$$\frac{h\,Dp}{k} = 16.3 \quad \ldots\ldots\ldots\ldots 5.15$$

A disadvantage of the heat transfer coefficient h, as defined by these equations is that its use depends upon a knowledge of the surface area available for the heat transfer and this is not readily measured or estimated for particles of irregular shape. A choice of specific surface areas was provided by the work described in Section 2 of this thesis. The smallest estimates were 3587 and 2525 m^2/m^3 for S.23 and Sabrina respectively. They were calculated from respective volume-surface diameters of 1.181 and 1.584 mm, which had been derived from sieving results. They represent the surface area of the particle in relation to its own volume. The

surface-area within an incremental layer of seeds must be related to the total volume they occupy i.e. the area must be adjusted for void space which in ryegrass is of the order of 75%.

For comparative purposes these figures can be used by substitutioninto equation 5.13 to obtain simplified expression for hS, the product of h and S_v, termed the volumetric heat transfer coefficient. At 30°C the expressions are:-

For S.23 $hS = 1113.8\ G^{0.59}$ 5.16

For Sabrina $hS = 741.6\ G^{0.59}$ 5.17

Using the/data of Bakker-Arkema et al [7] and assuming a specific surface porosity of 51% *, the equivalent expression for barley is

$$hS = 552.7\ G^{0.59} \quad \text{..... 5.18}$$

These simplified expressions have been developed to allow comparison with an alternative description of the heat transfer coefficient proposed by Boyce [18]. He avoided the difficulty of measuring specific surface area by determining the value of the volumetric coefficient hS directly. The integral of the differential heat transfer in a layer in which no mass transfer occurs has been shown to be [18,94]

$$hS = -\frac{Cpg\ \rho}{\theta} \ln\left(\frac{T_a - T_g}{T_a - T_{go}}\right) \quad \text{..... 5.19}$$

Boyce used this relation to obtain for barley a series of values of hS at a series of air flows, G. The values were then fitted by least squares to give the equation

$$hS = 4286.5 \left(G\ \frac{(T_a + 273)}{P_{at}}\right)^{0.6011} \text{ kJ/min K m}^3 \quad \text{..... 5.20}$$

For $T_a = 30°C$ this simplifies to

$$hS = 130.3\ G^{0.6011} \quad \text{..... 5.21}$$

---

* Bakker-Arkema appears to use specific surface area uncorrected for porosity in his heat transfer equation.

The dependence of this expression on G (and on T_a) is very similar to that of equation 5.13 but the size of the constant is only $\frac{1}{4}$ of that of equation 5.18. If the uncorrected specific surface area had been used in the calculation of equation 5.18 the comparison would have been worse. The increase in hS for barley given by equation 5.18 compared with 5.21 is greater than the increase of either ryegrass equation 5.16 or 5.17 over equation 5.18 although these increases would clearly be greater if the larger estimates of S_v obtained in Section 2 were used.

In 1972 an attempt was made to use the method of Boyce to determine hS for ryegrass seeds. The procedure was as follows. From a bulk of seed which had previously been brought into approximate moisture equilibrium with air at 60°C and which was kept in a sealed container, a 100 g sample was taken and spread in the drier pan. It was placed on the drier and allowed to dry for a further 30 minutes at 60°C or until there was no further change in weight. The pan was quickly removed and placed together with a thermometer and without disturbing the seed in a large plastic bag which was sealed with adhesive tape. After the seed had cooled to room temperature once more the pan was quickly removed from the bag and replaced on the drier. After 5 minutes, timed by stop-watch, the seed was rapidly tipped into an insulated container. This transfer was estimated to take 1 second. The temperature in the container was monitored by means of a thermocouple connected to a Honeywell Brown Potentiometric recorder and the maximum temperature reached was taken as the final grain temperature. The final moisture content of the seed was then determined.

It soon became apparent that the temperature of the seed was approaching a maximum value in less than 5 minutes and a series of runs was carried out at each of 2 air flows at various intervals from $2\frac{1}{2}$ seconds to $2\frac{1}{2}$ minutes. This series demonstrated that

the final measured temperature could be seriously affected by the speed and efficiency of the physical transfer of the seed from the drying pan to the insulated container. Further the temperature-time curves plotted with the best of this data indicated an asymptotic temperature of 54°C rather than the hot-air temperature of 60°C. This implied a relatively large heat loss in the transfer from pan to insulated container even allowing for the possibility that the air entering the pan was slightly cooler than at the point its temperature was sensed and controlled. Finally, and this may have been in large part an effect of the deficiencies already described, plots of θ against $\ln\left(\frac{T_a - T_{go}}{T_a - T_g}\right)$ derived from the smoothed temperature time curves were not straight lines and this brings into question the validity of equation 5.19. At this point it was concluded that the deficiencies of the method were such that any further work should be delayed until significant improvements could be made or a new method developed. However the work had confirmed that the rate of heat transfer was a function of airflow and had indicated that the value of hS for ryegrass seed was probably several times that for barley grain predicted by the Boyce equation 5.20.

The drying model was developed using the Boyce relation, but later versions allowed this equation to be modified by a multiplier and provided for the alternative use of the Gamson, Thodos and Hougen equation 5.13.

5.2.2. Solution of the equation of the wet-bulb line

Under adiabatic drying conditions, the maximum drying rate which might be achieved from a bed in which a complete drying zone is established would be that resulting from adiabatic saturation of the air. This value is used as a yardstick by which to judge the drying

rate predicted by the model. It is found by solving the equation of the wet-bulb line given the temperature of the dry bulb and the absolute or relative humidity.

From Brooker [21] and converting to SI units the equation of the wet-bulb line is

$$P_{swb} - P_v = \left[-1.007\ (P_{swb} - 1013.5)\ (T_{db} - T_{wb})\right] / 0.62194 * L \quad \ldots\ldots\ldots 5.22$$

where

P_{swb} = saturation vapour pressure at T_{wb}, mbar (= xN/m^2)

P_v = vapour pressure at T_{db}, mbar.

L = latent heat of vapourisation of water at T_{wb}

= $2502.535 - 2.38576\ (T_{wb} - 273)$ kJ/kg/C*

T_{db} = temperature of the dry bulb, ^oK

T_{wb} = temperature of the wet bulb, ^oK

The expression for saturation vapour pressure, P_s at temperature T was taken from the I.H.V.E. guide.[56]

$$P_s = \exp\left(a + bT + \frac{c}{T} + d \ln T\right) \quad \ldots\ldots\ldots 5.23$$

where $a = 72.73974$

$b = 0.0057113$

$c = -7235.4261$

$d = -8.2$

Given ambient humidity H, then from

$$H = 0.622 \left(\frac{P_v}{P_{at} - P_v} \right) \quad \ldots\ldots\ldots 5.24$$

$$P_v = P_{at} \cdot H / (0.622 + H) \quad \ldots\ldots\ldots 5.25$$

---

* Obtained by direct conversion of the relationship given by Brooker [21] in British units.

Given relative humidity, rh as a decimal then $P_v = rh \times P_{sdb}$

Substituting for latent heat in 5.22 and simplifying.

$$P_{swb} = P_v - \left[\frac{P_{swb} (T_{db} - T_{wb}) - 1013.5 (T_{db} - T_{wb})}{1947.866 - 1.473485\ T_{wb}} \right] \quad \ldots\ldots 5.26$$

An approximate solution to equation 5.26 can be obtained by Newton's Method.

Let $p = 1947.866$, $r = 1.473485$, $s = 1013.5$

$q = 1 + r = 2.473485$

Then if $f(T_{wb}) = 0$

$$f(T_{wb}) = P_{swb} (p - q\,T_{wb} + T_{db}) + T_{wb} (rP_v + s) - pP_v - sT_{db} \quad \ldots\ldots 5.27$$

$$\therefore f'(T_{wb}) = P_{swb} \left(- q + (T_{db} - qT_{wb} + p)\left(b - \frac{c}{T_{wb}^2} + \frac{d}{T_{wb}}\right)\right) + rP_v + s \quad \ldots\ldots 5.28$$

and for Newton's method, the adjustment Δ is given by

$$\Delta = \frac{f(T_{wb})}{f'(T_{wb})} \quad \ldots\ldots 5.29$$

Using T_{db} as the initial estimate of T_{wb}, this procedure converges to within 0.005 degrees very rapidly.

Substitution of T_{wb} back into equation 5.23 gives the saturation vapour pressure and a further substitution back into equation 5.24 gives the absolute humidity at saturation.

5.2.3. Other properties

5.2.3.1. Specific heat capacity: The following constants are written into the programme:-

$$Cpa = 1.005 \quad kJ/kg\ K$$

$$Cpw = 1.88 \quad kJ/kg\ K$$

$$Cpl = 4.187 \quad kJ/kg\ K$$

The programme was developed on the assumption that the specific heat of the seed dry matter, Cpg, was the same as that of wheat[65], 1.298 kJ/kg K. Provision is now made for the value to be read in with the input data although the author recently discovered some data which confirmed that 1.298 is a reasonable value for ryegrass seed.

This data had been obtained in 1966 by R.B. Sharp[107] using S.24 ryegrass seed rewetted in the moisture range 16.3 to 99.5% m.c.d.b. The method of determination used was that of Sharp and Nash [106] modified to cope with larger volumes of seed. The results are tabulated in Table 5.4. The specific heat of the dry matter, Cpg, in the final column was calculated from the measured

TABLE 5.4

Specific heats of S.24 ryegrass - unpublished data of R.B. Sharp [107]

C kJ/kg.K	M ratio d.b.	Cpg kJ/kg.K
1.611	0.1625	1.192
1.754	0.2037	1.258
1.757	0.2200	1.223
1.872	0.2604	1.269
1.961	0.3120	1.266
2.212	0.3887	1.443
2.378	0.4715	1.525
2.336	0.545	1.290
2.409	0.6380	1.274
2.483	0.7838	1.148
2.709	0.9952	1.237

value for the wet seed, C , from the equation.

$$C(1+M) = Cpg + Cpl\ M \qquad \ldots 5.30$$

where the specific heat of liquid water, Cpl was taken to be 4.187 kJ/kg.K. The mean of 1.284 has a standard error of 0.0327 and therefore the validity of the value of 1.298 is confirmed.

5.2.3.2. Latent heat: In the development of the heat and mass transfer equations the enthalpy of the air was approximated as the sum $Cpa\ T_a + H\ (CpwT_a + La)$. Treybal[123] shows that this is a valid expression if La is the latent heat of water at the reference temperature, $0^{\circ}C$ in this case. A value of 2500.8 kJ/kg was assumed and written into the programme. The dependence of the latent heat of the moisture held within the seed upon the concentration of that moisture was described by the equation of Gallaher[35]

$$Lg = La\ (1 + 23.0 \exp(-40M)) \qquad \ldots 5.31$$

5.2.4. The computer programme

A simplified flow chart of the computer programme is given in Fig 5.3 and specimen output. A FORTRAN listing is given in Appendix 5. Much of the action of the programme has been indicated in the previous paragraphs and will not be repeated. Additional features are summarised below:-

(i) Initial seed moisture and temperature profiles could be input as depth-dependent arrays and were interpolated linearly to initialise the layers.

(ii) Inlet air temperature and humidity could be input as time-dependent arrays and interpolated linearly to initialise inlet air conditions at the start of each time iteration.

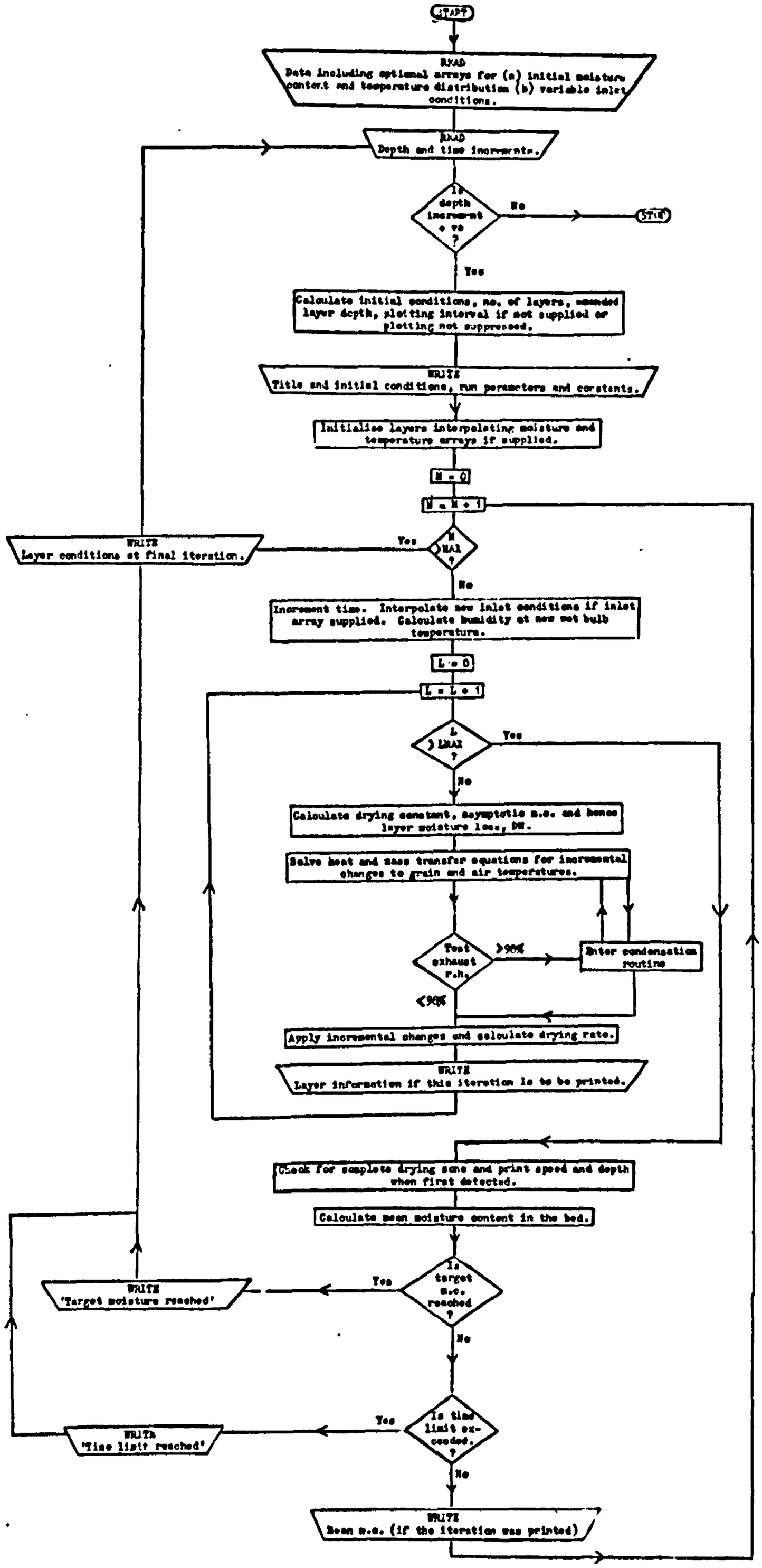

Fig. 5.3 Simplified flow chart of parallel-flow deep bed drying programme.

(iii) Bed depth and depth increments were of type real. The programme automatically adjusted the supplied depth increment to subdivide the total depth into an integer number of layers.

(iv) The formation of a complete drying zone was recognised when the drying rate in a layer fell below 0.00001 kg/kg of air and was succeeded in the same time iteration by a layer in which the maximum permissible relative humidity was exceeded. The depth, speed and time when the zone was first formed was printed.

(v) An output file of layer temperatures and bed mean moisture content could be produced for input to either of the plotting programmes SIMPLT or RADPLT. The printing interval for the plotting file was independent of that for the main output file.

(vi) A simulation was normally terminated by the mean bed moisture content reaching a target value but could also be terminated by exceeding either a time limit or a maximum number of time iterations. Both of these limits were declared on input. The programme terminated when a negative depth increment was read from the input data file.

(v) For simulating radial-flow drying, the airflow per unit area of the inner wall was reduced through each successive annular layer in proportion to R_1/R_L where R_1 and R_L are the radii at the bin wall and at the centre of the layer respectively.

5.3. SIMULATION OF EXPERIMENTAL RESULTS

5.3.1. Preliminary tests

The experimental results were used as specimen input data during the development of the model. In the course of this various parameters were adjusted to determine their effect on the final solution. These tests were not entirely systematic because at the same time other constants were being adjusted as the analyses of the thin layer results were completed and minor errors in the programme corrected as they were found.

5.3.1.1. Sensitivity to increment size: Irrespective of whether or not the model was a reasonable description of the drying process, it was necessary first of all to establish the ranges of values of the increments $\Delta\theta$ and Δz which would give convergence to the same solution. Clearly the smaller the intervals chosen the greater the likely "accuracy" but the greater the computing time and quantity of redundant information calculated. Clearly for practical purposes the intervals chosen need to be in reasonable proportion to the depth of bed and probable total drying time.

It was found that the model was stable over a wide range of depth and time increments. The results of the most systematic tests are presented in Table 5.5. Time increments from 1 to 60 minutes and depth increments from 0.005 to 0.24 metres had only marginal effects on predicted total drying times either for the low temperature Run 9 or the high temperature Run 7. At the constant depth increment of 0.013 m, the differences in drying times for Run 9 given by increments from 1 to 60 min. reflect the inevitable rounding caused by the use of large time increments.

TABLE 5.5.

Effect of depth and time increments on predicted drying time, minutes, for Run 7 (Ta = 55.4°C) and Run 9 (Ta = 26.0°C).

	Δθ min.	Δz, m.				
		0.005	0.013	0.025	0.12	0.24
Run 7	5.0	-	900	-	-	-
	15.0	915	900	900	-	-
	30.0	-	900	-	-	-
Run 9	1.0	-	4186	-	-	-
	5.0	4195	4185	4175	-	-
	15.0	-	4200	-	-	-
	30.0	-	4170	-	-	-
	60.0	4200	4140	-	-	-
Run 9*	1.0	-	-	-	4020	-
	5.0	-	4115	4105	4020	4020
	15.0	-	-	-	4020	-

* Differences in time between this and the previous series for Run 9 are due to a change in the constants used to define the drying constant, k.

Increasing Δz at constant Δθ caused only slight reductions in predicted total time, even up to 0.24 m in Run 9. In practice a Δz of 0.24 m is too large because it fails to give sufficient information about the moisture profile. This is illustrated by Figure 5.4. which compares the final moisture profiles predicted using depth increments of 0.0127 and 0.24 m and the experimental observations. The smaller increment divided the bed into 75 layers from which it was possible to plot a smooth curve. The larger increment divided the bed into only 4 layers and was clearly inadequate to fully describe the moisture profile.

Thus the conclusion was that increments, chosen to be in reasonable proportion to the total drying time and bed depth, were unlikely to influence the predicted results to a significant extent. In the present work, increments of 5 minutes and 0.025 m were used in the majority of cases.

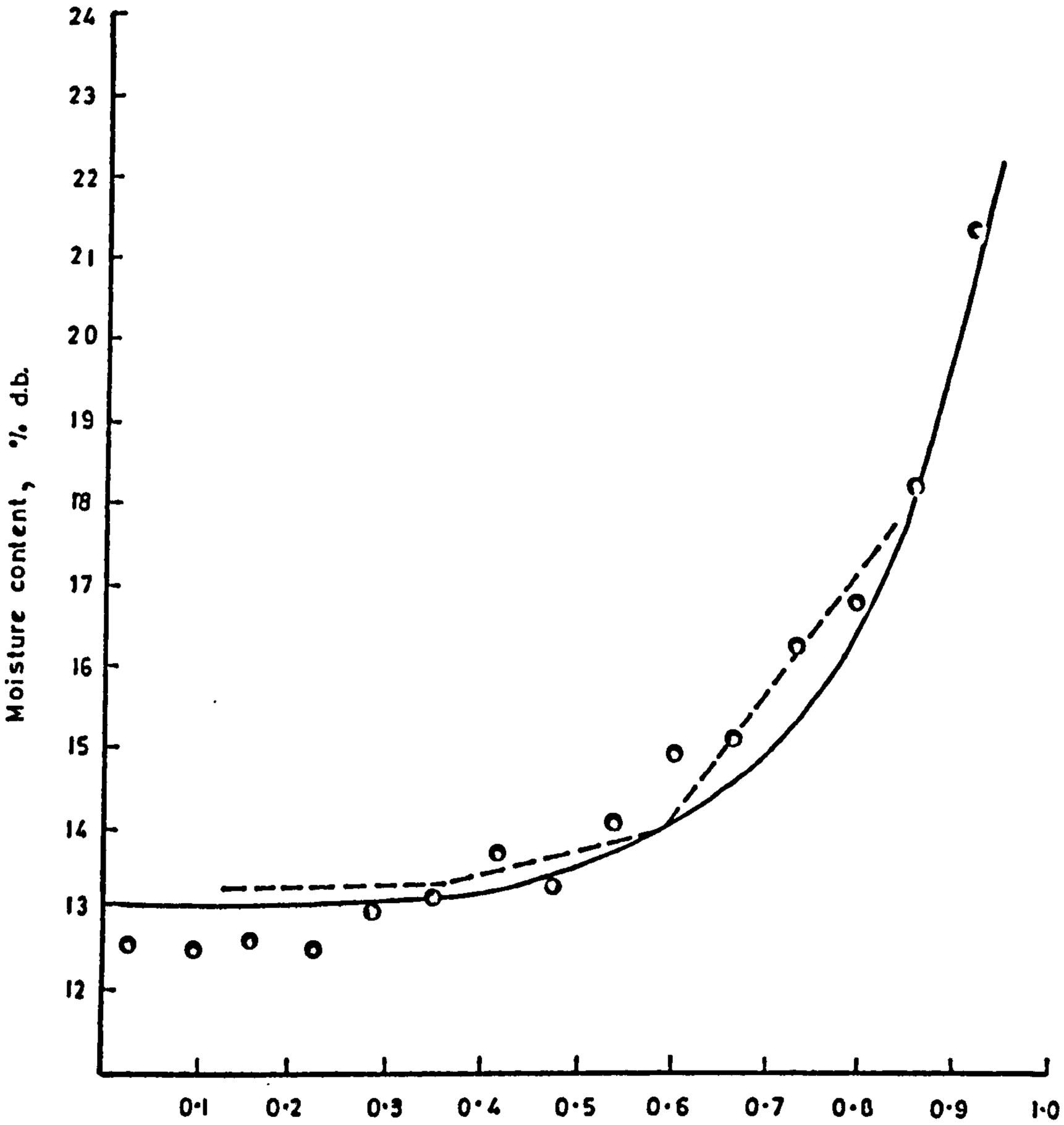

Fig. 5.4 Effect of depth increment on predicted final moisture profile in Run 9.

o Experimental readings.

——— $\Delta z = 0.0127 = 75$ layers.

– – – – $\Delta z = 0.23812 = 4$ layers.

5.3.1.2. Sensitivity to heat transfer coefficient: The effect of varying the heat transfer coefficient, hS was investigated because there was some doubt as to the values which should be used (Section 5.2.7.1.). No firm conclusion had been reached about the specific surface area, S, to use in conjunction with the Gamson, Thodos and Hougen equation (Eqn. 5.13) and attempts to determine volumetric heat transfer coefficients by the method of Boyce had been inconclusive.

The effect of hS on model predictions was investigated by multiplying the value given by the Boyce equation (5.20) for barley by factors between 0.1 and 1000 for the high temperature (55.4°C) for Run 7. This effectively altered the heat transfer coefficient from 46 to 46 x 10^4 kJ/min K m^3.

The quantity most affected by this variation was the predicted seed temperature. In Figure 5.5. are plotted the temperature profiles through the bed at the end of drying given by hS x n, for n = 0.1 and 1000. When the heat transfer coefficient is small the seed temperature tends to stay several degrees below that of the air. In constrast when the ccefficient is large, the difference between the air and seed temperatures is small and in the opposite direction, i.e. the seed is warmer than the air. This reversal occurred at a value of hS just a little greater than that given by Boyce equation alone. In Figure 5.6. the seed and air temperatures within a single layer are plotted against hS x n for (a) the first layer in the first time iteration and (b) the last layer in the last time iteration. In both cases the pattern is similar but more pronounced in the starting iteration because of the much larger initial temperature difference and predicted moisture loss. Clearly hS x 0.1 predicts much too little heat transfer and the heat for evaporation is taken out of the seed (which cools to 4°C) with very little cooling of the air.

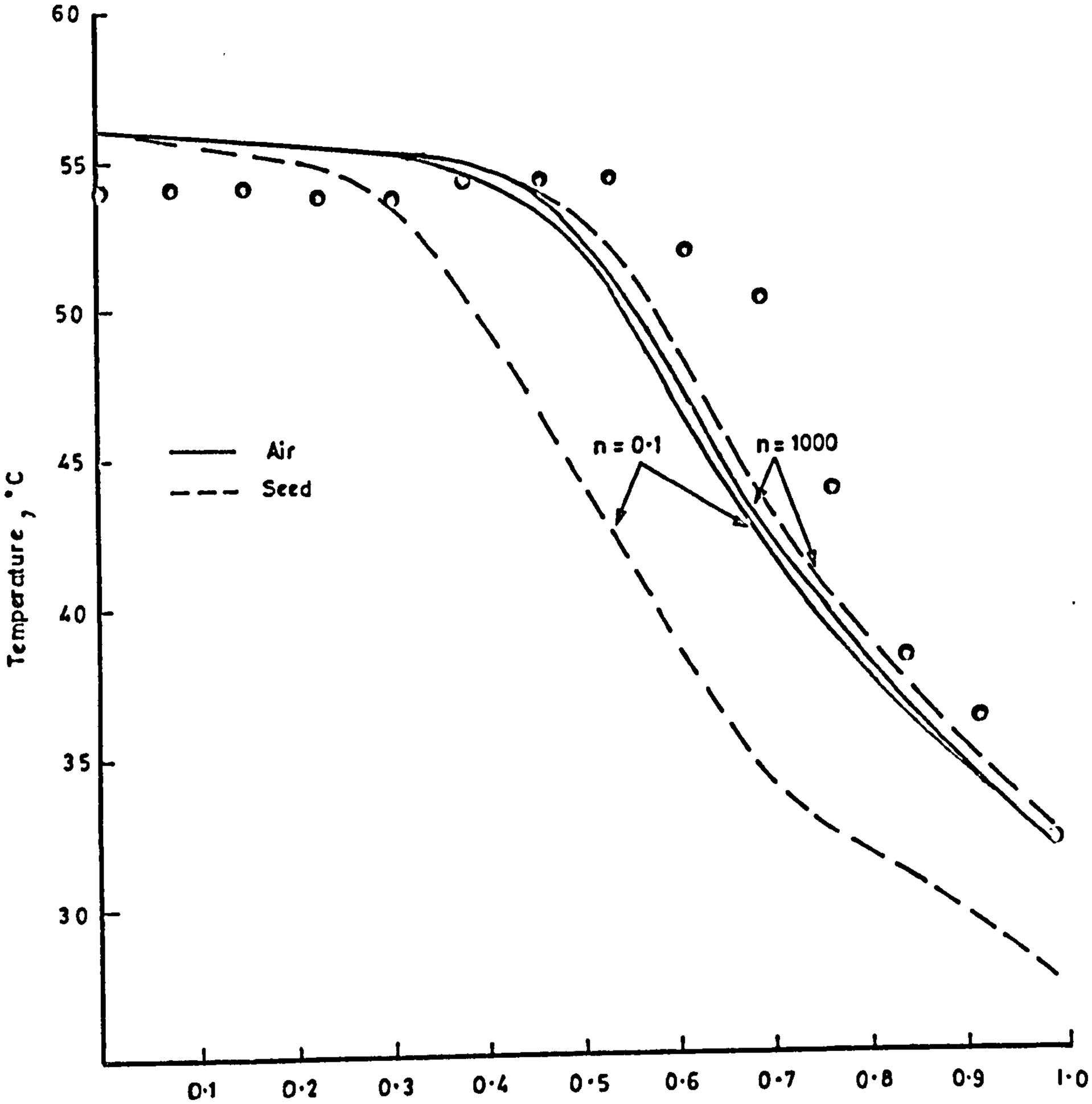

Fig. 5.5 Effect of heat transfer coefficient on final temperature profile predicted for Run 7. Experimental observations at real final time donated by o .

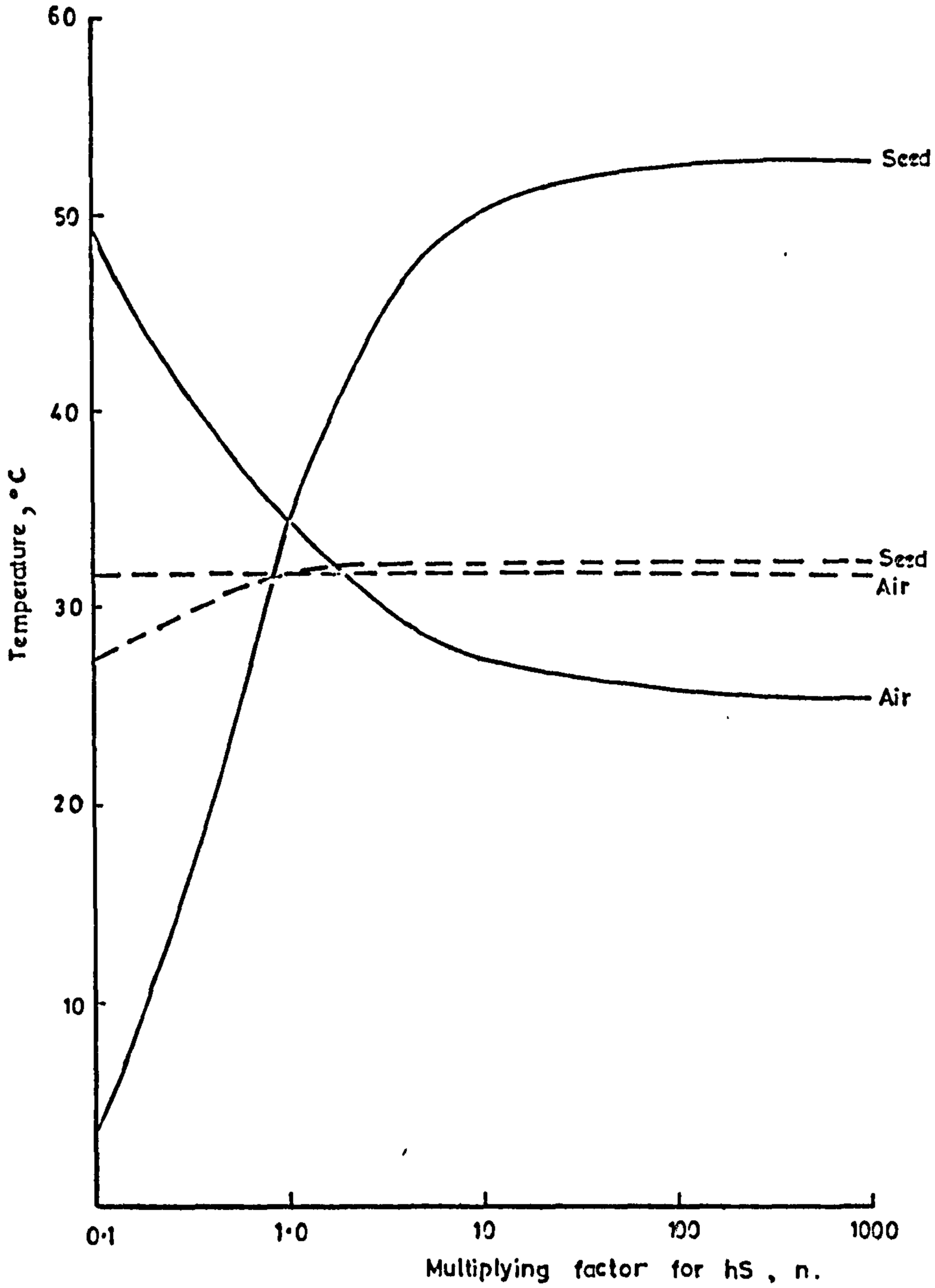

Fig. 5.6 Effect of heat transfer coefficient hS on temperatures in layer 1 at iteration 1 (———) and in the 39th layer of the last iteration(----).

This is an unrealistic situation. Above hS x 1 the opposite occurs; so much heat is transferred that the air is greatly cooled and the seed warmed close to the inlet air temperature. Increases in hS of x50 to x 1000 have very little effect on this pattern. It is interesting that inspite of these differences the total drying times and final moisture profiles are affected only slightly (Table 5.6.)

TABLE 5.6.

Effect of value of heat transfer coefficient on predicted drying time and final moisture profile in Run 7. (hS ≏ 460 kJ/min K m^3)

Multiplier for hS	Drying time		Final moisture content, % d.b.	
	Min	Iteraticns	Mean	Range
0.1	865	173	16.81	5.27 - 43.59
1.0	870	174	16.84	5.27 - 44.22
5.0	870	174	16.85	5.27 - 44.29
50	870	174	16.86	5.27 - 44.31
100	870	174	16.88	5.27 - 44.32
1000	875	175	16.75	5.27 - 44.18

This is probably because in the model the drying rate is calculated from, and, depends upon, the air temperature and this is much less affected by hS than is the seed temperature (Figure 5.5.). In real life the amount of moisture lost is determined simultareously with the heat transfer and the rate of heat transfer is almost certainly more important than the approximate method of solution used in the model allows it to be. This aspect clearly requires more detailed investigation.

Before this investigation of hS had been completed and when it was thought that hS for ryegrass seed would be of the order of 5 times that of cereals, work began on simulating all the experimental runs with hS x 5. In the light of the above results this was a reasonable choice.

5.3.2. Comparison of observed and predicted results

5.3.2.1. Input data

All 15 experimental runs were simulated using as much input data as was available for each. That is, if information, on the initial moisture and temperature profiles was available it was used and if variable input air conditions were available these were also used. In the case of Runs 2 and 3 it was found necessary to extend the drying period to include the cooling after drying.

The drying curve was assumed to be described by the diffusion equation for a plane sheet (equation 3.38) and the drying constant, k, was evaluated from equation 3.44 using the appropriate constants given in Table 3.7, page 85. The correction for initial moisture content, Mo, was applied before the constants were read into the programme so that the input values were as listed in Table 5.7.

TABLE 5.7.

Simulation of experimental runs. Constants used in equation 3.44 for evaluating the drying constant, k.

$$k = A \exp (bT+cH+dMo)$$

Run	Crop	Mo	A exp (dMo)	b	c
1	Sabrina	82.0	0.0001661	0.0830	46.48
2	S23	69.4	0.0004075	0.0725	25.31
3	"	56.0	0.0004500	0.0725	25.31
6	Sabel	104.5	0.0001368	0.0830	46.48
5	"	92.7	0.0001517	"	"
6	"	63.1	0.0001966	"	"
7	"	49.0	0.0002224	"	"
8	"	23.5	0.0002784	"	"
9	S23	72.4	0.0003985	0.0725	25.31
10	"	64.2	0.0004235	"	"
11	"	35.8	0.0005229	"	"
12	Sabel	80.2	0.0001692	0.0830	46.48
13	"	46.9	0.0002266	"	"
14	S23	75.1	0.0003905	0.0725	25.31
15	"	36.7	0.0005194	"	"

Asymptotic moisture contents, M_e, were evaluated from equation 3.42 using the appropriate constants from Table 3.8. (page 91) and also, in some runs, the constants derived from the fit of equation 3.42 to all the final moisture contents of the 1971 and 1972 thin-layer tests. These values are summarised in Table 5.8.

TABLE 5.8.

Simulation of experimental runs. Constants used in equation 3.42 for evaluating the asymptotic moisture content, M_e.

$$M_e = a - b \ln T - c \ln(1-rh)$$

Source	Crop	Constant		
		a	b	c
Exponential series for plane sheet	Sabel	5.06	0.63	13.18
	S23	15.70	2.82	9.11
Final moisture contents, 1971 + 1972	All	16.25	3.00	9.28

5.3.2.2. Comparison of drying times and final moisture contents:

The two simplest measures of agreement betweer simulated and experimental results are:-

(a) The total drying time necessary to reach the mean final bed moisture content.

(b) The mean final bed moisture content at the experimental time.

These quantities are compared in Table 5.9 and Figure 5.7. In general agreement is better between the final moisture contents (r=0.968) than between final drying times (r=0.897). This is to be expected and for three main reasons:-

1. The accuracy of determination of the experimental final moisture contents is far less than that of drying time.

2. Towards the end of most runs, small changes in moisture content are equivalent to large changes in time (c.f. Run 8 in next paragraph 5.3.2.3.).

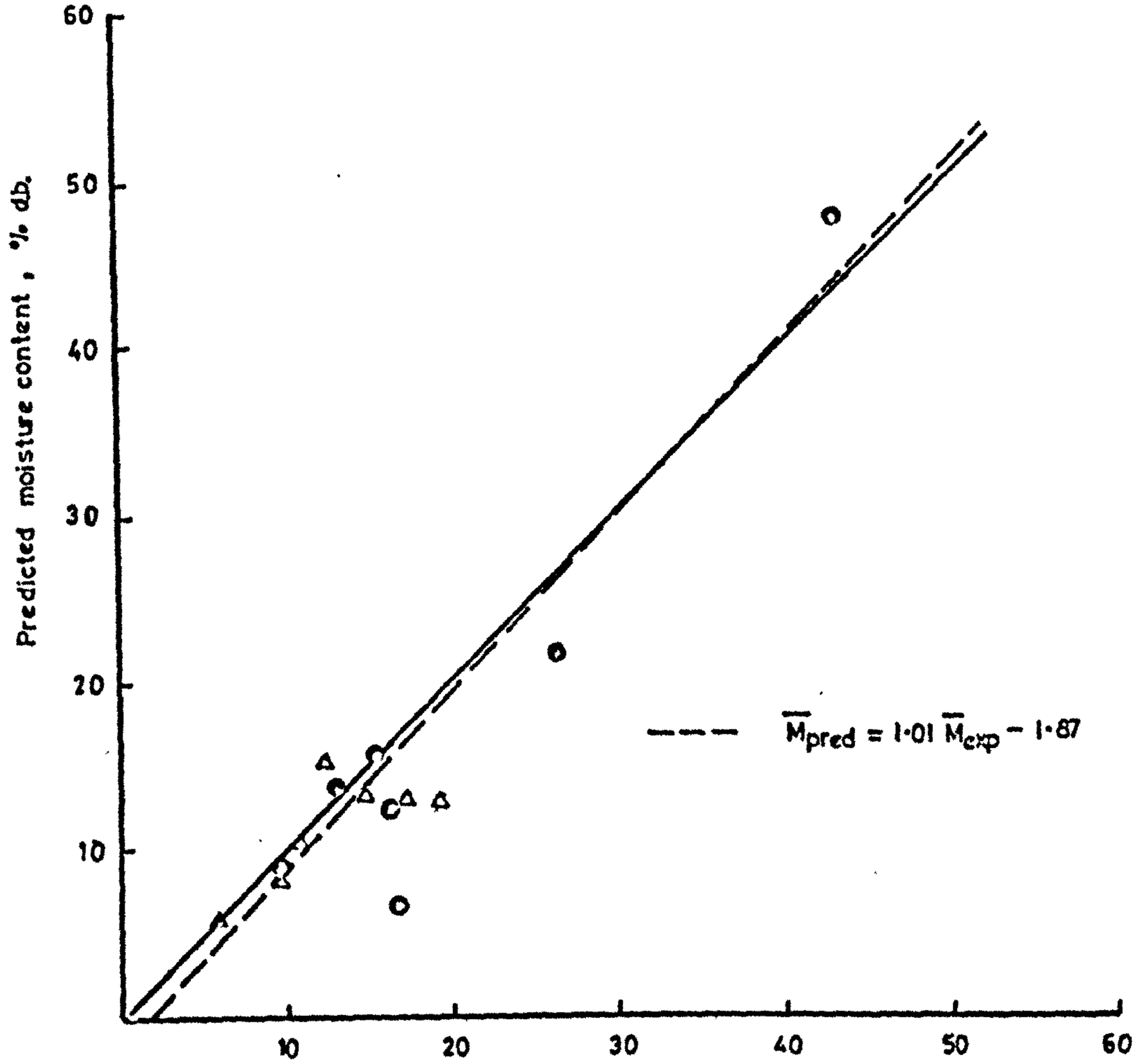

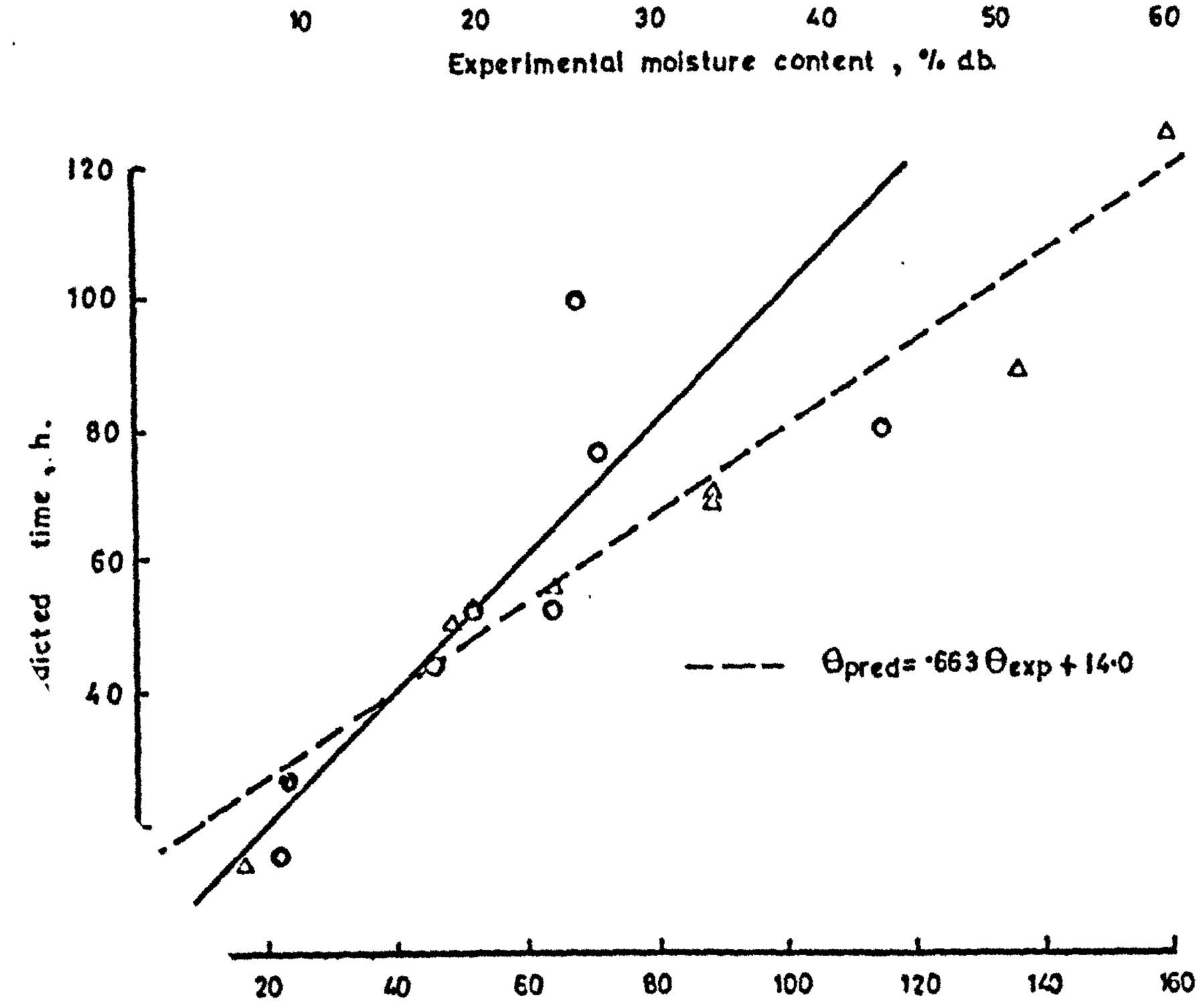

parison of experimental and predicted final moisture
nts (Top) and drying times (Bottom) for Sabel a
Sabrina (o) and S23 (Δ).

3. In long runs with several diurnal cycles, differences between calculated and target values, which in practice might be negligible, may cause the target value to be reached up to 24h earlier or later than the experimental time.

There is, however, a consistent tendency for the model to reach the target moisture content more rapidly than the experimental run. The particular features of individual runs are examined more fully in the next paragraph (5.3.2.3.)

TABLE 5.9.

Simulation of experimental runs. Comparison of drying times and final mean bed moisture contents.

Run	Seed	Bed depth, m	Ta, °C	G, kg/min m²	Moisture content, % d.b.			Drying time, h	
					Initial	Final	Predicted 1	Experimental	Predicted 2
1	Sabrina	0.61	32.5	14.08	82.0	9.32	9.34	52.5	52.7
2	S23	0.91	32.5	15.14	69.4	12.1	15.1	65.0	55.5
3	S23	0.91	49.7	11.99	56.0	9.6	8.9	49.0	49.8
4	Sabel	0.20	25.2	10.21	104.5	43.1	47.5	23.0	26.4
5	"	0.99	24.2	10.36	92.7	16.2	12.8	115.0	179.4
6	"	0.99	24.3	9.47	63.1	26.5	21.6	65.0	52.2
7	"	0.99	55.4	7.55	49.0	16.9	6.7	21.75	15.0
8	"	0.99	26.4	5.96	23.5	13.0	13.8	69.0	99.8
9	S23	0.95	26.0	8.36	72.4	14.6	13.4	89.0	70.0
10	"	0.96	26.0	4.77	64.3	17.1	12.9	136.0	88.5
11	"	0.64	48.6	8.12	35.8	5.5	5.6	16.0	14.5[3]
12	Sabel	1.22	25.7	5.97	80.2	60.0	58.6	46.5	43.8
13	"	1.55	22.2	35.5[4]	46.9	15.3	15.4	71.0	75.5
14	S23	1.55	24.2	18.0[4]	75.1	19.4	12.6	160.5	125.0
15	"	1.55	27.4	19.8[4]	36.7	10.5	10.6	88.0	68.9

1. Predicted at experimental time
2. Predicted time to reach experimental mean m.c.
3. Time to reach 5.53% d.b.
4. Per square metre of bin inner wall

5.3.2.3. Examinations of individual runs

Run 1. The agreement between observed and calculated final moisture contents and drying times in this run is excellent. For practical purposes there are no differences.

The observed and calculated final moisture profiles are compared in Figure 5.8. The calculated profile is steeper than the observed but the differences are small.

The dashed curves in Fig. 5.8. illustrate the importance of the asymptotic moisture content relationship in determining the predicted answer when the bed is close to equilibrium. Curves 2 and 3 were obtained using, in equation 3.42, the constants derived from the analysis of the final moisture contents, Mf, in the thin layer tests.

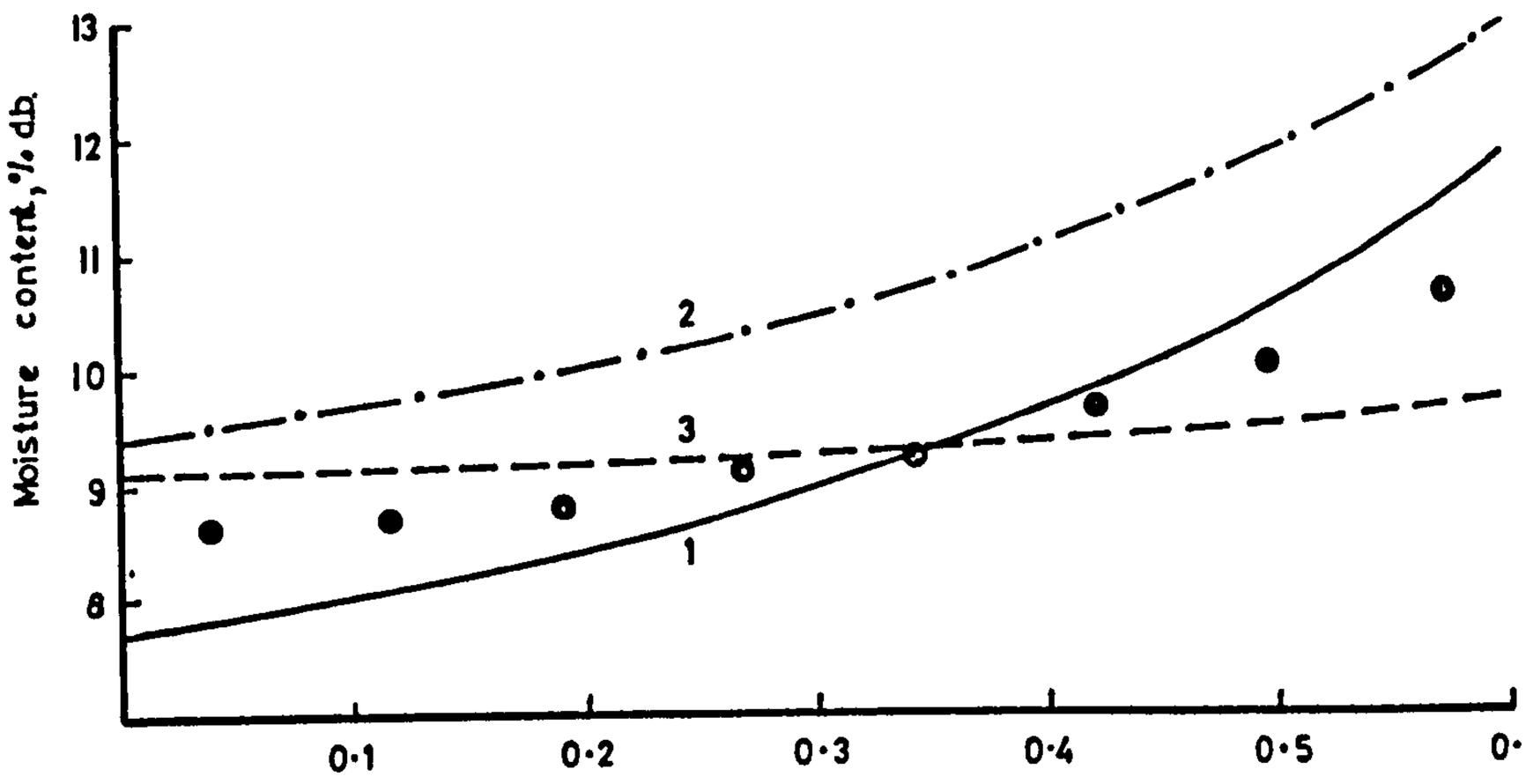

Fig. 5.8 Run 1. Observed (●) and calculated (1) final moisture profiles. The effect on calculated profile of using an alternative relation for M_e is shown at the experimental time and at the time required to reach the final mean bed moisture content.

At the experimental time calculated profile (curve 2) has the same slope as that calculated originally (curve 1) but was 1½% above it. Another simulated 20 hours were necessary to reach the experimental mean bed moisture content and by this time the profile (curve 3) was much flatter than the experimental. Note that the values of Me at the inlet temperature and relative humidity given by the two sets of constants are 7.5% d.b. for curve 1 and 9.1% for curves 2 and 3. Thus in the second case, the experimental profile could never have been predicted.

Run 2. An important feature of this run, and of Run 3, was the cooling after drying. In presenting the experimental results in Section 4 the possibility of some moisture regain during cooling was speculated upon but cooling periods were excluded from the total drying times. The simulation results indicated that they ought not to be excluded and the simulation inputs were adjusted accordingly.

The effect of the cooling on the mean bed moisture content is shown by the drying curve of Fig. 5.9. The run was similar in air temperature and flow to Run 1 and after 45 hours, when the heat was switched off, was calculated to have reached a similar mean bed moisture content of 9.2%. Thereafter moisture was condensed back into the bed until a mean of 15.1% d.b. was predicted at the experimental time of 65 h. Compared with the experimental final moisture content of 12.1% the regain appears to be excessive. This could be because the absolute humidity of 0.009 kg/kg used throughout the simulated run should have been reduced to a value nearer 0.007 kg/kg during the periods when the cooling temperature fell as low as 15.6°C.

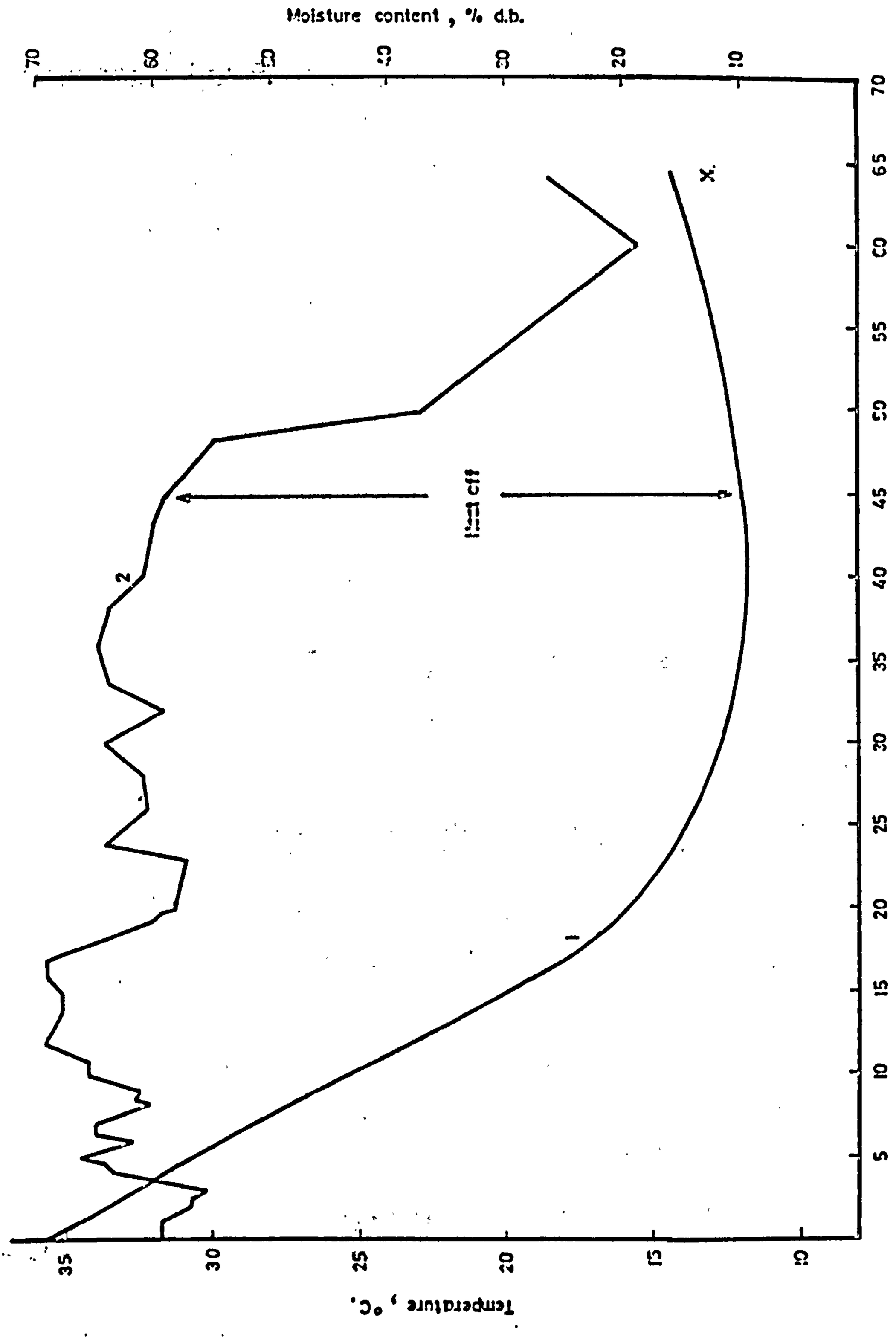

Fig. 5.9 Run 2. Predicted drying curve (1) and input air temperature (2).
X = experimental final moisture content.

It should also be noted that the constants for Me used for simulating S.23 runs were those obtained from the analysis of Mf since these were virtually the same as those obtained for Me for the plane sheet for S.23. It is possible that the constants for Sabel would have given better agreement.

Even so the predicted result is regarded as reasonable. The drying curve of Fig. 5.9 puts these differences into perspective and shows that, in the context of the run as a whole, they were slight. Fig. 5.10 compares the predicted and experimental final moisture profiles.

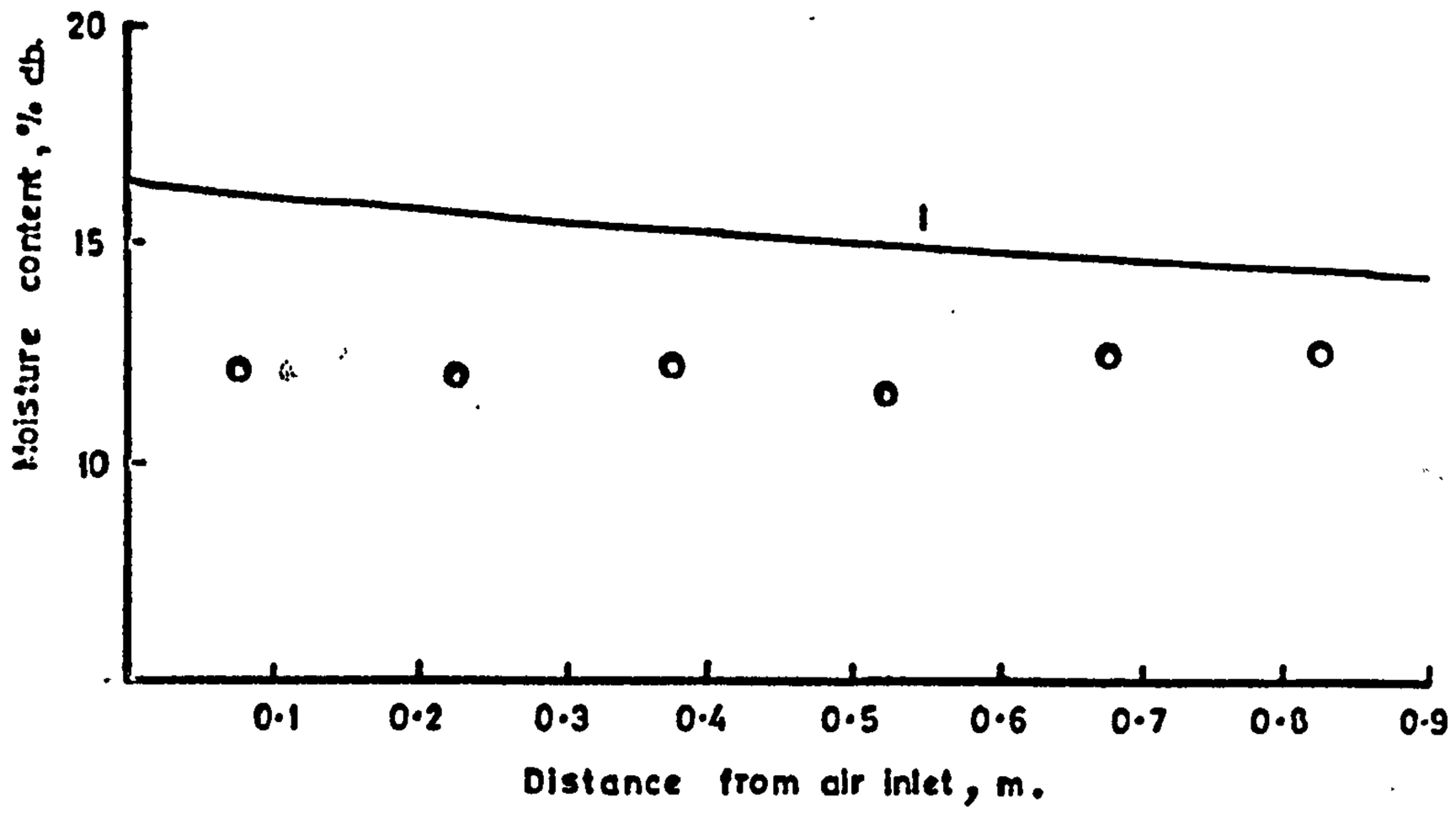

Fig. 5.10 Run 2. Calculated (-) and observed (o) final moisture contents within the bed.

Run 3. In contrast to Run 2 the moisture regain during the cooling period in this run was under rather than over estimated. However the discrepancy is small (0.7%) and the agreement between predicted (49.8h) and observed (49.0h) drying times is also good.

But there is evidence to suggest that the cooling corrects and also masks too rapid simulated drying. In the experimental bed, the wettest seed was furthest from the air inlet whereas in the simulated bed it was closest to the air inlet (Fig.5.11). Also the predicted drying curve (Fig. 5.12) reaches equilibrium nearly 25 h before the heat is switched off. Finally the predicted temperature of the air within the bed changes at a greater rate than the recorded temperatures. Predicted and observed exhaust air temperatures are compared in Fig. 5.12. Within the first hour, the predicted curve drops to 22°C, about 3°C below the wet bulb temperature of the inlet air. It then rises equally rapidly back to about 24°C, about 1°C below inlet wet bulb. After about 15 h the drying zone is emerging from the top of the bed and the exhaust temperature rises to approach that of the inlet air. In contrast, the initial fall of the observed exhaust temperature is much greater (≏ 8°C below inlet wet bulb) and this much lower temperature is not disturbed by the progression of the drying zone for about 30 h. The implication is that the simulation underestimates the amount of heat transferred into the seed.

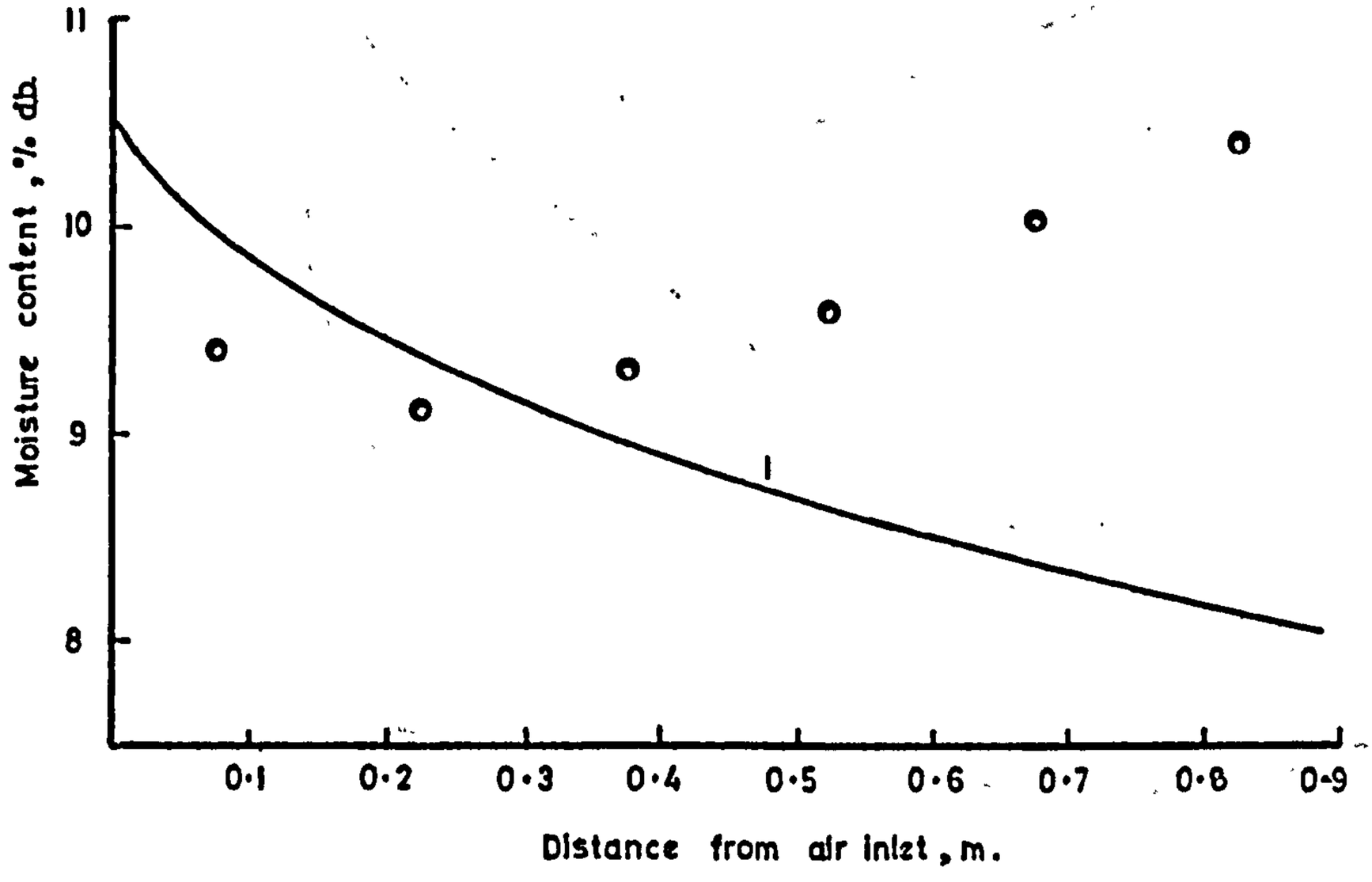

Fig. 5.11 Run 3. Observed (o) and calculated (1) final moisture profile.

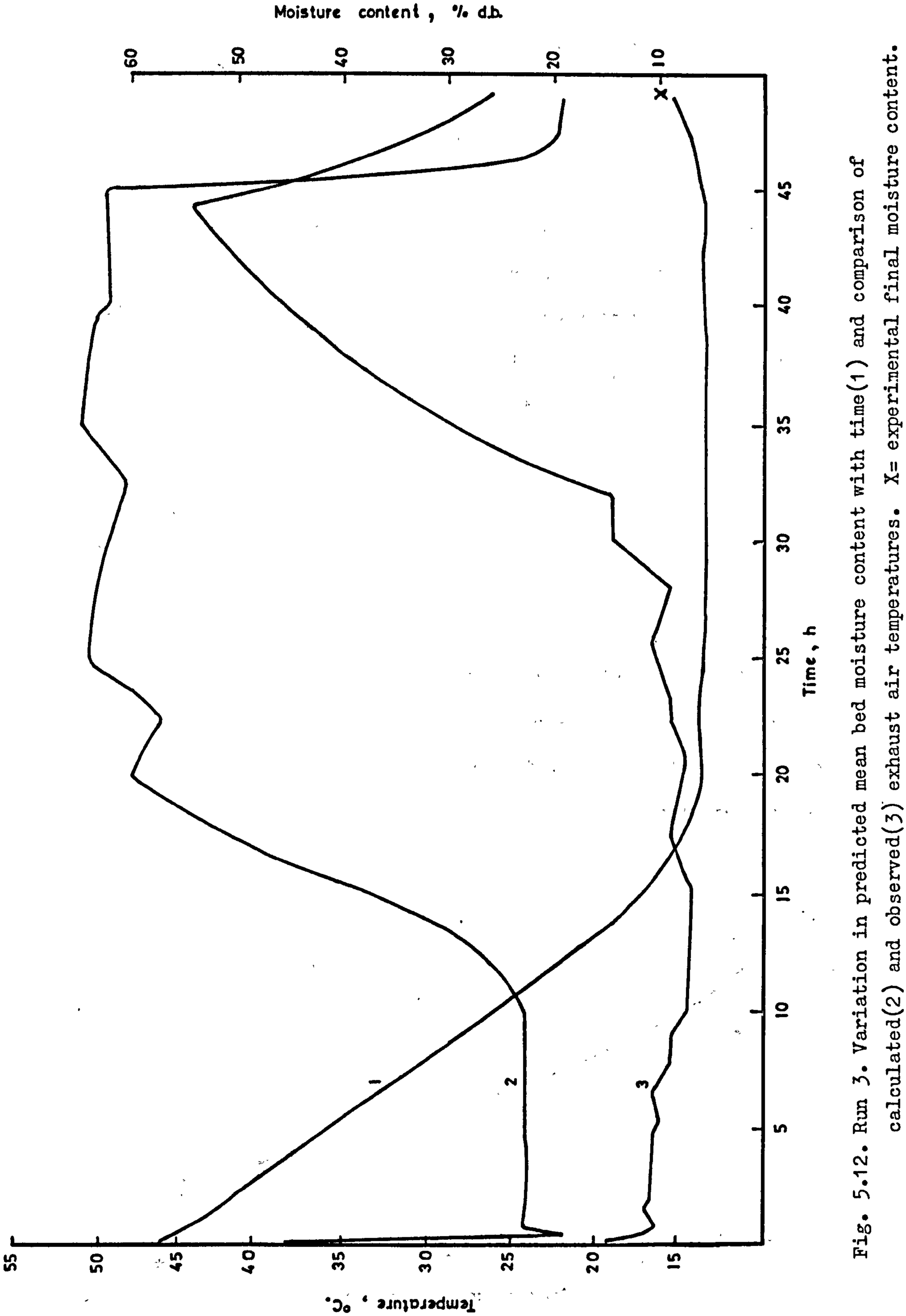

Fig. 5.12. Run 3. Variation in predicted mean bed moisture content with time(1) and comparison of calculated(2) and observed(3) exhaust air temperatures. X= experimental final moisture content.

Run 4. This run differed from other runs in being a shallow layer (0.2m) dried to a high (43.1%) final moisture content. It was one of the few runs for which the calculated drying time was greater (in this case by 3.4h) than the observed. The final moisture profiles are compared in Figure 5.13. and show good agreement.

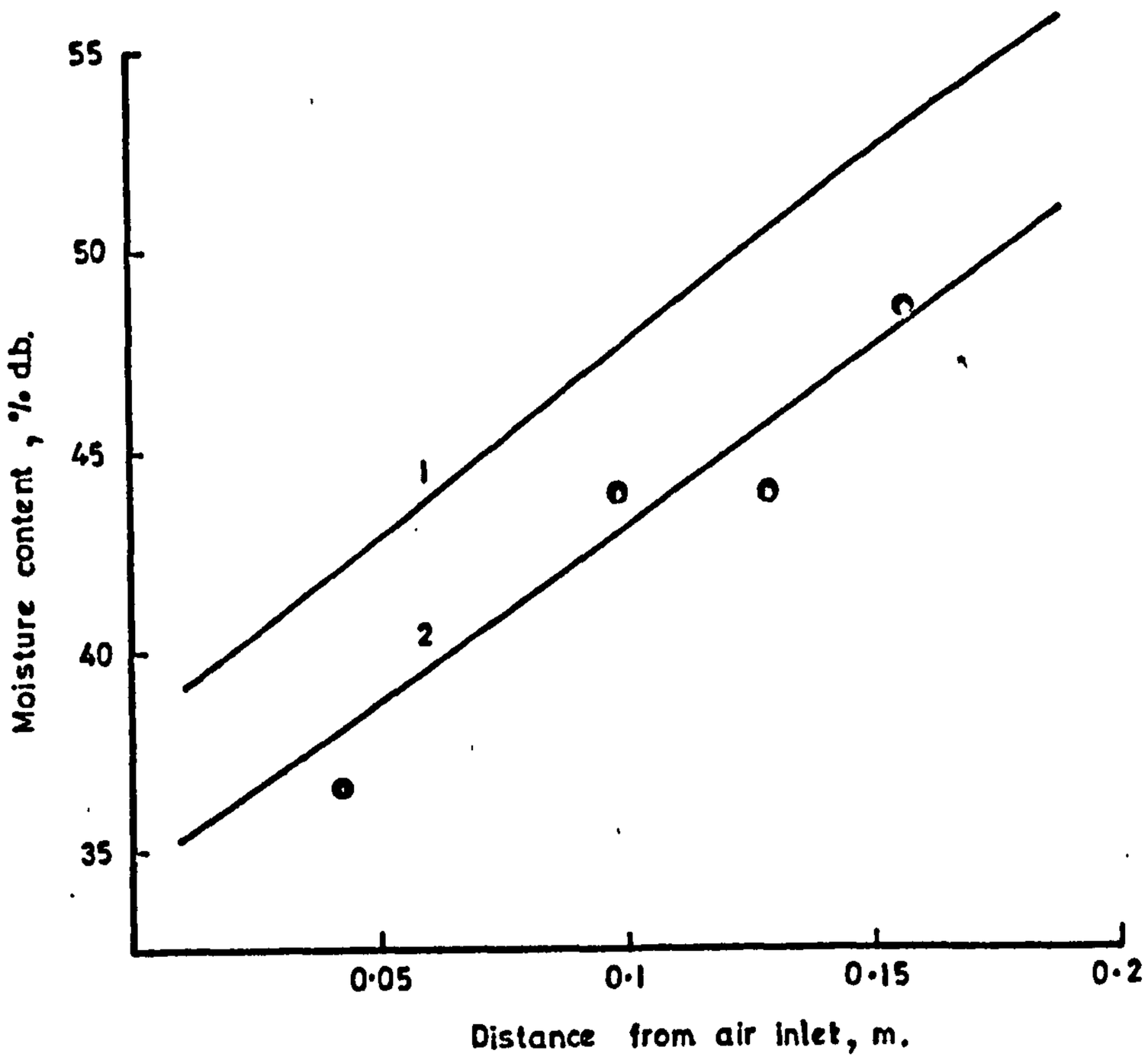

Fig. 5.13. Run 4. Final moisture profiles predicted at (1) experimental time (=23.0 h) and (2) calculated final time (=26.3 h) compared with experimental data (o).

Run 5. This run differed from Run 4 in having a lower initial moisture content (92.7%) and much greater depth of seed (0.99 m). The experimental run took 114 h to reach a mean of 16.2% d.b. The simulation predicted 79.4 h; a shorter rather than the longer time which might have been expected from the result for Run 4. Comparison of the final moisture profile in Fig. 5.14 indicates a much narrower predicted drying zone than was observed in practice. In fact the top layer was calculated to be still at 91% m.c. and the air exhausting at 99% r.h. Thus the predicted drying rate was very close to the maximum possible adiabatic rate.

The average drying curve in Fig. 5.15 shows that when the simulation was continued to the experimental time some rewetting was calculated to occur but, like Run 3, the experimental final moisture profile does not show much evidence of rewetting.

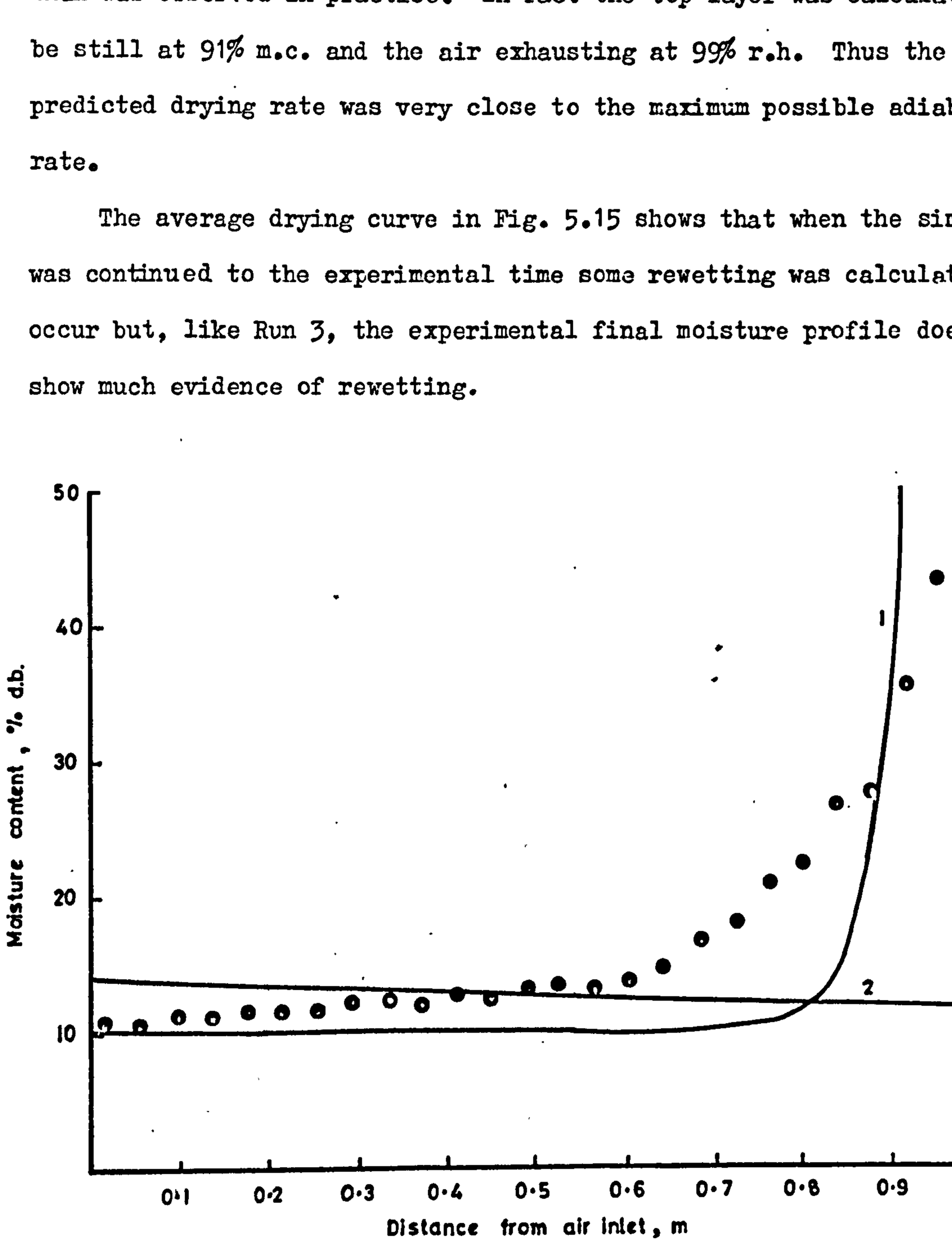

Fig. 5.14. Run 5. Final moisture profiles predicted at 79.4 h (1) and at 114 h (2) compared with experimental data (o).

Re-running the simulation with the exhaust r.h. limited to 94% only slightly increased the predicted drying time (85 h) and had virtually no effect on the predicted moisture profile. Substitution of the m.c. relationship for M_f rather than M_e had no effect on the predicted drying time and only a slight effect on the final moisture profile. The basic problem appears to be the narrowness of the drying zone and its excessive speed; this appears to result more from inadequate prediction of air temperature change than from an overestimate of incremental drying rate.

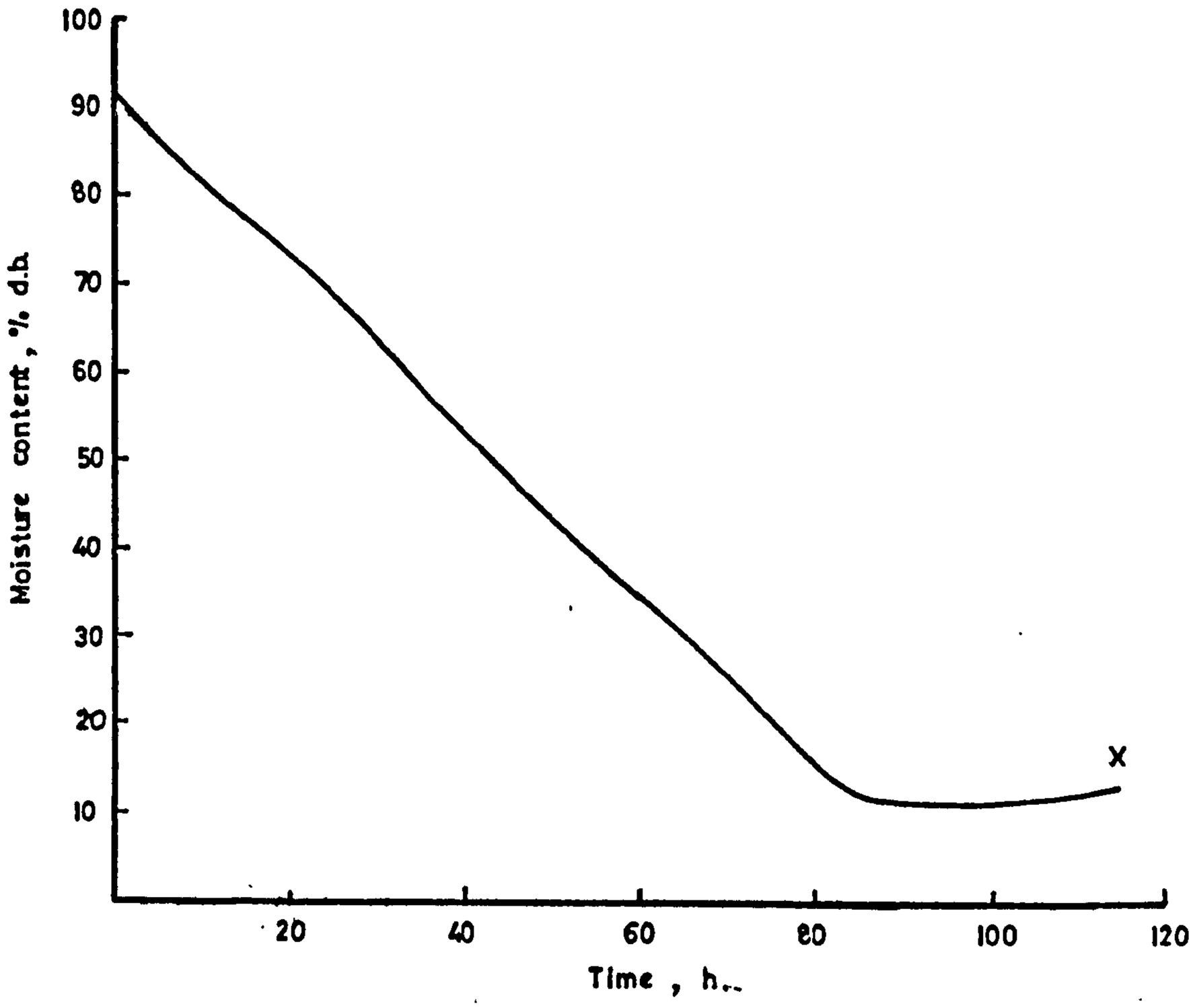

Fig. 5.15. Run 5. Predicted drying curve. X = experimental final moisture content.

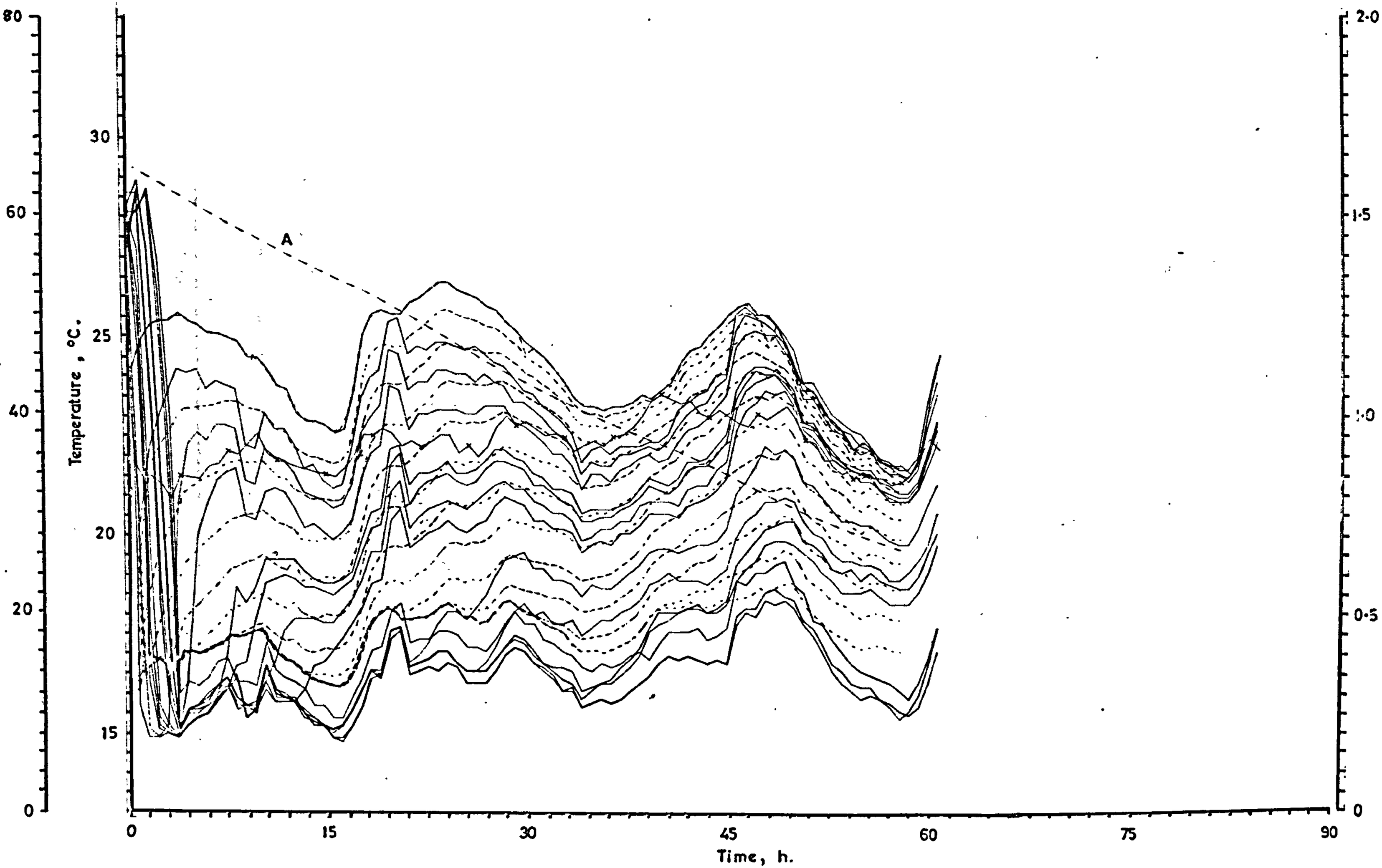

Fig. 5.16. Run 6. Predicted temperature-time profiles (- - - -) compared with observed profiles (———) from Fig. 4.14. A = predicted average drying curve.

Run 6. A similar run to Run 5 but with a lower airflow and much lower initial moisture content. The simulation also predicted a shorter (52.2 h) than observed (65.0 h) drying time and displays similar symptons to Run 5. Thus in Fig. 5.16, the pseudo-saturation temperature preceding the drying zone was higher in the predicted than in the experimental run. Also the predicted initial cooling was much faster than the observed. Apart from this the predicted run was very similar to the experimental and the final moisture content profiles (Fig. 5.17) agree quite well, although the slower spread of heat through the experimental bed is reflected in the slightly steeper profile.

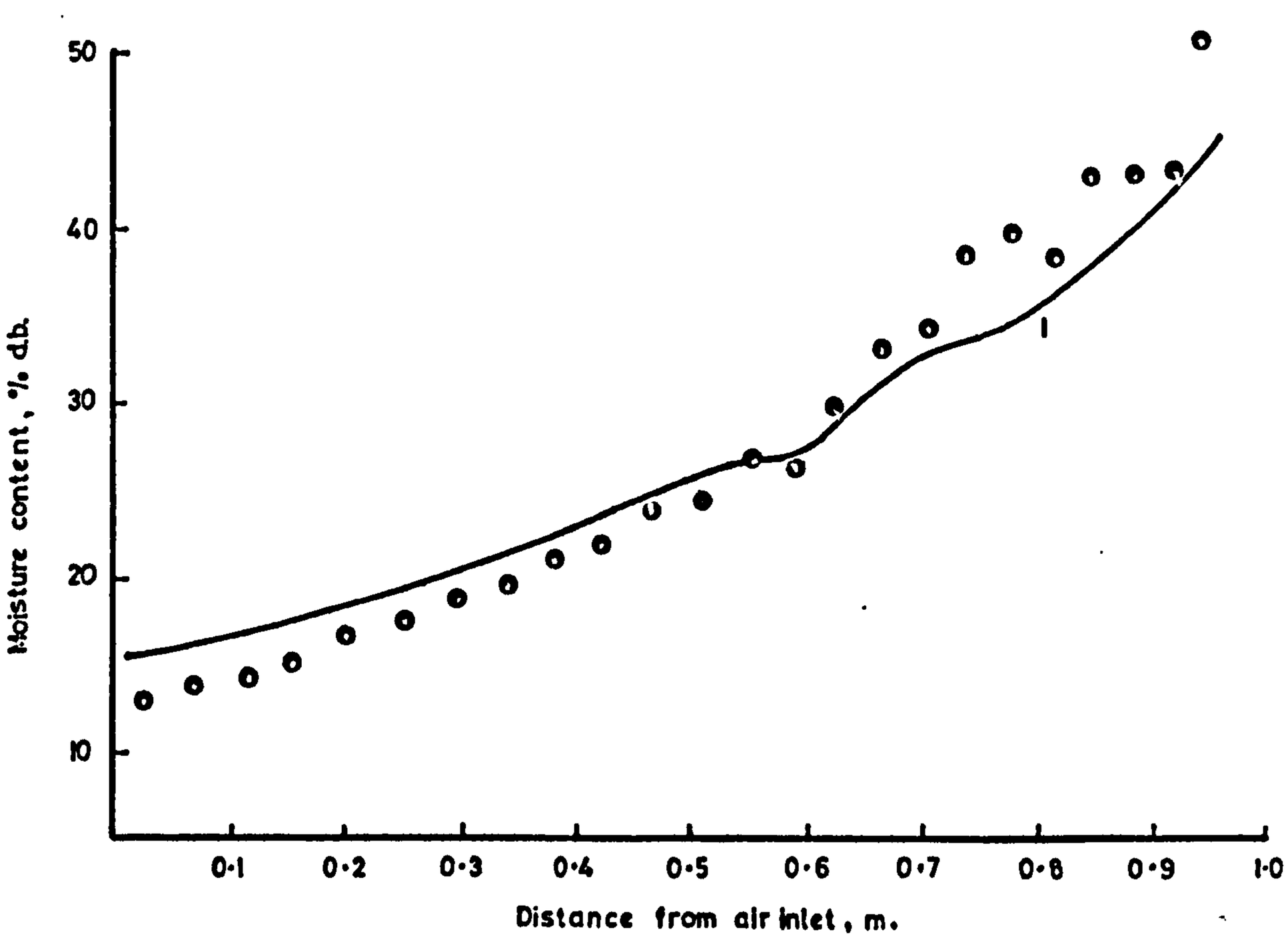

Fig. 5.17. Run 6. Final moisture profile at predicted drying time (1) compared with experimental data (●).

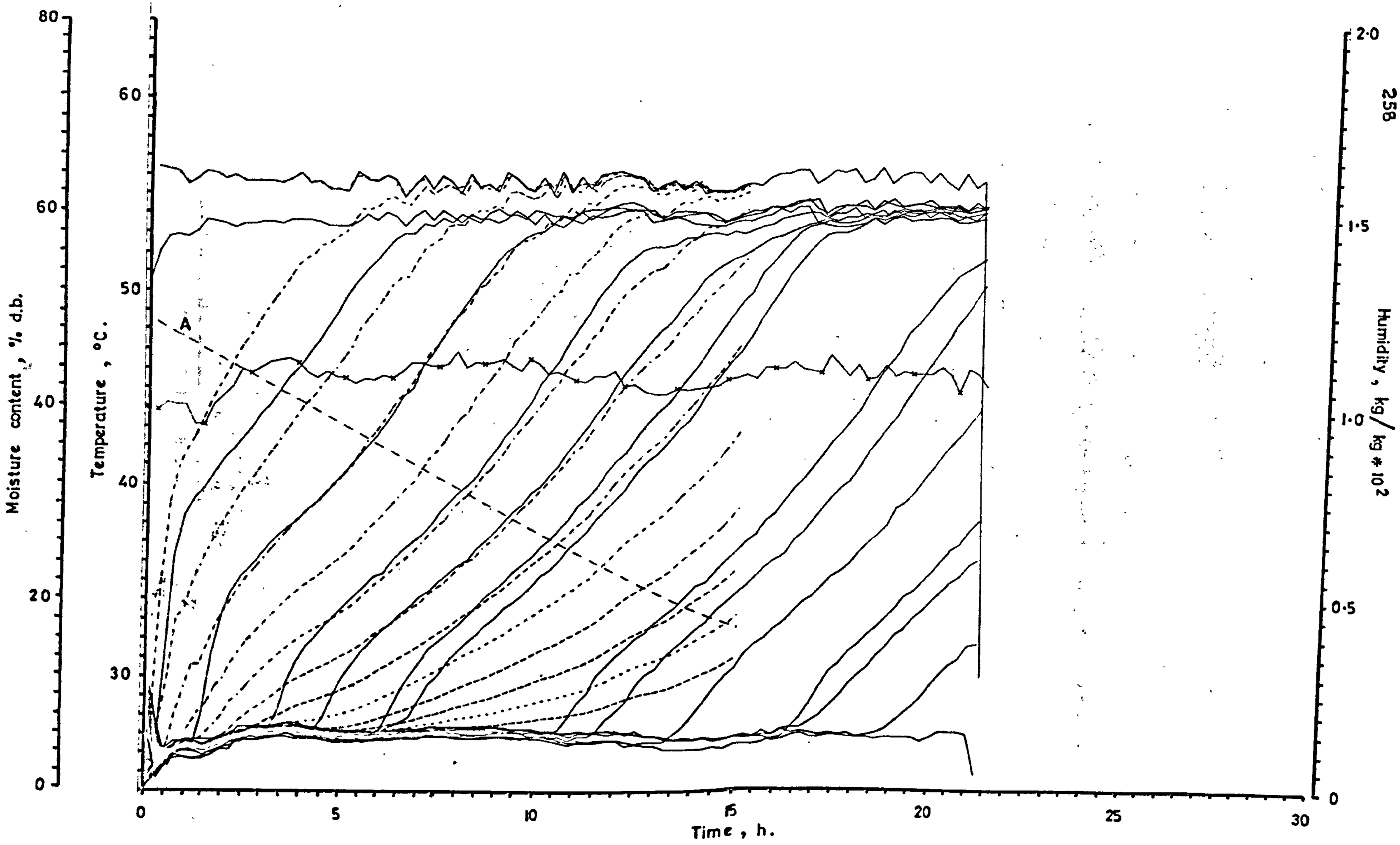

Fig. 5.18. Run 7. Predicted temperature-time profiles (- - - -) compared with observed profiles (———) from Fig. 4.16. A = predicted average drying curve.

Run 7. This was the run with the highest inlet air temperature. Once again the predicted drying time (15 h) was less than the observed (21.8 h) and is associated with the more rapid passage of the drying zone through the bed. This can be seen in the comparison of predicted and observed temperatures in Fig. 5.18. It is interesting to note that in this case, in contrast to Runs 6 and 3, the predicted and observed pseudo-saturation temperatures are comparable. Agreement between the observed and predicted final moisture profiles (Fig. 5.19) is alsc good. It was shown for this run in Section 5.3.2.1. that the simulated result is very little affected by the value of the heat transfer coefficient.

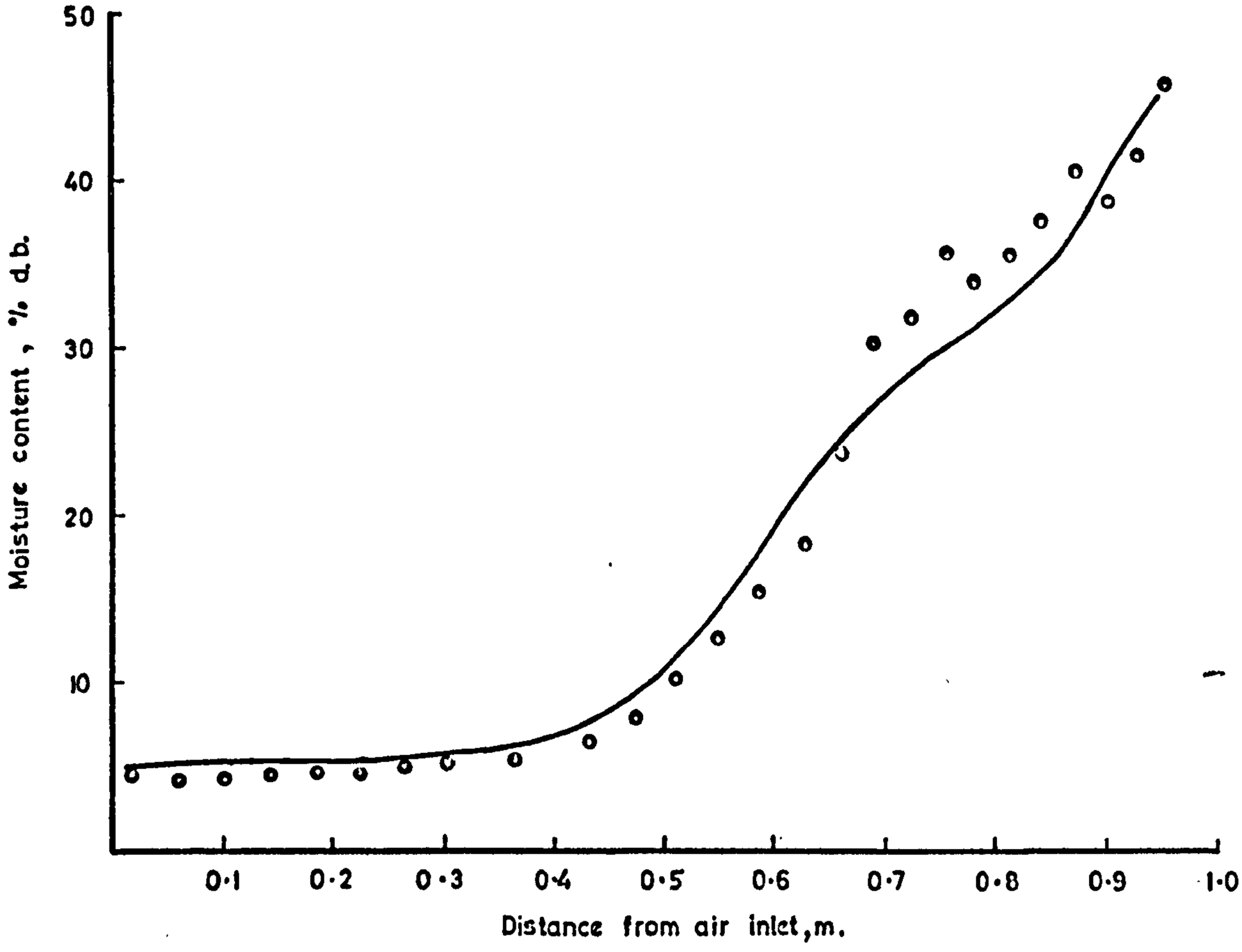

Fig. 5.19. Run 7. Final moisture profile at predicted drying time (1) compared with experimental data (o).

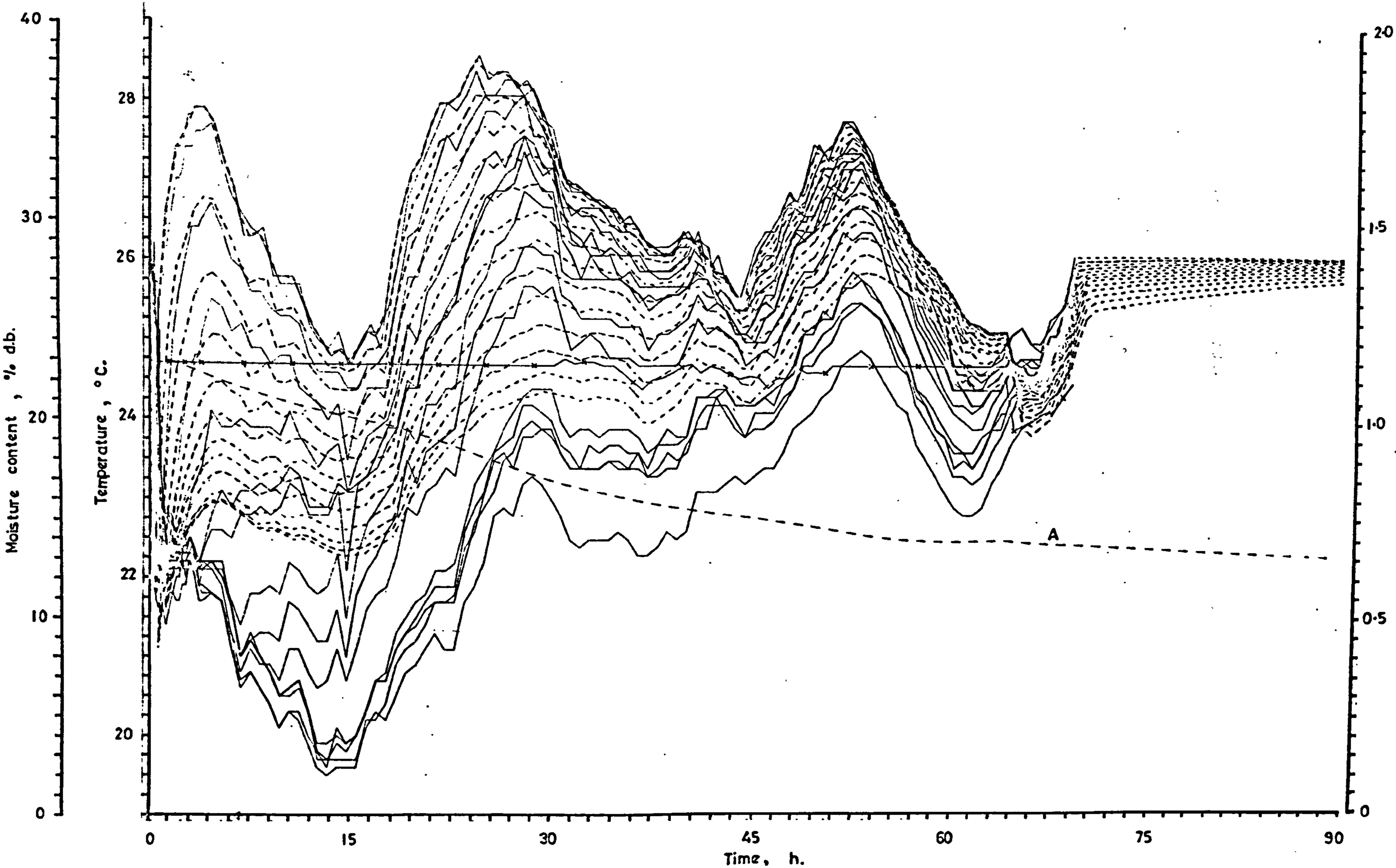

Fig. 5.20. Run 8. Predicted temperature-time profiles (- - - -) compared with observed profiles (———) from Fig. 4.17. A = predicted average drying curve.

The effect of latent heat of vapourisation from the seed, Lg, was investigated by adjusting the constants in Gallaher's equation, equation 5.31, from 23.0 and 40.0 to 0.4 and 11.5 respectively. This adjustment had very little effect.

Run 8. This run was one of the few for which the predicted drying time (99.8 h) was greater than the observed (69 h). However, this was because the equilibrium to which the model was tending was slightly higher than that for the experimental bed. Prior to this being approached closely, the temperature time profile (Fig. 5.20) suggests that this simulation also dried at an excessive rate.

At 69 h the model predicts a moisture content of 13.8% and the extra 30 h are needed to remove just 0.8%. This illustrates how small differences in target moisture content can cause large differences in predicted drying times.

Final moisture profiles are plotted in Fig. 5.21.

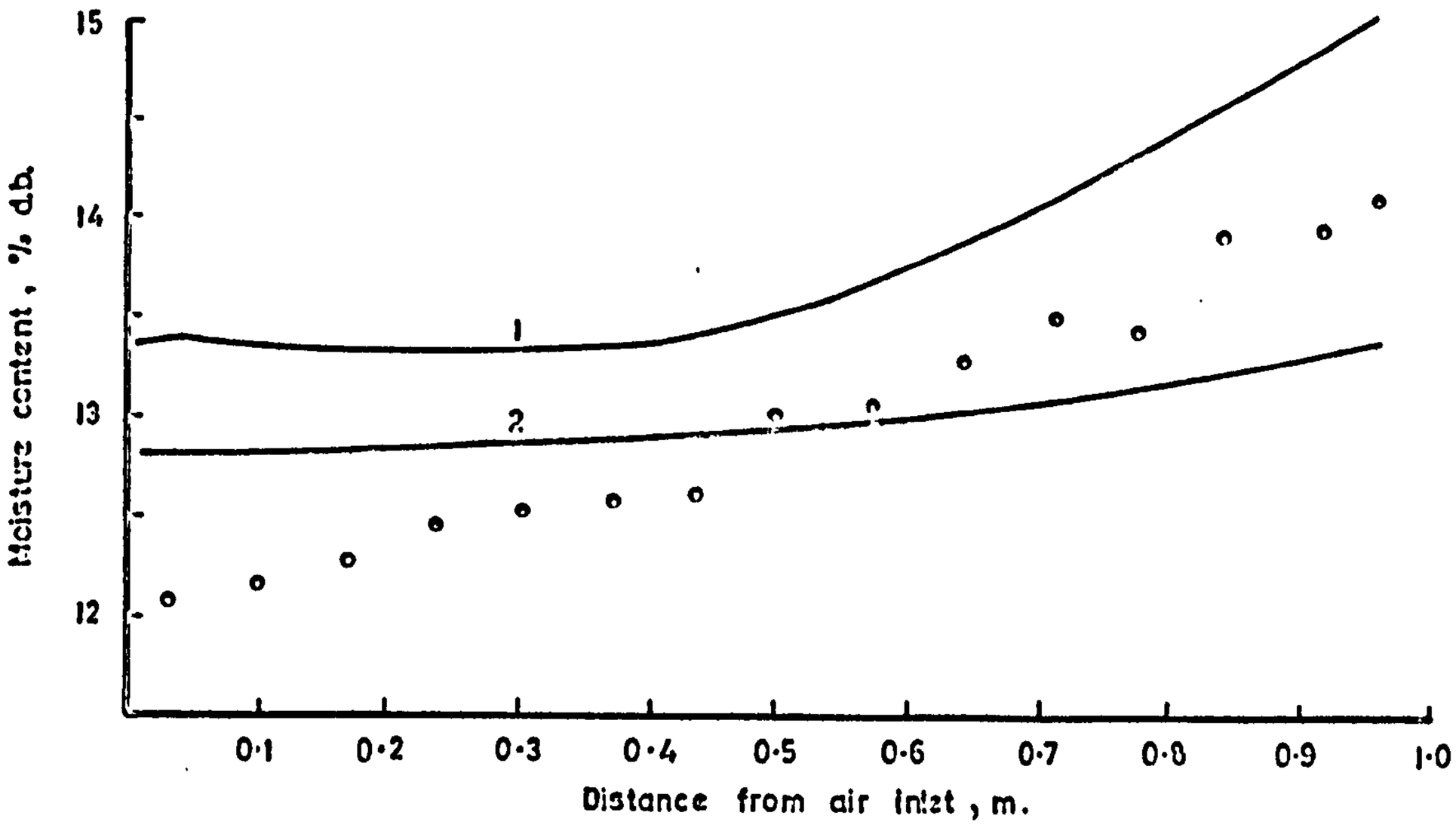

Fig. 5.21. Run 8. Final moisture profiles predicted at experimental time (1) and at 99.8 h (2) compared with experimental data (o).

Run 9. This was the first run with S.23 seed at ambient temperatures but in spite of the change of constants the simulated results follow the same general pattern as those for Sabel. The predicted drying time (70 h) was again less than the observed (89 h) and for the same reasons. This was one of the runs used in the study of increment size and the final moisture profile has already been presented in Fig. 5.4. There was good agreement between the observed and predicted values.

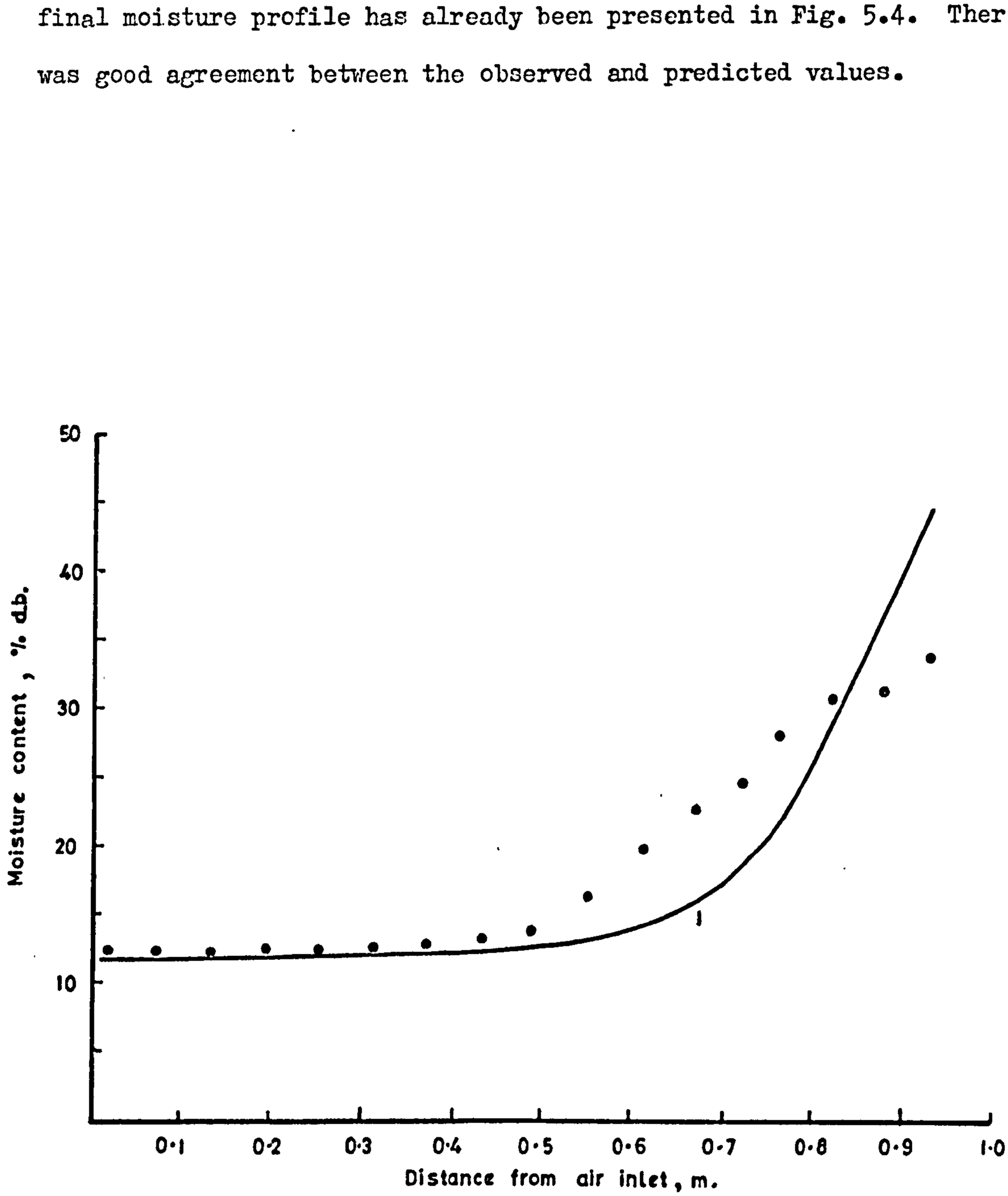

Fig. 5.22. Run 10. Final moisture profile predicted at 88.5 h (1) compared with experimental profile at 136 h (•).

Run 10. A similar run to Run 9 but with a lower airflow and longer drying time (136 h). Once again the model underestimated the drying time (88.5 h). As in Run 5, continuing the simulation to the experimental time indicated some rewetting of the lower layers but this time the experimental profile (Fig. 5.22) with its sharp transition in slope could be consistent with some rewetting. There is good agreement between the observed and predicted pseudo-wet bulb temperatures (Fig. 5.23)

Run 11. Run 11 was similar to Run 3 without the cooling. Like most of the other runs the predicted air temperatures suggest that it dried too rapidly although the bed reached equilibrium without ever reaching the target value. The predicted time (14.5 h) was taken as that at which the predicted moisture content approached most closely to the target value (a difference of only 0.03%). The predicted moisture profile was thus almost completely flat whereas the experimental profile sloped from 4.8 to 6.8%.

Run 12. Agreement between observed and predicted drying times for Run 12 was much better because, for such a deep layer (1.2 m), the drying time was relatively short and the final moisture content high (60% d.b.). Run 12 provoked particular interest in Section 4 because of the evidence of considerable moisture reduction in front of the drying zone caused by evaporative cooling. The simulation failed to predict this to the same degree although it did predict some. As a result the calculated moisture profile shows a greater moisture loss from the lower layers than does the experimental (Fig. 5.25). One reason why the model predicted less moisture loss from the upper layers than was obtained experimentally was because it predicted that the air in those wet layers would cool to lower temperatures and thus be unable to exhaust at such a high absolute humidity (Fig. 5.24).

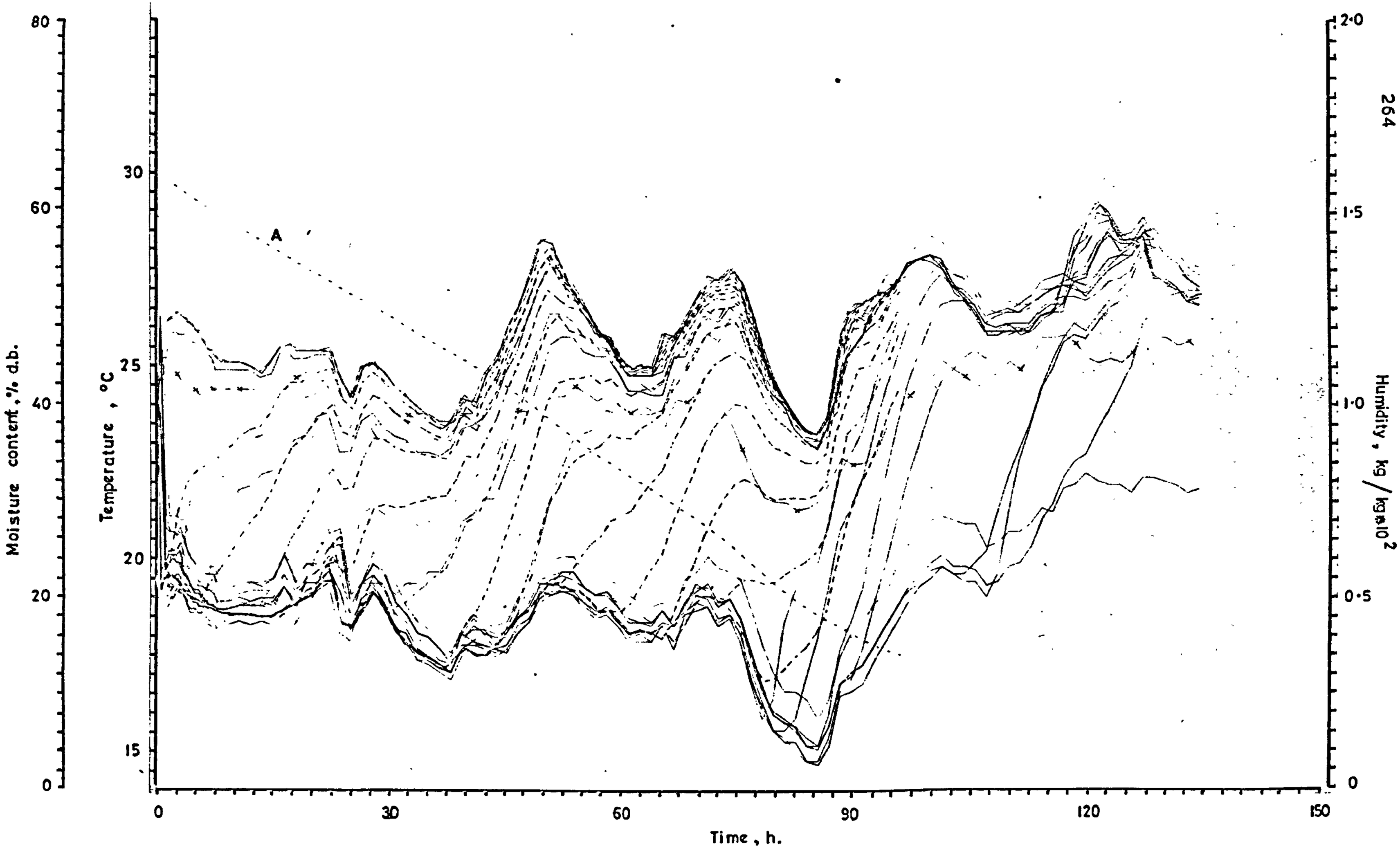

Fig. 5.23. Run 10. Predicted temperature-time profiles (- - - -) compared with observed profiles (————) from Fig. 4.20. A = predicted average drying curve.

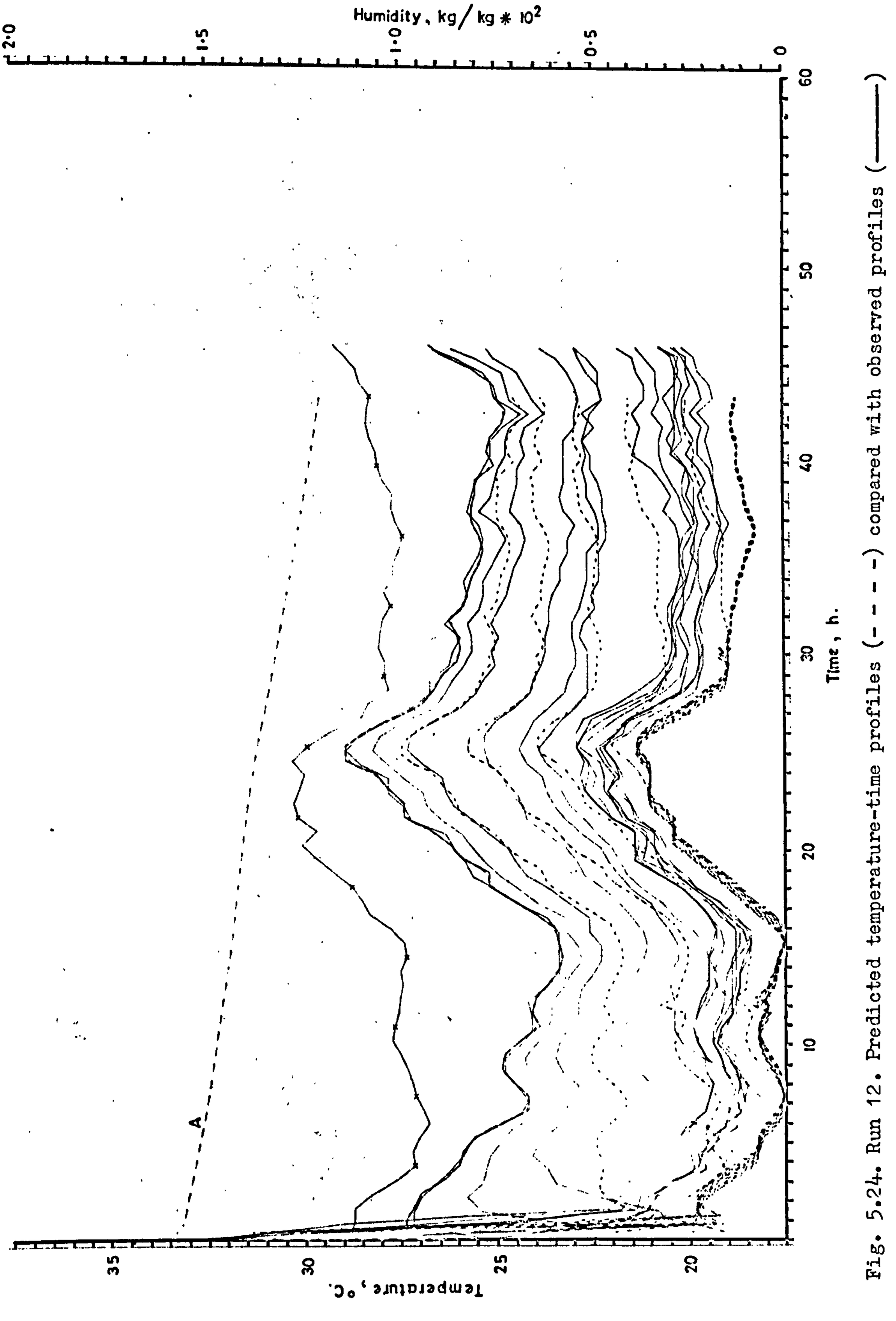

Fig. 5.24. Run 12. Predicted temperature-time profiles (— — —) compared with observed profiles (——)
from Fig. 4.23. A = predicted average drying curve.

This was the only run in which the pseudo-wet bulb temperatures predicted by the model were significantly less than the recorded values.

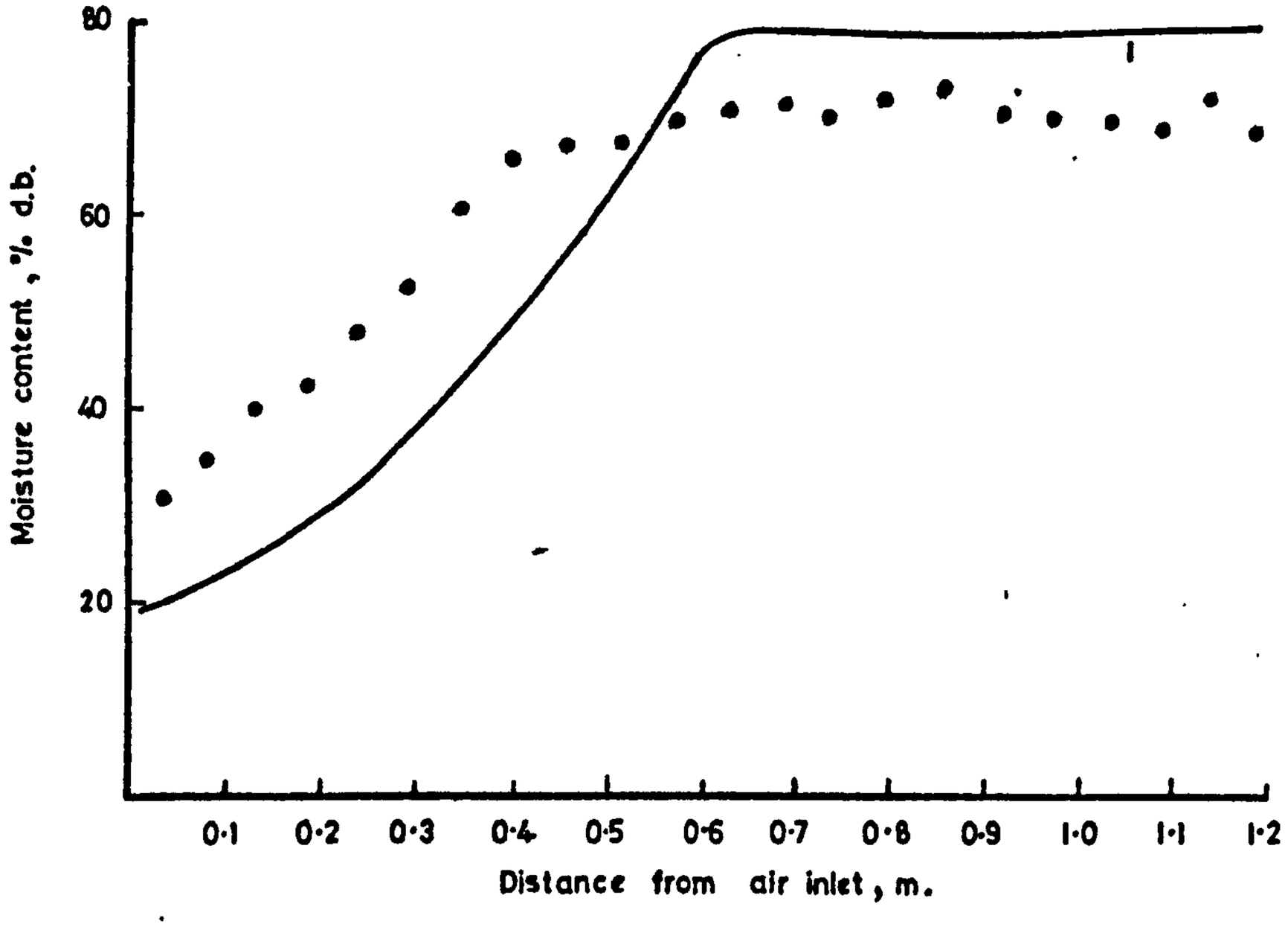

Fig. 5.25. Run 12. Final moisture profile at predicted drying time (1) compared with experimental data (•).

Runs 13, 14 and 15. These three radial-flow runs are taken together since they are all similar. It should be noted that the target moisture contents represented a mean of the profile values and not a true mean of the bed. The profile mean is easier to use than the true mean although the latest version of the programme calculates both.

Run 13 was one of those runs for which the model predicts a longer than actual drying time although comparison of predicted and observed temperatures suggests that like most of the parallel flow runs the drying was too rapid and was only slowed down towards the end by approaching close to equilibrium. However the error (5 h in 70 h) is small and predicted and observed moisture profiles were comparable (Fig. 5.26).

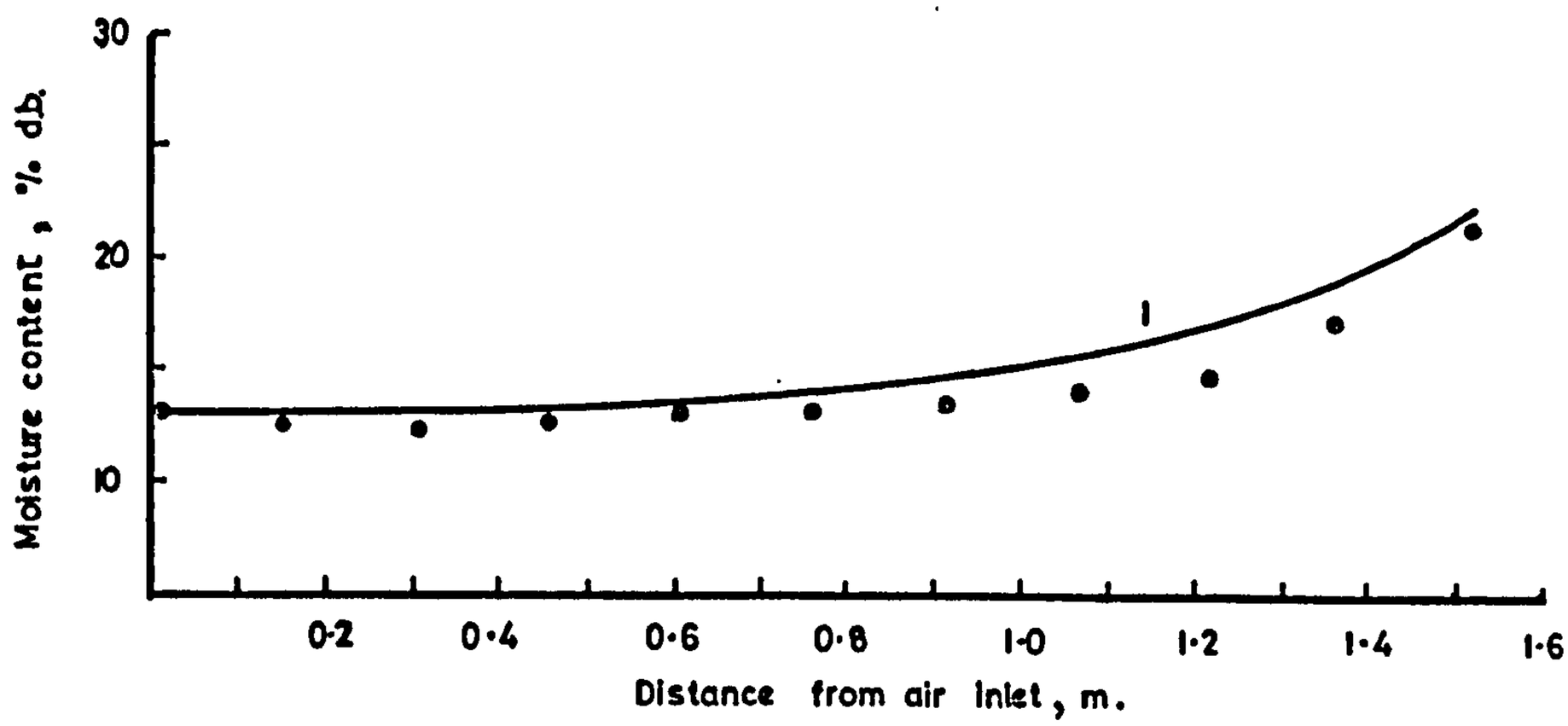

Fig. 5.26. Run 13. Final moisture profile at predicted drying time (1) compared with experimental data (•).

Run 14 also dried too rapidly and the temperature-time profile of Fig. 5.27 exhibits the familiar pattern of predicted temperatures moving ahead of the observed. It is interesting to note that, like Run 12, the predicted pseudo-wet bulb temperature is less than the observed. Run 15 was very similar but because the final moisture content of the bed was close to equilibrium continuing the simulation up to the experimental time still gave a similar predicted final moisture content.

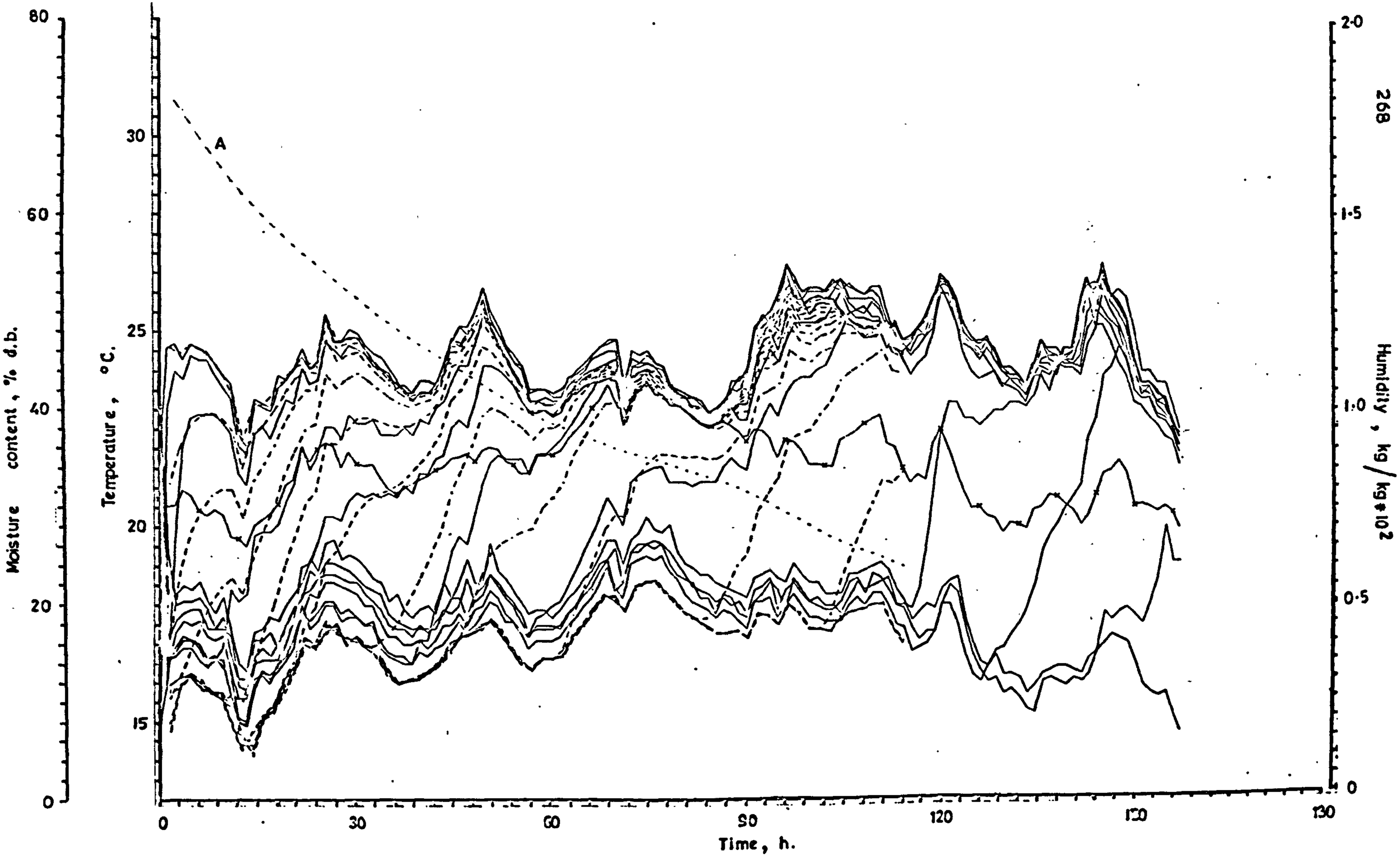

Fig. 5.27. Run 14. Predicted temperature-time profiles (- - - -) compared with observed profiles (————) from Fig. 4.27. A = predicted average drying curve.

5.4. DISCUSSION

5.4.1. Validation.

To be of practical use a mathematical model must be stable, convenient to use and accurate. The model presented here is certainly extremely stable and is convenient to use. For example, because increment size can be altered over a wide range, it is possible to reduce the computing time, even for simulations of several days real time, to within the bounds required for normal day-time running on a multi-access computer. This quality will also make it possible to use the model within larger programmes of the optimising type.

The third attribute, that it should be accurate, is far more difficult to assess because of the difficulty of defining suitable objective criteria by which to compare experimental and predicted results. No one single criterion is likely to be adequate because the model output is multi-valued and good agrecment of one quantity may be associated with poor agreement of another. Good agreement would normally be expected with those quantities for which the model is inherently convergent. The model is concerned with predicting changes associated with proceeding from the equilibrium state of the unventilated seed to a new equilibrium with the ventilating air. Thus the solution will ultimately be convergent provided the equilibrium properties are known, but in the process small errors may propagate considerable divergence in the imtermediate conditions. Such propagated divergence is most clearly demonstrated by the temperature profiles of Run 7, Fig. 5.18. Clearly the deeper the drying bed and hence the longer this transient period, the more serious will be such divergence.

The main cause of such systematic errors will be the crude simplification of the real life process made in setting up the equations and their method of solution.

To a lesser extent they may be due to bias in the experimental results either for the seed properties or for the deep bed runs. Since the seed properties used in this study are based on a large number of experimental data, the defining equations are thought to be reliable but an examination of the standard errors of the coefficients of these equations indicates considerable random or unexplained variation in properties. For example, if the standard errors of the coefficients* of equation 3.42, the equilibrium moisture content equation, are applied to act in the same direction, they can cause differences of several per cent in the predicted value of Me. Now if such variation is typical of the thin-layer data, it will also be typical of the measurements of the deep bed runs but here it was only possible to carry out a few runs and each of these was a unique combination of several variables.

O'Callaghan et al[88], for example, state that even under the most stringent testing conditions for deep beds, errors of 10% of total evaporation may occur and they use this 10% as a measure of the acceptability of the simulation results, i.e. they make no allowance for error in model formulation of in seed properties. Clearly this is somewhat optimistic and their own static bed simulations had a mean error from 24 separate tests of +13.7%. The mean of the 15 tests reported in this present work was +9.6% but this figure conceals a greater variation in error (Table 5.10) than obtained by O'Callaghan et al. Indeed, the fact that the mean value falls below 10% is fortuitous and owes much to the large negative (slow drying) error of Run 8. This run was a special case in which the slow drying was entirely associated with discrepancy between observed and predicted equilibrium moisture values. Excluding this the general tendency is for the model to be over-optimistic in its prediction by up to 35% (see also Fig. 5.7).

* Appendix tables 3.2.18. - 3.2.20. pages 393-395.

TABLE 5.10

Differences between experimental and predicted drying times and mean bed moisture contents in relation to total drying time and percentage moisture removed

Run	Moisture content removed, % d.b.	Relative errors[1]		
		in time		in final moisture content
		% experimental time	h/% moisture removed	% m.c./% moisture removed
1	72.7	-0.4	-0.0028	-0.0003
2	57.3	14.6	0.166	-0.052
3	46.4	-1.6	0.0172	0.015
4	61.4	-14.8	-0.0554	-0.072
5	76.5	31.0	0.465	0.044
6	36.6	19.7	0.3497	0.134
7	32.1	31.0	0.2103	0.38
8	10.5	-44.6	-2.933	-0.076
9	57.8	21.3	0.3287	0.021
10	47.2	34.9	1.006	0.089
11	30.3	9.4	0.0495	0.0033
12	20.2	5.8	0.1337	0.069
13	31.6	-6.33	-0.1424	-0.0032
14	51.5	22.1	0.689	0.132
15	26.2	21.7	0.729	-0.0038
Mean	43.9	+9.6	+0.0674	+0.0454

Mean m.c. error = 43.9 x 0.0454 = 1.99% m.c.
Mean time error = 43.9 x 0.0674 = 2.96 h

1 = Negative if drying too slow.

At first sight this may seem poor but it has to be considered against the other criteria of agreement given in Table 5.10. These are differences in drying times and final moisture contents as decimal fractions of the total percentage of moisture removed. Some of these indices are very small and illustrate that the model must be very good indeed if substantial errors are not to accumulate.

Furthermore the effect of such errors can be minimised if predicted drying times are modified by the equation of the line of best fit given in Fig. 5.7.

$$\theta_{exp} = 1.51\ \theta_{pred} - 21.0 \qquad \ldots 5.32$$

Prediction of mean moisture content requires no such correction. Correspondence between predicted and observed moisture contents at given experimental times was excellent.

$$M_{exp} = 1.85 + 0.99\, M_{pred.} \qquad \ldots 5.33$$

This is because mean bed moisture content changes very slowly with time, i.e. the simulation tends to be convergent for moisture content. Thus the model is sufficiently accurate for general use and may be preferred in those applications, e.g. within a system model, in which computing speed is an essential requirement.

It has to be recognised, however, that the model has a systematic error which is typically associated with the too rapid passage of heating or cooling fronts through the bed. The temperature profiles of Fig.5.28, which is taken from the paper of O'Callaghan et al, show that the Newcastle model has the same characteristic.

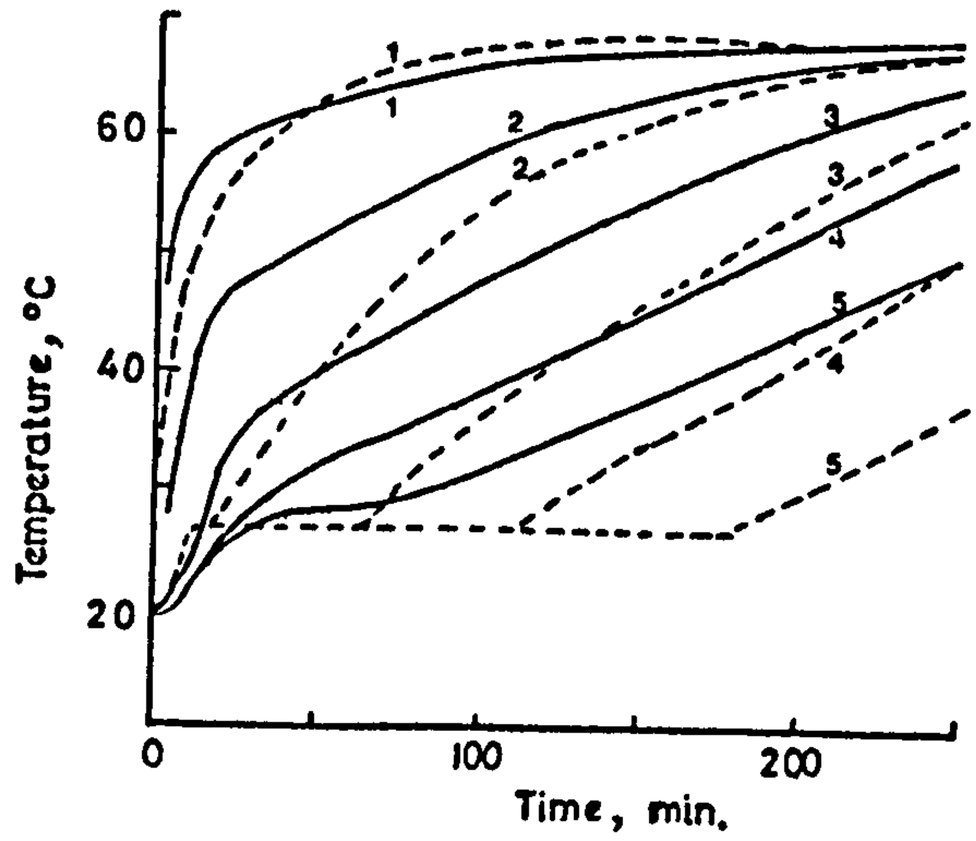

Fig. 5.28. Example of predicted (———)and experimental (-------) deep bed profiles given in reference 88. Depths from surface:- 1=0.28 m, 2=0.23 m, 3=0.15 m, 4=0.075 m, 5= surface.

Since the only common features of the two models are the basic heat and mass balances and the method of integration it would seem that it is in these that improvement should be sought. However, it is only likely to be achieved at a considerable cost in computing time.

As formulated the equations are solved in a single pass at each step and are extremely insensitive to step size. This stability is inconsistent with the initial assumptions that the layer and time steps are sufficiently small for the least important partial derivatives to be neglected. If this is a reasonable assumption and the equations are formulated in correct differential terms, the half-incremental terms included in the heat transfer term of equation 5.3. are unnecessary.

$$hS.\Delta z.\ ((T_a + \tfrac{1}{2}\Delta T_a)-(T_g + \tfrac{1}{2}\Delta T_g))\Delta\theta$$

If these incremental terms are removed, then the model does only become stable for extremely small depth and time steps. An examination of the simpler equations which result, suggest that they would probably also be more sensitive to the heat transfer coefficient but does not suggest that the overall effect on the results will be very great. A small improvement may be all that is required, however, for the divergence is accumulating over large times for large depths and for large moisture reductions. Advanced numerical integration procedures, which have safeguards against truncation and induced-instability errors, are now becoming available. Bakker-Arkema[6] has found these to give "excellent and fast" results in drying simulations, including cases where the more conventional Runge-Kutta method either failed or was prohibitively slow. These advanced procedures are not expected to be available on the ICL 4/70 computer until April 1974. If the use of the revised equations and these new methods still fail to increase appreciably the accuracy of the model, then it is clear that some means of including the neglected partial differential terms should be sought. Such an exercise is beyond the scope of the present work.

It seemed possible that another factor which might have made some contribution towards the optimistic model predictions could be the neglect of lateral heat losses to the walls of the experimental

bin. To test this a conductive heat transfer term was introduced of the form

$$q = U.S_s.(T_s-T_{amb})$$

where U = rate of heat transfer through edges of layer, i.e. conductance of the bin wall, KJ/m^2 min K

A_s = surface area of layer edge

T_s = temperature of surface of seed and air at layer edge (assumed T_a)

T_{amb} = ambient temperature

and tested for the highest temperature run, Run 7. The effect was extremely small and the original assumption that it could be neglected was confirmed.

5.4.2. Application

The aim in developing the model was to provide a convenient means of calculating moisture and temperature changes within deep beds of seeds. It was intended also that this information would be used to predict the effect of drying on seed quality with the ultimate intention of studying the technical and economic interactions of such factors as depth, moisture content, drying conditions and pressure resistance to provide a basis for making recommendations.

There are a number of situations for which the model could be used in its existing form to determine the course of subsequent experimentation. For other applications it still remains to introduce biological restraints. Prediction of the effect of drying temperatures on germinations can be incorporated using equation 3.53 of Section 3.5.3. in differential form and integrating in parallel with moisture content. Prediction of deterioration in quality at low to medium temperatures and high humidity will be more difficult. There are two problems.

The first is to define the deterioration that is unacceptable, the second is to measure and express the rate of deterioration in mathematical terms. When this work was begun it was thought that damage could be measured in terms of germination depression. It was found, however, that seed could show considerable visible moulding but still germinate quite well after drying and cleaning. Mouldy

seed could be a health hazard and is commercially unacceptable so that any advisory recommendations would have to ensure that visible mould did not develop. Experience suggests that the first indication of the presence of fungal mycelium in the seed bed may be an increase in the pressure resistance to airflow. It may be that a series of small-scale experiments to monitor pressure resistance changes in seeds subjected to constant temperatures and humidities would allow limiting moulding times to be expressed as a function of temperature and interstitial relative humidity.

5.5. SUMMARY AND CONCLUSIONS

1. A mathematical model of the deep bed drying process in parallel and radial flow was developed and programmed in FORTRAN IV. The model is based on the simple stepwise solution in time and distance of a set of differential equations describing the heat and mass changes within a small element of the bed. The equations used are similar to those of the Newcastle University model but there are differences in subsidiary procedures and in equations used for defining seed properties.

2. The chief differences are:-

   (a) The condensation procedure

   (b) Optional use of exponential series equations for evaluating the drying rate

   (c) Optional use of the Gamson, Thodos and Hougen equation for the heat transfer coefficient

   (d) Facility for initialising seed moisture and temperature profiles

   (e) Facility for interpolating experimental records of varying inlet air temperature and humidity

   (f) Facility for plotting predicted temperature profiles in comparison with observed.

3. The model was developed and validated by simulation of the experimental runs in Section 4. It was found to be stable and tolerant of a wide range of increments of time and distance so that computing times could be kept short.

4. It was found to be insensitive to the value of the heat transfer coefficient.

5. In general the model gave a realistic description of the progress of the drying of deep beds of ryegrass seed. The use of alternative seed properties produced minor variations in results but did not affect the basic tendency for predicted drying times to be over-optimistic. Predicted and observed drying times and moisture contents were related by the equations

$$\Theta_{pred} = 14.0 - 0.663\ \Theta_{exp} (r=0.897) \quad \ldots 5.32$$

$$\overline{M}_{pred} = 1.01\ \overline{M}_{exp} - 1.87\ (r=0.968) \quad \ldots 5.33$$

where Θ is in hours and M is in % d.b.

6. The extreme stability of the model stems from the inclusion of incremental terms in the expression for the heat transferred between the air and seed. These included terms also gave the model its insensitivity to the heat transfer coefficient. Solution of the very much less stable equations, obtained when the terms are omitted, was not possible because conventional methods are too slow for deep bed runs of the depths, moisture contents and drying times of this study. More advanced and faster integration procedures are not available yet on the A.R.C. computer. It may be that to achieve a marked improvement in accuracy partial differential terms at present neglected will have to be introduced.

7. Incorporation of biological restraints into the model was not attempted. In low temperature drying, germination is not a satisfactory index of deterioration in quality.

6. CONCLUSIONS.

6. CONCLUSIONS

The objective of this study was to develop a mathematical simulation of the drying of ryegrass seeds in deep layers, to provide a means of extrapolating a limited number of experimental observations to a wide range of conditions. The work was carried out under four main headings.

6.1. RYEGRASS SEED - RELEVANT PROPERTIES

6.1.1. The experimental work was carried out with 2 types of ryegrass seed, Aberystwyth S.23, a small-seeded diploid cultivar of Lolium perenne, and Aberystwyth Sabrina and Sabel, both large-seeded tetraploid hybrid crosses of Lolium perenne with Lolium multiflorum.

Structurally the seeds are similar to cereal grains although there are differences of shape, size and proportions of various tissues. The grain or kernel is contained within a pair of bracts which do not become fused to the grain as they do in barley but are nevertheless firmly attached and are not readily removed at threshing as they are in wheat or rye. Naked grains are a sign of excessive threshing damage.

6.1.2. The seeds are normally harvested before fully ripe and hence seed moisture content and potential germination are functions of maturity. The following equations related the germination and initial moisture contents of control samples taken during 3 harvest years and dried with ambient air only.

For Sabel and Sabrina.

$$G_o = 94.9 - 3.336 \exp (0.173\ M_D) \quad \ldots 2.1.$$

For S.23

$$G_o = 96.0 - 0.1588 \exp (0.0445\ M_D) \quad \ldots 2.3.$$

Thus 90% germination, the normal commercial minimum is reached by S.23 at 45% w.b. (82% d.b.) and by the tetraploid hybrids at 18% w.b. (22% d.b.). This important difference in sensitivity to premature harvesting was not known at the start of this study.

6.1.3. The diploid and tetraploid types were used because of the contrast in size albeit apparent similarity of shape. Measurements on individual seeds confirmed the common shape. The average ratio of length and width to thickness was 6.68:1.5:1 and the mean dimensions of Sabrina seeds were 1.3 times those of S.23 seeds. Mean 1000 seed weights were 4.124 g and 1.744 g respectively. There was a wide distribution in size within each type so that there was some overlap between them.

Volume - surface mean diameters derived from sieving tests were 1.181 and 1.584 mm for S.23 and Sabrina respectively. These indicated specific surface areas in the range 3587-5081 m^2/m^3 for S.23 and 2525-3787 m^2/m^3 for Sabrina. Much higher values (11,000 - 19.000 m^2/m^3) were obtained by an air permeability method.

6.2. DETERMINATION OF DRYING PROPERTIES - THIN-LAYER EXPERIMENTS

6.2.1. An iterative least-squares procedure was developed to fit 4 alternative diffusion equation to thin-layer drying curves for Sabel and S.23 seeds. Each equations contained an exponentional rate constant k and an asymptotic value, M_e. Similar values of k were given by the fits of all 4 equations but the closest agreement was obtained between those given by equations 3.39 and k_2 of 3.10.

$$M = A.\exp(-k_1\theta) + B.\exp(-k_2\theta) + M_e \qquad \cdots\cdots\cdots 3.10$$

$$M = (M_0 - M_e)\frac{8}{\pi^2}\sum_{n=1}^{\alpha}\frac{1}{(2n-1)^2}\exp(-(2n-1)^2.k\theta + M_e \qquad \cdots\cdots\cdots 3.39$$

These two equations and especially 3.10 also gave the best fits of the drying curves. Equation 3.10 was shown to be the solution of a second-order differential equation.

Equation 3.39 is the solution for a plane sheet of Fick's equation for the rate of change of concerntration of diffusing substance with time. Since it has only 2 constants it is more convenient to use than equation 3.10. It may be argued also that although the fit is not quite as good as that of equation 3.10 the more inflexible shape of 3.39 smooths out experimental errors which 3.10 attempts to follow.

6.2.2. Differences between the rate constants of Sabel and S.23 were shown to be in proportion to their size although diminished by increasing temperature. Hence the two ryegrasses have similar diffusivities.

Differences between the rate constants for ryegrasses and cereal seeds were not a function of size and indicated lower diffusivities in the former. These differences probably reflect differences in tissue ratios.

The rate constant, k, was expressed as a function of drying air temperature and humidity and seed initial moisture content.

$$k = A \exp (bT + cH + dMo) \quad .. 3.44$$

6.2.3. The asymptotic moisture contents, M_e, and the final moisture contents, M_f were expressed as a function of drying air temperature and relative humidity by equation 3.42.

$$M_e = a - b.\ \ln T - c \ln (1-rh) \quad .. 3.42$$

Differences in M_e between varieties were small. In general under similar conditions values for Sabel were 1% d.b. less than those for S.23. Differences between M_e and M_f were less than this.

6.2.4. Under conditions of prolonged exposure, depression in germination began to occur at drying air temperatures between 35 and 40°C and reached unacceptable levels at 50°C. Similar depressions occurred in both varieties even though their potential germinations were different.

Experiments in which time of exposure was varied, showed that as temperatures are increased above 40°C there is a rapid decline in critical exposure times and above 68°C they are a matter of minutes only. An empirical exponential function was developed to describe the decline in germination with drying air temperature and exposure time.

$$G = (G_o - G_e) \exp(-kg\,\theta) + G_e \qquad .. 3.53$$

The constants kg and G_e were described as linear functions of temperature and of temperature and initial moisture content respectively.

6.3. DEEP BED EXPERIMENTS

6.3.1. Experimental data were recorded for 15 deep bed drying runs. Each run was a unique combination of several variables. 12 were carried out with parallel airflow at bed depths from 0.2 to 1.23 m ($\bar{x}$ = 0.87 m) and the remaining 3 employed radial flow at a common radial depth of 1.5 m. Drying air temperatures varied from ambient for two-thirds of the runs to between 32.2 and 55.6°C for the remaining third. Drying times varied from 16 to 160½ h ($\bar{x}$ = 69.6h) and seed initial moisture contents from 23.5 to 104.5% d.b. Inlet air conditions were recorded as a function of time and saved in a form suitable for input to the simulation model. For eventual comparison with predicted values, temperature-time profiles, at each depth recorded, were plotted by computer. The experiments confirmed that attempts to understand the deep-bed drying process by purely empirical experimentation would be prohibitively costly in equipment, seed and labour and the results would, in any case, be almost impossible to interpret in more than very general terms.

6.3.2. The most air per unit of water removed ($662 m^3/kg$) was used in Run 8 which had the lowest initial moisture content (23.5% d.b.) and for which a complete drying zone was not established within the bed.

The least air ($171 m^3/kg$) was used in Run 7 where the highest drying air temperature ($55.4^{\circ}C$) was combined with termination of the run shortly after the drying zone began to emerge from the top of the bed.

6.3.3. No reduction in germination was detected even in seed which had moulded sufficiently to be caked and smelly.

6.3.5. Pressure resistance to airflow in parallel flow was adequately described by the equation $P = a V^n$. Values of a and n were obtained from measurements made in both parallel and radial flow. They appeared to be affected more by differences in seed condition and compaction than by varietal differences of size.

6.4. SIMULATION OF DRYING IN DEEP LAYERS

6.4.1. A mathematical model of the deep bed drying process was developed based upon the simple stepwise solution in time and distance of a set of differential equations describing the heat and mass changes within a small element of bed. The equations used are similar to those of Newcastle University model but are programmed in FORTRAN IV and are asscciated with different subsidiary procedures. These proçedures include a condensation routine, alternative options for drying rate and heat transfer equations, and input/output routines adapted for studying drying runs of several days real time under fluctuating air inlet conditions.

6.4.2. The model was developed and validated by simulation of the experimental runs of Section 4. It was fcund to be stable and tolerant of a wide range of increments of time and distance so that computing times could be kept short. This extreme stability, and an associated insensitivity to the heat transfer coefficient, stems from the inclusion of incremental terms in the expression for the heat transferred between the air and seed.

It was thought that these terms account for some at least of the cumulative over-optimism of the drying time predictions but this cannot be tested until more advancedand faster integration procedures become available on the A.R.C. computer. It may be that to achieve a marked improvement in accuracy, partial differential terms at present neglected will have to be introduced.

6.4.3. In general the model gave a realistic description of the progress of the drying of deep beds of ryegrass seed. Prediction of mean moisture contents and moisture profiles was more accurate than the prediction of drying times. Predicted and observed drying times for the 15 experimental runs of Section 4 were related by the equations

$$\Theta_{pred} = 14.0 - 0.663.\Theta_{exp} \qquad ...5.32$$

$$\bar{M}_{pred} = 1.01\ \bar{M}_{exp} - 1.87 \qquad ...5.33$$

where Θ = time in hours and M is in % d.b.

7. REFERENCES.

7. REFERENCES

1. ALLEN J.R. Application of grain drying theory to the drying of maize and rice. J. agric. Engng, Res., 1960, 5 (4), 363-385

2. BABBIT, J.D. Observations on the absorption of water vapor by wheat. Can. J. Res., 1949, 27 (F), 55-72

3. BAILEY, P.H. High temperature drying of cereal grain. M.Sc. Thesis., Univ. Newcastle-upon-Tyne, 1972

4. BAILEY, P.H. Private Communication. December, 1972

5. BAKKER-ARKEMA, F.W.; BICKERT, W.G.; MOREY, R.V. (Simultaneous heat and mass transfer during grain drying.) Landtech. Forsch. 1967, 17 (6), 175-180. (G)

6. BAKKER-ARKEMA, F.W. Numerical techniques in cooling and drying simulations (1) Solution of ordinary differential equations. (11) Solution of partial differential equations. Proc. Inst. Simulation of Cooling and Drying of Agricultural Products, Michigan State University, 1970

7. BAKKER-ARKEMA, F.W.; ROSENAU, J.R.; CLIFFORD, W.H. The effect of grain surface area on the heat and mass transfer rates in fixed and moving beds of biological products. Trans. am. Soc. agric. Engrs. 1971, 14 (5), 864-867

8. BARKER, J.J. Heat transfer in packed beds. Industrial Engineering Chemistry, 1965, 57 (4), 43.

9. HAUGHMAN, G.R.; BARRE, H.J.; HAMDY, M.Y. Experimental study and simulation of concurrent flow driers. A.S.A.E. Paper No. 71-319

10. BECKER, H.A.; SALLANS, H.R. A study of internal moisture movement in the drying of wheat grain. Cereal Chem., 1955, 32, 212

11. BECKER, H.A.; SALLANS, H.R. A study of the desorption isotherms of wheat at 25 and 50 deg.C. Cereal Chem., 1956, 33 (2), 79

12. BECKER, H.A.; SALLANS, H.R. A theoretical study of the mechanism of moisture diffusion in wheat. Cereal Chem., 1957, 34 (6), 395-409

13. BECKER, H.A. A study of diffusion in solids of arbitrary shape with application to the drying of the wheat kernel. J. of App. Polymer. Sci., 1959, 11 (2), 212-226

14. BLOOME, P.D.; SHOVE, G.C. Near equilibrium simulation of shelled corn drying. Trans. am. Soc. agric. Engrs., 1971, 14 (4), 709-712

15. BLOOME, P.D.; SHOVE, G.C. Simulation of low temperature drying of shelled corn leading to optimisation. Trans. am. Soc. agric. Engrs., 1972, 15 (2), 310-316

16. BOYCE, D.S. Grain moisture and temperature changes with position and time during through drying. J. agric. Engng. Res., 1965, 10 (4), 333-341

17. BOYCE, D.S. Heat and moisture transfer in ventilated grain. J. agric. Engng. Res., 1966, 11 (4), 255-265

18. BOYCE, D.S. Heat and moisture transfer in ventilated grain. Ph.D. Thesis. Univ. of Newcastle upon Tyne. 1966

19. BRITISH STANDARDS INSTITUTION. Methods for the measurement of fluid flow in pipes, Part 1: Orifice plates, nozzles & venturi tubes. B.S. 1042: Part 1 : 1964, B.S.I., London

20. BRITISH STANDARDS INSTITUTION. Methods of test for agricultural grain driers. British Standard 3986: 1966. B.S.I., London

21. BROOKER, D.B. Mathematical model of the psychometric chart. Trans. am. Soc. agric. Engrs., 1967, 10 (4), 558

22. CADLE, R.D. Particle size determination. Interscience Publishers Inc., New York, 1955

23. CHEN, C.S.; CLAYTON, J.T. The effect of temperature on sorption isotherms of biological materials. Trans. am. Soc. agric. Engrs., 1971, 14 (5), 927-929

24. CHIEN, K.S.; MATTHES, P.K.; VERMA, B.P. Dimensional analysis of seed moisture movement in deep-bed drying. A.S.A.E. Paper No. 69-833

25. CHITTENDEN, D.H.; HUSTRULID, A. Deterministic drying constants for shelled corn. Trans. am. Soc. agric. Engrs., 1966 9 (1), 52-55

26. CHU, S-T.; HUSTRULID, A. Numerical solution of diffusion equations. Trans. am. Soc. agric. Engrs., 1968, 11 (6), 705-708

27. CHU, S-T; HUSTRULID, A. General characteristics of variable diffusivity process and the dynamic equilibrium moisture content. Trans. am. Soc. agric. Engrs., 1968, 11 (6), 709-715

28. CHUNG, D.S.; PFOST, H.B. Absorption and desorption of water vapour by cereal grains and their products. II. Development of the general isotherm equation. Trans. am. Soc. agric. Engrs., 1967, 10 (4), 552-555

29. COLBURN, A.P. A method of correlating forced convection heat transfer data and a comparison with fluid friction. Trans. am. Inst. chem. Engrs., 1933, 29, 174-209

30. CRANK, J. The mathematics of diffusion. O.U.P., 1964

31. CRAVEN, F.W. Varieties for seed production in the U.K., imports & exports. Paper to A.D.A. course on herbage seed production, Winchester, 1971

32. DAY, D.L.; NELSON, G.L. Desorption isotherms for wheat. Trans. am. Soc. agric. Engrs., 1965, 8 (2), 293-297

33. DENCH, J.A.L.et al. Break crops. An economic study in Southern England with a technical appraisal from A.D.A.S. Agricultural enterprise studies in England & Wales. Economic Report No. 13. University of Reading, 1972

34. FLOOD, C.A.; SABBAH, M.A.; MEEKER, D.; PEART, R.M. Simulation of a natural-air corn drying system. Trans. am. Soc. agric. Engrs., 1972, 15 (1), 156-159, 162

35. GALLAHER, G.L. A method of determining the latent heat of agricultural crops. Agric. Engng., 1951, 32 (1), 34

36. GAMSON, B.W.; THODOS, G.; HOUGEN, O.A. Heat mass and momentum transfer in the flow of gases through granular solids. Trans. amer. Inst. chem. Engrs, 1943, 39 1-35

37. GREIG, D.J. The determination of the rate constant in the thin-layer drying of agricultural crops. J. agric. Engng. Res., 1970, 15 (2), 106-110

38. GROVES, J.F. Temperature and life duration of seeds. Botanical Gazette, 1917, 62 (3), 169-189

39. GUEST, P.G. Numerical methods of curve fitting. Cambridge University Press, 1961

40. HALL, C.W.; RODRIGUES-ARIAS, J.H. Equilibrium moisture content of shelled corn. Agric. Engng., 1958, 39, 466-470

41. HAMDY, M.Y.; BARRE, H.J. Theoretical analysis and simulation of deep-bed grain drying. A.S.A.E. Paper No. 69-328 presented at the 1969 A.S.A.E. Annual Meeting, Purdue University, June 1969

42. HAMDY, M.Y.; BARRE, H.J. Analysis and hybrid simulation of deep-bed drying of grain. Trans. am. Soc. agric. Engrs., 1970, 13 (6), 752-757

43. HARRIES, O. A photoelectric control circuit for a self balancing weigher for use in an experimental drying installation. N.I.A.E. Departmental Note, 1971. DN/CI/006/1720

44. HARTLEY, H.O. The modified Gauss-Newton method for the fitting of non-linear regression function by least squares. Technometrics, 1961, 3 (2), 269-280

45. HENDERSON, S.M. A basic concept of equilibrium moisture. Agric. Engng., 1952, 33, 20-32

46. HENDERSON, S.M.; PABIS, S. Grain drying theory I. Temperature effect on drying coefficient. J. agric. Engng. Res., 1961, 6(3), 169-174

47. HENDERSON, J.M.; HENDERSON, S.M. A computational procedure for deep-bed drying analysis. J. agric. Engng. Res., 1968, 13 (3), 87-95

48. HINTON, J.J.C. Resistance of the testa to entry of water into the wheat kernel. Cereal Chemistry, 32, (4), 1955

49. HUGHES, J.M.; MITCHELL, T.J. Through-circulation drying of vegetable materials. V. Barley grain. J. Sci. Food. Agric., 1959, 10, 39-45

50. HUGHES, M. Experiments to define the normality of response to heat treatment of wheat samples used for drier tests. Bulletin of Research Ass. of British Flour-Millers, 1964, 15 (4), 129-134

51. HUSAIN, A.; CLAYTON, J.T. Coupled heat and moisture diffusion in porous food product an application to rough rice. A.S.A.E. Paper No. 70-833

52. HUSAIN, A.; CHEN, C.S.; CLAYTON, J.T.; WHITNEY, L.F. Mathematical simulation of mass and heat transfer in high moisture foods. Trans. am. Soc. agric. Engrs., 1972, 15 (4), 732-736

53. HUSTRULID, A.; FLIKKE, A.M. Theoretical drying curve for shelled corn. Trans. am. Soc. agric. Engrs., 1959, 2 (1), 112-114

54. HUTCHINSON, J.B. The drying of wheat. III. The effect of temperature on germination capacity. Journ. Soc. Chem. Industry, 1944, 63, 104-7

55. International Rules for Seed Testing. Proc. Int. Seed Test Assoc., 1966, 31 (1)

56. Institution of Heating and Ventilation Engineers. IHVE Guide Book C. 1970. IHVE London

57. IRANI, R.R.; CALLIS, C.F. Particle size: Measurement, interpretation and application. J. Wiley & Sons. London 1963

58. JASON, A.C. A study of evaporation and diffusion processes in the drying of fish muscle. Fundamental aspects of the dehydration of foodstuffs, 1958. Society Chem. Ind., London

59. KAHRE, L.; SALLVIK, G.; WRANELL, L. Present testing for germination and future research, review of Swedish experience of herbage, oilplant, beet, vegetable, flower and forestry seeds. Proc. Int. Seed. Test. Ass. Vol 36 (1971) 2, 313-324

60. KREYGER, J. Drying of seeds. Proc. Int. Seed Test. Ass., 1960, 25 (1), 590-601

61. KULIK, M.M.; JUSTICE, O.L. Some influences of storage fungi, temperatures and relative humidity on the germination of grass seeds. J. Stored Prod. Res., 1967, 3, 335-343

62. LAWTON, P.J. Resistance to airflow of some common seeds. J. agric. Engng. Res., 1965, 10 (4), 298-300

63. McCORMICK, J.M.; SALVADORI, M.G. Numerical methods in FORTRAN. Prentice-Hall,Inc., 1964

64. McKNIGHT, K.E.; MOYSEY, E.B. The effect of temperature and airflow rate in the quality of dried rapeseed. A.S.A.E. Paper No. 72-386

65. MENZIES, D.J. Private Communication. December, 1970

66. MENZIES, D.J. Heat and mass transfer relationships in the drying of grass. Ph.D. Thesis. Univ. Newcastle-upon-Tyne, 1971

67. M'EWEN, F.; SIMMONDS, W.H.C.; WARD, G.I. The drying of wheatgrain. Part III. Interpretation in terms of its biological structure. Trans. Instn. Chem. Engrs., 1954, 32 (2), 116-120

68. M'EWEN, E,; SIMMONDS, W.H.C.; WARD, G.T. The drying of wheatgrain, Part V. Resistance to airflow of beds of agricultural products. A correlation of results. Trans. Instn. Chem. Engrs., 1954, 32 (2), 130-140

69. M'EWEN, E.; O'CALLAGHAN, J.R. Through drying of deep beds of wheat grain. The Engineer. 1954, Dec. 10

70. M'EWEN,; O'CALLAGHAN, J.R. The effect of air humidity on through drying of wheatgrain. Trans. Instn. Chem. Engrs., 1955, 33, 135-154

71. MOREY, R.V.: PEART, R.M. Optimum horsepower and depth for a natural air corn drying system. Trans. am. Soc. agric. Engrs., 1971, 14 (5) 930-934

72. MOREY, R.V.; CLOUD, H.A. Simulation and evaluation of a multiple column cross-flow drier. A.S.A.E. Paper No. 72-831

73. MORRIS-THOMAS, A. Grain drying of through-circulation. J. agric. Engng. Res., 1962, 7 (4). 328-341

74. NELDER, J.A. et al. Genstat. A general statistical program Statistics Department, Rothamsted Experimental Station, 1972 Also published by Scientific and Social Sciences Program Library, Inter-University/Research Councils Series, Report No. 3, June 1972

75. NELLIST, M.E.; REES, D.V.H.; HIGGS, D.M.J. The drying of Timothy seed. I. Effect on quality. J. Brit. Grassl. Soc., 1965, 20 (4), 273-282

76. NELLIST, M.E. Harvesting cereal and grass seeds. Farm and Country. June, 1967, 333-334

77. NELLIST, M.E.; REES, D.V.H. A comparison of direct-and swath-harvesting of S.24 ryegrass seed. J. of the British Grassland Soc., 1968, 23 (4), 336-342

78. NELLIST, M.E. An examination of methods of evaluating drying constants from experimental data. Departmental Note. DN/HC/29/70. May 1970

79. NELLIST, M.E. The drying of grass seed. N.A.A.S. Quarterly Review, 1970, No. 88, 167-177

80. NELLIST,M.E.; ABRAHAMS, S.J. An examination of the size and shape of ryegrass seeds. Departmental Note. DN/HC/008/1720. June 1970

81. NELLIST, M.E.; O'CALLAGHAN, J.R. The measurement of drying rates in thin-layers of ryegrass seed. J. agric. Engng. Res., 1971, 16 (3), 192-212

82. NELLIST, M.E.; HUGHES, M. Some physical and biological processes in the drying of seeds. Seed Sci. Technol. (In press 1973)

83. NELSON, G.L. A new analysis of batch grain-drier performance. Trans. am. Soc. agric. Engrs., 1960, 3 (1), 81-88

84. NGODDY, P.O.; BAKKER-ARKEMA, F.W. A generalised theory of sorption phenomena in biological materials. I. The isotherm equation. Trans. am. Soc. agric. Engrs. 1970, 13 (5), 612-617

85. NGODDY, P.O.; BAKKER-ARKEMA, F.W. A generalised theory of sorption phenomena in biological materials. II. Adsorption compression on sorbing biological materials. A. Trans. am. Soc. agric. Engrs (in print) 71

86. NGODDY, P.O.; BAKKER-ARKEMA, F.W. A generalised theory of sorption phenomena in biological materials. III. A pore size distribution function of the power law type for biological materials. Trans. am. Soc. agric. Engrs. (in print) 71

87. NGODDY, P.O.; BAKKER-ARKEMA, F.W. A generalised theory of sorption phenomena in biological materials. IV. Sorption hysteresis. A.S.A.E. Paer No. 71-325 (To be published) 71

88. O'CALLAGHAN, J.R.; MENZIES, D.J.; BAILEY, P.H. Digital simulation of agricultural drier performance. J. agric. Engng. Res., 1971, 16 (3), 223-244

89. OLIVER, F.R. Estimating the exponential growth function by direct least squares. Applied Statistics, 1970, 19 (1), 92-100

90. ORR, C.; DALLAVALLE, J.M. Fine particle measurement. Size, surface and pore volume. The Macmillan Company, New York, 1959

91. OSBORNE, L.E. Resistance to airflow of grain and other seeds. J. agric. Engng. Res., 1961, 6 (2), 119-122

92. OTHMER, D.F. Correlating vapour pressure and latent heat data. Ind. Engng. Chem., 1940, 32, 841

93. PARIS, S.; HENDERSON, S.M. Grain drying theory II. A critical analysis of the drying curve for shelled maize. J. agric. Engng. Res., 1961, 6 (4), 272-77

94. PABIS , S.; HENDERSON, S.M. Grain drying theory III. The air/grain temperature relationship. J. agric. Engng. Res., 1962, 7 (1), 21-26

95. PABIS, S.; HENDERSON, S.M. Grain drying theory IV. The effect of airflow rate on the drying index. J, agric. Engng. Res., 1962, 7 (2), 85-89

96. PABIS, S. Grain drying in thin layers. Proc. Agric. Engng. Symposium, 1967, Publ. Instn. Agric. Engrs., 1969

97. PIXTON, S.W.; WARBURTON, S. Moisture content/relative humidity equilibrium of some cereal grains at different temperatures. J. Stored Prod. Res., 1971, 6 (4), 283-295

98. PTITSYN, S.D. Determination of the principal parameters of the drying conditions of seed grain. Mekhan. I. Elektr. Sots Sels. Khoz., 1953, No. 3, 32-39. (N.I.A.E. Translation by E. Harris)

99. PURDY, J.L.; CRANE, P.L. Influence of pericarp on differential drying rate in "mature" corn (Zea mays L). Crop Sci., 1967, 7 (4), 379-381

100. REES, D.V.H.; NELLIST, M.E. Recording automatic weighing apparatus for experimental driers. J. agric. Engng. Res., 1966, 11 (4), 310-314

101. Report of the Committee on Herbage Seed Supplies. CMND 3748. H.M.S.O. London, 1968

102. ROBERTS, E.H. The viability of cereal seed (in storage) in relation to temperature and moisture. Annals of Botany, 1960, 24 (93), 12-31

103. ROBERTS, H.M. Harvesting tetraploid ryegrass for seed. J. Brit. Grassl. Soc., 1971, 26, 59-62

104. SAUL, R.A. Deterioration rate of moist shelled corn at low temperatures. A.S.A.E. Paper No. 70-301

105. SAUL, R.A.; LIND, F. Maximum time for safe drying of grain with unheated air. Trans. am. Soc. agric. Engrs., 1958, 1 (1), 29-33

106. SHARP, R.B.; NASH, J.F. A method of determining the specific heat of seeds. J. agric. Engng. Res. 1965, 10 (4), 355-358

107. SHARP, R.B. Private Communication, 1966

108. SHOVE, G.C. Transient low temperature deep-bed drying. A.S.A.E. Paper No. 72-323

109. SIJBRING, P.H. Results of experiments on the moisture relationships of seeds. Proc. Int. Seed Test Assn., 1963, 28 (4), 837-44

110. SIMMONDS, W.H.C.; WARD, G.T.; M'EWEN, E. The drying of wheatgrain, Part I. The mechanism of drying. Trans. Instn. Chem. Engrs. 1953, 31 (3), 265-278

111. SMITH, S.E. The sorption of water vapour by high polymers. Jour. Amer. Chem. Soc., 1947, 69, 646-651

112. SOUTHWORTH, R.W.; DELEEUW, S.C. Digital computation and numerical methods. McGraw-Hill Book Co. 1965

113. SPENCER, H.B. A mathematical simulation of grain drying. J. agric. Engng. Res., 1969, 14 (3), 226-235

114. SPENCER, H.B. A revised model of wheat drying process. J. agric. Engng. Res., 1972, 17 (1), 189-194

115. STEELE, J.L.; SAUL, R.A.; HUKILL, W.V. Deterioration rate of shelled corn as measured by carbon-dioxide production. Trans. am. Soc. agric. Engrs., 1969, 12 (5), 685-689

116. STROHMAN, R.D.; YOERGER, R.R. A new equilibrium moisture-content equation. Trans. am. Soc. agric. Engrs., 1967, 675-677

117. THOMSON, J.R. New tolerances in seed testing. J. Natn. Inst. Agric. Bot., 1963, 9, 372-377

118. THOMPSON, T.L.; PEART, R.M.; FOSTER, G.H. Mathematical simulation of corn drying - a new model. Trans. am. Soc. agric. Engrs., 1968. 11 (4), 582

119. THOMPSON, T.L. Simulation for optimal grain-drier design. Trans. am. Soc. agric. Engrs., 1970, 13 (6), 844-848

120. THOMPSON T.L.; PEART, R.M. Useful search techniques to save research time. Trans. am. Soc. agric. Engrs., 1968, 11 (4),461-467

121. THOMPSON, T.L.; VILLA, L.G.; CROSS, O.E. Simulation and experimental performance of temperature-control systems for chilled high-moisture grain storage. Trans. am. Soc. agric. Engrs., 1971, 14 (3), 554-59

122. THOMPSON, T.L. Temporary storage of high-moisture shelled corn using continuous aeration. Trans. am. Soc. agric. Engrs., 1972, 15 (2), 333-337

123. TREYBAL, R.E. Mass transfer operations. McGraw-Hill.

124. TROEGER, J.M.; HUKILL, W.V. Mathematical description of the drying rate of fully-exposed corn. A.S.A.E. Paper No. 70-324

125. TUITE, J.; FOSTER, G.H. Effect of artificial drying on the hydroscopic properties of corn. Cereal Chem. 1963, 40, 630-637

126. VAN ARSDEL, W.B. Simultaneous heat - and mass-transfer in a non-isothermal system, through-flow drying in the low-moisture range. Am. Inst. Chem. Eng., 1955, Chem. Eng. Progress Symposium Series No. 16, Mass-Transfer, Transport Properties, 47-58

127. VAN REST, D.J.; ISAACS, G.W. Exposed-layer drying rates of corn. Trans. am. Soc. agric. Engrs., 1968, 11 (2), 236-239

128. WARNER, M.G.R.; BROWNE, D.A. Apparatus for the assessment of drying damage and some initial results with barley and wheat. J. agric. Engng, Res., 1962, 7 (4), 359-366

129. WELLINGTON, P.S.; BRADNOCK, W.T. Studies on the germination of cereals. 6 The effect of heat during artificial drying on germination and seedling development in barley. J. Nat. Inst. Agric. Bot. 1964, 10, 129-143

130. WESTERMAN, P.W.; WHITE, G.M.; ROSS, T.J. Effect of relative humidity on the high-temperature drying of shelled corn. A.S.A.E. Paper No. 72-818

131. WHITAKER, T.; BARRE, H.J.; HAMDY; M.Y. Theoretical and experimental studies of diffusion in spherical bodies with a variable diffusion coefficient. Trans. am. Soc. agric. Engrs., 1969, 12 (5), 668-672

132. WHITE, G.M.; ROSS, I.J.; WESTERMAN, P.W. Drying rate and quality of shelled corn as influenced by dew point temperature. A.S.A.E. paper 71-817

133. WILLIAMS, M. The moisture content of grass seed in relation to drying and storing. Welsh J. Agric., 1937, 14, 213-232

134. WOODFORDE, J.; LAWTON, P.J. The drying of seeds. J. agric. Engng. Res., 1965, 10 (4) 283-297

135. YOUNG, J.H.; NELSON, G.L. Theory of hysteresis between sorption and desorption isotherms in biological materials. Trans. am. Soc. agric. Engrs., 1967, 10 (2), 260-263

136. YOUNG, J.H.; NELSON, G.L. Research of hysteresis between sorption and desorption isotherms of wheat. Trans. am. Soc. agric. Engrs., 1967, 10 (6), 756-761

137. YOUNG, J.H. Simultaneous heat and mass transfer in a porous hygroscopic solid. Trans. am. Soc. agric. Engrs., 1969, 12 (6), 720-725

138. YOUNG, J.H.; WHITAKER, T.B. Numerical analysis of vapour diffusion in a porous composite sphere with concentric shells. A.S.A.E. Paper No. 70-336

139. YOUNG. J.H.; WHITAKER, T.B. Evaluation of the diffusion equation for describing thin-layer drying of peanuts in the hull. Trans. am. Soc. agric. Engrs., 1971, 14 (2), 309-312.